

Durham E-Theses

Copper and zinc ligands of pisum sativum and expression of psMT(_A)

Wilson, Jonathan Robert

How to cite:

Wilson, Jonathan Robert (1995) *Copper and zinc ligands of pisum sativum and expression of psMT(_A)*, Durham theses, Durham University. Available at Durham E-Theses Online:
<http://etheses.dur.ac.uk/5320/>

Use policy

The full-text may be used and/or reproduced, and given to third parties in any format or medium, without prior permission or charge, for personal research or study, educational, or not-for-profit purposes provided that:

- a full bibliographic reference is made to the original source
- a [link](#) is made to the metadata record in Durham E-Theses
- the full-text is not changed in any way

The full-text must not be sold in any format or medium without the formal permission of the copyright holders.

Please consult the [full Durham E-Theses policy](#) for further details.

Copper and zinc ligands of *Pisum sativum* and expression of *PsMT_A*

by

Jonathan Robert Wilson

(B.Sc. Hons. University of Leeds)

The copyright of this thesis rests with the author.
No quotation from it should be published without
his prior written consent and information derived
from it should be acknowledged.

thesis submitted for the degree of Doctor of Philosophy
to the University of Durham

Department of Biological Sciences

July 1995



27 NOV 1995

ABSTRACT

Copper and zinc ligands of *Pisum sativum* and expression of *PsMT_A* (Jonathan R. Wilson, Ph.D. 1995)

The gene, *PsMT_A* is highly expressed in the roots of the garden pea, *Pisum sativum*. The predicted primary structures of homologues of the *PsMT_A* gene from a range of plant species were compared. Common features are amino and carboxyl terminal domains of approximately 20 residues which are rich in cysteine residues many of which are arranged in the cysteine-Xaa-cysteine (Xaa is not a cysteine) motifs characteristic of metallothionein. The greatest degree of sequence conservation between these predicted gene products occurs within the cysteine rich domains. Two principal (most highly represented in the available sample) categories of sequence were identified on the basis of the arrangement of the cysteine residues within the amino terminal domain. A secondary structure motif (β -strand) was predicted (using a computer algorithm) to occur in a conserved position in the central domain linking the two cysteine rich domains of these predicted proteins. This feature is not apparent in the structure of metallothioneins from other species.

A recombinant GST-*PsMT_A* fusion protein was isolated from crude lysates of *Escherichia coli* containing the plasmid pGEX3X with *PsMT_A* coding sequence. When isolated from *Escherichia coli* cells grown in zinc supplemented media it was demonstrated that zinc was associated with the *PsMT_A* moiety of the fusion protein. In aqueous solution the *PsMT_A* moiety of the fusion protein formed discreet degradation products. The fusion protein was insoluble at concentrations greater than 20 mg ml⁻¹ which rendered it unsuitable for a structural study of the putative metal binding site(s) by ¹¹³Cd NMR. An antibody to the GST-*PsMT_A* fusion protein was characterised and the epitope was found to lie within the GST moiety.

Comparison of the arrangement of cysteines in the amino terminal domains with the different domains of mammalian metallothionein suggested that the two principal categories of predicted plant metallothionein-like gene products may have different affinities for zinc. The predicted products of the metallothionein-like gene highly expressed in the leaves of *Arabidopsis thaliana* (*AtMT-t2*) and the *PsMT_A* gene are representative of the two principal categories identified by sequence analysis. The *AtMT-t2* coding sequence was amplified from an *Arabidopsis thaliana* leaf cDNA library and cloned into the pGEX3X plasmid to allow expression of the protein as a fusion to GST in *Escherichia coli*. Zinc was associated with the *AtMT-t2* moiety of the fusion protein. The pH of 50 % displacement for the GST-*AtMT-t2* fusion protein with respect to zinc was 0.25 pH units lower than that for the GST-*PsMT_A* fusion protein indicating that putative metallothionein-like protein from *Arabidopsis thaliana* may have a higher affinity for zinc. It is feasible that this difference allows *AtMT-t2* to compete with endogenous ligands of zinc more effectively than *PsMT_A*. Expression of the *AtMT-t2* gene in a zinc metallothionein deficient strain of *Synechococcus* (in collaboration with Dr. J.S. Turner) partially restored zinc tolerance to the transformed cells.

The similarity of the cysteine rich domains of the predicted metallothionein-like proteins with metallothionein and the demonstration of metal binding *in vitro* suggested that these genes may be metal regulated. The effect of variations in the exogenous concentration of the trace metals copper, zinc and iron on the expression of the *PsMT_A* gene in the roots of *Pisum sativum* seedlings was investigated by northern analysis. Induction of *PsMT_A* expression was seen with increasing iron concentrations up to 2.0 μ M iron chelate. At this concentration of iron chelate, and above, expression of *PsMT_A* decreased. At concentrations of copper above 100 nM induction of *PsMT_A* expression was seen. Below 100 nM copper *PsMT_A* expression increased with decreasing copper concentrations. This response has not been reported for metallothioneins from other species and may be significant for the role of *PsMT_A* in root tissue. In the presence of 2.0 μ M iron zinc concentrations above 5.0 μ M induced expression of *PsMT_A*. The response to changes in exogenous metal concentrations was rapid. Complete repression of *PsMT_A* transcription occurred within 1 h of transfer to media supplemented with 2.0 μ M iron.

To date no translational products of plant metallothionein-like genes (excluding the E_c protein from *Triticum aestivum*) have been identified in plant tissue. Two copper and one zinc complex were identified following ion exchange chromatography of soluble extracts from roots of *Pisum sativum*. The quantity of the zinc complex eluted from the matrix was reduced by the addition of iron chelate to the growth media. There was no consistent change in the quantity of copper complex recovered in response to iron. Two copper and one zinc component of low molecular weight were identified following gel filtration chromatography of the above complexes. Following polyacrylamide gel electrophoresis of extracts from roots of *Pisum sativum*, labelled *in vivo* with ³⁵S cysteine, a band was identified with the characteristics predicted for the product of the *PsMT_A* gene. On two dimensional polyacrylamide gels a doublet of spots was identified (migrating to a low pH as predicted for *PsMT_A*) in an extract from roots of seedlings grown in media not supplemented with iron which were not observed on gels of extracts from seedlings grown in media supplemented with iron. The identity of these polypeptides was not established by sequence analysis.

STATEMENT

No part of this thesis has been previously submitted for a degree in this or any other university. I declare that, unless otherwise indicated, the work herein is entirely my own.

The copyright of this thesis rests with the author. No quotation from it should be published without his prior written consent and information derived from it should be acknowledged.

ACKNOWLEDGEMENTS

I would like to thank my supervisor, Professor Nigel Robinson, for continuous help and guidance throughout my Ph.D. research which is greatly appreciated. I am very grateful to Drs. Jen Turner, Amit Gupta, Andy Morby, Andy Tommey and Quentin Groom for advice, assistance and encouragement. I am grateful for the use of the facilities of the Department of Biological Sciences, particularly the technical assistance of Mrs. Julia Bartley and Mr. John Gilroy and the photographic work of Mr. David Hutchinson.

I would especially like to thank my parents, Carole and Robert, for their ever present support and Mary for being a true friend.

ABBREVIATIONS

2-ME	-	2-mercaptoethanol;
ACC	-	1-aminocyclopropane-1-carboxylate;
ATP	-	adenosine-5' triphosphate;
BCIP	-	5-bromo-4-chloro-3-indolyl phosphate;
BSA	-	bovine serum albumin;
BSO	-	L-buthionine sulphoxamine;
cAMP	-	cyclic-adenosine monophosphate;
CD	-	circular dichroism;
CPM	-	counts per minute;
dCTP	-	2'-deoxycytidine-5'-triphosphate;
DEAE	-	diethylaminoethyl;
DNA	-	deoxyribonucleic acid;
DTNB	-	5,5'-dithiobis-(2-nitrobenzoic acid);
EDTA	-	ethylenediaminetetraacetic acid;
g	-	acceleration due to gravity (9.8 ms^{-2});
GST	-	glutathione-S-transferase;
(γ -EC) _n G	-	(gamma-glutamylcysteinyl) _n glycine;
h	-	hour(s);
HPLC	-	High Performance Liquid Chromatography;
IPTG	-	isopropyl thio- β -D-galactosidase;
l	-	litre(s);
LB	-	Luria-Bertani;
m	-	minute(s);
M	-	molar;
mA	-	milliampere;
μ g	-	microgram;
mM	-	millimolar;
μ M	-	micromolar;
Mes	-	4-morpholineethansulphonic acid;
MRE	-	metal regulatory element;
mRNA	-	messenger RNA;
MT	-	metallothionein;
nm	-	nanometer;
nM	-	nanomolar;
nmol	-	10^{-9} moles;
NBT	-	nitro blue tetrazolium;
NCBI	-	National Centre for Biological Information;
NMR	-	nuclear magnetic resonance;
PCR	-	polymerase chain reaction;
PPi	-	pyrophosphate;
PVDF	-	polyvinylidene difluoride
RNA	-	ribonucleic acid;
SDS	-	sodium dodecyl sulphate (lauryl sulphate);
TEMED	-	N,N,N',N'-tetramethylethylenediamine;
Tris	-	tris(hydroxymethyl)methylamine;
v/v	-	volume for volume;
w/v	-	weight for volume;
Xaa	-	an amino acid other than cysteine;
Yaa	-	any amino acid.

Plant species referred to in this thesis		plant species continued	
Scientific Name	Common Name	Scientific Name	Common Name
<i>Actinidia delectiosa</i>	kiwifruit	<i>Ricinus communis</i>	castorbean
<i>Arabidopsis thaliana</i>	mouse ear cress	<i>Silene cucubalus</i>	campion
<i>Brassica campestris</i>	field cabbage	<i>Silene vulgaris</i>	bladder campion
<i>Brassica capitae</i>	cabbage	<i>Tifolium repens</i>	clover
<i>Brassica juncea</i>	Indian mustard	<i>Triticum aestivum</i>	wheat
<i>Brassica napus</i>	rape	<i>Vicia faba</i>	long pod bean
<i>Coffea arabica</i>	coffee	<i>Zea mays</i>	maize
<i>Cucumis sativus</i>	cucumber	Other species	
<i>Datura innoxia</i>	sacred datura		
<i>Deschampsia cespitosa</i>	tussak grass	<i>Agaricus bisporus</i>	mushroom
<i>Dianthus caryophyllus</i>	carnation	<i>Candida glabrata</i>	pathogenic yeast
<i>Glycine max</i>	soyabean	<i>Saccharomyces cerevisiae</i>	bakers yeast
<i>Hordeum vulgare</i>	barley	<i>Chlorella fusca</i>	algae
<i>Lupinus albus</i>	white lupin	<i>Drosophila melangaster</i>	fruit fly
<i>Lycopersicon esculentum</i>	tomato	<i>Equus caballus</i>	horse
<i>Mimulus guttatus</i>	monkey flower	<i>Euglena gracilis</i>	algae
<i>Nicotiana tabacum</i>	tobacco	<i>Neurospora crassa</i>	fungus
<i>Nicotiana rustica</i>	tobacco	<i>Noemacheilus Barbatulus</i>	loach
<i>Oryza sativa</i>	rice	<i>Scenedesmus acutiformis</i>	algae
<i>Phaseolus vulgaris</i>	kidney bean	<i>Schistosoma japonicum</i>	fluke
<i>Physcomitrella commune</i>	moss	<i>Schizosaccharomyces pombe</i>	fission yeast
<i>Pisum sativum</i>	garden pea	<i>Scylla serrata</i>	crab
<i>Rauvolfia serpentina</i>	Java devilkeeper	<i>Synechococcus</i> species	blue green algae

Gene names referred to in this thesis		
Gene	Description of product	Reference
<i>ACE1</i>	copper dependent transcription factor of metallothionein in <i>S. cerevisiae</i>	Fürst <i>et al.</i> 1988
<i>AMT1</i>	copper dependent transcription factor of metallothionein in <i>C. glabrata</i>	Zhou and Thiele 1991
<i>AtMT-t2</i>	type-2 metallothionein-like protein in <i>A. thaliana</i>	this thesis, chapter 5
<i>CTR1</i>	putative copper import protein in <i>S. cerevisiae</i>	Dancis <i>et al.</i> 1994
<i>CTT1</i>	cytosolic catalase in <i>S. cerevisiae</i>	Jungmann <i>et al.</i> 1993h
<i>CUP1</i>	copper metallothionein in <i>S. cerevisiae</i>	Fogel <i>et al.</i> 1982
<i>Ec</i>	Class II metallothionein in <i>T. aestivum</i>	Kawashima <i>et al.</i> 1992
<i>FET3</i>	putative ferrous iron transport protein in <i>S. cerevisiae</i>	Askwith <i>et al.</i> 1994
<i>FRE1</i>	putative ferric iron reductase in <i>S. cerevisiae</i>	Dancis <i>et al.</i> 1990
<i>GEF1</i>	putative iron transport protein in <i>S. cerevisiae</i>	Greene <i>et al.</i> 1993
<i>GEF2</i>	vacuolar proton ATPase in <i>S. cerevisiae</i>	Eide <i>et al.</i> 1993
<i>MAC1</i>	transcription factor for <i>FRE1</i> and <i>CTT1</i> in <i>S. cerevisiae</i>	Jungman <i>et al.</i> 1993b
<i>PsMT_A</i>	type-1 metallothionein-like protein in <i>P. sativum</i>	Evans <i>et al.</i> 1990
<i>SOD1</i>	copper, zinc superoxide dismutase in <i>S. cerevisiae</i>	Tardat and Touati 1991
<i>UBC7</i>	ubiquitin conjugating enzyme in <i>A. thaliana</i>	Jungman <i>et al.</i> 1993

TABLE OF CONTENTS

	PAGE
ABSTRACT	i
STATEMENT	ii
ACKNOWLEDGEMENTS	iii
ABBREVIATIONS	iv
TABLE OF CONTENTS	v
LIST OF FIGURES	xi
LIST OF TABLES	xiii

CHAPTER 1 - INTRODUCTION

1.1 An overview of the introductory chapter	1
1.2 A general introduction to trace metals in biological systems	2
1.2.1 Copper.....	2
1.2.2 Iron.....	3
1.2.3 Zinc.....	3
1.2.4 A brief comment on non-essential trace metals.....	4
1.3 Metallothionein	5
1.3.1 A general introduction to metallothionein.....	5
1.3.2 Occurrence of metallothionein.....	5
1.3.3 Function of metallothionein.....	6
1.3.3.1 Metal ion homoeostasis.....	6
1.3.3.2 Metal tolerance.....	8
1.3.3.3 Other potential metallothionein functions.....	9
1.4 The structure and function of mammalian metallothionein	9
1.4.1 Introduction.....	9
1.4.2 Methods employed in structural studies of metallothionein.....	10
1.4.3 Basic structural characteristics.....	10
1.4.4 Metal ion binding properties of the metallothionein domains.....	12
1.4.5 The inter-domain region.....	13
1.4.6 Dimerisation.....	13
1.4.7 Alternative metallothionein conformations.....	13
1.5 Metallothionein and trace metal ion homoeostasis in yeast	16
1.5.1 Introduction.....	16
1.5.2 Yeast metallothionein.....	16
1.5.2.1 Identification of metallothionein in <i>S. cerevisiae</i>	16
1.5.2.2 Structure and properties of CUP1.....	16
1.5.2.3 Transcriptional regulation of yeast metallothionein expression.....	17
1.5.2.4 ACE1 a metal dependent transcription factor of yeast metallothionein.....	18
1.5.2.5 The metallothionein gene family in <i>Candida glabrata</i>	19
1.5.3 Other aspects of trace metal ion homoeostasis in yeast.....	21
1.5.3.1 Genes with products proposed to have a role in iron and copper uptake and metabolism in <i>S. cerevisiae</i>	21
1.5.3.2 Oxidative stress, copper/zinc superoxide dismutase and metallothionein.....	24
1.5.3.3 Summary.....	25
1.6 Metal binding polypeptides in plants, algae and some fungi	27

1.6.1 Introduction	27
1.6.2 Induction of phytochelatin synthesis.....	27
1.6.3 Properties of phytochelatin	28
1.6.4 Inorganic sulphur is involved in stabilisation of some cadmium phytochelatin complexes.....	29
1.6.5 Biosynthesis of phytochelatin.....	30
1.6.6 Function of phytochelatin	31
1.7 Iron accumulation in higher plants.....	35
1.7.1 Introduction	35
1.7.2 Strategy 1.....	35
1.7.2 Strategy 2.....	35
1.8 Isolation of low molecular weight metal containing compounds from plants.....	37
1.9 Gene encoded metallothionein in higher plants.....	38
1.9.1 Introduction	38
1.9.2 The E _c protein from <i>Triticum aestivum</i>	38
1.9.3 A plant metallothionein-like gene in the root of <i>P. sativum</i> - <i>PsMT_A</i> , and characterisation of the translational product.....	39
1.10 Objectives of this research.....	43
<u>CHAPTER 2 - MATERIALS AND METHODS</u>.....	45
2.1 Materials	45
2.1.1 Chemicals, reagents and laboratory consumables	45
2.1.2 <i>E. coli</i> strains	45
2.1.3 Plasmids.....	46
2.2 Media and buffers.....	46
2.2.1 Buffers used in DNA manipulations.....	46
2.2.2 Maintenance of <i>E. coli</i> cultures.....	46
2.2.3 Hydroponic growth media for <i>P. sativum</i> seedlings.....	47
2.2.3.1 Preparation of Iron(III)-EDDHA	47
2.2.4 Buffers required for proton displacement experiments.....	48
2.2.5 Other commonly used buffers	48
2.3 General methods in protein biochemistry.....	48
2.3.1 Expression of GST fusion proteins in <i>E. coli</i>	48
2.3.2 Purification of fusion proteins from a crude <i>E. coli</i> extract using a glutathione affinity matrix.....	49
2.3.3 Estimation of protein concentration	49
2.3.4 Cleavage of the GST fusion protein with Factor Xa.....	50
2.3.5 Methods used to increase the concentration of protein solutions	50
2.3.5.1 Acetone precipitation.....	51
2.3.5.2 Microconcentrator centrifuge vials.....	51
2.3.6 One-dimensional polyacrylamide gel electrophoresis in SDS.....	51
2.3.6.1 Standard electrophoresis.....	51
2.3.6.2 Tricine buffer electrophoresis.....	52
2.3.7 Two-dimensional polyacrylamide gel electrophoresis in SDS.....	52
2.3.7.1 Isoelectrofocusing.....	52
2.3.7.2 Second phase electrophoresis.....	53
2.3.8 Semi-dry electroblotting of polyacrylamide gels onto membrane.....	53
2.3.9 Western Blotting	53

2.3.10 Crude protein extraction from roots of <i>P. sativum</i>	54
2.3.10.1 Original protein extraction protocol	54
2.3.10.2 Revised protein extraction protocol	54
2.3.11 Chromatography	55
2.3.11.1 Ion exchange chromatography	55
2.3.11.2 Gel filtration chromatography	55
2.3.12 Protein sequencing	55
2.3.13 Atomic absorption spectrophotometry	55
2.4 Growth of <i>P. sativum</i> seedlings in hydroponic solution	55
2.5 General methods in molecular biology	56
2.5.1 Small scale isolation of plasmid DNA from <i>E. coli</i>	56
2.5.1.1 Alkaline lysis method	56
2.5.1.2 Isolation with DNA extraction resin	57
2.5.2 Agarose gel electrophoresis of nucleic acids	57
2.5.2.1 Agarose gel electrophoresis of DNA	57
2.5.2.2 Denaturing electrophoresis of RNA	57
2.5.3 Isolation of DNA restriction fragments from agarose gels	57
2.5.4 Further purification of DNA	58
2.5.4.1 Phenol / chloroform extraction	58
2.5.4.2 Ethanol precipitation	58
2.5.5 DNA restriction digests	58
2.5.6 Preparation and transformation of competent <i>E. coli</i> cells	58
2.5.7 Oligonucleotide synthesis and DNA sequence analysis	58
2.5.8 Polymerase chain reaction (PCR) for <i>in vitro</i> amplification of DNA	59
2.5.9 Preparation of radiolabelled DNA probes	59
2.5.10 Total RNA extraction from pea roots	59
2.5.11 Hybridisation of radiolabelled DNA probes to filter-immobilised nucleic acids	60
2.5.11.1 Southern transfer of DNA	60
2.5.11.2 Southern hybridising conditions	61
2.5.11.3 Northern transfer of RNA	61
2.5.11.4 Northern hybridisation conditions	61

CHAPTER 3 - COMPARISON OF THE PREDICTED PRODUCTS OF PLANT METALLOTHIONEIN-LIKE GENES

3.1 Introduction and objectives	62
3.1.1 Published reports of plant metallothionein-like genes	62
3.1.1.1 <i>Mimulus guttatus</i>	62
3.1.1.2 <i>Pisum sativum</i>	63
3.1.1.3 <i>Zea mays</i>	63
3.1.1.4 <i>Hordeum vulgare</i>	64
3.1.1.5 <i>Triticum aestivum</i>	65
3.1.1.6 <i>Glycine max</i>	65
3.1.1.7 <i>Actinidia deleciosa</i>	66
3.1.1.8 <i>Vicia faba</i>	66
3.1.1.9 <i>Arabidopsis thaliana</i>	67
3.1.1.10 <i>Brassica napus</i>	68
3.1.2 Analysis of 5' flanking sequences of plant metallothionein-like genes	68
3.2. Methods	69

3.2.1 Database searching.....	69
3.2.2 Prediction of protein characteristics.....	69
3.2.3 Sequence comparison.....	70
3.2.3.1 Multiple sequence alignment.....	70
3.2.3.2 Pairwise sequence alignment.....	70
3.2.3.3 Evolutionary relationships.....	70
3.2.4 Secondary structure prediction.....	70
3.3 Results and discussion.....	71
3.3.1 Plant metallothionein-like genes reported in the literature and in sequence databases.....	71
3.3.2 Classification of the products of plant metallothionein-like genes based on their predicted primary structure.....	71
3.3.3 Comparison of the predicted products of plant metallothionein-like genes with other Swissprot protein database entries.....	72
3.3.4 Sequence alignment of the plant metallothionein-like gene products.....	72
3.3.5 Phylogenetic relationships between the products of the plant metallothionein-like genes.....	76
3.3.6 Sequence conservation in type-1 and type-2 gene products.....	77
3.3.7 Predicted secondary structure within plant metallothionein-like gene products.....	82
3.4 Conclusions.....	86

<u>CHAPTER 4 - CHARACTERISATION OF THE PRODUCT OF THE <i>PsMT_A</i> GENE AND AN ANTI GST-<i>PsMT_A</i> IMMUNE SERUM</u>	88
4.1 Introduction and objectives.....	88
4.1.1 Characterisation of the product of the <i>PsMT_A</i> gene.....	88
4.1.2 Characterisation of an a rabbit anti GST- <i>PsMT_A</i> fusion protein immune serum.....	89
4.2 Methods.....	89
4.2.1 Expression of <i>PsMT_A</i> in <i>E. coli</i>	89
4.2.2 The association of metal with the <i>PsMT_A</i> portion of the fusion protein.....	90
4.2.3 Preparation of bulk quantities of GST- <i>PsMT_A</i> fusion protein for structural studies.....	90
4.2.4 Characterisation of an anti GST- <i>PsMT_A</i> immune serum by western blotting.....	91
4.2.4.1 Purification of the immune serum on a GST affinity matrix.....	91
4.2.4.2 Further refinement of the immune serum characterisation.....	91
4.2.5 Characterisation of an anti- <i>PsMT_A</i> antibody.....	91
4.3 Results and discussion.....	92
4.3.1 Expression of the GST- <i>PsMT_A</i> fusion protein in <i>E. coli</i>	92
4.3.2 Metal association with the <i>PsMT_A</i> protein.....	93
4.3.3 Preparative protein purification for [¹¹³ Cd] NMR.....	93
4.3.4 Characterisation of a rabbit anti GST- <i>PsMT_A</i> fusion protein immune serum.....	102
4.3.4.1 Purification of the immune serum on a GST affinity matrix.....	102
4.3.4.2 Further refinement of the immune serum characterisation.....	104
4.3.5 Characterisation of an anti- <i>PsMT_A</i> antibody.....	104
4.4 Conclusions.....	107

<u>CHAPTER 5 - CLONING AND CHARACTERISATION OF THE TYPE-2 METALLOTHIONEIN-LIKE GENE FROM <i>ARABIDOPSIS THALIANA</i></u>	109
5.1 Introduction and objectives.....	109
5.2 Methods.....	110

5.2.1 Design of primers for the Polymerase Chain Reaction	110
5.2.2 PCR of the coding sequence of the <i>AtMT-t2</i> gene	110
5.2.3 Cloning of <i>AtMT-t2</i> into pGEX3X	111
5.2.4 Genomic analysis	111
5.2.5 Overexpression of <i>AtMT-t2</i> in <i>E. coli</i>	112
5.2.6 Confirmation of zinc association with the AtMT-t2 protein	112
5.2.7 Measurement of zinc affinity for recombinant plant metallothionein-like peptides	112
5.2.8 Expression of <i>AtMT-t2</i> in <i>Synechococcus</i>	113
5.2.8.1 Design of PCR primers	113
5.2.8.2 PCR and initial cloning of <i>AtMT-t2</i> , for the expression of <i>AtMTt2</i> in <i>Synechococcus</i>	114
5.2.8.3 Transformation of <i>Synechococcus</i> and examination of the zinc phenotype	114
5.3 Results and discussion	116
5.3.1 PCR	116
5.3.1.1 <i>AtMT-t2</i> primers	116
5.3.1.2 <i>PsMT_A</i> primers	116
5.3.2 Cloning of the <i>AtMT-t2</i> coding sequence	117
5.3.3 Genomic analysis	117
5.3.4 Expression of <i>AtMT-t2</i> in <i>E. coli</i>	118
5.3.5 Confirmation of zinc binding with the AtMT-t2 peptide	118
5.3.6 Comparison of the zinc affinity of AtMT-t2 and <i>PsMT_A</i> GST fusion proteins	124
5.3.7 Expression of <i>AtMT-t2</i> in a zinc metallothionein deficient mutant of <i>Synechococcus</i>	125
5.4 Conclusions	129

CHAPTER 6 - REGULATION OF THE EXPRESSION OF *PsMT_A* IN THE ROOTS OF *PISUM SATIVUM* BY TRACE METALS

6.1 Introduction	131
6.2 Methods	131
6.2.1 Growth conditions	131
6.2.2 Extraction of RNA from <i>P. sativum</i> roots and northern analysis	131
6.2.3 Metal treatments used in the study the expression of <i>PsMT_A</i>	132
6.2.3.1 The response of <i>PsMT_A</i> to different exogenous copper concentrations with and without added iron	132
6.2.3.2 The response of <i>PsMT_A</i> to different exogenous iron concentrations with and without added copper	133
6.2.3.3 The response of <i>PsMT_A</i> to different exogenous zinc concentrations with and without added iron	134
6.2.4 Time course experiments to study the responsive of <i>PsMT_A</i> gene expression to changes in copper and iron concentrations	135
6.2.4.1 Conditions for time course experiment 1	135
6.2.4.2 Conditions for time course experiment 2	136
6.3 Results and Discussion	137
6.3.1 The response of <i>PsMT_A</i> to different exogenous copper concentrations with and without added iron	137
6.3.2 The response of <i>PsMT_A</i> to different exogenous iron concentrations with and without added copper	138

6.3.3 The response of <i>PsMT_A</i> to different exogenous zinc concentrations with and without added iron	139
6.3.4 Time course experiments to study the responsive of <i>PsMT_A</i> gene expression to sudden changes in copper and iron concentrations	148
6.3.4.1 Time course experiment 1	148
6.3.4.2 Time course experiment 2	149
6.4 Conclusions	154
<u>CHAPTER 7 - COPPER AND ZINC LIGANDS IN <i>PISUM SATIVUM</i> :</u>	
<u>EVIDENCE FOR THE <i>PsMT_A</i> PROTEIN IN ROOT EXTRACTS</u>	157
7.1 Introduction	157
7.2 Methods	157
7.2.1 Basic strategy for the isolation of ligands from roots of <i>P. sativum</i>	157
7.2.2 Copper and zinc ligands from <i>P. sativum</i> seedlings grown in media with and without added iron-EDDHA	157
7.2.3 Revised protocol for the isolation of ligands from <i>P. sativum</i> seedlings	158
7.2.4 Purification of a putative copper ligand by thiol affinity chromatography	159
7.2.5 Copper and zinc ligands from the leaves of <i>P. sativum</i> seedlings	159
7.2.6 <i>In vivo</i> labelling of plant material with [³⁵ S] SO ₄	160
7.2.7 Labelling of the recombinant <i>PsMT_A</i> peptide with [³⁵ S] cysteine and spiking of a crude extract from <i>P. sativum</i> roots	161
7.2.8 Electrophoresis of pea root extracts labelled with [³⁵ S] cysteine	161
7.2.8.1 Carboxymethylation of proteins	162
7.3 Results and discussion	162
7.3.1 Basic ligand isolation procedure	162
7.3.2 Copper and zinc ligands from peas grown with and without added exogenous iron	162
7.3.3 Extraction of copper and zinc ligands from <i>P. sativum</i> seedlings, grown with and without added iron, using the revised protocol (7.2.3)	169
7.3.4 Identification of a high apparent molecular weight copper species and purification of the putative copper ligand by thiol affinity chromatography	175
7.3.5 Copper and zinc ligands from the leaves of <i>P. sativum</i> seedlings	180
7.3.6 Extraction of ligands from pea roots labelled with [³⁵ S] SO ₄	180
7.3.7 Copper and zinc ligands in roots <i>P. sativum</i> seedlings grown in media without added copper and zinc	186
7.3.8 Chromatographic properties of <i>PsMT_A</i>	193
7.3.9 Polyacrylamide gel electrophoresis of root extracts from <i>P. sativum</i>	195
7.3.9.1 One dimensional polyacrylamide gel electrophoresis of pea root extracts labelled with [³⁵ S] cysteine	195
7.3.9.2 One dimensional electrophoresis of pea root extracts labelled with [³⁵ S] methionine	197
7.3.9.3 Two dimensional electrophoresis of [³⁵ S] cysteine labelled protein	202
7.4 Conclusions	208
<u>CHAPTER 8 - GENERAL DISCUSSION</u>	212
8.1 Plant metallothionein-like genes	213
8.2 Characterisation of the products of the <i>PsMT_A</i> and <i>AtMT-t2</i> genes	217
8.3 The regulation of expression of <i>PsMT_A</i> in response to trace metals	219

8.4 Copper and zinc ligands in <i>P. sativum</i>	225
8.5 Evidence for the PsMT_A protein in crude root extracts	228
8.6 Concluding remarks	228
8.7 Future work	230
8.7.1 Isolation of the translational products of plant metallothionein-like genes from plant tissue	230
8.7.2 Structural characterisation of the plant metallothionein-like gene translational products	231
8.7.3 Structure / function relationships between the different categories of plant metallothionein-like gene products	231
8.7.4 Control of expression of plant metallothionein-like genes	232
<u>BIBLIOGRAPHY</u>	233

LIST OF FIGURES

1.1 A simplified schematic diagram demonstrating how the chelation of metal by metallothionein could reduce it's own expression	7
1.2 Co-ordination of cysteines to cadmium in cadmium(7)-metallothionein	11
1.3 Summary of components involved in trace metal metabolism in <i>S. cerevisiae</i>	26
3.1 Schematic diagram showing the arrangement of cysteine residues and interdomain regions in the different categories of plant metallothionein-like gene products	74
3.2 Amino acid sequence alignment of the known plant metallothionein-like gene products	78
3.3 Phylogenetic tree for the type-1 and type-2 plant metallothionein-like proteins	80
3.4 Conservation of primary structure in the type-1 and type-2 plant metallothionein-like proteins	81
3.5 Secondary structure prediction for the PsMT _A predicted amino acid sequence	83
3.6 Secondary structure prediction for all the type-1 and type-2 plant metallothionein-like proteins	84
4.1 Polyacrylamide gel electrophoresis of crude cell extracts and purified protein obtained from <i>E. coli</i> containing the pGEX3X and pGPMT3 plasmids	95
4.2 Polyacrylamide gel electrophoresis of the purified GST-PsMT _A fusion protein showing the susceptibility of the protein to proteolysis	96
4.3 Calibration curve for molecular weight markers in figure 4.2	97
4.4 Gel filtration chromatography of factor Xa enzyme and cleavage products eluted from glutathione Sepharose matrix	98
4.5 a Nucleotide sequence and translation of the GST to PsMT _A linking region in the pGPMT3 plasmid	99
4.5 b Primary structure of the PsMT _A gene product	99
4.6 Polyacrylamide gel electrophoresis of the purified GST-PsMT _A fusion protein before and after concentration by acetone precipitation	100
4.7 Western blot of recombinant PsMT _A protein probed with anti GST-PsMT _A immune serum	103

4.8 Dot blot of PsMT _A samples probed with anti GST-PsMT _A immune serum.....	105
4.9 ELISA of BSA, GST-PsMT _A and PsMT _A probed with anti-Cd ₆ -PsMT _A and anti-GST-PsMT _A immune sera	106
5.1 AtMT-t2 primer design	115
5.2 Diagnostic PCR of <i>P. sativum</i> and <i>A. thaliana</i> DNA samples with primers homologous to the metallothionein-like gene coding sequences.....	119
5.3 Nucleotide sequence of insertion into pGEX3X from clone pJWNR1.1	120
5.4 Genomic analysis of <i>A. thaliana</i> and <i>P. sativum</i> DNA	121
5.5 Polyacrylamide gel confirming the production of the GST-AtMT-t2 fusion protein in <i>E. coli</i>	122
5.6 Gel filtration chromatography of the eluent from affinity matrix bound GST-AtMT-t2 fusion protein following cleavage with factor Xa	122
5.7 Proton dissociation curves for PsMT _A and AtMT-t2 GST fusion proteins.....	127
5.8 Growth curves for <i>Synechococcus</i> (R2-PIM8) cells expressing <i>AtMT-t2</i> and control cultures (data courtesy of Dr. J.S. Turner)	128
6.1A Northern analysis of RNA extracted from <i>P. sativum</i> roots from plants grown in media containing a range of copper concentrations (with zinc)	141
6.1B Northern analysis of RNA extracted from <i>P. sativum</i> roots from plants grown in media containing a range of copper concentrations (without zinc)	142
6.1C Northern analysis of the effect of growth in low copper media.....	143
6.2A Northern analysis of RNA extracted from <i>P. sativum</i> roots from plants grown in media containing a range of iron concentrations (with and without 0.5 μM CuSO ₄).....	144
6.2B Northern analysis of RNA extracted from <i>P. sativum</i> roots from plants grown in media containing a range of iron concentrations (with and without 1.0 μM CuSO ₄).....	145
6.3A Northern analysis of RNA extracted from <i>P. sativum</i> roots from plants grown in media containing a range of zinc concentrations	146
6.3B Northern analysis of RNA extracted from <i>P. sativum</i> roots from plants grown in media containing a range of zinc concentrations	147
6.4 Northern analysis of RNA extracted from <i>P. sativum</i> roots from plants over a range of times following the final solution change, experiment 1	151
6.5 Northern analysis of RNA extracted from <i>P. sativum</i> roots from plants over a range of times following the final solution change, experiment 2	152, 153
7.1 Ion exchange chromatography of an extract from roots of <i>P. sativum</i> seedlings.....	165
7.2 a., b. Ion exchange chromatography of an extract from roots of <i>P. sativum</i> seedlings (supplemented and not supplemented with iron)	166
7.2 c., d. Gel filtration chromatography of representative metal containing fractions from Zn-1 / Cu-1 peaks figures 7.2a and b	167
7.2 e. Gel filtration chromatography of representative metal containing fractions from peak Zn-2 figure 7.2a.....	168
7.3 a., b. Ion exchange chromatography of an extract from roots of <i>P. sativum</i> seedlings (supplemented and not supplemented with iron)	171
7.3 c. Gel filtration chromatography of representative metal containing fractions from peak Zn-1 figure 7.3a.....	172
7.4 a., b. Ion exchange chromatography of an extract from roots of <i>P. sativum</i> seedlings (supplemented and not supplemented with iron).....	173

7.4 c. Gel filtration chromatography of representative metal containing fractions from peak Zn-1 figure 7.4a	174
7.5 a., b. Ion exchange chromatography of an extract from roots of <i>P. sativum</i> seedlings (supplemented and not supplemented with iron)	177
7.5 c., d. Gel filtration chromatography of representative metal containing fractions from Cu-1 peaks figure 7.5a and b	178
7.5 e. Gel filtration chromatography of representative metal containing fractions from peak Zn-1 / Cu-2 figure 7.2a	179
7.6 a. Ion exchange chromatography of an extract from leaves of <i>P. sativum</i> seedlings.....	182
7.6 b., c. Gel filtration chromatography of representative metal containing fractions from peaks Cu-1 and Zn-1 figure 7.6a	183
7.7 a. Ion exchange chromatography of a [³⁵ S] labelled extract from roots of <i>P. sativum</i> seedlings.....	184
7.7 b., c. Gel filtration chromatography of representative [³⁵ S] containing fractions from figure 7.7a	185
7.8 a., b. Ion exchange chromatography of an extract from roots of <i>P. sativum</i> seedlings (supplemented and not supplemented with iron, not supplemented with copper and zinc) ..	189
7.8 c., d. Gel filtration chromatography of representative metal containing fractions from peak Zn-1 / Cu-1 figure 7.8a and 7.8b.....	190
7.9 a., b. Ion exchange chromatography of an extract from roots of <i>P. sativum</i> seedlings (supplemented and not supplemented with iron, not supplemented with copper and zinc) ..	191
7.9 c., d. Gel filtration chromatography of representative metal containing fractions from peak Zn-1 / Cu-1 figure 7.9a and 7.9b.....	192
7.10 a. Ion exchange chromatography of root extract spiked with labelled PsMT _A	194
7.10 b. Gel filtration chromatography of representative fractions from peak P-1 figure 7.10a	195
7.11 One dimensional electrophoresis of [³⁵ S] cysteine labelled crude pea extract.....	198
7.12 Molecular weight calibration curve for figure 7.11.....	199
7.13 Northern analysis of root extract identical to that used in figure 7.11	200
7.14 One dimensional electrophoresis of [³⁵ S] methionine labelled crude pea extract	201
7.15 a Two dimensional electrophoresis of [³⁵ S] cysteine labelled crude pea extract, Coomassie blue stained membranes.....	204
7.15 b Two dimensional electrophoresis of [³⁵ S] cysteine labelled crude pea extract, autoradiographs.....	205
7.16 a Two dimensional electrophoresis of [³⁵ S] cysteine labelled crude pea extract, Coomassie blue stained membranes.....	206
7.16 b Two dimensional electrophoresis of [³⁵ S] cysteine labelled crude pea extract, autoradiographs.....	207

LIST OF TABLES

3.1 Summary of published information on plant metallothionein-like genes.....	75
4.1 Estimated molecular weights of the GST-PsMT _A degradation products in figure 4.2	93
6.1 Hydroponic solution copper concentrations for copper response experiments.....	132
6.2a Hydroponic solution iron concentrations for iron response experiment, figure 6.2A...	133

6.2b Hydroponic solution iron concentrations for iron response experiment, figure 6.2B...	133
6.3a Hydroponic solution zinc concentrations for zinc response experiment, figure 6.3A...	134
6.3b Hydroponic solution zinc concentrations for zinc response experiment, figure 6.3B...	134
6.4 Conditions for time course experiment 1	135
6.5 Conditions for time course experiment 2	136
7.1 Yield of each amino acid at each cycle from automated microsequencing of copper species Cu-X figure 7.5c following cleavage with CNBr	176
7.2 Incorporation of [³⁵ S] cysteine into PsMT _A protein	193
7.3 Incorporation of [³⁵ S] cysteine into non iron supplemented and iron supplemented root extract.....	196
7.4 Incorporation of [³⁵ S] methionine into non iron supplemented and iron supplemented root extract.....	197
7.5 Incorporation of [³⁵ S] cysteine into non iron supplemented and iron supplemented root extract.....	202
7.6 Summary of estimated metal contents of chromatogram peaks following ion exchange chromatography of root extracts from seedlings of <i>P. sativum</i>	209

CHAPTER 1

INTRODUCTION

1.1 Overview of the introductory chapter

In general transition metal ions are represented in biological systems only in trace amounts. Some are essential components of these systems whilst others have no known biological function. Supraoptimal concentrations of metal are toxic. Homoeostatic mechanisms have evolved to regulate the intracellular concentration of available metals. Such mechanisms may scavenge essential metals or detoxify excess metal. *

The trace metals considered in detail in this thesis are copper and zinc. Before reviewing the molecular mechanisms involved in their regulation some aspects of their biological chemistry will be briefly discussed in sections 1.2.1 and 1.2.3. During the development of this project the importance of iron uptake and regulation in the metabolism of copper became apparent and therefore some aspects of the biological chemistry of iron will also be discussed in section 1.2.2.

A class of protein which has been implicated in the regulation of copper and zinc in many organisms is metallothionein. Before dealing with the regulation of metals in plants specifically some of the available knowledge concerning the structure and function of metallothionein in other organisms and how it relates to trace metal regulation and tolerance will be discussed in section 1.3. Specifically the structural studies which have been reported on mammalian metallothionein (sections 1.4), and the regulation of iron and copper metabolism in yeast will be reviewed (section 1.5). Although molecular mechanisms vary between different classes of organisms there are often broad similarities and this may be true for metallothionein which may be common to all species. Before the identification of genes encoding predicted metallothionein-like proteins in higher plants (de Miranda *et al.* 1990, Evans *et al.* 1990) it was thought that the analogues of metallothionein in plants were non gene encoded peptides based on glutathione, phytochelatin. Phytochelatins will be reviewed in section 1.6.

The importance of the interrelation of iron and copper metabolism in yeast will be discussed in section 1.5.3, the mechanisms involved in iron accumulation in higher plants will be reviewed in section 1.7. In section 1.8 methods employed in the isolation of low molecular weight metal binding compounds in higher plants will be reviewed. In section 1.9

the reported information relating to gene encoded metallothionein in higher plants, essentially that available at this start of this project, the E_c protein from *Triticum aestivum*, and genes encoding metallothionein-like proteins from *Pisum sativum* (Evans *et al.* 1990) and *Mimulus guttatus* (de Miranda *et al.* 1990), will be reviewed. Specifically the E_c protein and the metallothionein-like gene from *Pisum sativum* will be discussed in detail. In the introduction to chapter 3 there will be a more comprehensive review of the plant metallothionein-like genes reported from other species.

1.2 A general introduction to trace metals in biological systems

The transition metals which are considered essential for all organisms are boron, cobalt, copper, iron, zinc, manganese, molybdenum, and nickel (da Silva and Williams 1991). In addition to these metals da Silva and Williams state that there are trace metals which may not be generally required but may be essential in certain species or that the data concerning their biological role may be ambiguous or incomplete, these include; aluminium, arsenic, chromium, tin and vanadium. Non essential trace metals have no known biological function but some, for example cadmium and mercury can be highly toxic.

1.2.1 Copper

In aqueous solution at physiological pH copper can be either a divalent or monovalent ion enabling it to take part in redox and free radical reactions and it is often associated with oxidative enzymes especially in the extracellular matrix (da Silva and Williams, 1991). When bound to organic molecules divalent copper often assumes tetragonal co-ordination geometry whilst monovalent copper often assumes tetrahedral co-ordination (da Silva and Williams 1991). In biological systems the common ligands of copper are the nitrogen of amine groups or the sulphur of thiolate groups, although divalent copper ions can form a bond with the nitrogen of the peptide group and monovalent copper ions can bind O₂ and CO₂ (summarised in da Silva and Williams 1991). Copper toxicity arises due to unfavourable interactions with nucleic acids, alterations of enzyme active sites and oxidation of membrane components (Cervantes and Gutierrez-Corona, 1994). It is proposed that at high intracellular concentrations copper may be involved in the generation of free radicals by a metal catalysed Fenton-like reaction in actively respiring cells $\{Cu^+ + H_2O_2 \rightarrow Cu^{2+} + \bullet OH + OH^-\}$ (Halliwell and Gutteridge 1984). DNA cleavage by the hydroxyl free radical occurs by abstraction of a

hydrogen atom from the deoxyribose backbone (Hertzberg and Dervan 1984). Free radicals can also attack proteins and lipids (cited in Tamai *et al.* 1993).

1.2.2 Iron

Iron is also found in more than one ionic state, ferric iron (Fe^{3+}) or ferrous iron (Fe^{2+}). In the presence of water and oxygen iron forms insoluble ferric iron hydroxide complexes, this has important consequences for iron availability and uptake in oxygenated environments. Upon entering the cytoplasm iron is transported to a host of enzymes and proteins with a wide spectrum of activities or is stored as ferric iron in ferritin (Theil, 1987). As a co-factor in many non-haem iron proteins, predominantly the iron-sulphur proteins, eg. ferredoxin, iron has a redox role in electron transfer systems and assumes tetrahedral co-ordination geometry (da Silva and Williams 1991). Whereas iron is found with octahedral co-ordination geometry in other enzymes which have a range of functions, eg. iron superoxide dismutase and a host of oxidative and reductive enzymes.

In a large number of proteins and enzymes, iron is associated with the polypeptide via the haem group, a porphyrin ring at the centre of which is a ferrous iron ion (described in da Silva and Williams 1991). Iron in haem does not dissociate and is therefore a distinct species from free iron in the cell.

1.2.3 Zinc

The divalent ionic state of zinc is highly stable and zinc is inert to oxireduction (da Silva and Williams 1991). Tetrahedral co-ordination geometry is common although the co-ordination sphere of zinc is highly flexible. This flexibility and zinc's amphoteric nature at neutral pH makes it suitable for a wide variety of ligand types with a broad range of stability constants, reactivities and functions. Common biological ligands of zinc are the nitrogen of amine groups, the sulphur of thiolate groups and the oxygen of carboxylate groups (da Silva and Williams 1991).

Zinc is known to have roles in catalysis, gene expression, stabilisation of protein and nucleic acid structure, preservation of the integrity of subcellular organelles, participation in transport processes and it plays important roles in viral and immune phenomena (Vallee and Auld, 1990). In their review in 1990, Vallee and Auld report that zinc has been identified as a component of as many as 300 different enzymes across all species and phyla. Crystal

structures are available for many zinc containing proteins and are found to be of two types (Vallee and Auld, 1993). Where zinc is involved in a catalytic site it is co-ordinated to three amino acids (generally His, Glu, Asp or Cys) of the polypeptide chain and the oxygen of an activated water molecule. When zinc plays a structural role affecting local protein conformation and stability the four ligands are amino acid residues, often cysteine or histidine.

1.2.4 A brief comment on non-essential trace metals


Non-essential trace elements are important in biological systems because of their potential toxic effects and are often associated with industrial pollution. For example mercury and lead are associated with damage to the central nervous system in humans (da Silva and Williams 1991). In terms of the study of molecular toxicology an important element is cadmium. Cadmium toxicity arises because it resembles zinc in its chemistry, in fact the name cadmium is derived from 'cadmia' an old name for zinc ore. In general, compared to zinc, cadmium forms weaker bonds with oxygen groups and stronger bonds with sulphhydryl groups (da Silva and Williams 1991). Cadmium may substitute for zinc in binding sites in proteins and cause the inactivation of a large number of enzymes which require zinc for activity (Vallee and Ulmer 1972).


1.3 Metallothionein

1.3.1 General introduction to metallothioneins

In 1957 a protein was isolated from equine renal cortex which contained a high proportion of cadmium and zinc (Margoshes and Vallee, 1957). In addition to a high metal content the protein had a high cysteine content and was termed metallothionein (MT). Proteins and polypeptides showing broad structural homology to equine metallothionein have been isolated from a diverse range of animals and micro-organisms, principally fungi (reviewed in Hamer, 1986). The salient features of metallothionein is its small size (equine metallothionein has only 60 amino acids) and a high cysteine content (as high as 33 %) arranged in characteristic Cys-Xaa-Cys motifs (Kägi and Schäffer 1988). Structural studies, for example proton NMR (Vašák *et al.* 1980), of mammalian metallothionein have demonstrated that metal ions (copper, cadmium and zinc) are bound to the metallothionein via thiol bonds with the sulphur of the cysteine.

1.3.2 Occurrence of metallothionein

Any polypeptides meeting the criterion of small, cysteine rich, metal binding polypeptides are often termed metallothioneins irrespective if functional homology has been demonstrated (Hamer 1986). In an attempt to classify metallothioneins from other organisms on the basis of their structural characteristics, those with a pattern of cysteine residues resembling equine metallothionein were described as class-I metallothionein, whilst structurally divergent and biosynthetic peptides were grouped into class-II and class-III metallothionein respectively  (Fowler *et al.* 1987). This nomenclature system, although widely adopted, can lead to confusion as different isoforms of metallothionein from the same organisms are often described as MT-I, MT-II etc. (Hamer 1986).

Metallothioneins from non-mammalian sources which are sufficiently homologous to equine renal MT to be designated class-I have been found in many species, for example *Neurospora crassa* (Lerch 1980), *Drosophila melanogaster* (Maroni *et al.* 1986), *Agaricus bisporus* (Munger and Lerch 1985) and *Scylla serrata* (Otvos *et al.* 1982). Genes occur in higher plants which encode putative translational products with regions possessing some sequence similarity to class-I metallothionein, for example in the garden pea, *Pisum sativum* (Evans *et al.* 1990) and the flowering plant *Mimulus guttatus* (de Miranda *et al.* 1990) and  many more (refer to section 3.1.1).

Class-II metallothioneins have been isolated from a variety of sources, for example the yeast *Saccharomyces cerevisiae* (Winge *et al.*, 1985), in cyanobacteria for example *Synechococcus* TX-20 (Olafson, 1979), and in higher plants, for example the wheat Ec protein (Lane *et al.*, 1987).

At present class-III metallothioneins have been found in plants, algae and some fungi but to date this class has not been reported from animal sources. For example in the yeast *Schizosaccharomyces pombe* (Murasagi *et al.* 1981) and *Candida glabrata* (Mehra *et al.* 1988), many algae including *Chlorella fusca* (Gekeler *et al.* 1988) and *Euglena gracillus* (Shaw *et al.* 1989), and is ubiquitous in higher plants for example *Datura innoxia* (Jackson *et al.* 1987) and *Zea mays* (Leblova *et al.* 1986). Class-III metallothioneins have been variously referred to as, cadystin (Kondo *et al.* 1985), phytochelatin (Grill *et al.* 1985), and poly (γ -glutamylcysteinyl)glycine (Robinson and Jackson 1986) amongst others.

1.3.3 Function of metallothionein

1.3.3.1 Metal ion homoeostasis

Non metal induced calf liver metallothionein can be isolated as zinc(4)copper(3)-thionein (Briggs and Armitage, 1982). It has been demonstrated *in vitro* that metal bound to metallothionein could be used in subsequent cellular functions such as the formation of metalloenzymes. For example equine MT-1a donates zinc to bovine apocarbonic anhydrase (Li *et al.* 1980). The inactive, apo form of dopamine β -monoxygenase can be activated by the addition of copper from copper-thionein and conversely the holoenzyme can be inactivated by removal of copper by apo-thionein (Markossian *et al.* 1988). Apo-metallothionein has been shown *in vitro* to modulate DNA binding in the zinc finger transcription factors TFIIIA and Sp1 resulting in transcription inactivation (Zeng *et al.* 1991a, Zeng *et al.* 1991b). However it remains to be established whether or not metallothionein can donate metal ions to metallo-proteins *in vivo*.

Metallothionein can chelate excess free copper and zinc ions in the cell, the reduction of which may lead to the down regulation of metallothionein synthesis (Wright *et al.* 1988, Richards 1989). If metal levels are low there will be no activation of metal responsive transcription factors. Conversely if the influx of copper and zinc overwhelms the existing thionein pool then these metals can interact with other cell components including the *trans*-acting factors influencing metallothionein production leading to the synthesis of more

metallothionein which in turn would chelate the excess metal and thus reduce the stimulus for its own production (Richards, 1989), see figure 1.

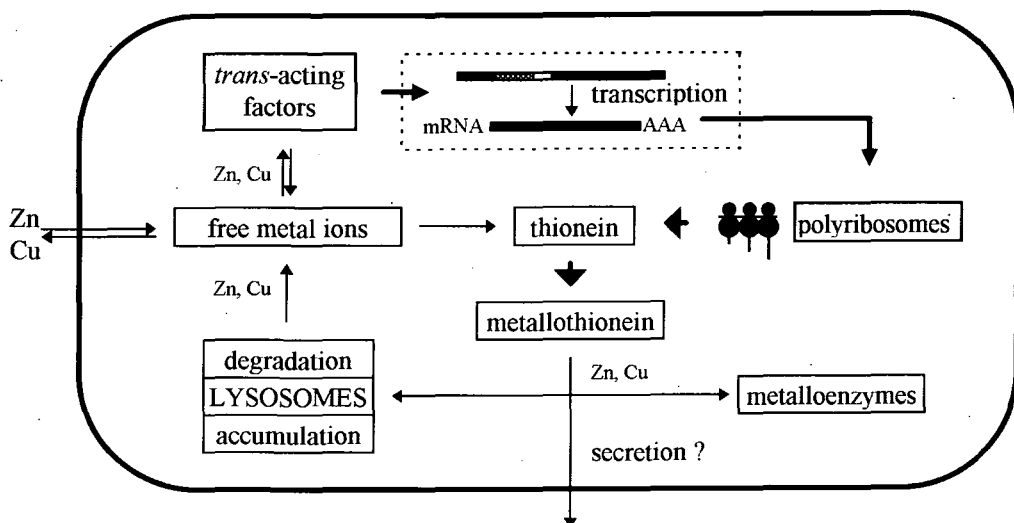


Figure 1.1 A simplified schematic diagram demonstrating how the chelation of metal by metallothionein could reduce its own expression (adapted from Richards, 1989).

In the yeast *Saccharomyces cerevisiae*, in cells in which the metallothionein gene (*CUP1*) has been deleted, a reporter gene construct of the *CUP1* promoter fused to the *E. coli* galactokinase gene (*galk*) show high constitutive expression, even in low copper levels (Hamer *et al.* 1985). Expression can be repressed (effectively reduced to wild type levels) by introducing the *CUP1* gene back into the cell (Wright *et al.* 1987). The repression of the reporter gene construct also occurs when monkey metallothionein is introduced into the yeast cells (Hamer 1986). The different structures of monkey and yeast metallothionein make it improbable that the mammalian metallothionein would bind to the yeast promoter element. Furthermore, by introducing genes coding for various truncations of *CUP1* and modifications in which normal metal binding is altered by specific changes to cysteine codons, the reduction of repression was shown to be related solely to the ability of the metallothionein to chelate copper (Wright *et al.* 1988).

1.3.3.2 Metal Tolerance

Metal tolerance has been linked to metallothionein in a number of organisms. For example, in mammals it has been demonstrated that chronic exposure to high levels of copper and zinc leads to accumulation of copper- and zinc-metallothionein (summarised in Richards, 1989). In cultured mammalian cell lines, increased sensitivity has been shown to cadmium if metallothionein production is blocked whereas cadmium resistant strains overproduce metallothionein as a result of gene amplification (Crawford *et al.* 1985). Targeted disruption leading to the inactivation of the the metallothionein I and II genes in mice, although not effecting viability or reproduction under laboratory conditions, increases susceptibility to hepatic poisoning by cadmium (Masters *et al.* 1994). Induction of metallothionein by cadmium in mammalian cells is well established and has been exploited in the preparation of the protein for structural studies (for example, Vařák *et al.* 1985). In plants, algae, and some fungi resistance to cadmium and elevated copper concentrations is achieved by a biosynthetic peptide analogue of metallothionein with the structure $(\gamma\text{-EC})_n\text{G}$ (Jackson *et al.* 1986, Gekeler *et al.* 1988 and Kneer *et al.* 1992). In the cyanobacteria, *Synechococcus* PCC 6301, amplification (Gupta *et al.* 1992) and specific rearrangement (Gupta *et al.* 1993) of the metallothionein locus, *smt*, was shown to occur in cells selected for growth in elevated concentrations of cadmium.

In a number of cases it has been demonstrated that metallothionein is not essential for growth on non metal supplemented media. For example, deletion of the metallothionein locus from *Synechococcus* PCC 7942 creates sensitivity to zinc and cadmium but otherwise cells grow normally (Turner *et al.* 1993). Mice homozygous for a disruption preventing translation of the MT-1 and MT-II isoforms are reported to be viable and to grow and reproduce normally, they were however sensitive to cadmium poisoning compared with the wild type (Masters *et al.* 1994). Similarly *cup1* Δ mutants in *Sacchchromyces cerevisiae* are hypersensitive to copper poisoning (Hamer *et al.* 1985). The *cup1* Δ yeast mutants were reported to be “fully competent at mating, diplophase growth, sporulation, and germination. They [*cup1* Δ yeast mutants] also accumulate normal levels of total cell copper and of the copper-dependent form of superoxide dismutase” (Hamer, 1986). The implication therefore is that metallothionein does not play an essential role in “normal” cell metabolism in

laboratory conditions but is required for a detoxification function when cells are challenged with elevated trace metal concentrations.

1.3.3.3 Other potential metallothionein functions

Other potential functions for metallothionein have been suggested. A role in transport has been postulated and metallothionein has been identified in extracellular fluid such as urine, plasma and bile (Bremner 1987). Relatively large amounts of zinc and copper metallothionein are found in human foetal liver leading to speculation that metallothionein plays an important role in controlling copper and zinc levels during development (Riordan and Richards 1980). A twenty fold increase is observed in the concentration of metallothionein in neonatal compared to mature rat liver (Kern *et al.* 1981). The E_c protein in wheat is involved in zinc metabolism during embryogenesis (Kawashima *et al.* 1992).

1.4 The structure and function of mammalian metallothionein

1.4.1 Introduction

The structure of mammalian metallothionein has been intensely studied (reviewed in following sections). Mammalian metallothionein therefore serves as a model system when considering the structure / function relationships in this class of protein. Mammalian metallothionein consists of 60 or 61 amino acids and has 20 cysteines arranged predominantly in Cys-Xaa-Cys, or Cys-Cys motifs (Kägi and Schäffer 1988). The non cysteinyl residue is often lysine, serine or threonine and mammalian metallothionein has no aromatic or histidine residues. The positions of the cysteines are highly conserved in animals as is the amino-terminal sequence AcMet-Asp-Pro-Asn. It is usually found to bind up to 7 divalent or 11 to 12 monovalent ions (Hamer 1986).

Purification of mammalian metallothionein by ion exchange chromatography and analysis by HPLC and electrophoresis has led to the isolation of more than one structural isoform of metallothionein (for example Vašák *et al.* 1985). These isoforms differ slightly in their primary structure but NMR studies show that they have the same, or very similar tertiary structures (Nielson and Winge, 1983 and Winge and Miklossy, 1982). Other mass isoforms observed by various chromatographic techniques may reflect different metal contents and have been referred to as metalloforms (cited in Richards 1988).

Induction of metallothionein expression has been demonstrated in response to a wide range of factors in animals (Kägi 1992). These include the ionic species of the trace metals, cadmium, copper, zinc, mercury, silver, gold, cobalt, nickel, and bismuth, hormones and second messengers for example glucorticoids and cAMP, inflammatory agents and cytokines, tumour promoters and oncogenes, and vitamins for example ascorbic acid.

1.4.2 Methods employed in structural studies of metallothionein

A wide range of biophysical techniques have been employed in the determination of metallothionein structure. These include UV and Raman spectroscopy (for example Willner *et al.* 1987, Elgrin and Wilcox, 1989), ESR (for example Vašák and Kägi, 1981), proton NMR (for example Vašák *et al.* 1980) and [¹¹³Cd] NMR (for example Otvos and Armitage, 1980), circular dichroism (for example Rupp and West, 1987). Metallothionein has been shown to have a characteristic Raman band at $138 \pm 2 \text{ cm}^{-1}$ (Elgren and Wilcox, 1989). To study the importance of the cysteine residues to metal co-ordination, techniques such as single amino acid substitutions have been employed (Cismowski and Huang, 1991 and Chernaik and Huang, 1991). There is a full X-ray diffraction crystallographic determination available for rat metallothionein at 2.0 Å resolution (Robbins *et al.* 1991).

Metallothionein induction by subcutaneous injections of cadmium salts has become a standard method leading to recovery of quantities cadmium(5)zinc(2)-thionein, which can be further processed to give the spectroscopically homogeneous cadmium(7)-thionein (Vašák *et al.* 1985). The binding characteristics of zinc and cadmium are very similar and spectroscopic studies indicate that they induce similar, but not quite identical, tertiary structures in metallothionein, the differences arising from the different ionic radii of the two ions (Vašák *et al.* 1980). When applying spectroscopic methods cadmium metallothionein has some distinct advantages over copper or zinc species. The nucleus of the isotope [¹¹³Cd] has spin ½ and therefore a nuclear magnetic moment giving rise to a clear NMR signal (Otvos and Armitage 1980). The UV absorption envelope of cadmium is centred around 245-250 nm and differential CD effects can be seen at 248 nm (Willner *et al.* 1987).

1.4.3 Basic structural characteristics

Apometallothionein is a random chain in aqueous solution (Otvos and Armitage, 1980). When metal ions bind to metallothionein the protein forms two domains joined by a short

flexible linker region (Briggs and Armitage 1982). The different structural characteristics of the two domains are thought to account for their different metal binding characteristics (Bremner and Mehra, 1983 and Nielson and Winge, 1984). It has been demonstrated by NMR spectroscopy that the amino terminal or β domain can bind three divalent cadmium (or zinc) ions whilst the carboxyl terminal or α domain can bind up to four divalent cadmium (or zinc) ions (Dalgarno and Armitage, 1984). The divalent ions have tetrahedral co-ordination geometry and all four ligands are thiol bound cysteines. The overall shape of divalent metal metallothionein is ellipsoidal (Robbins *et al.* 1991). Each domain can bind up to six monovalent metal ions when reconstituted with copper (Nielson and Winge 1984). The structure of copper metallothionein has not been reported.

In the crystal structure of cadmium(5)zinc(2)-thionein each domain has a solvent exposed cleft with three cysteine residues at the base (Robbins *et al.* 1991). The sulphur atoms can make hydrogen bonds with water molecules in the cleft. Sulphur atoms also make hydrogen bonds with peptide amide groups and other side chains but a characteristic of metallothionein is that there are no di-sulphide bridges. The seven Cys-Xaa-Cys motifs have very similar conformations which mimic a type I reverse turn. The four Cys-Yaa-Yaa-Cys motifs form a typical type I reverse turn even when one of the Yaa residues is a cysteine. The Cys-Xaa-Xaa-Cys motifs observed in iron-sulphur proteins have a similar conformation (Adman *et al.* 1975).

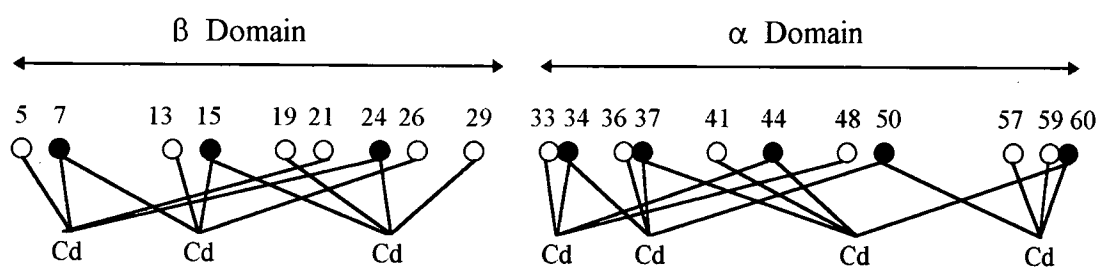


Figure 1.2 Co-ordination of cysteines to cadmium in the α and β domains of mammalian (Cd_7)-MT. Closed circles represent terminal cysteines and filled circles represent bridging cysteines. (Adapted from Chernaik and Huang, 1991).

There are two distinct types of cysteine to metal ion configurations (Chernaik and Huang 1991). Bridging cysteines form two thiolate bonds to the divalent metal ions and terminal cysteines form only one thiolate bond. In the α domain (formed from residues 33 to 61) there are 11 cysteines, five are bridging ligands to the divalent metal ion and six are terminal ligands. In the β domain (formed from residues 1 to 29) there are 9 cysteines, only three bridging ligands and six are terminal ligands, figure 2. This arrangement may account for the different metal binding characteristics of the two domains.

1.4.4 Metal ion binding properties of the metallothionein domains

The binding of metal ions to apometallothionein is site selective. Titration of apometallothionein with cadmium or zinc leads initially to co-operative formation of the α domain, similarly when EDTA was used to remove metal from the protein the β domain cadmium ions were the first to be removed (Nielson and Winge, 1983, Stillman and Zelazowski, 1988). When apometallothionein is titrated with copper the β domain is the site of initial binding (Nielson and Winge, 1984). Robbins *et al.* (1991), postulate that the first two cadmium ions bind to the Cys-Xaa-Cys-Cys motifs at either ends of the domain (residues 34 to 37 and 57 to 60 respectively). This would induce the folding of the domain creating a favourable conformation for the binding of the remaining two cadmium ions. The two domains fold independently (Winge and Miklossy 1982).

Various spectroscopic studies have suggested that metal ions in metallothionein are labile (for example NMR, Vařák *et al.* 1985, CD, Stillman and Zelazowski 1988 and UV Johnson and Armitage 1987). Furthermore, it has been demonstrated that divalent metal ions in the β domain are more likely to undergo metal exchange (Otvos *et al.* 1985). Zinc occupies the two highly labile sites in cadmium(5)zinc(2)-thionein (Robbins *et al.* 1991). Single amino acid substitution experiments in which individual cysteines were targeted and replaced with serine (Chernaik and Huang, 1991) or tyrosine (Cismowski and Huang, 1991) demonstrate that the lower the proportion of bridging cysteines in the metal cluster the more labile the metal ions will be. By measuring the growth characteristics of *cup1* Δ yeast mutants in which different Chinese hamster metallothionein constructs were introduced Huang and colleagues were able to identify the importance of individual cysteines to metal tolerance. It was found that changes in the β domain in which metal ions are labile in the native protein

had little effect on cadmium tolerance. Substitutions in the α domain, making the metal ions more labile reduced the effectiveness of the metallothionein to detoxify cadmium.

1.4.5 The inter-domain region

Residues 30 to 32 (Lys-Lys-Ser) form a “hinge” or “linker” region between the two domains (Robbins *et al.* 1991). In their solution of the crystal structure for cadmium(5)zinc(2)-thionein Robbins *et al.* (1991) predict a single hydrogen bond between the side chain of residue 31 in the “hinge” to the β domain. The sequence Cys-Xaa-Cys-Xaa-Xaa-Xaa-Cys-Xaa-Cys incorporating this “hinge” region is highly conserved (Nemer *et al.* 1995). Oddly, although highly conserved the length of this region does not appear to be functionally important. Insertion of up to twelve or sixteen amino acid residues into the “hinge” region was found to have no significant effect on metallothionein activity *in vivo* (Rhee *et al.* 1991). Replacement of the two highly conserved lysines in the hinge region with positively or negatively charged amino acids had no effect on metallothionein activity (Cody and Huang, 1993). An unexplained reduction in metallothionein accumulation was observed if both lysines were replaced with neutral amino acids.

1.4.6 Dimerisation

Aggregation of metallothionein has been observed with high concentrations of copper (Riordan and Richards 1980, Bremner and Mehra 1982 and Nielson and Winge 1982). It has been suggested that metal exchange may occur via direct intramolecular contacts (Robbins *et al.* 1991). This is supported by the observation that crystal packing of metallothionein contains pairs of molecules related by a two fold axis. The exposure of monomeric cadmium(7)-thionein to increased cadmium concentration in the presence of inorganic phosphate leads to the formation of the dimer (cadmium(9)-thionein)₂ (Palumaa and Vašák, 1992). Inorganic phosphate is an extra cadmium ligand.

1.4.7 Alternative metallothionein conformations

Vašák *et al.* 1985, noted that the [¹¹³Cd] NMR studies suggest that metallothionein does not possess a unique rigid structure but undergoes a great deal of structural variability and flexibility. Comparison of the various NMR solutions with the crystal structure shows the

greatest difference, and by inference greatest flexibility, in the β domain (Braun *et al.* 1992). Compared to proteins with a highly ordered secondary structure the polypeptide backbone is less well defined. As a consequence of this flexible structure metallothionein is capable of near isomorphous binding of seven mole equivalents of a wide range of divalent metal ions of bismuth, cobalt, lead, iron and mercury (Kägi and Kojima, 1987).

Despite having the same overall structure there is an 18 % difference in cluster volume between the zinc(7) and cadmium(7) forms of metallothionein (Messerle *et al.* 1992). This ability is thought to be a feature of the flexibility of the inter cysteine loops. Pountney and Vašák (1992) report that binding of cobalt to zinc-thionein is site selective. This is believed to occur as the binding of different metal ions of different ionic radii create different local steric strains on the polypeptide chain. However, Ding *et al.* (1994) report that the conformation of the β domain of iron(7)-thionein is different than zinc- or cadmium-thionein. They predict a pseudo planar geometry of the $(\text{Fe}^{2+})_3\text{Cys}_9$ cluster with a normal α domain conformation. A further variation in metallothionein, cadmium(13)(Pi)₂-thionein, has been observed *in vitro* (Palumaa *et al.* 1993). It has different spectroscopic properties than cadmium(7)-thionein and by inference a different structure. Non thiolate cadmium ligands are predicted including the inorganic phosphate.

The most biologically significant variations on metallothionein structure is found with copper containing metallothionein. In Wilson's disease copper accumulates in the intestine as copper(12)-thionein (Pountney *et al.* 1994). Failure to excrete copper into the bile results in copper toxicity leading to, for example, acute liver failure. Metal binding is proposed to occur in two six metal clusters involving both digonal and trigonal co-ordination geometry with cysteine thiolate ligands (Pickering *et al.* 1993). Other forms of copper metallothionein with different co-ordination chemistry have been reported. In reconstitution experiments *in vitro* the binding of fourteen to fifteen monovalent copper ion equivalents has been reported (Zelazowski *et al.* 1989). As with the highly metallated forms of divalent metallothionein this form is thought to involve non thiolate copper ligands (Li and Weser 1992). Recently it has been reported that the stoichiometry of copper metallothionein depends on the cellular location of the metallothionein, copper(8)-thionein was identified in the lysosome and copper(12)-thionein in the cytoplasm (Pountney *et al.* 1994). In the copper(8)-thionein form it is proposed that there are two four metal clusters similar to the clusters found in the

divalent metal metallothionein but with six to eight cysteine side chains which are not involved in metal co-ordination (Pountney *et al.* 1994). In such a structure cysteine residues could be involved in disulphide bridges.

The metal composition of metallothionein *in vivo* is likely to reflect both the cellular metal concentrations and the avidity of metallothionein for different metal ions. In mammalian cells not challenged by elevated trace metal concentrations a heterogenous copper/zinc-thionein has been observed (Richards 1989). However the lack of suitable NMR isotopes for copper and zinc make the study of the structure of this metalloform more difficult than the cadmium containing protein.

1.5 Metallothionein and trace metal ion homeostasis in yeast

1.5.1 Introduction

Trace metal metabolism in yeast may reflect that of higher plants more closely than mammals. In section 1.5.2 the structural properties and regulation of yeast metallothionein will be reviewed. In section 1.5.3 some aspects of the iron and copper regulation which have been reported recently will be reviewed.

1.5.2 Yeast metallothionein

1.5.2.1 Identification of metallothionein in *S. cerevisiae*

Copper resistance in certain strains of yeast was first established in 1951 (Minagawa *et al.* 1951). Classical genetic analysis identified a single chromosomal locus, denoted *CUP1*, responsible for this resistance (Brenes-Pomales *et al.* 1955). Two strains were characterised on whether they were sensitive (*cup1^S*) or resistant (*CUP1^R*) to 300 μ M copper sulphate. Copper resistance is due to amplification of the *CUP1* locus (Fogel *et al.* 1982). In different *CUP1^R* strains there are 2-14 copies of this locus and in *cup1^S* only a single copy of the locus (Fogel *et al.* 1983). Structural characterisation of the locus yielded the gene for a yeast copper metallothionein (also known as copper chelatin or CUP1) and an uncharacterised protein, designated protein X (Karin *et al.* 1984, Butt *et al.* 1984).

1.5.2.2 Structure and properties of CUP1

The predicted product of the copper metallothionein gene from *S. cerevisiae*, CUP1, has 61 amino acids including 12 cysteine residues (Karin *et al.* 1984). Prior to the sequencing of the *CUP1* gene a number of small cysteine rich copper binding proteins had been isolated from copper resistant yeast strains (for example, Prinz and Weser 1975, Premakumar *et al.* 1975 and Kimura *et al.* 1981). Different purification strategies produced proteins with different molecular weights and biochemical properties, but it has been suggested that these represent the same protein at different stages of degradation (Winge *et al.* 1985).

CUP1 is isolated from yeast as a copper rich protein of 53 residues (for example, Winge *et al.* 1985). Amino acid analysis reveals that the initial eight residues of the amino terminus of the predicted primary structure are absent in the purified protein. It is not clear if this represents the functional form of the protein *in vivo* or if the truncated structure is a result of proteolytic cleavage during purification. Genes encoding variations in this region introduced

into *cup1*Δ cell lines suggest that this motif has no determinable biological function (Wright *et al.* 1987). If the codons for residues 2-7 are deleted cells are wild type with respect to copper detoxification and copper inducible transcription. Similarly a gene with a double mutation resulting in substitution of Asn⁶-Phe⁷ with Arg⁶-Ile⁷ introduced on a high copy number plasmid results in phenotypically wild type cells despite the fact that this alteration leads to the recovery of a non truncated protein. The amino terminus of this protein is sensitive to proteolysis *in vitro* and so it is proposed that it does not participate in the tertiary protein fold (Wright *et al.* 1987). The peptide sequence is similar to mitochondrial targeting sequences in yeast, for example in cytochrome *c1* (Sädler *et al.* 1984). There is no evidence, however, that yeast metallothionein is localised in the mitochondria (Wright *et al.* 1987).

There is little sequence conservation between CUP1 and mammalian metallothionein. A common feature however is the high cysteine content (12 out of 61 (53) amino acids) in Cys-Xaa-Cys motifs and the formation of a copper(I)-thiolate cluster (George *et al.* 1988). This cluster is resistant to proteolysis (Weser *et al.* 1986). CUP1 can chelate up to 8 monovalent copper ions (Hartmann *et al.* 1992). It has variously been proposed that the copper-thiolate cluster has trigonal co-ordination geometry (George *et al.* 1988) or that each copper ion is co-ordinated by four cysteine thiolate ligands (Hartmann *et al.* 1992). The ambiguity arises due to the absence of biophysical techniques to directly determine the co-ordination geometry in the absence of a crystal structure. In addition to copper binding it has been demonstrated that CUP1 can bind 8 monovalent silver ions, or 4 divalent cadmium, zinc or cobalt ions (Butt and Ecker 1987). In a cadmium resistant strain of *S. cerevisiae*, designated 301N, *CUP1* expression was found to be inducible by divalent cadmium ions (Inhoue *et al.* 1991). A cadmium metallothionein was isolated from these cells which was shown to be homologous to CUP1 by amino acid analysis and immunoassay. However cadmium resistance in *S. cerevisiae* has been attributed to the *CAD2* gene which is independent of *CUP1* and is not thought to involve metallothionein (Tohoyama 1990). In both *cup1*Δ and wild type cells phytochelatin (see section 1.6) has been identified as a major cadmium binding complex (Kneer *et al.* 1991).

1.5.2.3 Transcriptional regulation of yeast metallothionein expression

Metallothionein gene expression is controlled by *cis*-acting metal regulatory elements (MRE) (Thiele, 1992) and *trans*-acting binding factors (Zhou and Thiele, 1993). The *CUP1* gene is

transcriptionally regulated in response to environmental copper concentrations (Butt and Ecker 1987). A region designated the upstream activation sequence (UAS_{CUP1}) was identified by the ability of a series of 3', 5' and internal deletions of the *CUP1* promoter to drive copper-inducible transcription of a *CUP1* promoter - *E. coli* galactokinase gene fusion introduced into wild-type yeast (Thiele and Hamer 1986). This region, -180 to -105 nucleotides downstream from the transcription start site, was identified as being essential for copper induced transcription. Most nucleotide mutations in the region -142 to -127 render the promoter non responsive to copper (Fürst *et al.* 1988). An increase in the basal level of expression was observed for mutations of nucleotides A-118 and T-122, implying that the *CUP1* gene is under both copper induced transcription and transcriptional repression.

In *cup1* Δ mutants in which the *CUP1* promoter driving a reporter gene has been inserted high levels of expression are observed which can be repressed if either yeast metallothionein or monkey MT are added to chelate copper (Wright *et al.* 1988). Using classical genetics mutants were identified which were unable to regulate *CUP1* expression in response to copper (Thiele *et al.* 1988, Welch *et al.* 1989). A yeast genomic fragment was identified which when introduced into these mutants could restore the copper response. The gene was designated *ACE1* (activation of *CUP1* expression) or *CUP2*.

The heat shock transcription factor (*HSF*) has also been shown to activate the transcription of *CUP1* in the absence of *ACE1* (Silar *et al.* 1991). The product of the *HSF* drives expression from the *CUP1* promoter indicating that biosynthesis of metallothionein is a factor in the heat shock response.

1.5.2.4 ACE1, a metal dependent transcription factor of yeast metallothionein

ACE1 encodes a 225 residue protein with a highly positively charged amino terminal domain (residues 1-105) and a highly negatively charged carboxyl terminal domain (residues 106-225) (Fürst *et al.* 1988). The amino terminal domain contains twelve cysteine residues 11 of which are involved in Cys-Xaa-Cys or Cys-Xaa-Xaa-Cys motifs and so are implemented in copper binding. The *ACE1* protein is activated by the co-operative binding of copper to this domain causing a conformational change (Fürst and Hamer 1989). A copper thiolate cluster is formed containing six monovalent copper ions which renders this domain resistant to proteolysis (Dameron *et al.* 1991). Copper co-ordination leads to the formation of a 'copper fist' structure which binds to the upstream activation sequences of the *CUP1* gene (Buchman

et al. 1990). There are three ACE1 binding sites in the *CUP1* promoter with a consensus binding site consisting of an A-T rich element followed by GCTG core. Differential occupation of these sites suggests that ACE1 may associate with other factors with different affinities for these sites (Huibregtse *et al.* 1989).

The other important component of the function of copper-ACE1 is the interaction with the yeast transcriptional machinery. The TATA element is another essential part of the *CUP1* promoter (Culotta *et al.* 1989). This is the site of binding of the TATA binding protein (TBP). It has been demonstrated with *in vitro* transcription assays that the presence of the TPB alone cannot support copper-ACE1 mediated expression of the *CUP1* promoter attached to a reporter gene construct (Kambadur *et al.* 1990). This implies a multi-component transcription complex. Along with ACE1 and TBP other components, termed co-activators are required to form the copper activated transcription initiation complex (Martin 1991). The acidic carboxyl terminal domain of ACE1 is proposed to participate in the intermolecular interactions leading to the formation of the transcription complex (Zhou and Thiele 1993). This activity has been shown to occur independently of the amino terminal domain and independently of copper (Hu *et al.* 1990). A fusion protein of amino acids 70-225 of ACE1 and the DNA binding domain of GAL4, a galactose utilisation gene transcription factor, specifically stimulates *GALI* transcription.

The copper hypersensitivity of *ace1Δ* mutants can be partially relieved by the presence of multiple copies of a gene *ACE2* (Butler and Thiele 1991). The gene encodes a 770 amino acid protein with similarity to a known yeast transcriptional activator. Expression of *ACE2* in the absence of *ACE1* allows induction of *CUP1* in a copper dependent manner but at lower levels than if *ACE1* was present. *ACE2* is a zinc finger protein and is involved in control of the basal expression of *CUP1* (Butler and Thiele 1991).

1.5.2.5 The metallothionein gene family in *Candida glabrata*

In response to elevated copper the pathogenic yeast *C. glabrata* synthesises a number of metallothioneins. These include the gene products MT-I, MT-II (Mehra *et al.* 1989, 1992) as well as γ -glutamyl peptides (Mehra *et al.* 1988). There are two MT-II genes, MT-IIa and MT-IIb which encode identical protein sequences but differ in the 5' and 3' flanking sequences. MT-I is a 62 amino acid protein, 18 of which are cysteine residues. MT-II is a 57 amino acid protein, 16 of which are cysteine residues. The predominant structural features

are Cys-Xaa-Cys or Cys-Xaa-Xaa-Cys motifs. MT-I and MT-II can bind up to 12 or 10 monovalent copper ions respectively. MT-I and MT-IIb are single copy genes and MT-IIa is present as a multi copy locus (Mehra *et al.* 1992).

Probes made from *ACE1* DNA do not hybridise to *C. glabrata* genomic DNA on Southern blots (Zhou and Thiele, 1993). To identify a metal regulated transcription factor in *C. glabrata* analogous to ACE1 Zhou and Thiele undertook a complementation approach. An *ACE1/CUP1* deficient *S. cerevisiae* mutant was constructed containing the MT-I gene from *C. glabrata* and a gene fusion of the MT-I promoter driving a reporter gene. A genomic library was used to transform these cells and clones selected which could confer copper resistance and expression of the reporter gene. A copper regulated transcription factor was isolated and denoted AMT1 (activator of metallothionein transcription) (Zhou and Thiele 1991). AMT1 is a 265 amino acid protein which like ACE1 has a positively charged amino terminal domain (residues 1-115) and a negatively charged carboxyl terminal domain (residues 116-265). The structure of the binding site in the metallothionein promoter is also conserved, A-T rich region followed by GCTG (Zhou *et al.* 1992). The arrangement of cysteines in the amino terminal domain is conserved allowing the formation of the 'copper fist'. The primary structure of the carboxyl domains of ACE1 and AMT1 are not similar. AMT1 regulates all three metallothionein genes in *C. glabrata* in a copper dependant manner, furthermore if the *AMT1* gene is disrupted then the resulting phenotype is copper hypersensitive implying that AMT1 is the major and most important copper regulatory trans-acting factor in *C. glabrata* (Zhou *et al.* 1992).

A series of experiments were performed, by Thorvaldsen *et al.* (1993), to determine if ACE1 and AMT1 are functionally homologous. Both AMT1 and ACE1 conferred copper tolerance to *S. cerevisiae* mutants lacking a functional *ACE1* gene but containing a functional *CUP1* gene. However a chromosomal *ACE1* gene was unable to activate the expression of the *C. glabrata* *MT-IIa* gene introduced into *cup1Δ* cells. A combination of reporter gene constructs of MT gene promoters were co-transformed with either *ACE1* or *AMT1* into *ace1Δ* cells. It was found that AMT1 could confer copper mediated expression of *CUP1* and all three *C. glabrata* MT genes, but ACE1 could only confer copper mediated expression of *CUP1* and had no, or a limited, effect on the *C. glabrata* genes.

1.5.3 Other aspects of trace metal ion homeostasis in yeast

1.5.3.1 Genes with products proposed to have a role in iron and copper uptake and metabolism in *S. cerevisiae*

In the presence of oxygen and water soluble ferrous iron (Fe(II)) is rapidly oxidised to form insoluble ferric iron (Fe(III)) hydroxides (cited in Anderson *et al.* 1992). Iron uptake is achieved by two main mechanisms. In, for example *E. coli*, specific iron chelating compounds, siderophores are released which deliver iron to cell receptors (reviewed Bagg and Neilands 1987). The second strategy involves a cell surface iron reductase, iron is then transported into the cell as soluble divalent iron ions (Anderson *et al.* 1992). *S. cerevisiae* employs the latter strategy (Yamashoji and Kajimoto 1986). Fractionation experiments show that the yeast contains both plasma membrane and cytosolic ferric reductase components (Lesuisse *et al.* 1990). A number of genes have been identified which are involved in the uptake or metabolism of iron and / or copper metabolism and are described in the following section.

The *FRE1* gene was identified because it restored wild type ferric reductase activity to a mutant with an aberrant reductase phenotype (Dancis *et al.* 1990). The putative protein contains two membrane spanning motifs and a region with significant sequence similarity to the large subunit of the human plasma membrane cytochrome b_{558} (or X-CGD protein), an oxireductase present in the plasma membrane of human phagocytic cells which donates one electron to molecular oxygen (Dancis *et al.* 1992). It is proposed that *FRE1* product could be a plasmalemma oxireductase (or a component of a reductase complex) which donates one electron to ferric iron. Disruption of the *FRE1* gene produces a yeast phenotype with significantly reduced ferric reductase activity and reduced iron uptake and retarded growth characteristics (Anderson *et al.* 1992). In addition to iron reduction it has been reported that the *S. cerevisiae* ferric reductase has copper reductase activity (Lesuisse and Labbe 1992). Transcription regulation of the *FRE1* gene has been demonstrated in response to iron and a putative iron responsive element has been identified in the gene promoter region (Dancis *et al.* 1992). In addition to regulation by iron, ferric reductase activity can be regulated by cAMP (Lesuisse *et al.* 1991).

A gene encoding a putative copper dependent transcription factor of *FRE1*, *MAC1*, has been identified (Jungmann *et al.* 1993b). The *UBC7* gene, which encodes the ubiquitin conjugating enzyme (involved in cadmium resistance) was cloned and sequenced (Jungmann

et al. 1993a). Sequence analysis revealed a gene, subsequently designated *MAC1*, as a divergently transcribed gene downstream from *UBC7* (Jungmann *et al.* 1993b). The putative product of the gene has some sequence similarity to the copper dependent transcription factors ACE1 and AMT1. Reporter gene constructs indicate that *MAC1* has a nuclear location Jungmann *et al.* 1993b).

Jungmann *et al.* (1993b) constructed mutants lacking a functional *MAC1* gene and examined their phenotype. The cell lines grew more slowly than wild type cells and were unable to grow on non fermentable carbon sources indicating a respiratory defect. They had a severe reduction in oxygen uptake and were hypersensitive to stress by heat, hydrogen peroxide, cadmium, zinc and lead. The cells were not hypersensitive to copper and the addition of copper or iron to the medium rescued the stress and growth phenotype. Plasma membrane copper and iron reduction was reduced as was copper uptake. The *fre1Δ* mutant has a similar phenotype to cells with a non functional *MAC1* gene (Dancis *et al.* 1992). A yeast mutant (designated *MAC1*^{up1} cells) with elevated copper and iron reductase activity and strongly elevated copper uptake was found to have a single nucleotide substitution in the *MAC1* gene causing a Glu to His substitution (Jungmann *et al.* 1993b). *FRE1* expression is decreased in *mac1Δ* cells and increased in *MAC1*^{up1} cells, and together with the nuclear location of *MAC1* this has led to the proposal that *MAC1* is a transcriptional regulator of *FRE1* (Jungmann *et al.* 1993b).

The gene *CTTI* encodes a cytosolic catalase, which is involved in the reaction { $\text{H}_2\text{O}_2 \rightarrow \text{H}_2\text{O} + \text{O}_2$ }, with expression which is induced by hydrogen peroxide (Marcheler *et al.* 1993). In *mac1Δ* cells the induction of *CTTI* by hydrogen peroxide is absent and in the *MAC1*^{up1} cells there is no increase in *CTTI* transcription (Jungmann *et al.* 1993b). It is proposed that *MAC1* is also involved in the transcriptional activation of the *CTTI* gene.

The *GEF1* gene was found to be disrupted in *S. cerevisiae* mutants expressing a phenotype of slow growth on non fermentable carbon sources which could be alleviated by the addition of iron to the growth media (Greene *et al.* 1993). On iron rich media *gef1Δ* cells exhibited enhanced ferric reductase activity and increased ferrous iron uptake relative to wild type cells. Greene *et al.* compared the disrupted growth phenotypes of *gef1Δ* and *fre1Δ* cells. The *fre1Δ* mutant had wild type growth rate but reduced reductase activity whereas the *gef1Δ* had reduced growth rate but wild type reductase activity. It was concluded that

the reduced growth rate in *gef1Δ* cells was not due to a defect in ferric reductase activity. As the predicted product of the *GEF1* gene had significant sequence similarity to membrane spanning voltage-gated chloride channel proteins it was proposed that GEF1 may be involved in iron transport across an internal membrane (Greene *et al.* 1993). The mitochondria and vacuole were candidate organelles.

The vacuole has an important role in the storage and homoeostasis of metal ions especially iron and copper (Gadd and White 1989, Raguzzi *et al.* 1988). An important aspect of this function is the maintenance of a reduced vacuolar pH relative to the cytosol, pH 6.0 compared to pH 7.0, by a proton ATPase (Eide *et al.* 1993). A mutant with iron suppressible respiratory deficiency was traced to a disruption in a gene designated *GEF2* (Eide *et al.* 1993), this gene encodes a protoelipid subunit of a multicomponent proton ATPase which had previously been designated *VMA3* (Nelson and Nelson 1989).

Gef2Δ cells have deficiency in vacuolar acidification and are hypersensitive to growth inhibition by copper (Eide *et al.* 1993). It has not been determined if the copper hypersensitive phenotype is a consequence of the disruption in vacuolar acidification or if there is a more direct interaction with copper metallothionein. Disruption of the *GEF2/VMA3* gene reduces tolerance to the divalent ions of cadmium, manganese and zinc (Eide *et al.* 1993). The mutant phenotype could be relieved by increasing the availability of iron in the growth media which may indicate that disruption of the *GEF2/VMA3* gene effects the ability of the vacuole to act as an iron store.

A gene designated *FET3* was found to be disrupted in a *S. cerevisiae* mutant with wild type ferric reductase activity but with iron uptake less than 1 % of wild type and which was unable to grow on non fermentable carbon sources (Askwith *et al.* 1994). There is sequence similarity between the upstream activation sequence of *FET3* and *FRE1* and both genes show a similar pattern of regulation by iron (Askwith *et al.* 1994). The amino terminal domain of the putative product of *FET3* has sequence similarity to the 'blue' copper oxidase proteins which require copper for activation. Cells grown on copper deficient media had reduced ferrous iron transport activity, measured by incorporation of [⁵⁹Fe] or [⁵⁵Fe] (Askwith *et al.* 1994). A similar reduction in ferrous iron transport activity was noted for manganese and zinc but could only be recovered by the addition of copper. Askwith *et al.* have speculated that following trans membrane transport of ferrous iron the *FET3* protein could be required to oxidize ferrous iron and release it from the transporter.

It has been proposed that copper uptake in *S. cerevisiae* operates by a selective mechanism involving active facilitative transport (Lin and Kosman 1990). It has been demonstrated that ferrous iron and copper do not compete for uptake (Eide *et al.* 1992). Cell lines lacking a functional *CTR1* gene are apparently deficient in both a high affinity ferrous uptake system and a high affinity copper uptake system (Dancis *et al.* 1994). The ferrous iron uptake deficiency in *ctr1Δ* cells can be overcome by the addition of copper (500 μM) to the growth media implying that the deficiency in ferrous iron uptake could arise from a failure to assimilate copper (Dancis *et al.* 1994). To investigate this the phenotypes of cell lines with defects in either *CTR1* or *FET3* or both were compared (Dancis *et al.* 1994). It was found that the defect in ferrous iron uptake could only be relieved by the addition of copper in the *ctr1Δ* strain containing a functional *FET3* gene indicating that *FET3* is a copper dependent iron transport protein and that *CTR1* is involved in copper transport. Expression of *CTR1* was induced by copper deprivation and repressed by copper levels which did not induce the expression of the metallothionein (Dancis *et al.* 1994). The product of the *CTR1* gene has an amino terminal domain with some sequence similarity to the copper binding motifs of the P-type copper ATPases CopA and CopB in bacteria (Cha and Cooksey 1991 and Odermatt *et al.* 1993). Dancis *et al.* propose that *CTR1* is a plasma membrane copper import protein or a component of a copper import complex.

1.5.3.2 Oxidative stress, copper/zinc superoxide dismutase and metallothionein

Oxygen related toxicity has been reviewed in detail, by Halliwell and Gutteridge 1984 and 1992, and some aspects of the potentially damaging effects of oxygen metabolism will be cited in this paragraph. The superoxide radical [O_2^-] is formed when a single electron is accepted by a ground state dioxygen molecule and is formed in almost all aerobic cells. In aqueous solution [O_2^-] can undergo the “dismutation” reaction which can be summarised $\{2O_2^- + 2H^+ \rightarrow H_2O_2 + O_2\}$. Free iron and copper ions can cause the decomposition of H_2O_2 to H_2O and O_2 with the production of highly reactive hydroxyl radical intermediates. Hydroxyl radicals react with extremely high rate constants with all organic molecules, including sugars, amino acids, phospholipids, DNA bases and organic acids. The production of hydroxyl radicals is therefore highly damaging to living systems. Also biologically significant in the production of hydroxyl radicals is the Haber-Weiss reaction $\{O_2^- + H_2O_2 \rightarrow$

$\cdot\text{OH} + \text{OH}^- + \text{O}_2$ } (Halliwell and Gutteridge 1992). This reaction is also catalysed by iron and copper. The accumulation of highly reactive oxygen species is termed oxidative stress.

Superoxide dismutase (SOD) enzymes greatly increase the rate of the dismutase reaction effectively buffering $[\text{O}_2^-]$ ions produced in the cell and are believed to be ubiquitous (Tardat and Touati 1991). *S. cerevisiae* cells lacking a functional copper, zinc superoxide dismutase gene, *SOD1*, are hypersensitive to oxidative stress, and hypersensitive to oxygen and superoxide generating drugs such as paraquat (Tamai *et al.* 1993). *Sod1Δ* cells fail to grow on agar containing lactate, a respiratory carbon source and require the amino acids, cysteine, methionine and lysine for aerobic growth (Tamai *et al.* 1993). It would be expected that the addition of copper ions to *sod1Δ* cells would exacerbate the symptoms of oxidative stress. In fact the addition of CuSO_4 (in the range 200 μM to 1 mM) restores growth on lactate media provided the cells contains functional *CUP1* and *ACE1* genes (Tamai *et al.* 1993). By linking the *CUP1* gene to a galactose inducible promoter Tamai *et al.* demonstrated that the lactate growth defect in *sod1Δ* cells is relieved by elevated levels of the yeast copper metallothionein with similar results being obtained for copper induced expression of the monkey metallothionein in the *sod1Δ* cells. *CUP1* also relieved the requirement for cysteine and methionine for aerobic growth and partially restored tolerance to paraquat but expression of metallothionein did not alleviate hypersensitivity to oxygen, or the requirement for lysine for aerobic growth. Expression of *CUP1* was induced by growth in oxygen levels expected to cause oxidative stress (Tamai *et al.* 1993). In *in vitro* assays Tamai *et al.* have demonstrated that yeast copper metallothionein has antioxidant activity. The activity was significantly less for the apoprotein or silver, zinc or cadmium species. Copper-thionein reacts with radical species releasing divalent copper, this includes the dismutation of $[\text{O}_2^-]$ (Felix *et al.* 1993). The release of copper into the cell by the reaction could stimulate *de novo* synthesis of metallothionein accounting for the induction of metallothionein in response to oxidative stress. Glutathione (γ -glutamylcysteinylglycine) is an abundant molecule in the cell (cited in Felix *et al.* 1993). It has a major antioxidant role in the cell due to the reactivity of thiol groups with free radicals.

1.5.3.3 Summary

The description of the determined and predicted characteristics of the genes described above illustrates the relationship between various aspects of copper and iron metabolism. Some of

these relationships are represented in figure 1.3, but it should be stressed that that the components and relationships presented in this diagram represent only a small fraction of the

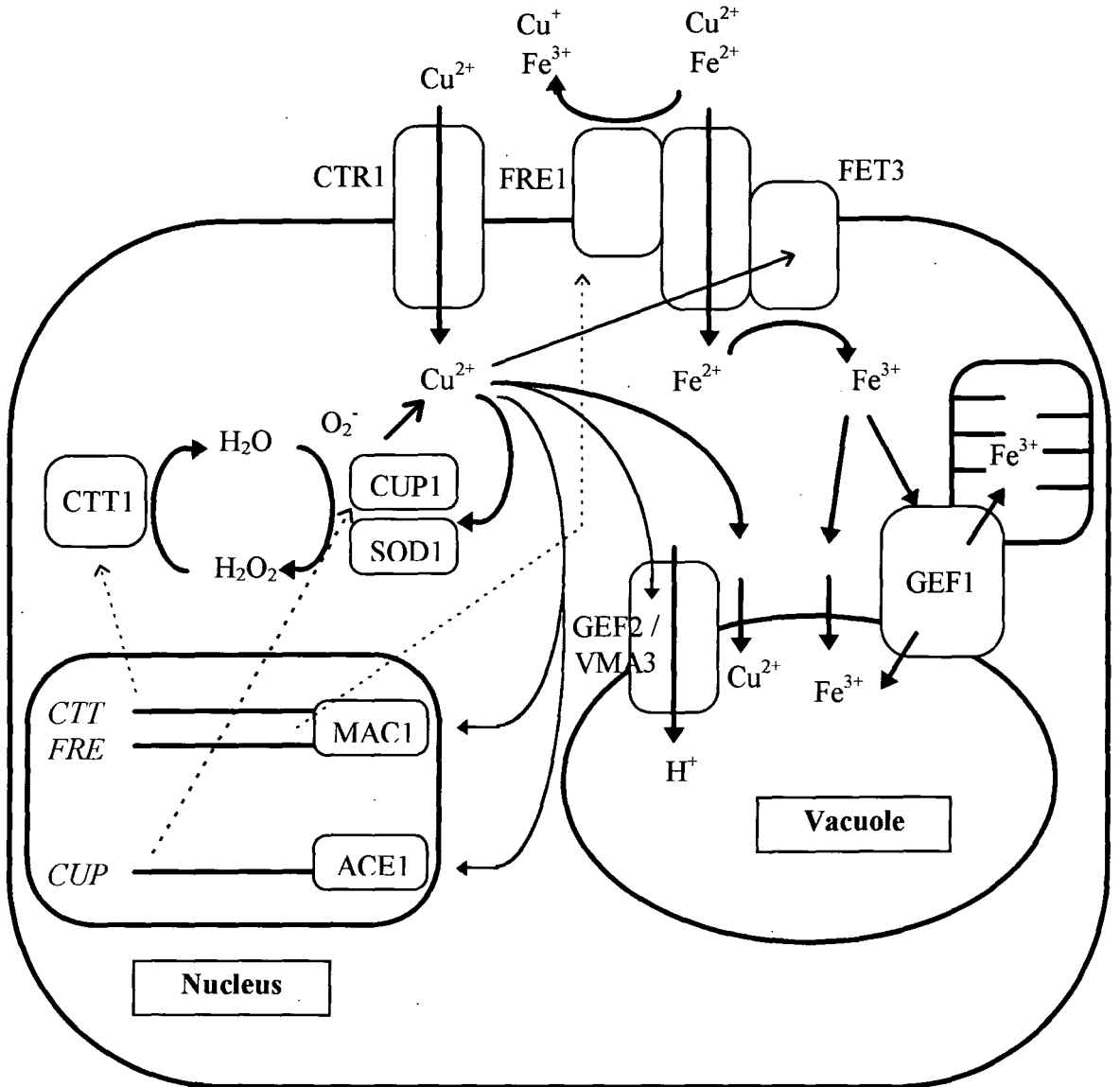


Figure 1.3 Diagram summarising the relationship between some of the components involved in iron and copper metabolism in *S. cerevisiae*.

true complexities of the interaction of the different components in a cell. Many aspects of metabolism, not necessarily directly related, may be effected by a fluctuation in a particular factor, for example fluctuations in exogenous concentrations of trace metals.

1.6 Metal binding polypeptides in plants, algae and some fungi

1.6.1 Introduction

In response to elevated environmental levels of cadmium and copper, plants, algae and some fungi produce metal binding polypeptides structurally related to glutathione (reviewed extensively for example, Tomsett and Thurman 1988, Rauser 1990, Steffens 1990, Robinson 1990). These polypeptides have been considered to be analogous to metallothionein in the animal kingdom. Cadmium binding polypeptides were first identified in extracts of the fission yeast, *Schizosaccharomyces pombe* and termed “cadystin” (Murashagi *et al.* 1981, Kondo *et al.* 1985). Homologous peptides were subsequently identified in plants and termed “phytochelatin” (Grill *et al.* 1985). Various workers have referred to essentially the same molecule by a number of different names; “poly-(γ -glutamylcysteinyl)glycines” (Jackson *et al.* 1987), “class-III metallothionein” (Fowler *et al.* 1987), “ γ -glutamyl metal binding peptides” (Reese *et al.* 1988) and more recently “ γ EC isopeptides” (Rauser and Meuwly 1993). In the following review the term phytochelatin will be used to represent γ -glutamyl metal binding peptides.

The general molecular formula for this class of compound is (γ -Glu-Cys)_n-Xaa, n has been reported to vary from 2 to 11, although n = 2 or 3 is most commonly reported (cited in above reviews). Xaa is usually glycine, but in some plants which contain homo-glutathione (γ -Glu-Cys- β -Ala) then Xaa is β -alanine, for example in *Glycine max* (Grill *et al.* 1986). In several species of Poaceae the tripeptide γ -glutamylcysteinylserine has been reported (Klapcheck *et al.* 1992) and there is a report of the tripeptide γ -glutamylcysteinylglutamic acid being produced in *Z. mays* in response to cadmium exposure (Meuwly *et al.* 1993). These tripeptides may undergo elongation to produce variations of (γ -EC)_nXaa.

1.6.2 Induction of phytochelatin synthesis

The production of phytochelatin has been observed in response to increased levels of a number of metal ions. In the algae *Chlorella fusca* and *Scenedesmus acutiformis* and the yeast *S. pombe* production of phytochelatin was induced by cadmium, copper, lead, silver and zinc (Grill *et al.* 1986, Gekeler *et al.* 1988). Phytochelatin production was observed in *Rauvolfia serpentina* cells in response to antimony, arsenate, bismuth, cadmium, copper, gold, lead, mercury, nickel, selenate, silver, tin, tellurium, tungsten and zinc but not

aluminium, caesium, calcium, chromium, cobalt, magnesium, manganese, molybdenum, potassium, sodium or vanadium (Grill *et al.* 1987). Despite the apparent production of phytochelatin as a general response to a wide variety of metals most of the research into this class of compound has been concerned with the metabolism / detoxification of copper and cadmium (see reviews cited in section 1.6.1).

1.6.3 Properties of phytochelatin

Direct sequencing of polypeptides from the cadmium binding complexes was hampered because they were insensitive to Edman degradation (Robinson and Jackson 1986) even following incubation with *S. aureus* V8 protease which cleaves the glutamyl α -carboxamide bond (Bernhard and Kägi 1987). However treatment with γ -glutamyl transferase liberates glutamic acid (Grill *et al.* 1985). The γ -carboxamide bond has been confirmed by ^{13}C NMR (Jackson *et al.* 1987).

Metal complexes involve aggregation of $(\gamma\text{-EC})_n\text{G}$ of different lengths which results in the determination of non integral values of n using certain methods (reviewed Rauser 1990). Proton displacement experiments to estimate the pH at which 50 % of the metal ions dissociate from the metal-peptide complex have been performed on a number of complexes. The cadmium complex from cabbage (*Brassica capitata*) had a pH of half displacement of 4.4 (Wagner 1984), and that for *Nicotiana tabacum* cadmium complex was pH 5-5.8 (Reese and Wagner 1987a). The pH of half displacement of yeast cadmium- $(\gamma\text{-EC})_n\text{G}$ for $n = 1, 2$ and 3 was found to be 6.4, 5.4 and 4.9 respectively (Hayashi *et al.* 1988), indicating that as the polypeptide chain becomes longer the affinity for cadmium increases.

The spectroscopic properties of metal-phytochelatin complexes are similar to mammalian metallothionein. They have a UV absorption shoulder between 250 and 275 nm which is dependent on metal co-ordination (Mehra *et al.* 1988). Luminescence emission of copper phytochelatin in *S. pombe* and cucumber was typical of copper metallothionein (Reese *et al.* 1988). The similarity of spectroscopic properties to mammalian metallothionein suggests that a metal cluster is formed with thiol-metal liganding. Differences in UV absorption CD spectra have been observed for different cadmium phytochelatin complexes (Plocke and Kägi 1992). A definite peak between 250 and 275 nm was absent in a sample containing $n=1$ and $n=2$ but was evident in complexes containing longer polypeptides. The CD spectra for three

complexes with different mixtures of chain length were distinctive which may indicate differences in structure.

1.6.4 Inorganic sulphur is involved in stabilisation of some cadmium phytochelatin complexes

The release of hydrogen sulphide from an acid treated cadmium complex was first reported in *S. pombe* (Murasagi *et al.* 1983). In a detailed HPLC analysis of three cadmium complexes extracted from *S. pombe* by gel filtration and ion exchange chromatography the stoichiometries, chain length, cadmium content and labile sulphide content were determined (Plocke and Kägi 1992). The smallest complex, designated complex I, was composed of $(\gamma\text{-EC})_n\text{G}$ with $n = 1$ and $n = 2$, it contained no acid labile sulphide and only one cadmium ion per complex. Complexes II and III contained progressively longer chain lengths and six or more cadmium ions, in these acid labile sulphide was an integral part of the complex. This led to the hypothesis that the sulphide component of the cadmium complex is required to stabilise or promote the longer cadmium phytochelatin with a concomitant increase in affinity for metal ions (Reese and Winge 1988). In tomato (*Lycopersicon esculentum*) roots the ratio of sulphur to cadmium in phytochelatin complexes increased with the concentration of cadmium to which the plants are exposed (Reese *et al.* 1988). Mutants of *S. pombe* which exclusively produce cadmium phytochelatin without incorporated sulphide are hypersensitive to cadmium poisoning (Mutoh and Hayashi 1988).

Large phytochelatin coated cadmium sulphide quantum semiconductor crystallites with a core of approximately 80 cadmium sulphide units have been observed in *C. glabrata* grown in minimal salt media (Dameron *et al.* 1989). Cadmium phytochelatin sulphide complexes have also been observed in *L. esculentum* (Reese *et al.* 1992) and the wild mustard *Brassica juncea* (Speiser *et al.* 1992). The accumulation of high molecular weight cadmium sulphide complexes in the vacuole requires the specific transporter, designated HTM1 (Ortiz *et al.* 1992). The vacuole has been determined as the main organelle of accumulation of both cadmium phytochelatin and total cadmium in *Nicotiana rustica* (Vögeli-Lange and Wagner 1990).

1.6.5 Biosynthesis of phytochelatin

There is evidence that the production of phytochelatin involves a biosynthetic pathway(s) which utilises the glutathione pool in the cell; Accumulation of phytochelatin in response to cadmium exposure still occurs in cells in which *de novo* protein synthesis has been inhibited with cyclohexamide (Scheller *et al.* 1987, Robinson *et al.* 1988). In cultured cells challenged with cadmium the glutathione pool decreases (Grill *et al.* 1987, Scheller *et al.* 1987), the same phenomena is observed in intact roots (Rauser 1987). In species containing homoglutathione the phytochelatin variant $(\gamma\text{-EC})_n\beta\text{-A}$ is produced (Grill *et al.* 1986). Depletion of ^{35}S glutathione in *Datura innoxia* cells exactly matched the biosynthesis of phytochelatin (Berger *et al.* 1989). Initially 70 % of the ^{35}S was present as glutathione but after 2 hours 90 % of the ^{35}S was incorporated into phytochelatin, predominantly the pentapeptide.

The addition of buthionine sulphoxamine (BSO) strongly inhibits glutathione synthesis by blocking the active site of the enzyme γ -glutamylcysteine synthetase which forms the γ -carboxamide linkage between Glu and Cys (Griffith and Meister 1979). Exposure of cells to BSO reduces cadmium and copper tolerance in *N. tabacum* along with the levels of cadmium and copper binding peptides, assumed to be phytochelatin (Reese and Wagner 1987b). Similarly, in *L. esculentum* cells treated with BSO there is little glutathione or phytochelatin production, phytochelatin synthesis can be rescued by addition of exogenous glutathione (Scheller *et al.* 1987).

The enzymes in the glutathione biosynthetic pathway, γ -glutamylcysteine synthetase and glutathione synthetase have been characterised (cited in Chen and Goldsbrough 1994). The depletion in cellular glutathione levels in response to elevated cadmium indicates that metal regulation of phytochelatin production occurs following, and independently of, glutathione synthesis (Meuwly and Rauser 1992). Rapid production of phytochelatin with $n = 2$ or 3 is observed in response to cadmium exposure (Grill *et al.* 1986, Grill *et al.* 1987, Robinson *et al.* 1988). The lack of any apparent lag phase supports constitutive expression of enzyme(s) involved in the production of phytochelatin.

In *Silene cucubalus* cell cultures phytochelatin synthesis from glutathione involves the proposed enzyme, γ -glutamylcysteinyl dipeptidyl transpeptidase (phytochelatin synthase) (Grill *et al.* 1989). The enzyme substrate is suggested to be either two glutathione molecules

or a glutathione molecule and phytochelatin. Activity of this enzyme has been shown to be strongly activated by cadmium, gold, lead, mercury and silver and more weakly by copper and zinc (Grill *et al.* 1989). Synthesis of phytochelatin *in vitro* ceases upon chelation of all the heavy metals (Löffler *et al.* 1989). Increased production of phytochelatin could occur by the allosteric effect of metal ions binding directly to and activating the biosynthetic enzyme(s) or via product removal. In *Arabidopsis thaliana* a mutation in the locus referred to as *CAD1* results in a cadmium sensitive phenotype (Howden and Cobbett 1992). It has been demonstrated that disruption of this locus leads to a deficiency in the ability to accumulate phytochelatin probably due to a disruption in the phytochelatin biosynthetic pathway (Howden *et al.* 1995a). Disruption to a second *A. thaliana* locus, *CAD2*, also leads to cadmium sensitivity and a decreased ability to accumulate phytochelatin, but in this case a decrease in the level of glutathione was also observed (Howden *et al.* 1995b). In the yeast *S. cerevisiae* two genes *CAD1* (Mortimer *et al.* 1989) and *CAD2* (Tohoyama *et al.* 1990) have been implemented in cadmium tolerance. In *S. pombe* two pathways for $(\gamma\text{-EC})_n\text{G}$ biosynthesis have been detected in cell-free systems (Hayashi *et al.* 1991). One of these is similar to that of *S. cucubalis* described above, the other involves polymerisation of γ -glutamylcysteine which is terminated by the addition of a glycine (Rauser and Meuwly 1993).

1.6.6 Function of phytochelatin

The accumulation of phytochelatin in response to elevated metal supports a putative role of phytochelatin in metal tolerance (see reviews cited in 1.6.1). Inhibition of phytochelatin production by BSO increases the susceptibility of plants and yeast to cadmium poisoning (Reese and Wagner 1987). Metal sensitive enzymes are 10- to 1000- fold more sensitive to free cadmium than to the equivalent amount of cadmium in a cadmium phytochelatin complex (Kneer and Zenk, 1992). Cadmium sensitive mutants in *A. thaliana* are deficient in the production of phytochelatin (Howden *et al.* 1995a and b). It has been postulated that in plants with higher tolerance to cadmium, phytochelatin production may be more rapid, have a higher capacity, or produce longer phytochelatin which are known to be more stable (Steffens *et al.* 1986, Huang *et al.* 1987, Delhaize *et al.* 1989). In cadmium tolerant *L. esculentum* cell lines the activity of the enzyme γ -glutamylcysteine synthetase was found to be

double that of the wild type strain, thus making more glutathione available for production of phytochelatin (Chen and Goldsborough 1994).

In cadmium resistant *Datura innoxia* cells increased synthesis of phytochelatin was detected after 5 minutes following exposure to cadmium (Robinson *et al.* 1988) but this was also the case for the wild type cell line (Delhaize *et al.* 1989). When exposed to the same external cadmium concentration, cadmium sensitive plants of the bladder campion *Silene vulgaris* produce more phytochelatin than the tolerant strain (de Knecht *et al.* 1992). Cadmium sensitivity in tolerant plants was not effected by BSO but it was in the sensitive plants. This suggests the presence of an alternative mechanism for cadmium tolerance. The investigation of phytochelatin production in sensitive and tolerant roots of *S. vulgaris* found no difference in the chain length and distribution of phytochelatin between the two *S. vulgaris* phenotypes (de Knecht *et al.* 1994). A similar situation was observed in root tips of *Zea mays* (Tukendorf and Rauser 1990).

It is likely that a variety of tolerance strategies have evolved in different plants. The degree of tolerance in agronomic plants varies considerably and differences can be as great or greater between different genotypes within a species as between higher phylogenetic groupings (Aniol and Gustafson 1990). In a study of the effect of cadmium on the *Phaseolus vulgaris* (bush bean) and *Pisum sativum* two tolerance mechanisms were evident (Leita *et al.* 1993). Huge amounts of cadmium accumulate in the root system of *P. vulgaris* but little is translocated to other tissues. The uptake of cadmium by *P. sativum* roots was substantially lower, so the toxic metal was largely excluded from the plant. In a study of cadmium uptake in *Lupinus albus*, it was estimated that 70 % of cadmium uptake in roots of whole plants in hydroponic solution was by active uptake involving a proton ATPase carrier (Costa and Morel 1993). It was proposed that this was non specific uptake utilising plasmalemma calcium carriers. In the same study parallel to active absorption excretion of cadmium from root cells was also observed. Introduction of a mammalian metallothionein gene into *Brassica campestris*, and the introduction of human MT-II into *Brassica napus* and *Nicotiana tabacum* imparted metal tolerance to the transgenic cell lines (Lefebvre *et al.* 1987, Mishra and Gedamu 1988). The implication of this result is that the expression of metal chelating proteins, in this case metallothionein, can confer a degree of metal tolerance in plants.

The production of metal chelating phytochelatin by certain plants and algae is an important defence against elevated concentrations of trace metals such as cadmium (for example Jackson *et al.* 1987, Kneer and Zenk 1992, Meuwly *et al.* 1993 and Chen and Goldsbrough 1994). However, in trace metal tolerant organisms mechanisms other than increased capacity for phytochelatin production have evolved (for example Schat and Kalff 1992 and Costa and Morel 1993). Proposed mechanisms for exclusion of metals from the cell include; immobilisation of metals at the cell wall, complexation of metals by chelates secreted at the cell wall, formation of a redox barrier at the plasma membrane and the formation of a pH barrier at the plasma membrane (reviewed Taylor 1987). Excretion of cadmium from root cells has been proposed as a possible cadmium tolerant mechanism in *Lupinus albus* (Costa and Morel 1993).

As with other metallothioneins the propensity to investigate the role of phytochelatin in cadmium detoxification may have obscured a constitutive physiological role in the cell. Studies of the production of cadmium complexes in cell culture lines often involve the use of cadmium concentrations several orders of magnitude higher than could be expected in even the most contaminated of environments (Rauser 1990, Meuwly and Rauser 1992). The production of phytochelatin in both metal tolerant and sensitive plants of the same species (de Knecht *et al.* 1994), constitutive expression of enzymatic pathways involved in phytochelatin biosynthesis (Robinson *et al.* 1988), and the detection of phytochelatin in both tolerant and sensitive *L. esculentum* cells in the absence of elevated trace metal concentrations (Steffens *et al.* 1986), all suggest that phytochelatin may have a constitutive function.

There is ample evidence that phytochelatin chelates copper ions *in vivo* (for example Premakumar *et al.* 1975, Robinson and Thurman 1986, Robinson *et al.* 1987, Reese *et al.* 1988, Salt *et al.* 1989). In support of a role for phytochelatin in normal cell metabolism is the donation of copper and zinc to metal requiring enzymes *in vitro* from metal-phytochelatin complexes (Thumann *et al.* 1991). Differential copper tolerance in sensitive and tolerant strains of *S. vulgaris* was demonstrated to be independent of production of phytochelatin in response to elevated copper concentrations by these plants (Schat and Kalff 1992). The inhibition of thiol production, including phytochelatin in tolerant and sensitive *Deschampsia cespitosa* had no effect on copper tolerance (Schultz and Hutchinson 1988). In metal tolerant *N. tabacum* cells, inhibition of phytochelatin by BSO reduced tolerance of cadmium but not copper or zinc (Reese and Wagner 1987).

There is less evidence that phytochelatin chelates zinc *in vivo*, it has been postulated that zinc binding to phytochelatin at physiological pH would be too weak to have significance for sequestration or homeostasis (Reese and Wagner 1987, Robinson, 1990). In an investigation of metal complexes in *Euglena gracilis*, cadmium was observed to be bound to $(\gamma\text{-EC})_n\text{G}$, but zinc was associated with a pool of very low relative molecular mass, possibly glutathione (Shaw *et al.* 1989). As with cadmium and copper, accumulation of thiols including phytochelatin and glutathione was observed as a response to elevated zinc concentrations in *S. vulgaris* and there was no observed difference in this response between tolerant and sensitive plants (Harmens *et al.* 1993). The primary mechanism of zinc tolerance in barley is exclusion mechanisms in the root and compartmentalisation of free zinc into the vacuole and protoplasts (Brune *et al.* 1994). Zinc accumulation in the ear-leaf of *Zea mays* was reported to vary considerably between different strains (El-Blendary *et al.* 1993). Through cross-breeding experiments with the highest and lowest accumulators four genes were implicated as segregating factors but were not identified or characterised. Zinc-phytochelatin has been successfully used to restore activity to zinc requiring carbonic anhydrase (Thumann *et al.* 1991). Restoration of activity was not as effective as free zinc ions or as effective as the restoration of activity to copper requiring diamino oxidase by copper-phytochelatin.

The association of sulphide with the phytochelatin complex and the sulphur content of thiol groups has also lead to speculation that $(\gamma\text{-EC})_n\text{G}$ could be involved in, for example assimilatory sulphate reduction (Steffens *et al.* 1986). Furthermore as glutathione and phytochelatin are quite similar it has been suggested that they may be functional analogs (Robinson 1990). Glutathione is a cofactor in oxidative and reductive reactions, the detoxification of pesticides, and detoxification of hydrogen peroxide and free radicals, but phytochelatin have not been assigned such a role. (Renenberg 1982).

1.7 Iron accumulation in higher plants

1.7.1 Introduction

Two discrete mechanisms have evolved for iron uptake in higher plants under conditions of low iron availability (Marschner *et al.* 1986). 'Strategy 1' is found in all dicotyledonous species and all non graminaceous monocots. It involves reduction of ferric iron compounds by an inducible plasma membrane iron reductase. This system of uptake is believed to be analogous to that found in *S. cerevisiae* (Anderson *et al.* 1992). 'Strategy 2' occurs in graminaceous species. It involves secretion of ferric iron chelating phytosiderophores and subsequent absorption of the iron complex by the root. A similar mechanism is observed in many bacteria including *E. coli* (Bagg and Neilands 1987).

1.7.2 Strategy 1

Strategy 1 plants, including *P. sativum*, accumulate iron via a plasma membrane ferric-chelate reductase system (Grusak *et al.* 1990). A reduction in iron availability stimulates ferric iron reduction capacity, and increases proton extrusion and the release of phenolics from the root. The lower pH increases the solubility of ferric iron compounds and the reduction increases the concentration of ferrous iron at the root surface. It is ferrous iron which is transported across the root-cell plasmalemma (Chaney *et al.* 1972). The ferric reductase system and ferrous transport system are linearly correlated up to the point of influx saturation (Grusak *et al.* 1990).

A mutant strain of *P. sativum*, E107 accumulates extremely high levels of iron in its leaves (Kneen *et al.* 1990). The E107 strain has an iron deficient phenotype irrespective of the actual availability of iron and has a permanently active iron reductase activity (Welch and LaRue 1990). This mutant has been a useful tool for studying the role of the ferric reductase in *P. sativum* (Grusak *et al.* 1990). It has been found that under iron deficient conditions, when the iron chelate reductase is active, wild type *P. sativum* shoots accumulate up to three times as much manganese, twice as much copper and potassium and an extra 60 % magnesium compared to 'control' (iron sufficient) conditions (Welch *et al.* 1993). In reductase assays Welch *et al.* found that iron deficient conditions stimulated not only the reduction of ferric iron but divalent copper as well. Copper limited treatments stimulated iron and copper reductase activity after a slightly longer period, this lag is probably due to the difficulty of inducing truly copper deficient conditions in *P. sativum* seedlings.

The regulation of the iron deficiency response by hormone levels, specifically ethylene, has been investigated in *Cucumis sativus* (Romera and Alcántara 1994). Treatment of plants grown in iron deficient condition with inhibitors of ethylene synthesis was demonstrated to reduce the induction of iron deficiency responses; iron reductase activity, swelling of the subapical root tip and net proton extrusion. Furthermore it was demonstrated that if ethylene production was artificially increased, by the introduction of the ethylene precursor ACC (1-aminocyclopropane-1-carboxylic acid), then iron reductase activity could be stimulated even in plants grown in iron sufficient conditions. These findings would be in keeping with the proposal that enhanced activity of the iron reductase was a general response to stress.

1.7.2 Strategy 2


Biosynthesis of phytosiderophores by strategy 2 plants is induced by low iron conditions (Mihashi *et al.*, 1991). The biosynthetic pathway has been described for *Hordeum vulgare* (Shojima *et al.* 1990). The precursor molecule is L-methionine and in a pathway involving a number of intermediary molecules and enzymes various forms of mugineic acid are synthesised which are secreted as phytosiderophores. It has been demonstrated in wheat plants, that the rate of iron translocation is directly related to the rate of phytosiderophore release by the root (Zhang *et al.*, 1991). Phytosiderophore chelation was found to be responsible for the uptake of more than 90 % of the iron in hydroponic wheat plants. Young rice plants which express very low amounts of phytosiderophore in iron limited conditions, and for only a short time, are hypersensitive to low iron concentrations (Mori *et al.*, 1991). Chlorosis rapidly develops as a result of iron deficiency in the shoots, accompanied by the appearance of reduced root elongation and an increase in lateral roots. Experiments on iron deficient barley demonstrated that they daily secreted a 1000-fold excess of mugineic acid relative to amount of ferric iron which was actually taken up by the plant (Mihashi *et al.* 1991).

The siderophore based iron uptake system of *E. coli* is regulated by an iron dependent transcriptional co-repressor, the Fur protein (Bagg and Neilands 1987). Fnr protein, a transcriptional regulator of *E. coli*. anaerobic respiratory genes, is activated by iron (Green *et al.* 1991). It is possible that higher plants contain analogous iron dependent regulatory proteins.

1.8 Isolation of low molecular weight metal containing compounds from plants

Most buffers used to extract such complexes have been based on Tris or potassium in the pH range 7.2 to 8.6 with agents such as NaCl, 2-mercaptoethanol, dithiothreitol or thiourea added to stabilise the compound during purification (Rauser 1990). Exceptions include a copper binding complex from *Mimulus guttatus* extracted using a HEPES buffer at pH 6.5 (Thurman *et al.* 1989). Further initial purification of the crude extract often involves gel permeation chromatography on Sephadex G-50 or G-75 or ion exchange chromatography on DEAE based columns (Rauser 1990). In some cases the first chromatographic step is gel permeation (for example; Bartolf *et al.* 1980, Wagner and Trotter 1982, Kaneta *et al.* 1983, Grill *et al.* 1985, Robinson and Thurman 1986) and in others the anion exchange chromatography (for example; Murasagi *et al.* 1981, Lue-Kim and Rauser 1986, Reese *et al.* 1988). However if the first chromatographic step is gel permeation chromatography then often a preceding concentration step is required, for example dialysis against polyethylene glycol (Robinson and Thurman 1986) or ammonium sulphate precipitation (Grünhage *et al.* 1985). Alternatively quite large volumes can be applied to anion exchange resins as the charged metal complexes will adhere to the resin in low salt concentrations. Another purification procedure used is affinity chromatography using thiopropyl Sepharose-6B, which forms a covalent bond with thiol groups (for example, Wagner 1984, Jackson *et al.* 1987, Reese *et al.* 1987). Metal chelation chromatography based on metal affinity matrices has been less successful (Wagner and Trotter 1982). Preparative and analytical PAGE has also been applied (Wagner 1984).

On gel permeation columns the apparent molecular weight of the metal complex has been observed to decrease with increasing ionic strength of the gel filtration medium, ranging from 13,000 down to 1700 (summarised in Rauser 1990). The use of columns to size complexes by their retention time therefore needs to be approached carefully.

Chromatography in denaturing 6 M guanidine hydrochloride produces apparent sizes in broad agreement with the value of n determined subsequently by other methods (Grill *et al.* 1985, Jackson *et al.* 1987). 

One of the most powerful techniques for resolving individual phytochelatin complexes is the application of high performance liquid chromatography (HPLC) to metal complexes which have been isolated using gel permeation and / or anion exchange chromatography (for example Reese *et al.* 1988, Salt *et al.* 1989, Meuwly *et al.* 1993). Metal dissociates from the

complexes if organic solvents are used but the absorbance of the peptide bond at 214-220 nm can be used as a detection method (Reese *et al.* 1988). An alternative method is the derivitisation of thiols with Ellmans reagent (Gekeler *et al.* 1988) or Clelands reagent (Kneer *et al.* 1992) and measuring the absorbance at 410 nm. On HPLC polypeptides are resolved into peaks corresponding to the length of chain allowing accurate determination of the distribution of the size of synthesised under particular conditions (for example, Kaneta *et al.* 1983, Jackson *et al.* 1987, Meuwly *et al.* 1993, de Knecht *et al.* 1994). Further detailed analysis of complexes has been obtained by applying conventional and tandem mass spectroscopy to isolates (Meuwly and Rauser 1993).

To date, these methods have only lead to the purification and characterisation of phytochelatin-metal complexes. The products of plant metallothionein-like genes have not been unequivocally identified by these techniques.

1.9 Gene encoded metallothionein in higher plants

1.9.1 Introduction

In addition to phytochelatins, genes have been isolated from a number of plant species encoding predicted proteins with some similarity to metallothionein (reviewed Robinson *et al.* 1993). Their identification in representative monocotyledonous, for example *Hordeum vulgare* and *Zea mays*, as well as dicotyledonous, for example *Pisum sativum*, *Mimulus guttatus*, *Glycine max* and *Arabidopsis thaliana*, species suggest that they are widely distributed across the plant kingdom. The predicted products of these genes are characterised by amino and carboxyl terminal cysteine rich domains containing the Cys-Xaa-Cys motif characteristic of metallothionein. The published reports of these genes will be reviewed in detail in a later chapter. The wheat-germ E_c protein is a cysteine rich, zinc containing protein which has been isolated from plant tissue and has been designated a class-II metallothionein (Lane *et al.* 1987). To date the E_c protein is the only plant metallothionein (excluding phytochelatin) which has been isolated from plant tissue.

1.9.2 The E_c protein from *Triticum aestivum*

The protein was first identified due to its high incorporation of [³⁵S] cysteine radiolabel following *in vitro* translation of mRNA isolated from dry wheat embryos (Hanley-Bowdoin and Lane 1983). E_c from early cysteine rich protein. The protein is synthesised almost

immediately following the uptake of water by isolated embryos at the onset of germination (Hofmann *et al.* 1984). Post imbibition the abundance of these transcripts and the E_c protein rapidly decline. The transcripts are undetectable after 5 to 10 hours post imbibition (Hanley-Bowdoin and Lane 1983, Kawashima *et al.* 1992). The protein may have an role in early embryogenesis with residual transcripts surviving in the desiccated seed to be briefly translated immediately post-imbibition (Kawashima *et al.* 1992). It has been proposed that the protein may have a role in zinc storage although it is estimated that only 5 % of total zinc is associated with E_c in mature *T. aestivum* embryos (Lane *et al.* 1987, Kawashima *et al.* 1992).

E_c is a zinc containing protein with a molecular weight of 6000 (Lane *et al.* 1987). The arrangement of cysteines in the sequence is similar to the patterns found in mammalian metallothionein, that is predominantly Cys-Xaa-Cys repeats (Kawashima *et al.* 1992). Purified E_c protein has a stoichiometry of 5 gram-atoms of zinc for every mole of protein (Lane *et al.* 1987). The E_c genes have been isolated, they are located in single copies on the long arms of chromosome 1A, 1B and 1D in hexaploid wheat (Kawashima *et al.* 1992). This arrangement differs from mammalian metallothionein genes which are located in multi-gene clusters (for example in mice Masters *et al.* 1994). Sequence analysis has identified no obvious metal responsive elements in the 5' flanking region of E_c genes, but they do have abscisic acid (ABA)-responsive elements (Kawashima *et al.* 1992). Transcripts of the E_c genes accumulate in response to the addition of ABA but not zinc in the germination media.

The highest levels of E_c transcripts are found in immature wheat embryos shortly following the onset of rapid cell differentiation (Kawashima *et al.* 1992). A parallel is drawn with the 20-fold greater concentration of rat metallothionein in neonatal compared to mature rat liver (Kern *et al.* 1981). It was observed that the deposition of animal metallothionein coincided with a shift between proliferative and differentiating stages of embryo development. A role for E_c in zinc homeostasis during development has been proposed (Kawashima *et al.* 1992).

1.9.3 A plant metallothionein-like gene expressed in the root of *P. sativum* - *PsMT_A*, and characterisation of the translational product

The *PsMT_A* gene was identified in *P. sativum* on the basis of the relative abundance of its transcripts in root tissue (Evans *et al.* 1990). A cDNA library was differentially screened for

clones more abundant in root tissue than other organs (green leaf, etiolated leaf and cotyledon). Of the 64 clones selected 5 were identified as being particularly abundant in roots. The clone, pPR179, strongly hybridised to a single abundant transcript in Northern blots of root RNA. Much weaker hybridisation was detected with a similar sized transcript (640 bases) in leaf and a smaller transcript in developing cotyledonous tissue. Transcripts were identified in roots of 14 day old seedlings but not in the embryonic radicle at day 4 (Robinson *et al.* 1992). The clone hybridised to multiple bands in restricted *P. sativum* genomic DNA, suggesting the possibility of a multigene family (Evans *et al.* 1990). A genomic clone to which the sequence hybridised was isolated from a *P. sativum* genomic DNA library (Evans *et al.* 1990). The genomic sequence is identical to the cDNA sequence apart from a 643 nucleotide intron.

The putative product of the gene is a 75 residue polypeptide. The predominant features of the sequence are two cysteine rich domains separated by a region of about 40 amino acids. The arrangement of cysteines in the two domains, in the form of three Cys-Xaa-Cys motifs, is characteristic of metallothionein. The gene was designated *PsMT_A* (Evans *et al.* 1990). *
Identification of the *P. sativum* gene coincided with the isolation of a related cDNA from copper tolerant *Mimulus guttatus* (de Miranda *et al.* 1990). There is 66 % identity at the nucleotide level between the coding sequences of the two genes, and the predicted products share the same overall features. Subsequently, gene sequences with predicted products with these same features have been isolated from a growing number of plant species (table 3.1). The significant features of these plant metallothionein-like genes will be detailed in chapter 3.

To date there are no reports of the isolation of the translational product of a plant metallothionein-like gene from plant tissue. However, the *PsMT_A* product has been partially characterised by the expression of the gene in *E. coli*. Two approaches have been reported; expression of the protein as a carboxyl terminal extension of glutathione-S-transferase using the pGEX3X expression vector system (Tommeay *et al.* 1991), and expression of the protein in a heat-inducible expression vector pPW1 (Kille *et al.* 1991). The fusion protein system has the advantage of a single step purification procedure, using glutathione affinity chromatography, which leads to a good recovery rate (Smith and Johnson 1988). The heat inducible vector system has the advantage of expressing the protein without the constraint of being anchored at one end to another protein but the purification procedure was more protracted (Kille *et al.* 1991).

Cells expressing the *P. sativum* metallothionein-like protein from the heat inducible pPW1 plasmid were reported to accumulate cadmium added to the culture medium (Kille *et al.* 1991). A control culture with the wild-type plasmid (no insert) did not accumulate cadmium. The *P. sativum* metallothionein-like protein cadmium complex was purified from a crude *E. coli* protein extract using gel permeation chromatography and ion exchange (Kille *et al.* 1991). The PsMT_A protein was identified in fractions containing cadmium by amino terminal Edman sequencing and visualised on 20 % acrylamide gels. Several coincident sequences were present, the amino terminal sequence and several attributable to internal regions within the protein. This was attributed to multiple proteolytic cleavages within the link region between the cysteine rich regions (Kille *et al.* 1991). Multiple bands were resolved on the gel. The cysteine rich domains were resistant to proteolytic cleavage by proteinase K, suggesting that a metal binding cluster analogous to those found in mammalian metallothionein may be formed. An average stoichiometry of approximately 6 gram-atoms of cadmium per mole of protein was calculated across the three pools selected from the chromatogram (Kille *et al.* 1991).

The GST- PsMT_A fusion protein was isolated from cells containing the pGPMT3 plasmid (pGEX3X plasmid with the *PsMT_A* coding sequence inserted in the correct frame and orientation for expression as a carboxyl terminal extension of GST) using a glutathione affinity matrix (Tommey *et al.* 1991). Metal stoichiometries were calculated for the fusion protein extracted from cells grown in media which had been supplemented with 500 μ M zinc, cadmium or copper (Tommey *et al.* 1991, Robinson *et al.* 1992). As a control this was repeated for GST extracted from cells expressing the wild-type pGEX3X vector. In three replicate experiments the fusion protein bound zinc in the ratio 4.27, 7.80, 5.98 gram-atoms per mole of protein, 4.10, 4.41, 4.82 gram-atoms of cadmium per mole of protein and 3.53, 3.21 and 2.94 gram-atoms of copper per mole of protein (Tommey *et al.* 1991). The GST protein alone did not bind significant quantities of any of the metal. The values determined were quite variable, especially for zinc. The suggested cadmium stoichiometry (an average of 4.4) is lower than that found by Kille *et al.* (1991). In a later paper revised values for metal stoichiometries of the GST-PsMT_A fusion protein of copper 6.27:1, cadmium 7.07:1 and zinc 5.99:1 were reported (Robinson *et al.* 1992). This inconsistency probably reflects both the difficulty in determining an accurate value for protein concentrations and in maintaining the protein in a reduced state. The procedure for protein determination for the fusion protein

was a modified Bradford assay using BSA as a standard which will be affected by differences in reactivity between the fusion protein and BSA to the assay reagents. Kille *et al.* estimated protein concentration by amino acid analysis but they had a heterogenous protein sample. Although the assignment of appropriate stoichiometries is difficult it is clear that the PsMT_A protein is capable of binding copper, zinc and cadmium ions, supporting the inference from the sequence analysis that it may have an analogous function to metallothionein. The GST-PsMT_A fusion protein did not bind any detectable quantities of iron (Robinson *et al.* 1992).

In addition to estimating the stoichiometries of the PsMT_A-GST fusion protein for copper, zinc and cadmium Tommey *et al.* estimated the relative affinity of the protein for the three metals by measuring the pH at which 50 % of the metal dissociates from the protein. Those values determined for protein isolated from *E. coli* supplemented with the particular metals are; copper pH 1.45, cadmium pH 3.95 and zinc pH 5.25. As a control the equivalent values were calculated for a commercially obtained sample of equine MT-1 and found to be; copper-pH 1.80, cadmium-pH 3.00 and zinc-pH 4.50 which agreed with previously reported values (cited in Tommey *et al.* 1991). The implication of these results is that the *P. sativum* root metallothionein-like protein has a relatively higher affinity for copper and a relatively lower affinity for cadmium and zinc than mammalian metallothionein and strongly suggests that the PsMT_A protein would selectively bind copper *in planta*. The value for pH of half dissociation for phytochelatin, isolated from the yeast *S. pombe* for cadmium is pH 4.0 in the presence of inorganic sulphide and pH 5.4 without sulphide (Reese *et al.* 1988). For copper the value was pH 1.3. Other reports of values of pH of half displacement of cadmium for phytochelatin isolated from various plant and yeast sources vary from 4.4 to 6.4 (Wagner 1984, Reese *et al.* 1987a, Hayashi *et al.* 1988). If this range of values is representative for phytochelatin synthesised in *P. sativum* then on this basis the apo-PsMT_A protein could compete with phytochelatin for cadmium in plant cells challenged with that metal.

Evidence of copper binding by the PsMT_A gene product in plants was obtained from studies of metal accumulation in transgenic *Arabidopsis thaliana* (Evans *et al.* 1992). The plants were transformed with a construct containing the PsMT_A gene under the control of the cauliflower mosaic virus 35 S (CaMV 35 S) promoter. In a segregating progeny, derived from a single F₁ parent expressing PsMT_A, 75 % of individuals accumulated more copper than any of the control plants. Although it was not confirmed by genetic analysis, this data

strongly suggests that the constitutive expression of *PsMT_A* resulted in the increased accumulation of copper.

1.10 Objectives of this research

It has been proposed that metal binding to the product of the plant metallothionein-like gene from *P. sativum* could involve the formation of a metal complex involving the two cysteine rich domains of the protein. The metal ligands are predicted to be exclusively thiol bonds to cysteine side chains (Kille *et al.* 1991). An initial aim of this project was to attempt to address this question using [¹¹³Cd] NMR spectroscopy to determine the structure of the metal binding complex formed by the recombinant GST-*PsMT_A* fusion protein (chapter 4). A limitation to the determination of the role of the plant metallothionein-like genes and their products has been the failure to identify the translational products of the genes in plant tissue. An antibody which recognised the gene product would be a useful tool in achieving this aim. An immune sera had been produce in rabbits inoculated with the GST-*PsMT_A* fusion protein (A.M. Tommey unpublished). A further aim was to characterise the epitope of this immune sera with the long term objective of using it to identify, and potentially help isolate, the translational product of the *PsMT_A* gene in plant tissue (chapter 4).

As this project has progressed the number of plant species in which plant metallothionein-like genes have been identified has greatly increased and reported information which has accumulated on these genes will be reviewed in chapter 3. With an increased sample size extensive analysis of the primary structures predicted by these genes has been possible (chapter 3). Arising out of this analysis has been the proposal that there may be more than category of these predicted gene products and that the different categories of protein could have different metal binding properties. To examine this possibility it was proposed that the plant metallothionein-like gene expressed in the leaves of *A. thaliana* should be cloned and the product of the gene produced as a GST fusion protein in *E. coli* allowing direct comparison to be made of the zinc preferences of this peptide and the GST-*PsMT_A* fusion protein (chapter 5). To further explore the potential zinc binding properties of the product of the *A. thaliana* gene it was proposed to study the effect on zinc tolerance of expressing the gene in a zinc metallothionein deficient mutant of the cyanobacteria *Synechococcus* PCC 7942 (strain R2-PIM8) (in collaboration with Dr. J.S. Turner).

Insight into the function of a protein can be gained from a study of the factors influencing the expression of the gene. To gain more information on the potential role of the putative PsMT_A protein an objective of this project was to determine the effects of variations of exogenous trace metal concentrations on expression of the *PsMT_A* gene in roots (chapter 6).

Finally the characterisation of the recombinant PsMT_A protein reported prior to the start of this project lead to the proposal that the protein would be associated with metal, probably copper or zinc, in plant tissue (Tommeey *et al.* 1991). A further aim of the project therefore was to isolate copper and zinc ligands from the roots of *P. sativum* with the same characteristics as those predicted for the putative product of the *PsMT_A* gene (chapter 7). Initially it was planned to screen extracts from pea roots with the anti-GST-PsMT_A immune sera. As the project developed alternative strategies to identify the plant metallothionein-like protein in root extracts were developed (chapter 7).

CHAPTER 2

GENERAL MATERIALS AND METHODS

2.1 Materials

2.1.1 Chemicals, reagents and laboratory consumables

Unless otherwise stated, general laboratory chemicals were obtained from the Sigma Chemical Company (Poole, Dorset). Other reagent and consumable suppliers are stated below:

3 MM chromatography paper; Whatman Ltd. (Maidstone, Kent, U.K.).

Radiochemicals, hybridisation membranes; Amersham International Ltd. (Bucks., U.K.).

Gel permeation products (Sephadex G-50, DEAE Sephadex, PD-10, glutathione Sepharose 4B; Pharmacia LKB (Milton Keynes, U.K.).

Electrophoresis grade agarose; GIBCO-BRL Ltd. (Paisley, Scotland).

Protein assay reagent: Bio-Rad Laboratories Ltd. (Hemel Hempstead, Hertfordshire, U.K.).

Scintillation fluid (Ecoscint A); National Diagnostics (Mannville, New Jersey).

Fuji X-ray film; Fuji Photo Film Co. Ltd. (Japan).

Yeast extract, Bacto-Agar; Difco (Detroit Michigan, USA).

Trypticase peptone; Beckton Dickinson (F-38240, Maylan, France).

Restriction enzymes, DNA modification enzymes, IPTG; Northumbria Biologicals Ltd. (Cramlington, Co. Durham) or Boehringer Mannheim Ltd. (Lewes U.K.).

Immobilon PVDF transfer membranes: Millipore Corporation (Bedford, U.K.).

DNA purification kits; Promega Ltd. (Enterprise Rd., Southampton, U.K.), Qiagen Ltd (Surrey, U.K.)

DNA labelling kit: Appligene Ltd. (Chester-le-Street, Co. Durham, U.K.).

P. sativum seeds: Samuel Yates Ltd. (Macclesfield, Cheshire, U.K.).

2.1.2 *E. coli* strains

The *E. coli* (K12) strains used in this research were: JM101 [*supE*, Δ (*lac-proAB*), {F'*traD36*, *proAB*, *lacI*^{qZ} Δ M15}, (*r_k*⁺, *m_k*⁺), *mcrA* (+)], and SURE [e14' (*mcrA*), Δ (*mcrCB-hsdSMR-mrr*)171, *sbcC*, *recB*, *recJ*, *umuC*::Tn5(*kan*^r), *uvrC*, *supE44*, *lac*,

gyrA96, relA1, thi-1, endA1 {F' *proAB, lacI^qZΔ M15, Tn10, (tet^r)*}. Obtained from Northumbria Biologicals Ltd. (Cramlington, U.K.).

2.1.3 Plasmids

Commercially supplied plasmid, pGEX3X, obtained from Pharmacia LKB Biotechnology (described in Smith and Johnson 1988). The plasmid pGPMT3 (Tommeey *et al.* 1991), transformed into *E. coli* strain JM101 (section 2.1.2) was available for this research. The pGPMT3 plasmid consists of the pGEX3X vector containing the coding sequence of the *PsMT_A* gene as an insert in the correct orientation for the expression of the protein as a carboxyl extension of GST. The advantage of expressing a protein as a GST fusion protein is the ability to recover high yields of the purified fusion protein using a glutathione-sepharose affinity matrix (section 2.3.2). The bridge between the GST moiety and the attached protein of interest is such that that GST and the attached protein form independent domains allowing both to retain their activity (Smith and Johnson 1988). Additionally the linking amino acid sequence includes the cleavage site for the proteolytic factor Xa enzyme.

2.2 Media and buffers

Distilled water was used in pea growth media. The water used for DNA manipulation was double-deionised (MilliQ). Water used for RNA manipulation was further treated for denaturation of RNAases by addition of 0.1 % (v/v) diethylpyrocarbonate, incubated at 25 °C for 16 h, followed by autoclaving. Unless otherwise stated distilled water was used in buffer solutions.

2.2.1 Buffers used in DNA manipulations

Restriction enzyme and DNA modification enzyme reaction buffers were supplied with the enzymes. Other buffers used in DNA or RNA manipulations were as described by Sambrook *et al.* (1989).

2.2.2 Maintenance of *E. coli* cultures.

E. coli were grown in Luria-Beltrami (LB) media (Sambrook *et al.* 1989) at 37 °C with constant shaking. Transformed cultures were supplemented with 100 µg ml⁻¹ as required.

Solid LB medium used for plating contained 1.5 % (w/v) agar. Cultures maintained in long term storage were stored in 1 ml aliquots containing 50 % (w/v) glycerol at -80 °C.

2.2.3 Hydroponic growth media for *P. sativum* seedlings

The hydroponic solution was based on that used for the study of the phenotype of the *P. sativum* iron uptake mutant E107 (Grusak *et al.* 1990). The macronutrient solution was used within one day of being made, a stock of 100 x micronutrients was prepared and used within 2 weeks.

Macronutrients		Micronutrients	
KNO ₃	1.2 mM	CaCl ₂ ·2H ₂ O	25 µM
Ca(NO ₃) ₂ ·4H ₂ O	0.8 mM	H ₃ BO ₃	25 µM
NH ₄ H ₂ PO ₄	0.1 mM	MnSO ₄ ·4H ₂ O	2 µM
MgSO ₄	0.2 mM	NaMoO ₄	0.5 µM
		NiSO ₄ ·7H ₂ O	0.1 µM

In the original hydroponic solution specified by Grusak *et al.* (1990) zinc, copper and iron were included as;

ZnSO₄·7H₂O - 2.0 µM

CuSO₄·5H₂O - 0.5 µM

Iron-EDDHA - 1.0 µM and 2.0 µM day 12 to harvest (for recipe section 2.2.3.1)

In all metal treatments, from day 8 the hydroponic solution was supplemented with 1 mM Mes buffer (pH 5.5).

2.2.3.1 Preparation of Iron(III)-EDDHA

Iron EDDHA (N,N'-ethylenebis[2-(2-hydroxyphenyl) glycine] was prepared for the hydroponic media as follows: EDDHA (0.36 g) was dissolved in 1 l of an ice cold solution of 4 mM sodium hydroxide. As there is a 4-fold excess of NaOH compared to EDDHA the solution is greater than pH 11. The ferric iron salt, Fe₂Cl₃·6H₂O (0.27 g) was added. The ferric iron salt displaces protons from the chelate and the pH falls to between pH 6 and pH 7. The solution was filtered to remove any undissolved salt and the iron concentration checked

by atomic absorption spectrophotometry. The solution was stored in a foil covered container at 4 °C.

2.2.4 Buffers required for proton displacement experiments

<u>Buffer</u>	<u>pH range</u>
potassium chloride - hydrochloric acid	1.5 to 2.3
glycine - hydrochloric acid	2.4 to 3.7
sodium acetate - hydrochloric acid	3.8 to 5.6
potassium phosphate - orthophosphoric acid	5.8 to 9.0

2.2.5 Other commonly used buffers

SSC (1 x): 0.15 M NaCl, 0.015 M sodium citrate, pH 7.0

SSPE (1 x): 0.18 M NaCl, 0.01 M Na₂HPO₄, 1 mM EDTA, pH 7.4.

PBS: 16 mM Na₂HPO₄, 150 mM NaH₂PO₄, 4mM NaCl, pH 7.3.

TBE: 0.089 M Tris, 0.089 M boric acid, 2 mM EDTA, pH 8.0.

TBS: 150 mM NaCl, 20 mM Tris, pH 7.4

2.3 General methods in protein biochemistry

2.3.1 Expression of GST fusion proteins in *E. coli*

Proteins were expressed in *E. coli* as carboxyl terminal extensions of the glutathione-S-transferase protein from *Schistosoma japonicum* using the pGEX3X vector system (Smith and Johnson 1988). Plasmids based on the pGEX3X vector were over-expressed in *E. coli* essentially according to the method of Smith and Corcoran (1990). An overnight culture of the pGEX3X vector in *E. coli* in LB medium was diluted 1:10 with fresh media and incubated with shaking at 37 °C, for 45 minutes. Metal, as sulphate, was added to 500 µM if required and growth continued for 15 minutes. Expression of the fusion protein was induced by addition of isopropyl-β-D-thiogalactoside (IPTG) to a final concentration of 1 mM. Growth was continued in the above conditions until harvest.

As an approximate indication of cell density the absorbance of 200 µl of the culture was determined using a microtitre plate reader at 595 nm. Upon reaching a value of approximately 0.500 absorbance units cells were harvested, and pelleted by centrifugation at 3500 x g for 10 minutes (Beckman rotor JA-20 at 5500 rpm). The pellet was resuspended in

ice cold PBS (1 % (v/v) of the original culture volume). Cells were lysed by mild sonication of the suspension at 4 °C and the anionic detergent Triton X-100 added to 1 % (v/v) to prevent association of the fusion proteins with bacterial proteins. Cell debris was removed by centrifugation at approximately 10000 x g for 10 minutes at 4 °C (Beckman rotor JS-13.1 at 10000 rpm) and the supernatant stored on ice.

2.3.2 Purification of fusion proteins from a crude *E. coli* extract using a glutathione affinity matrix

The fusion protein was separated from the crude *E. coli* lysate by a single step affinity purification step using glutathione-Sepharose 4B essentially according to the manufacturers protocol. A column containing approximately 2 ml affinity matrix per litre of original culture was prepared and equilibrated with at least 10 bed volumes of PBS. The crude *E. coli* extract was loaded onto the column and allowed to pass through the matrix with a flow rate of approximately 1 ml min⁻¹. The column was washed with one bed volume of ice cold PBS + 1 % (v/v) Triton X-100 followed by 3 to 4 bed volumes of ice cold PBS. The matrix was finally washed with one volume of 50 mM Tris-HCl, pH 8.0 before elution of the fusion protein with a solution of 5 mM reduced glutathione in 50 mM Tris-HCl, pH 8.0 (5 to 10 ml elution buffer for 2 ml matrix).

[Note; in later purifications the elution buffer was changed to 10 mM reduced glutathione in 50 mM Tris-HCl, pH 8.0 in accordance with the manufacturers revised protocol].

The affinity matrix was regenerated for re-use. The column was washed with 5 volumes of 5 mM reduced glutathione in 50 mM Tris-HCl, pH 8.0 to remove any residual fusion protein. The matrix was washed with 3 bed volumes of 0.1 M Tris-HCl + 0.5 M NaCl, pH 8.5 followed by 0.1 M sodium citrate + 0.5 M NaCl, pH 4.5. This was repeated three times and then the column was re-equilibrated in an excess of PBS.

2.3.3 Estimation of protein concentration

Protein concentration was estimated using a Bradford assay (Bradford 1976) modified for the microtitre plate reader. A commercial protein assay reagent based on Coomassie Brilliant Blue G-250 was used. The colour change shift from 465 nm to 595 nm when protein binding occurs was followed. The absorbance, at 595 nm, of a measured volume of the unknown protein sample was compared to a calibration curve constructed from known concentrations

of bovine serum albumin (BSA) over a range of 0 to 2 μg . A standard curve was determined coincident with each set of estimations and duplicates of the unknown sample were used. It should be noted that the protein estimation method does not account for differences in dye binding between the standard, BSA, and the unknown protein. The molecular weight of the fusion protein is approximately 35,000, which is about half that of BSA. As the method gives yields for the GST gene fusion purification system compatible with the published protocol (Smith and Corcoran 1990), it was assumed that estimated protein concentrations were a reasonable approximation. The reagent was also used as an indicator of bulk protein in the analysis of chromatography fractions. In this case the protein concentration was not estimated as only a proportional response to the amount of protein in solution was required.

2.3.4 Cleavage of the GST fusion protein with Factor Xa

The design of the multi-cloning site, downstream from the GST gene, in the pGEX3X vector includes a coding sequence for an enzyme cleavage site which allows separation of the coupled protein (Smith and Johnson 1988). This is the specific cleavage site of the blood coagulation factor Xa, which is activated by Russel's viper venom. Cleavage of GST fusion proteins was performed essentially as described by Smith and Corcoran (1990) with the following modifications.

The fusion protein purification was performed up to, and including, washing the column bound protein with PBS. The column was washed with one column volume of wash buffer, 50 mM Tris-HCl, pH 7.5 containing 150 mM NaCl, and then once with the same volume of cleavage buffer (the wash buffer + 2.5 mM CaCl_2). The column was drained and closed. A reaction mixture containing cleavage buffer (2.5 ml) and 5 units of activated bovine Factor Xa was added and the Sepharose slurry thoroughly mixed. The column was incubated overnight at 25 °C. The Sepharose was mixed again and the cleavage buffer eluted from the column, a further 1 ml of cleavage buffer was passed through the column and pooled with the reaction mixture. The fusion protein was separated from the Factor Xa by gel filtration chromatography on Sephadex G-50.

2.3.5 Methods used to increase the concentration of protein solutions

Reduced glutathione was removed from the protein samples (obtained by the method described in section 2.3.2) by desalting on Sephadex G-25 columns (Pharmacia PD-10).

2.3.5.1 Acetone precipitation The protein solution was thoroughly mixed with 4 volumes of acetone and incubated at -80 °C for 3 h. The solution was cleared by centrifugation (approximately 900 x g) for 20 min. The acetone was decanted and the pellet allowed to air dry at 4 °C for 10 to 15 min. The pellet was not allowed to dry out completely and whilst still opalescent it was resuspended in the minimum possible volume of buffer.

2.3.5.2 Microconcentrator centrifuge vials The protein solution in 2 ml aliquots were placed in Centricon C-10 microconcentrator tubes (Centricon Corporation). The membrane in the C-10 tube has a molecular weight cut-off of 10 000, this is well below the molecular weight of the fusion protein. The tubes were centrifuged at approximately 900 x g in the desk top centrifuge for 20 minutes giving an approximately 10-fold reduction in volume. After concentration the protein solutions were assayed for protein as described in section 2.3.3.

2.3.6 One-dimensional polyacrylamide gel electrophoresis in SDS

Slab gel electrophoresis was performed on either the Bio-Rad 'Mini-Protean II' electrophoresis apparatus with gels 0.75 mm thick, or on the 'Protean II' apparatus with gels 1 mm thick. A stock solution of 30 % (w/v) acrylamide and 0.8 % (w/v) bisacrylamide was prepared and deionised by mixing the solution with Amberlite monobed resin for 2 h before filtering the solution through Whatman No. 1 filter paper.

Protein samples were treated prior to loading in a sample buffer solution consisting of, 0.1 M Tris-HCl, pH 6.8, 10 % (v/v) glycerol, 0.4 % (w/v) SDS, 1 % (v/v) 2-mercaptoethanol. Bromophenol blue was added as required.

2.3.6.1 Standard electrophoresis Polyacrylamide gel electrophoresis of proteins was performed essentially as described by Laemmli (1970). A continuous buffer system was used; 25 mM Tris base, 192 mM glycine, 0.1 % (w/v) SDS, pH 8.3. The gel buffers were as follows; Stacking gel buffer (4x) - 0.5 M Tris-HCl, 0.4 % (w/v) SDS, adjusted to pH 6.8. Resolving gel buffer (4x) - 1.5 M Tris-HCl, 0.4 % (w/v) SDS, adjusted to pH 8.8. A 4 % (w/v) acrylamide stacking gel and 12.5 % (w/v) acrylamide resolving gel was prepared with cross linking catalysts, ammonium persulphate and TEMED. Electrophoresis was performed

at a constant voltage of 200 V (mini-Protean II) or 140 V (Protean II) until the tracking dye had reached the bottom of the gel.

2.3.6.2 Tricine buffer electrophoresis A tricine buffer electrophoresis system was used essentially as described by Schägger and von Jagow (1987). A discontinuous buffer system was used; Cathode buffer (10 x) 1 M Tris base, 1 M tricine, 1 % (w/v) SDS, pH 8.25. Anode buffer (10x) 2 M Tris-HCl, adjusted to pH 8.9. The following gel buffer was used; Gel buffer (3x) 3 M Tris base, 0.3 % (w/v) SDS, adjusted to pH 8.45. 7.5 % (v/v) glycerol was added to give the gel mechanical strength.

A 5 % (w/v) acrylamide stacking gel and a 15 % (w/v) acrylamide resolving gel was prepared with cross linking catalysts, ammonium persulphate and TEMED. Electrophoresis was performed at a constant voltage of 100 V for approximately 18 h (Protean II). Gels were stained for 30 - 60 min with Coomassie brilliant blue G - 250 in 40 % (v/v) methanol, 8 % (v/v) acetic acid and destained with the same buffer until adequate band definition was achieved.

2.3.7 Two-dimensional polyacrylamide gel electrophoresis in SDS

Two dimensional gel electrophoresis was performed essentially as described by Sinclair and Rickwood (1981)

2.3.7.1 Isoelectrofocusing. The protein extract was resuspended in isoelectrofocusing sample buffer (9 M urea, 5 % (v/v) 2-ME, 2 % (v/v) pharmalyte (ampholine mixture), 2 % (v/v) nonidet P-40). Aliquots of the sample (approximately 100 μ l) were loaded onto 5 % (w/v) acrylamide rod gels (pre-run at 200 V for 15 min, 300 V for 30 min and 400 V for 30 min with 20 mM NaOH cathode buffer and 10 mM phosphoric acid anode buffer). The sample was overlaid with 9.5 M urea and the rod gels run overnight at 300 V and then 1 h at 800 V. A blank gel, loaded with sample buffer alone was included. To estimate the pH gradient following electrophoresis this gel was cut into 1 cm segments which were incubated for 1 h in 500 μ l 0.025 M KCl and the pH of the solution was measured using a glass electrode.

2.3.7.2 Second phase electrophoresis. The rod gels were incubated at -20 °C for 1 h and the gel removed by water pressure and incubated in Laemmli sample buffer for 2 h. The rod gels were laid onto tricine gels and electrophoresis performed as described in section 2.3.6.2. Protein was transferred to PVDF membrane by electroblotting (section 2.3.8), stained with Coomassie blue, air dried and exposed to photographic film.

2.3.8 Semi-dry electroblotting of polyacrylamide gels onto membrane

Protein samples were transferred to nitrocellulose or PVDF membrane by the semi-dry method (Sartorius electro-blotter with graphite plates) using either the discontinuous buffer system (described by Kyhse-Anderson 1984) or the continuous buffer system (described by Beisiegel 1986). The components were soaked in an appropriate buffer and a sandwich made of the nitrocellulose or PVDF membrane and gel between several layers of filter paper, the sandwich was placed on the anode plate membrane side down. Electrotransfer was performed at a current of 0.8 mA per square centimeter of gel for 1 to 2 h depending on the thickness of the gel.

2.3.9 Western Blotting

Following electroblotting, nitrocellulose was stained with a 0.1 % (w/v) solution of Ponceau S in 1 % (v/v) acetic acid for 5 to 10 min, partially destained in 1 % (v/v) acetic acid (2 min) and photographed. The blot was completely destained in PBS (5 min). The blot was placed in a solution of 4 % (w/v) BSA in TBS for 10 to 20 min at room temperature with shaking to block unoccupied sites on the filter. After washing in TBS the blot was incubated overnight in primary antibody (1:500 dilution) in TBS + 0.05 % (v/v) Tween-20. After thoroughly washing in TBS to remove the primary antibody the blot was incubated for 2 h in secondary antibody (1:9000 dilution of goat anti-rabbit IgG conjugated to alkaline phosphatase) in TBS + 0.05 % (v/v) Tween-20. After a final wash to remove the excess secondary antibody the blot was developed. The developer was a 1:200 fold dilution of a stock solution of BCIP (50 mg ml⁻¹ in 100 % (v/v) dimethylformamide) and a 1:100 dilution of a stock solution of NBT (35 mg ml⁻¹ in 70 % (v/v) dimethylformamide) in 100 mM NaCl, 100 mM Tris-HCl, 5 mM MgCl₂, pH 9.5. The reaction was stopped in 1 % (v/v) acetic acid after the image had developed.

2.3.10 Crude protein extraction from roots of *P. sativum*

Two methods were employed to produce crude protein extracts from roots of *P. sativum*. An initial method based on that described by Robinson *et al.* 1992 (described in section 2.3.10.1) and a subsequent method based on that of on Hurkman and Tanaka (1985) (described in section 2.3.10.2). *P. sativum* seedlings were grown as described in section 2.4.1.

2.3.10.1 Original protein extraction protocol Roots of *P. sativum* (30 to 40 g) were harvested, rinsed in distilled water and blotted dry. An equal volume of extraction buffer (0.1 M ammonium acetate, 1 % (v/v) 2-ME, pH 5.5) was added and roots were homogenised with a hand held electric blender. The resulting slurry was strained through two layers of sterilised muslin and remaining debris removed by centrifugation (MSE Centaur 2) at 900 x g for 15 minutes. This extract was concentrated by acetone precipitation as described in section 2.3.5.1. The resuspension buffer was 10 mM Tris, 1% (v/v) 2-ME, pH 7.2.

2.3.10.2 Revised protein extraction protocol Roots of *P. sativum*, approximately 0.5 g were ground to a fine powder under liquid nitrogen. The roots were allowed to thaw and mixed thoroughly with 4 ml sample buffer (0.7 M sucrose, 0.5 M Tris, 30 mM HCl, 0.1 M KCl, 2 % (w/v) 2-ME). The mixture was incubated on ice for 30 min and debris was removed by centrifugation (Beckman JA-20 rotor 5000 rpm, 5 min). One volume of phenol was added, mixed and the sample incubated on ice for 45 min. Phases were separated by centrifugation (Beckman JS-13.1 rotor, 6000 rpm, 10 min). The upper phenol phase was transferred to a fresh tube and 5 volumes of ice cold 0.1 M ammonium acetate in methanol added. Protein was precipitated overnight at -20 °C. A pellet was produced by centrifugation (Beckman JS-13.1 rotor, 5000 rpm, 10 min) and washed in methanol/NH₄Ac three times and once in acetone. The pellet was air dried and resuspended in a minimum volume of Laemmli sample buffer (200 - 300 µl).

2.3.11 Chromatography

All chromatography was performed at 4 °C.

2.3.11.1 Ion exchange chromatography Sephadex DEAE (A-25) anion exchange matrix was used for ion exchange chromatography. The matrix (10 g) was swollen by boiling in 10 mM Tris-HCl, pH 7.2 (2 h) and transferred to a glass column (1 cm diameter). The column was connected to a peristaltic pump to control the flow rate and allowing collection of fractions. Before use the matrix was equilibrated in 10 mM Tris-HCl, 1 % (v/v) 2-ME, pH 7.2 and packed by a slightly increased flow rate.

2.3.11.2 Gel filtration chromatography Sephadex G-50 (course) media was used for gel filtration chromatography. The media was hydrated by boiling for 2 h in 50 mM Tris-HCl, pH 8.0. The media was transferred to a glass column (approx. 2 cm x 100 cm) and linked to a peristaltic pump and packed under pressure. Prior to use the column was equilibrated in the appropriate buffer by running overnight under gravity. The sample was loaded by pipetting and the column connected to the peristaltic pump.

2.3.12 Protein sequencing

Protein samples were blotted onto Immobilon PVDF microporous membrane and subjected to automated amino acid sequence analysis on an ABI model 477A gas-phase microsequencer using standard operating procedures.

2.3.13 Atomic absorption spectrophotometry

The concentration of metal ions in solution was measured by atomic absorption spectrophotometry using a Perkin Elmer Model HGA spectrophotometer according to the manufacturer's protocols. Metal was quantified using a calibration graph constructed from measurements of known standards. A calibration graph was constructed for each set of measurements.

2.4 Growth of *P. sativum* seedlings in hydroponic solution

Pea seedlings were grown in hydroponic solution essentially as described by Grusak *et al.* (1990) with minor modifications;

Day 0 - Desiccated *P. sativum* seeds (*P. sativum* L. Feltham First, untreated with anti-fungicidal agents) were surface sterilised by soaking in a 10 % (w/v) sodium hypochlorite solution for 1 h. The seeds were thoroughly rinsed in distilled water, then imbibed overnight in distilled water with aeration. The peas were transferred to a seed tray, lined with tissue paper and soaked in distilled water to germinate.

Day 1 - The tray was placed in a 'spray room'. A dark chamber, at 22 - 25 °C, kept constantly moist by a light spray of water at regular intervals.

Day 3 - The germinated seedlings were transferred to hydroponic solution (described in section 2.2.3). The seedlings were suspended in a black foam float, in a blackened 2 l polypropylene bottle. (3 seedlings per bottle) The bottles were transferred to a growth chamber, 16 h light cycle, at 22 °C daytime temperature.

Day 8,10,12,13,14, - Hydroponic solution changed.

Day 15 - Hydroponic solution changed, seedlings harvested. *P. sativum* seedlings were removed intact from the hydroponic solution, the root system was rinsed briefly in distilled water and blotted dry with tissue paper. The entire root system was removed by cutting approximately 1 cm below the seed and either used immediately or immersed in liquid nitrogen and stored frozen at -80 °C.

2.5 General methods in molecular biology

Unless otherwise stated methods were performed as described by Sambrook *et al.* (1989).

2.5.1 Small scale isolation of plasmid DNA from *E. coli*

Two main methods of plasmid DNA preparation were employed. An adaptation of the alkaline lysis method of Mierendorf and Pfeffer (1987), and commercial kits utilising purification resins.

2.5.1.1 Alkaline lysis method; Small (5 ml) overnight cultures of *E. coli* were used as a source of bacteria. The solutions and method were as described by Mierendorf and Pfeffer (1989). Following the initial isolation plasmid DNA was precipitated by incubation with 400 µl of propan-2-ol for 20 min and pelleted by centrifugation in a microcentrifuge (1000 x g in a MSE Microcentaur). DNA was washed in 70 % (v/v) ethanol, dried in a vacuum desiccator and resuspended in distilled deionised water (30 µl). The method typically yields about 5 µg DNA.

2.5.1.2 Isolation with DNA extraction resin; Commercial extraction kits; Promega 'Magic' miniprep (renamed 'Wizard') kit or on a larger scale Qiagen midiprep kits. These kits were used according to the manufacturers instructions with minor modifications in the volume of buffer used for washing the DNA. These methods were employed chiefly to supply very pure DNA for automated sequencing.

2.5.2 Agarose gel electrophoresis of nucleic acids

2.5.2.1 Agarose gel electrophoresis of DNA Performed as described by Sambrook *et al.* (1989). Gels of 0.8 % (w/v) or 1.5 % (w/v) agarose in Tris-borate buffer were employed. The DNA loading dye contained 0.25 % (w/v) each of bromophenol blue and xylene cyanol, and 15 % (w/v) Ficoll 400. Electrophoresis was performed at a constant voltage of 100 V in Tris-borate running buffer. Electrophoresed DNA was visualised by ethidium bromide staining.

2.5.2.2 Denaturing electrophoresis of RNA Performed as described by Sambrook *et al.* (1989). A 1.2 % (w/v) agarose gel in MOPS running buffer (20 mM MOPS, 5 mM sodium acetate, 1 mM EDTA, pH 7.2) and 15 % (v/v) formaldehyde was prepared. An aliquot of RNA solution (approx. 15 µg) was denatured by mixing 1:2 with denaturing solution (67 % (v/v) formamide, 20 % (v/v) formaldehyde, 13 % (v/v) 10 x running buffer) and incubating at 60 °C for 5 min. The denatured solution was mixed with loading buffer and loaded onto the gel. Electrophoresis was performed at a constant 100 V for 4 to 6 h.

2.5.3 Isolation of DNA restriction fragments from agarose gels

Following ethidium bromide staining DNA bands were cut from the agarose gel and placed in Eppendorf tubes. The gel slice was incubated in 1 ml sodium iodide solution (NaI and Na₂SO₄) at 65 °C until the agarose had melted. An aqueous suspension of silica fines (5 µl) was added and the mixture incubated for 15 minutes at room temperature with frequent mixing. The silica-DNA suspension was pelleted by centrifugation (1000 x g) for 15 seconds, washed with 70 % (v/v) ethanol and dried in a vacuum desiccator. The DNA was eluted from the silica fines by incubation in water at 37 °C for 10 to 15 minutes.

2.5.4 Further purification of DNA

2.5.4.1 Phenol / chloroform extraction. One volume of phenol:chloroform:isoamyl alcohol (24:24:1) was added to the DNA solution and thoroughly mixed. The mixture was separated into an aqueous and phenol phase by centrifugation for 30 seconds. The upper aqueous phase was removed and precipitated with ethanol.

2.5.4.2 Ethanol precipitation. Sodium acetate, pH 5.5 was added to the DNA solution to 0.1 M. Two volumes of ethanol were added, the solution mixed and incubated at -80 °C for 15 minutes or -20 °C for 60 minutes. The DNA was pelleted by centrifugation, washed in 70 % ethanol and dried in a vacuum desiccator. DNA was resuspended in an appropriate volume of deionised distilled water.

2.5.5 DNA restriction digests

DNA restriction was performed as described by Sambrook *et al.* (1989). DNA was incubated with restriction enzyme in the diluted manufacturers buffer at the specified temperature for 2 h. For double restrictions where different buffers were required by individual enzymes '1-phor-all buffer plus' (Promega) was substituted.

2.5.6 Preparation and transformation of competent *E. coli* cells

Competent *E. coli* cells were prepared and transformed according to the method of Chung *et al.*, (1989). Aliquots of the transformed cells were plated onto solid LB medium containing antibiotic selection. Resulting colonies were screened by restriction analysis and inserts checked by sequence analysis.

2.5.7 Oligonucleotide synthesis and DNA sequence analysis

Oligonucleotides were synthesized using an Applied Biosystems 381A DNA synthesiser operated with a standard synthesis program. After cleavage and deprotection the oligonucleotides were dried under vacuum, resuspended in water and vacuum dried. Oligonucleotides were stored at -20 °C in aqueous solution and used without further purification.

Plasmid sequencing was performed by the dideoxy-sequencing method of Sanger *et al.* (1977), using dye linked M13 primers. Sequences were analysed using an Applied

Biosystems 370A DNA sequencing system as described in the suppliers protocol (Users manual version 11.3A, October 1988, pp. 3.22-3.25).

2.5.8 Polymerase chain reaction (PCR) for *in vitro* amplification of DNA

PCR reaction was carried out essentially as described by Tommey *et al.*, (1991). The PCR reaction mixture was prepared as follows;

Primers	10 μ l of both primers (60 pM stock)
dNTP	16 μ l (200 μ M dATP, dCTP, dGTP, dTTP)
10 x buffer	10 μ l
Taq polymerase	1 μ l
DNA	5 μ l (~15 to 100 ng depending on source, plasmid or cDNA)
Water	48 μ l
Mineral oil	100 μ l

The reaction conditions followed those described in Tommey *et al.* (1991). A Hybaid intelligent heating block provided 3 cycles of temperatures and times as follows; denaturation - 92 °C - 1.5 min, annealing - 45 °C - 2.0 min and extension - 72 °C - 2.0 min. This was followed by a single cycle with an extended extension time of 5.0 min after which the samples were stored at -20 °C.

2.5.9 Preparation of radiolabelled DNA probes

DNA fragments were obtained by restriction (section 2.5.5) of plasmid DNA and isolation of the DNA fragment from agarose gels using silica fines (section 2.5.3). [α -³²P] dCTP was incorporated into the fragment by random priming using the procedure of Feinberg and Vogelstein, 1983. The DNA was separated from unincorporated label by either gel filtration chromatography on a small (10 ml total volume) Sephadex G-50 column, or using an 'Appligene nonprimer probe purification' kit according to the manufacturers instructions.

2.5.10 Total RNA extraction from pea roots

Total RNA was extracted from the roots of *P. sativum* seedlings essentially as described by Logemann *et al.* (1986) with minor modifications. Glassware was baked at 400 °C for 3 h to inhibit RNAase activity. Roots of *P. sativum* (approx. 1 g fresh weight) were ground to a fine powder, under liquid nitrogen. The roots were allowed to thaw slightly and mixed to a

paste with 2 ml fresh, filter sterilized extraction buffer (8 M guanidine hydrochloride, 20 mM Mes, 20 mM EDTA, 50 mM 2-ME, pH 7.0). Phenol:chloroform:isoamyl alcohol (24:24:1) was added (2 ml) and the solution transferred to a corex tube and thoroughly vortexed. The phases were separated by centrifugation at 3200 x g (4500 rpm Beckman JS 13.1 rotor) at 15 °C for 30 min. The upper, aqueous, phase was removed and the phenol:chloroform extraction repeated. The aqueous phase was made up to 5 ml with water and 0.4 ml 1M acetic acid and 3 ml ice cold 95 % (v/v) ethanol were added. The nucleic acid was precipitated by incubation at -20 °C for 1 h.

The nucleic acid was pelleted by centrifugation at 9000 x g (Beckman JS 13.1 rotor) for 30 min and washed with 70 % (v/v) ethanol. The pellet was dried on the bench (15 min) and resuspended in 500 µl water. The resulting solution was centrifuged for 30 sec in a microfuge to remove any undissolved material. To 470 µl of the solution in a fresh tube 117.5 µl 10 M lithium chloride was added and thoroughly mixed. The RNA was precipitated overnight at 4 °C.

The RNA was pelleted by centrifugation at full speed in a microfuge (15 minutes at 4 °C). The pellet was washed with 3M sodium acetate (pH 5.2) and then 70 % (v/v) ethanol. The RNA was dried briefly in a vacuum dessicator and resuspended in 80 µl water. The yield, 30 to 60 µg was determined by measurement of UV absorbance at 260 and 280 nm.

2.5.11 Hybridisation of radiolabelled DNA probes to filter-immobilised nucleic acids

Prehybridisation and hybridisation reactions were carried out in sealed glass tubes in a hybridisation oven.

2.5.11.1 Southern transfer of DNA

Following electrophoresis DNA was transferred to and immobilised onto membranes essentially by the method of Southern (1975) with modifications of Sambrook *et al.* (1989). The DNA was denatured by soaking the gel in 0.5 M NaOH, 1.5 M NaCl for 30 min and neutralised by soaking in an excess of 1.5 M NaCl, 0.5 M Tris-HCl, pH 7.5. Onto the gel was placed an appropriately sized piece of Hybond-N nylon membrane and DNA was transferred overnight in a reservoir of 6 x SSC by capillary action. The filter was removed and fixed by baking in a vacuum oven at 80 °C for 1 h.

2.5.11.2 Southern hybridisation conditions

The filter was incubated in prehybridisation solution (6 x SSC, 1 x Denhardt's solution, 0.05 % (w/v) PPI, 0.01 % (w/v) denatured herring sperm DNA, 0.5 % (w/v) SDS) for 4 h at 65 °C. The solution was replaced with hybridisation solution (6 x SSC, 0.5 x Denhardt's, 0.05 % (w/v) PPI, 0.5 % (w/v) SDS, 10 mM EDTA). The DNA probe was denatured by boiling for 10 minutes and added to the hybridisation solution and the filter incubated overnight. The filter was washed successively in 2 x SSC + 0.1 % (w/v) SDS and 1 x SSC + 0.1 % (w/v) SDS at room temperature for about 30 minutes, sealed in a plastic bag and placed in an X-Ray cassette next to photographic film. The cassette was sealed and stored at -80 °C for 7 days. After thawing the film was developed with standard photographic developer and fixer.

2.5.11.3 Northern transfer of RNA

Northern transfer of RNA was performed essentially as described by Sambrook *et al.* (1989) with modifications. The transfer buffer was 10 x SSC. The RNA was transferred to the nylon membrane overnight by capillary action. The RNA was fixed either by baking in a vacuum oven for 1 h at 80 °C or crosslinking under UV light.

2.5.11.4 Northern hybridisation conditions

The filter was incubated at 42 °C for 1 h in hybridising solution (50 % (v/v) deionised formamide, 5 x Denhardt's solution, 2.5 % (w/v) SDS, 0.01 % (w/v) denatured herring sperm DNA, 5 x SSPE). The DNA probe was denatured by boiling (10 min) and added to the hybridisation solution. The filter was incubated with the probe overnight. The filter was washed successively in 2 x SSC + 0.1 % (w/v) SDS and 1 x SSC + 0.1 % (w/v) SDS at room temperature (15 min each) and finally in 0.5 x SSC + 0.1 % (w/v) SDS at 60 °C (10 min). The filter was sealed in a polythene bag and placed in an X-Ray cassette next to the photographic film. The cassette was stored at -80 °C for 2 to 7 days (depending on apparent level of incorporation in the probe). The cassette was removed from the freezer and allowed to thaw for 30 minutes. The X-ray film was removed and developed using standard photographic developer and fixer.

CHAPTER 3
COMPARISON OF THE PREDICTED PRODUCTS OF
PLANT METALLOTHIONEIN-LIKE GENES

3.1 Introduction and objectives

At the start of this project genes with similarity to metallothionein had been reported from *M. guttatus* and *P. sativum* (de Miranda *et al.* 1990 and Evans *et al.* 1990). Homologues have subsequently been reported in a number of plant species by researchers studying a variety of phenomena, detailed in table 3.1 and section 3.1.1. Random sequencing of cDNA's (expressed sequence tags) account for an increasing number of submissions of plant metallothionein-like sequences to nucleotide databases. As a result many of the reports of these genes consist only of a database entry and very little information about the expression of the gene. To date there are still no reports of the isolation of the translational products of metallothionein-like genes from plant tissue. The only plant metallothionein for which the gene, mRNA and protein have been identified in plant tissue is the E_c protein from wheat embryo (Kawashima *et al.* 1992). An essential part of this project was to monitor the appearance of metallothionein-like genes from other species. In section 3.2 the published information relating to the isolation and characterisation of metallothionein-like genes in species in which they have been identified will be summarised. In section 3.4 a series of computer analyses of the predicted products of these genes are presented.

3.1.1 Published reports of plant metallothionein-like genes

3.1.1.1 *Mimulus guttatus*

A cDNA library was constructed from roots of copper-tolerant *M. guttatus* plants grown in media which had been supplemented with 10 µM CuSO₄ 24 hours before harvest (de Miranda *et al.* 1990). This library was probed with cDNA constructed from RNA isolated from plants grown with or without added copper. A total of 40 differentially expressed clones were identified, half repressed and half induced by copper shock. Five of these copper repressible clones were sequenced and found to have one of two distinct sequences, with minor differences in the coding region, with the same predicted amino acid sequence. The

presence of these two sequences was attributed to there being two copies of the gene in the genome.

Northern analysis confirmed that transcripts of the gene were repressed by copper shock but that plants grown continuously in the presence of 5 μM CuSO_4 had transcript levels approximately equivalent to plants grown in the absence of copper (de Miranda *et al.* 1990). The transcript levels were reduced in plants grown continuously in the presence of 5 μM CdSO_4 or 15 μM ZnSO_4 . Transcript levels were very low in RNA extracted from leaf tissue.

The cDNA sequence encodes a putative 72 residue polypeptide with 12 cysteine residues arranged in three Cys-Xaa-Cys motifs at both the carboxyl and amino terminal ends of the protein (de Miranda *et al.* 1990).

3.1.1.2 *Pisum sativum*

Published information relating to the metallothionein-like gene from *P. sativum* is presented in detail in section 1.9.3 of the introduction. A full genomic clone was obtained which contains a 634 base pair intron (Evans *et al.* 1990). During the course of this research it was shown that levels of gene transcripts in seedlings of *P. sativum* are reduced by the addition of iron to the growth media and can be restored by the addition of copper (Robinson *et al.* 1993).

The gene encodes a 75 residue polypeptide with 12 cysteine residues arranged in three Cys-Xaa-Cys motifs at both the carboxyl and amino terminal ends of the protein (Evans *et al.* 1990).

3.1.1.3 *Zea mays*

A cDNA library was constructed from RNA extracted from *Z. mays* roots (de Frammond 1991). This library was probed with RNA extracted either from root or from seed to identify clones which were expressed in root but not in seed. A clone was identified whose transcript consisted of approximately 600 nucleotides and which was shown by northern analysis to be abundant in roots, less abundant in leaves and pith and much less abundant in seed. The clone was used to probe a *Z. mays* genomic library and a homologous genomic clone identified (de Frammond 1991). The genomic clone was identical to the cDNA apart from a 176 base pair intron between codons 17 and 18.

Southern blots of restricted genomic DNA revealed intense bands corresponding to the genomic clone and less intense bands attributed to a related gene which hybridized weakly to the *Z. mays* metallothionein-like gene were observed (de Frammond 1991). Transcriptional and translational start sites were identified at approximately 35 and 105 base pairs from a TATA box respectively. The open reading frame encodes a 76 residue polypeptide with 12 cysteine residues arranged in three Cys-Xaa-Cys motifs at both the carboxyl and amino terminal ends of the protein. *In vitro* translation of hybrid-selected mRNA yielded a peptide with a molecular weight of 8000 (de Frammond 1991).

3.1.1.4 *Hordeum vulgare*

A cDNA library was constructed from iron-deficient *H. vulgare* roots and probed with RNA extracted from roots of *H. vulgare* grown in either iron-deficient or iron-sufficient conditions (Okumura *et al.* 1991). Seven truncated cDNA clones were identified, one of which was used to probe a new cDNA library and a full length clone obtained. The clone was designated *ids-1* (iron deficiency-specific clone 1). It was suggested that the *ids-1* gene may be involved in the regulation of mugineic acid synthesis in *H. vulgare* and may possibly chelate ferrous iron (Okumura *et al.* 1991).

The cDNA encodes a 74 residue polypeptide with 12 cysteines arranged in three Cys-Xaa-Cys motifs at both the carboxyl and amino terminal ends of the protein (Okumura *et al.* 1991). In northern analysis the gene was highly expressed in iron deficient roots but not in iron sufficient roots or iron-deficient or sufficient leaves (Okumura *et al.* 1992). In the same study after returning to iron sufficient conditions transcripts of the gene in roots were severely reduced after four but not two days.

In a study of differential gene expression during *H. vulgare* aleurone cell development a gene *B22E* was identified which is expressed in developing *H. vulgare* grains (Klemsdal *et al.* 1991). The putative product has an amino terminal domain with similarity to the amino terminal cysteine rich domain of the plant metallothionein-like gene products however the sequence subsequently diverges. *B22E* transcripts are repressed by ABA and in common with the gene for E_c protein in *T. aestivum* and the *H. vulgare* gene has a putative ABA responsive element (Klemsdal *et al.* 1991).

3.1.1.5 *Triticum aestivum*

A cDNA library was constructed from an aluminum sensitive cultivar of *T. aestivum* grown in media supplemented with 10 μM aluminium (Snowden and Gardner 1993). This library was probed with cDNA synthesized from RNA extracted from plants grown in media with either no aluminium supplement or supplemented with 10 μM aluminium. Five clones were identified *wali1* to *wali5* (wheat aluminium induced) and sequenced. The gene *wali1* encodes a putative product of 75 residues including 12 cysteine residues arranged in three Cys-Xaa-Cys motifs at both the carboxyl and amino terminal ends of the protein (Snowden and Gardner 1993).

In a time course study of aluminium sensitive plants in response to aluminium transcripts of the *wali1* clone increase dramatically in abundance after 24 hours of aluminium treatment and decreased to basal levels after 24 hours of transfer to aluminium free media (Snowden and Gardner 1993). An aluminium tolerant cultivar of *T. aestivum* required much higher levels of aluminium (100 μM) to induce elevation of transcripts of the *wali1* gene. Expression of the *wali1* gene was reduced by cadmium treatment and heat-shock stress (Snowden and Gardner 1993). *Wali1* transcripts were detectable in leaves of *T. aestivum* (at lower levels than in root) but in the leaves the gene was not induced by growth in aluminum supplemented media. Snowden and Gardner comment that the induction of the *wali1* gene by aluminum may not necessarily be a direct response to aluminium but may be due to the disruption of normal iron metabolism in aluminium stressed plants.

3.1.1.6 *Glycine max*

A cDNA library isolated from 6 day old *G. max* seedlings was probed with an oligonucleotide sequence designed from the consensus DNA sequence encoding the amino terminal 7 residues of rat, human and monkey metallothionein (MAPNCSC) (Kawashima *et al.* 1991). A 678 nucleotide cDNA clone was isolated and sequenced. The gene encodes a putative polypeptide of 79 residues.

In northern analysis levels of the transcripts in roots were not effected by treatment with 3 μM CuSO_4 but decreased slightly in 6 μM CuSO_4 (Kawashima *et al.* 1991). The level of the transcript was much higher in leaves than in roots.

3.1.1.7 *Actinidia deliciosa*

A cDNA library was made from young fruit of *A. deliciosa* (kiwifruit) collected 8-10 days after anthesis (Ledger and Gardner 1994). The library was probed with cDNA synthesized from 8-10 day old fruit or from leaf RNA. Of the 5 clones eventually isolated and sequenced two of them pKIWI503 and pKIWI504 encoded putative cysteine rich proteins (Ledger and Gardner 1994). Clone pKIWI504 encoded a putative 78 residue polypeptide including 14 cysteine residues arranged in a Cys-Cys, two Cys-Xaa-Cys and a Cys-Xaa-Xaa-Cys motif at the amino terminal end of the protein and three Cys-Xaa-Cys motifs at the carboxyl terminus. The pKIWI503 clone encodes a putative 63 residue polypeptide including 10 cysteines arranged in three Cys-Xaa-Cys pairs in the carboxyl terminus and 4 cysteines in the amino terminus (Ledger and Gardner 1994).

Northern analysis indicated that the pKIWI504 gene has a bimodal pattern of expression during fruit development reaching a maximum 6 and 44 days following anthesis (Ledger and Gardner 1994). The first peak in expression coincided with maximal levels of copper in *A. deliciosa* fruit (cited in Ledger and Gardner 1994). Transcript levels of clone pKIWI503 reached a maximum 147 days after anthesis. The level of both transcripts were relatively low in the flower before anthesis and in roots and leaves (Ledger and Gardner 1994).

3.1.1.8 *Vicia faba*

A cDNA library was constructed from leaves of *Vicia faba* (long pod bean) from which the mesophyll cells had been removed and probed with cDNA synthesized from either non-mesophyll cDNA or mRNA isolated from mesophyll protoplasts (Foley and Singh 1994). A total of 28 cDNA clones were isolated which were not expressed in mesophyll cells. A clone was identified which encoded a putative 77 residue polypeptide including 14 cysteine residues arranged in a Cys-Cys, two Cys-Xaa-Cys and a Cys-Xaa-Xaa-Cys motif at the amino terminal end of the protein and three Cys-Xaa-Cys motifs at the carboxyl terminus (Foley and Singh 1994).

Transcripts (approximately 500 bases) were most abundant in the stem but were also high in the leaf and flower (Foley and Singh 1994). Transcript levels were very low in the root and undetectable in the mesophyll cells. *In situ* hybridization studies showed that transcripts of were most abundant in trichomes (Foley and Singh 1994). Transcript levels were slightly reduced following 24 hour exposure high salt conditions but were unaffected by

exposure to cold or to dark for the same period. No significant variations in transcript levels in leaves were reported following growth in media supplemented with 5 or 50 μM CuSO_4 or with elevated levels of ZnSO_4 or CdSO_4 (Foley and Singh 1994).

3.1.1.9 *Arabidopsis thaliana*

An *A. thaliana* cDNA library was differentially screened for clones induced by ethylene (Zhou and Goldsbrough 1994). One of these clones (designated *MTI*) encoded a putative polypeptide of 45 residues including 13 cysteine residues arranged in three Cys-Xaa-Cys pairs in the amino terminus and three Cys-Xaa-Cys pairs and a single cysteine in the carboxyl terminus. There are 7 residues between the two cysteine rich domains.

MTI Transcripts are highly expressed in roots and in etiolated seedlings but transcript levels were much lower in leaves (Zhou and Goldsbrough 1994). After exposure to a range of copper concentrations (0 to 100 μM) for 30 hours prior to harvest, Zhou and Goldsbrough measured transcripts levels in 7-day old seedlings. The authors reported no response to copper, but a slight initial decrease in expression as exogenous copper was increased can be seen in the published data. No significant effect was observed following exposure to up to 150 μM cadmium or 1 to 2 μM zinc. In leaves excised from 2 week old plants, grown without metal supplement, and incubated in nutrient solution supplemented with no metal, copper (50 μM), cadmium (100 μM) or zinc (1 mM) for 17 hours a 3-fold induction of the gene was seen with copper and a lower induction with zinc and cadmium (Zhou and Goldsbrough 1994).

Previously another *A. thaliana* cDNA, isolated from mature leaf had been submitted to the nucleotide sequence databases (Takahashi, K. submitted 1991 EMBL accession number X62818). The cDNA was cloned using the same oligonucleotide used for soyabean (Kawashima *et al.* 1991). The coding sequence for this gene was amplified from an *A. thaliana* cDNA library by PCR and cloned (Zhou and Goldsbrough 1994). The putative product encodes a polypeptide of 81 residues including 14 cysteine residues arranged in a Cys-Cys, two Cys-Xaa-Cys and a Cys-Xaa-Xaa-Cys motif at the amino terminal end of the protein and three Cys-Xaa-Cys motifs at the carboxyl terminus. The sequence differed from that reported by Takahashi by a single base substitution resulting in a substitution of Ser⁶⁴ to Asn⁶⁴ (Zhou and Goldsbrough 1994).

This gene was submitted to the same northern analysis as the smaller *A. thaliana* gene (Zhou and Goldsbrough 1994). Transcripts were abundant in leaves but not seedlings or roots. A 5-fold increase in transcript levels in seedlings was induced by exposure to copper concentrations above 50 μM . The effect of exposure to cadmium and zinc was less significant. In a time course study levels of gene transcripts increased steadily up to 72 hours following exposure to 50 μM copper (Zhou and Goldsbrough 1994). In a published extract it is reported that using reporter gene fusions of *gusA* and the upstream regulatory sequences of the larger *A. thaliana* gene, expression is detected in older parts of plants and can be induced in root tips by heavy metal treatment (Fujiwara *et al.* 1994).

Both *A. thaliana* genes were introduced into a *cup1 Δ* strain of the yeast *S. cerevisiae* on high copy number expression vectors (Zhou and Goldsbrough 1994). Yeast cells carrying the vector alone were sensitive to 300 μM CuSO_4 , however yeast cells expressing either of the *A. thaliana* plant metallothionein-like genes or hamster MT were tolerant in copper concentrations up to 3 mM CuSO_4 . CdSO_4 became toxic to yeast cells expressing the shorter plant metallothionein-like protein above 10 μM , the longer metallothionein-like protein above 100 μM and cells expressing the hamster metallothionein were tolerant to 500 μM CdSO_4 .

3.1.1.10 *Brassica napus*

A cDNA library was made from RNA extracted from leaves of *B. napus* undergoing senescence (Buchana-Wollaston 1994). The library was probed with cDNA from green leaves or senescent leaves and clones identified which were expressed during senescence. One of these clones encodes a putative polypeptide of 45 residues including 13 cysteine residues arranged in three Cys-Xaa-Cys pairs in the amino terminus and three Cys-Xaa-Cys pairs and a single cysteine in the carboxyl terminus. There are 7 residues between the two cysteine rich domains.

In northern analysis transcript levels were very low during leaf development and in the mature leaf but were very high during senescence and increased steadily (Buchana-Wollaston 1994). Transcripts were not detected in the root or the seed but were detected in the flower.

3.1.2 Analysis of 5' flanking sequences of plant metallothionein-like genes

Full genomic clones have been reported for the genes from *P. sativum* and *Z. mays* (Evans *et al.* 1990 and de Frammond 1991). In addition genomic clones have been obtained for both

reported metallothionein-like genes from *A. thaliana* (J. Bartley (1994) MSc. thesis). The upstream sequences of these genes were analysed for common putative metal responsive elements but no candidate sequences were identified.

3.2. Methods

3.2.1 Database searching

Throughout this project the EMBL and GenBank nucleotide sequence databases and the Swissprot, PIR and OWL protein sequence databases were regularly searched for the submission of new sequences with similarity to the plant metallothionein-like sequences. A variety of search tools were used but predominantly the FASTA program (Pearson and Lipman 1988) was used which was available on the GCG* suite of programs on the SEQNET computer facility at the SERC Daresbury laboratory.

As the internet system expanded various tools such as 'Gopher' and 'Mosaic' were used to access the Genbank and Swissprot databases directly and to search the sequence records on the *A. thaliana* and *Z. mays* genome project databases. In cases where only a nucleotide sequence had been submitted the open reading frame was converted into an amino acid sequence using the GCG program TRANSLATE*.


The FASTA* program aligns each sequence in a database to a query sequence and gives the alignment a score according to an algorithm which takes into account not only the number of identical residues but also the similarity of different amino acids. The output from the program reports the sequences with the best scores and an optimum alignment. The programs was used with a gap weight of 3.0 and a length weight of 0.1.

3.2.2 Prediction of protein characteristics


The PEPSTATS* program was used to calculate a prediction of the molecular weight, isoelectric point and charge of each predicted sequence. The calculated values are estimates only and do not take into account factors which may effect the characteristics of the functional peptides. Such factors include any post translational modification of the protein and, most significantly in the case of metallothioneins, the effects of metal binding.

3.2.3 Sequence comparison

3.2.3.1 Multiple sequence alignment The PILEUP* program was used to provide the original multiple sequence alignments which were then subject to minor manual modifications. Program parameters were a gap weight of 3.0 and a length weight of 0.1.



3.2.3.2 Pairwise sequence alignment The GAP* program was used to produce pairwise alignment scores, with gap weight of 5.0 and a length weight of 0.3.



3.2.3.3 Evolutionary relationships The DISTANCE* program was used to generate a matrix of pairwise evolutionary relationships based on pairwise sequence comparisons expressed as substitutions per 100 amino acids. The distances were corrected for multiple substitutions by the Jukes-Cantor method (Swoffard and Olsen 1990). This matrix was then used to generate a phylogenetic tree (phylogram) using the program GROWTREE*. An unweighted pair group method using an arithmetic averages algorithm was used. The final diagram was independent of the order in which the sequences were input into the program.

* program manual for the Wisconsin package, Version 8, August 1994, Genetics Computer Group, 575 Science Drive, Madison, Wisconsin, USA 53711 and program manual for the EGCG package, Peter Rice, The Sanger Centre, Hinxton Hall, Cambridge, CB10 1RQ, U.K.

3.2.4 Secondary structure prediction

The program PHDsec (Rost and Sander 1993) was used to provide a secondary structure prediction from the predicted amino acid sequence of the plant metallothionein-like genes. The program was available on a mailserver at the European Molecular Biology Laboratory, Heidelberg, Germany. The program uses a recently developed profile fed neural network technique based on sequence alignment (Rost and Sander 1993, 1994). The authors claim that for the same data set the algorithm is rated at 5-10 percentage points higher three-state accuracy than any previously published method.

3.3 Results and discussion

3.3.1 Plant metallothionein-like genes reported in the literature and in sequence databases

A summary of all the plant metallothionein-like genes reported at time of submission of this thesis are presented in table 3.1. The reported genes cover a wide range of plant species and this suggests that these genes may well be ubiquitous. The genes, or in most cases more accurately cDNA clones, have been isolated by researches studying a range of phenomena but the basic properties of the predicted products of the genes remains the same.

3.3.2 Classification of the products of plant metallothionein-like genes based on their predicted primary structure

The plant metallothionein-like gene products can be placed into different categories according to the arrangement of cysteine residues and the length of the region between the two cysteine rich domains, summarised in figure 3.1. The type-1 and type-2 products share similar carboxyl terminal cysteine rich domains. The type-1 and type-3 products share similar amino terminal cysteine rich domains. The type-3 product differs from the type-1 and -2 products not only in the length of the inter-domain region but also in the number and arrangement of cysteines in the carboxyl terminal cysteine rich domain. The E_c metallothionein can be reduced to three cysteine rich domains, the central of which resembles the carboxyl terminal domain of the type-1 and -2 gene products. The arrangement of the blocks of data in table 3.1 reflects these categories. The possible significance of the differences in the arrangement of cysteines in these different categories of metallothionein-like proteins will be discussed in chapter 5.

From the available information on the expression of the plant metallothionein-like genes a pattern emerges supporting the assignment of the genes into categories, table 3.1. Generally expression of the type-1 genes has been observed in root tissue and the type-2 genes in leaf tissue. Genes of both type-1 and type-2 have been identified in *T. repens*, both in the same tissue, stolon node (EMBL Z26493 and Z26492). The stolon is a tissue which has both leaf and root characteristics. Expression of the type-2 gene from *A. deliciosa* was detected in the developing fruit but not the leaf (Ledger and Gardner 1994). The type-3 gene products of *A. thaliana* (Zhou and Goldsbrough 1994) and *B. Napus* (Buchanan-Wollaston

1994) are very similar yet one is apparently expressed constitutively in the root and the other is expressed in the leaf during senescence.

3.3.3 Comparison of the predicted products of plant metallothionein-like genes with other Swissprot protein database entries

For a recent (Jan. 1995) FASTA search, of the Swissprot protein database, using the sequence of PsMT_A as the query sequence, the top 6 scores were the plant metallothionein-like proteins represented in the database. Of the remaining top 34 scores 2 were E_c sequences 28 were metallothionein sequences and 4 were other cysteine containing proteins. In all cases the region of similarity was based on the cysteine rich domains.

3.3.4 Sequence alignment of the plant metallothionein-like gene products

The amino acid sequence alignments of the plant metallothionein-like gene products described in section 3.3.2 and summarised in table 3.1 are presented in figure 3.2. In addition to those reported previously a potential type-4 category is also shown with representatives from *O. sativa*, *A. deleciosa* and *A. thaliana*. This group appears to be superficially similar to the plant metallothionein-like proteins but have only 4 cysteine residues at an amino terminal domain and 5 (*O. sativa*), 6 (*A. deleciosa*), and 8 (*A. thaliana*) cysteines in a carboxyl domain. The domains are separated by a region of 30 amino acids.

A recent survey (June 1995) of the NCBI GenBank expressed sequence tag (EST) database revealed a large number of reports of cDNA's from *A. thaliana* encoding predicted products with similarity to metallothionein. The predicted products of these sequences fell into the four categories described in section 3.3.2 and figure 3.2. However it should be noted that there was some variation in the predicted products of the genes reported. There were two type-2 sequences represented, the sequence presented in figure 3.2 (12 occurrences) and a second very similar sequence with several conservative amino acid substitutions and an additional four residues in the inter domain region (14 occurrences). The cysteine rich domains are highly conserved between these sequences. Similarly in addition to the E_c type sequence presented in figure 3.2 (3 occurrences) there was a second sequence with a small number of amino acid substitutions (2 occurrences). The most highly represented sequence was the type-4 sequence (24 occurrences). The EST sequences are derived from random sequencing experiments and therefore there is little accompanying information. It is not clear

if all the differences between sequences are genuine or result from sequencing errors. However, this data may imply that the metallothionein-like type-2 and E_c genes in *A. thaliana* may be part of small multigene families. All subsequent references to the *A. thaliana* type-2 amino acid sequence refers to that presented figure 3.2.

When compared to representative metallothionein sequences from other species the arrangement of cysteines and the inter domain region are unique to the plant metallothionein-like proteins. The program GAP was used to compare representative sequences of the 3 metallothionein-like categories with metallothionein from horse, yeast and *N. crassa* and a similarity score calculated, table 3.2.

The type-1 gene from *P. sativum* scores particularly highly against the *N. crassa* metallothionein gene. It was this particularly high similarity to *N. crassa*, designated a class I metallothionein, that originally lead to speculation that the product of this plant gene may be a metallothionein (Evans *et al.* 1990). The protein database entries describe the plant gene products as metallothionein I homologs, a description which is unqualified. The type-3 plant metallothionein-like protein lacking the central domain and with an extra cysteine in the carboxyl domain scores consistently highly against the other metallothioneins.

When a FASTA search was performed for the predicted translational product of the *A. thaliana* type-3 metallothionein-like gene against the Swissprot protein database non plant metallothioneins scored as highly as, or higher than, other plant metallothionein-like proteins. This reflects the non metallothionein characteristics of the interdomain region in the type-1 and type-2 categories.

Type 1 plant metallothionein-like gene product

CxCxxxCxCxxxCxC ————— CxCxxxCxCxxCxC

Type 2 plant metallothionein-like gene product

CCxxxCxCxxxCxCxxxCxxC ————— CxCxxxCxCxxCxC

Type 3 plant metallothionein-like gene product

CxCxxxCxCxxxCxC — CxxCxCxxxCxCxxxCxC

Type Ec plant metallothionein

CxxxCxCxxxCxxxxCxC ————— CxCxxxCxCxxCxC ————— CxCxxxCxCxxC

Mammalian metallothionein

CxCxxxxxCxCxxxCxCxxCxCxxCxxxCCxCCxxxCxxxCxCxxxxxCxC
←—————→ ←—————→
β-domain α-domain

Figure 3.1 Schematic diagram showing the arrangement of cysteine residues and inter-domain regions in the different categories of plant metallothionein-like gene products. The arrangement of cysteines within equine MT-I is shown for comparison.

Table 3.1 Summary of the reported information relating to metallothionein-like genes. The table is grouped into type-1, type-2, type-3 and E_c categories. The information included is; the plant species in which the gene has been identified, whether the plant is monocotyledonous or dicotyledonous, the tissue types in which expression of the gene has been observed, the type of clone, the length of the gene product and the predicted molecular weight, the isoelectric point and charge of the predicted product, the nature of the research being undertaken which lead to the identification of the gene, the main reference (if published) and EMBL database accession number of the gene.

Plant	Monocot. or dicot.	Tissue	Clone	Length (MW)	IP Charge	Basis of isolation	Reference
Pea <i>Pisum sativum</i>	D	root	genomic, cDNA	75 (7 608)	4.3 (-4)	root specific expression	Evans <i>et al.</i> 1990 EMBL Z23097
Clover <i>Trifolium repens</i>	D	stolon node	cDNA	75 (7 659)	4.3 (-4)	not known	EMBL Z26493
Monkey Flower <i>Mimulus guttatus</i>	D	root	cDNA	72 (7 348)	4.4 (-3)	copper regulation	de Miranda <i>et al.</i> 1990 EMBL X51993
Maize <i>Zea mays</i>	M	root	genomic, DNA	76 (7 486)	4.7 (-3)	root specific expression	de Frammond <i>et al.</i> 1991
Barley <i>Hordeum vulgare</i>	M	root	cDNA	74 (7 469)	4.6 (-3)	iron deficiency	Okumura <i>et al.</i> 1991 X58540
Wheat <i>Triticum aestivum</i>	M	root tip	cDNA	75 (7 367)	4.3 (-3)	aluminium regulation	EMBL L11879

Plant	Monocot. or dicot.	Tissue	Clone	Length (MW)	IP Charge	Basis of isolation	Reference
Mouse ear cress <i>Arabidopsis thaliana</i>	D	leaf	genomic, cDNA	81 (8 136)	4.4 (-3)	sequence homology	(see text) EMBL X62818
Clover <i>Trifolium repens</i>	D	stolon node	cDNA	77 (8306)	5.6 (-2)	not known	EMBL Z26492
Long pod bean <i>Vicia faba</i>	D	leaf	cDNA	77 (7729)	4.4 (-3)	leaf specific expression	Foley and Singh 1994 EMBL X77254
Castorbean <i>Ricinus communis</i>	D	cotyledon	cDNA	80 (7 953)	4.7 (-3)	not known	EMBL L02306
Soyabean <i>Glycine max.</i>	D	leaf	cDNA	79 (7 939)	4.6 (-2)	sequence homology	Kawashima <i>et al.</i> 1991
Coffee <i>Coffea arabica</i>	D	immature leaf	cDNA	80 (7 913)	4.7 (-4)	not known	Moisyadi and Stiles 1995 EMBL U11423
Kiwifruit <i>Actinidia delectiosa</i>	D	fruit	cDNA	78 (7 800)	4.4 (-3)	fruit development	Ledger and Gardner 1994 EMBL L27812
Rice <i>Oryza sativa</i>	M	callus	cDNA	82 (7 777)	4.6 (-3)	random sequencing	EMBL D15602

Plant	Monocot. or dicot.	Tissue	Clone	Length (MW)	IP Charge	Basis of isolation	Reference
Mouse Ear Cress <i>Arabidopsis thaliana</i>	D	root	cDNA	45 (4 580)	4.3 (-2)	ethylene regulation	Zhou and Goldsbrough 1994
Brassica <i>Brassica napus</i>	D	leaf	cDNA	45 (4 412)	3.97 (-3)	leaf senescence	Buchanan-Wollaston 1994

Plant	Monocot. or dicot.	Tissue	Clone	Length (MW)	IP Charge	Basis of isolation	Reference
Wheat <i>Triticum aestivum</i>	M	seed	protein, cDNA	81 (7 712)	4.4 (-3)	cysteine accumulation	Kawashima <i>et al.</i> 1992
Maize <i>Zea mays</i>	M	whole embryo	cDNA	77 (7705)	7.21 (+1)	random sequencing	EMBL U10696
Mouse Ear Cress <i>Arabidopsis thaliana</i>	D	seed	cDNA	84 (8306)	5.6 (-2)	random sequencing	EMBL Z27049

	Mammal	Yeast	<i>N. crassa</i>	Type-1	Type-2	Type-3
Type-1	37 % 19 %	48 % 27 %	67 % 46 %	-- --	71 % 51 %	60 % 53 %
Type-2	43 % 22 %	39 % 26 %	54 % 35 %	71 % 51 %	-- --	42 % 29 %
Type-3	56 % 33 %	48 % 23 %	65 % 46 %	60 % 53 %	42 % 29 %	-- --

Table 3.2 Gapped pairwise alignment scores for the plant metallothionein-like type-1 (*P. sativum*), type-2 (*A. thaliana*) and type-3 (*A. thaliana*) sequences against metallothionein from mammal (equine - Kojima and Kagi 1978), yeast (CUP1 - Winge *et al.* 1985) and the fungus *N. crassa* (Okada *et al.* 1989). The first score is percentage similarity and the second score is percentage identity.

3.3.5 Phylogenetic relationships between the products of the plant metallothionein-like genes

A phylogenetic tree was created for the type-1 and type-2 plant metallothionein-like sequences based on sequence similarity, figure 3.3. All the type-2 sequences have been grouped together, the shortness of the branch lengths reflecting the high degree of sequence conservation in the examples so far reported in this category. Likewise the majority of the type-1 sequences are grouped together. The separate branching for the type-1 sequences for *P. sativum* and *T. repens* is a result of the very high degree of similarity between this pair of sequences relative to the other sequences. The branch lengths in the type-1 grouping indicate that there is not as high a degree of conservation between the representatives in this category as in the type-2 category. The use of the type-1 and type-2 categorisation is supported by the fact that the program has independently reproduced the categories. If the arrangement of the cysteines in the amino terminal domain was due to simply random substitution over the evolutionary time scale then it would be expected that the sequence grouping would only have reflected evolutionary closeness.

The grouping within the type-1 sequences is consistent with the expected evolutionary closeness of the plant species represented. *P. sativum* and *T. repens* are both fabaceae and *H.*

vulgare, *Z. mays* and *T. aestivum* are poaceae. In the type-2 grouping the fabaceae *G. max*, *T. repens* and *V. faba* have been grouped together with very short branch lengths.

3.3.6 Sequence conservation in type-1 and type-2 gene products

From the consensus sequence derived from the alignment of all type-1 and all type-2 predicted plant metallothionein-like proteins, figure 3.2, the absolute conservation of the cysteine residues within each category is apparent. The conservation of amino acids within these two categories of protein is represented graphically in figure 3.4. The higher proportion of sequence conservation within the cysteine rich domains compared to the inter domain region supports strongly the idea that the cysteine rich domains are the key to the function of the putative proteins. The apparent higher overall conservation of sequences within the type-2 proteins compared to the type-1 sequences may just reflect the range of plant species so far represented in each category.

Although the central, cysteine region is generally not well conserved there is a short region in the centre of this domain which is relatively well conserved in both types. This region of conservation ends in the amino acids Gly-Val in both cases.

Figure 3.2 Amino acid sequence alignment of the known plant metallothionein-like gene products. The alignments are separated into different categories reflecting the arrangement of cysteines in the amino terminal domain. The sources are;

- | | |
|---|---|
| 1 - Evans <i>et al.</i> 1990, EMBL Z23097 | 14 - translated from EMBL D15602 |
| 2 - translated from EMBL Z26493 | 15 - translated from EMBL X62818 |
| 3 - de Miranda <i>et al.</i> 1990, SwissProt P20238 | 16 - Buchanan-Wollaston 1994 |
| 4 - de Frammond 1991, SwissProt P30571 | 17 - Kawashima <i>et al.</i> 1992 |
| 5 - Okumura <i>et al.</i> 1991, PIR S17299 | 18 - translated from EMBL U10696 |
| 6 - Snowden and Gardner 1994, EMBL L11879 | 19 - translated from EMBL Z27049 |
| 7 - SwissProt S18069 | 20 - translated from EMBL D21979 |
| 8 - translated from EMBL Z26492 | 21 - translated from EMBL L27811 |
| 9 - Foley and Singh 1994, EMBL X77254 | 22 - translated from EMBL T12945 |
| 10 - translated from EMBL L02306 | 23 - Klemsdal <i>et al.</i> 1991, PIR S16534 |
| 11 - Kawashima <i>et al.</i> 1991 | 24 - M. Leech personal communication |
| 12 - Moisyadi and Stiles 1995, EMBL U11423 | 25 - Wheat purothionin Bohlmann and Apel 1991 |
| 13 - Ledger and Gardner 1994, EMBL L27812 | 26 - SwissProt P02800 |
| | 27 - SwissProt D00381 |

Type-1 plant metallothionein-like gene products

*P. sativum*¹ .MSGCGCGSS CNCGDSCCKN KRSSGLSYSE METTE...TV ILGVGPAKIQ FEGAEMSAA. .SEDG.GCKC GDNCTCDPCN CK
*T. repens*² .MSGCNCGSS CNCGDSCCKN KRSSGLNYVE AETTE...TV ILGVGPAKIQ FEDAEEMGVA. .AEDS.GCKC GSSCTCDPCN CK
*M. guttatus*³ MSSGCSCGSG CKCGDNCSC. SMYPD.... METNTTV.TM IEGVAPLKMV SEGSEKSF. .AEGGNGCKC GSNCKCDPCN C.
*Z. mays*⁴ ..MSCSCGSS CGCGSSCKCG KKYPDL.EET STAAQ..PTV VLGVAPEKKA APEFVEAAAAE SGEAAHGCSG GSGCKCDPCN C.
*H. vulgare*⁵ ..MSCSCGSS CGCGSNCNCG KMYPDL.EEK SGATMQVTVI VLGVGSAKV. ...QFEAAAAE FGEAAHGCSG GANCKCNPCN C.
*T. aestivum*⁶ ..MSCCNCGSG CSCGSDCKCG KMYPDLTEQG SAAAQVAADV VLGVAPENKA G..QFEVAA. .GQSGEGCSG GDNCKCNPCN C.

ConsensusC.CG. C.CG..C.C.GV.....GC.C G..C.C.PCN C.
 C C C C C C C C C C

Type-2 plant metallothionein-like gene products

*A. thaliana*⁷ MSCCGGNCGC GSGCKCGNGC GGCKMYPDLG FSGETTTTET FVLGVAPAMK NQYEASGESN ..NAESDACK CGSDCKCDPC TCK.
*T. repens*⁸ MSCCGGNCGC GSACKCGNGC GGCKMNADLS YT.ESTTTET IVMGVGSAKA QFEGAEMG.. ...AESGGCK CGANCTCDPC TCK.
*V. faba*⁹ MSCCGGNCGC GSSCKCGSGC GGCKMYADLS YT.ESTTSET LIMGVGSEKA QYESAEMG.. ...AENDGCK CGANCTCNPC TCK.
*R. communis*¹⁰ MSCCGGNCGC GSGCKCGNGC GGCKMYPDMS FS.EKTTTET LVLGVGAEKA HFEGGEMGVV ..GAEEGGCK CGDNCTCNPC TCK.
*G. max*¹¹ MSCCGGNCGC GSSCKCGNGC GGCKMYPDLS YT.ESTTTET LVMGVAPVKA QYESAEMG.. ...AENDGCK CGANCTCNPC TCK.
*C. arabica*¹² MSCCGGNCGC GAGCKCSGGC GGCKMYPELS .YTENTAAET LILGVAPPKT TYLEGAGEEA ..AAENGGCK CGPDCKCNPC NCK
*A. deleciosa*¹³ MSCCGGKCGC GSSCSGSGC GGCGMYPDLS YS.EMTTTET LIVGVAPQKT YFEGSEMGV. ...AAENGCK CGSDCKCDPC TCK.
*O. sativa*¹⁴ MSCCGGNCGC GSGCQCGSGC GGCKMYPEMA ..EEVTTTQT VIMGVAPSKG HAEGLEAGAA AXAGAENGCK CGDNCTCNPC NCGK

Consensus MSCCGG.CG GS.C.CG.GC GGC.MY.DL. ...E.TT..T ...GV.....CK CG..C.C.PC .C..
 CC C C C C C C C C C C C

Type-3 plant metallothionein-like gene products

*A. thaliana*¹⁵ MADSNCGCGS SCKCGDSCSC EKYNKCEDN CSCGSNCSCG SNCNC
*B. napus*¹⁶ MAGSNCGCGS GCKCGDSCSC EKYNTECDN CSCGSNCSCG DSCSC
 C C C C C C C C C C

Type-E_c plant gene products

*T. aestivum*¹⁷.....M GCDDKCGCAV PCPGGTGCR C TSARSGAAAG .EHTTCGCGE HCGCNPCACG REGTPSGRAN RRANCSCGAA CNCASC GSAT A
*Z. mays*¹⁸M GCDDKCGCAV PCPGGKDCRC TSGSGG...Q REHTTCGCGE HCECSPCTCG RATMPSGREN RRANCSCGAS CNCASCASA
*A. thaliana*¹⁹ADTGKGSASA SCNDRCGCPS PCPGGESCRC KMMSEASGGD QEHNTPCPCGE HCGCNPCNCP KTQTQTS... .AKGCTCGEG CTCATCAA... .
 ConsensusC.D.CGC.. PCPGG..CRCEH TC.CGE HC.C.PC.C. ...T.....C.CG.. C.CA.C.... .
 C C C C C C C C C C C C C C C

Possible type-4 metallothionein-like gene products

*O. sativa*²⁰ MSDKCGNDC ADKSQCVKKG TSYGVVIVEA EKSHFE.... EVAAGXENGG ...CKCGTSCS CTDCKGK
*A. deleciosa*²¹ MSDKCGNDC ADSSQCVKKG NSI..DIVET DKS YIE.... DVVMGVPAE SGGKCKCGTSCP CVNCTCD
*A. thaliana*²² MSSNCGSCDC ADKTQCVKKG TSYTFDIVET QESYKEAMIM DVGAEENNA. .NCKCKGSSCS CVNCTCCPN
 C C C C C C C C C

Others cysteine rich plant sequences

*H. vulgare B22E*²³ MSCCGGKCGC GAGCQCGTGC GGCKMFPDVE ATAGAAAMVM PTASHKGSSG GFEMAGGETG
 GDCATCKCG TRAAAPAAAA SEPAPGRPAG RGEHEDERRT SNTNQAPSPS PSYHQ
*P. commune*²⁴ MAKDNGKCGA NDCPAGTCA KEN GKGRNC DCPAGTCANE NGKCGAN CDC PAGTCAKE
 Thionin²⁵ KSCCRSTLGR NCYNLCRARG AQLKAGVCR CKISSGLSCP KGFPK
 (*T. aestivum*)

Metallothionein

*E. Caballus*²⁶ MDPNCSCPTG GSCTCAGSCK CKECRCTSCK KSCCSCCPGG CARCAQGVCV KGASDKCSA
*N. Barbatulus*²⁷ MDP.CECSKT GTCNCGATCK CTNCQCTTCK KSCCSCCP SG CSK CASGVCV KGNSCDSSCC Q
*S. cerevisiae*²⁸ MFSELINFQN EGHECQCQCG SCKNNEQCQK SCSCPTGCNS DDKCPCGNKS EETKKSCCSG K
*N. crassa*²⁹ MGDCGCSGAS SCNCGSGCSC SNC GSK

Figure 3.3 Phylogenetic tree for the type-1 and type-2 plant metallothionein-like proteins.
The position and length of the branches is calculated on the basis of the number of amino acid substitutiona between sequences.

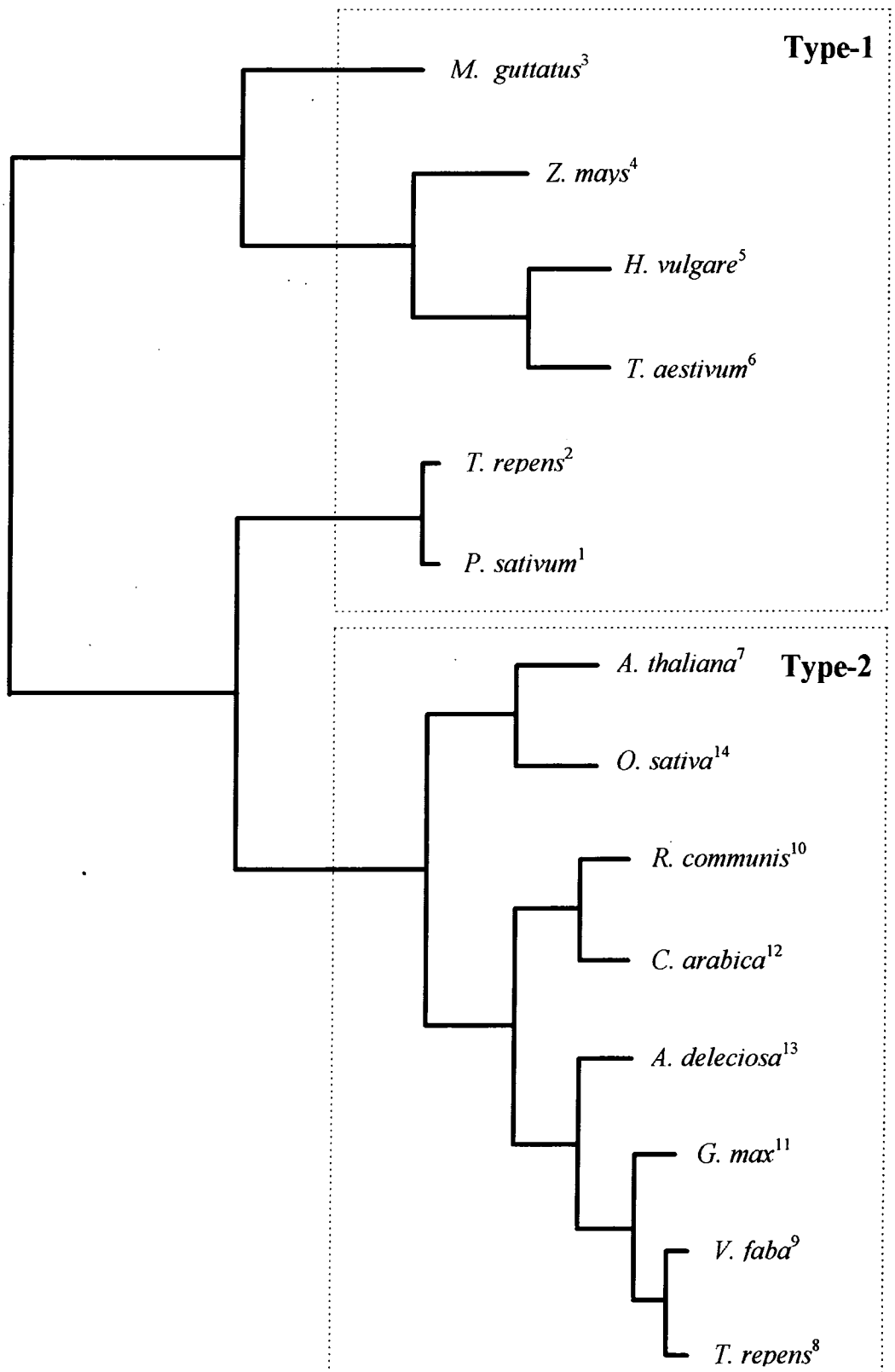
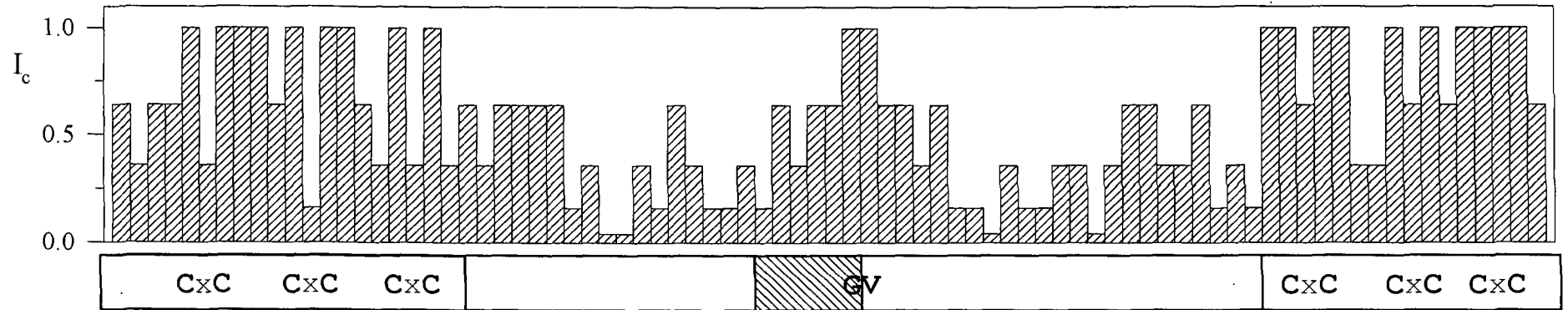


Figure 3.3 Phylogenetic tree for the type-1 and type-2 predicted metallothionein-like proteins. The grouping of sequences and length of branches was calculated on the basis of the amino acid substitutions between sequences. (Refs. figure 3.2.)

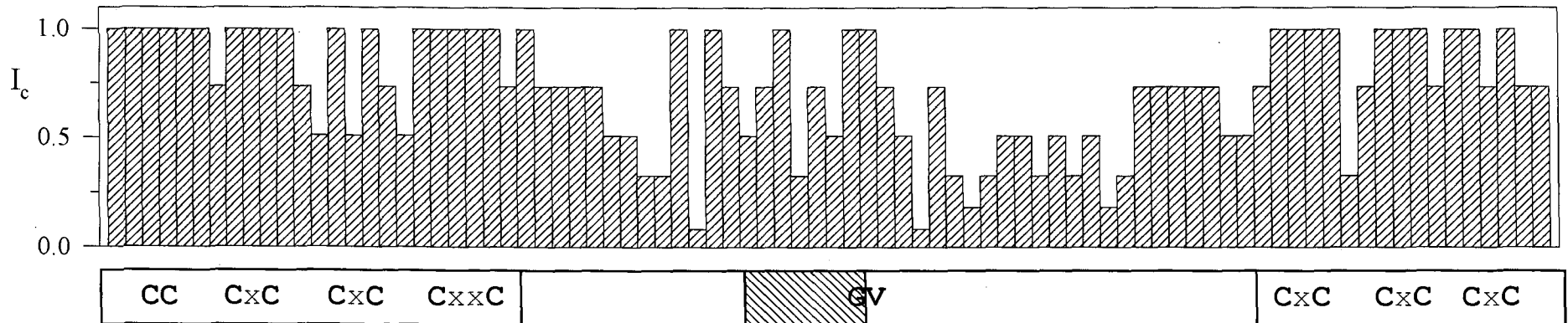
Figure 3.4 Conservation of primary structure in the type-1 and type-2 plant metallothionein like gene products. The x-axis represents the amino acid sequence, including gaps as shown in figure 3.2. The y-axis is a conservation index I_c based on the number of different amino acids at each position (v), and the total number of sequences in the alignment (n).

$$I_c = (n-v)^2 / (n-1)^2$$

If there is no sequence conservation then $I_c = 0$, if there is 100 % sequence conservation $I_c = 1$. I_c is not intended to have any special statistical significance but merely to allow the conservation of amino acids to be depicted graphically taking into account the number of sequences in the alignment. Unlike the phylograms, figure 3.3, this measurement of conservation does not take into account conservative substitutions of amino acids at particular positions between sequences.



Type-1 metallothionein-like gene products



Type-2 metallothionein-like gene products

3.3.7 Predicted secondary structure within plant metallothionein-like gene products

A secondary structure prediction for the *PsMT_A* predicted products is presented in figure 3.5. As expected the cysteine rich domains were predicted to be flexible loop regions, this lack of ordered secondary structure is characteristic of metallothionein allowing the polypeptide to fold around the metal-thiol cluster

The program predicted a region of β -strand in the centre of the inter-domain region. This assignment scored 9 on a reliability index provided with the program output, figure 3.5. This is the maximum score and correlates to a confidence in the prediction of around 95 %. There are no regions of α -helix predicted for *PsMT_A*.

The prediction program was used to generate secondary structure predictions for all the type-1 and type-2 plant metallothionein-like sequences, figure 3.6. All of these metallothionein-like gene products have a homologous region of β -strand in the centre of the inter-domain region. In all cases the prominent β -strand terminates in the residues Gly-Val (referred to hereafter as the β -strandGV motif). In all cases there is a predominance of potential β -strand forming sequences within the inter-domain region compared to the cysteine rich domains. The potential to form an ordered, possibly highly folded, secondary structure is the first indication of a potential function for the interdomain region. The formation of such a structure may explain why certain sites within the interdomain region of *PsMT_A* were more susceptible to proteolysis than others (Kille *et al.* 1991). Folding of the interdomain region may facilitate the movement of the cysteine rich domains into the correct juxtra-positioning for metal binding. Alternatively it may be involved in as yet unknown intermolecular interactions. The PHDsec program was used on the other categories of metallothionein-like gene products in plants, on CUP1 from yeast and on mammalian metallothionein, data not presented. The β -strandGV motif is unique to the type-1 and type-2 plant metallothionein-like gene products.

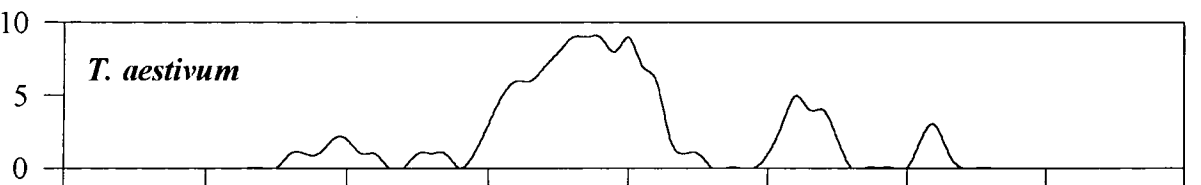
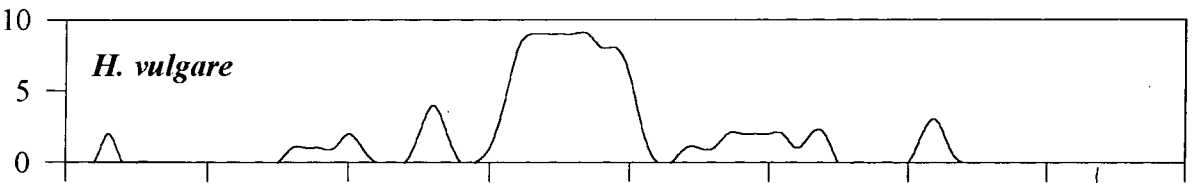
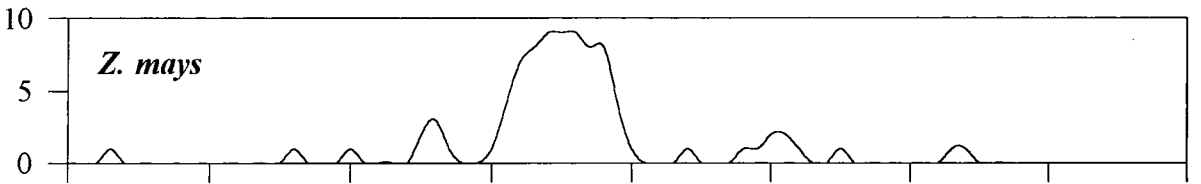
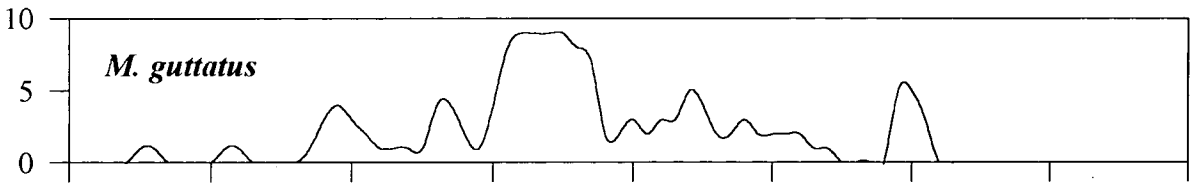
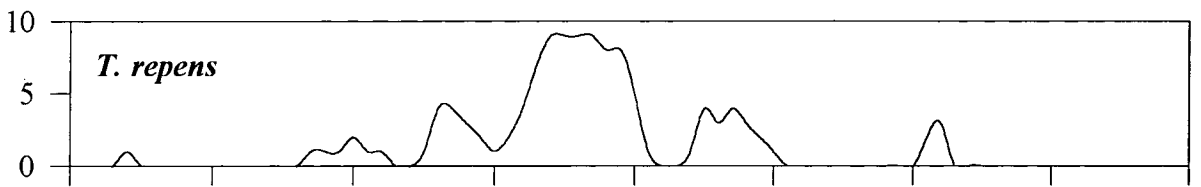
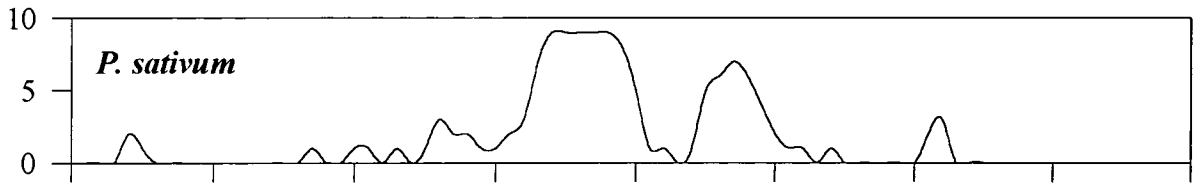
The amino acid sequence is by no means well conserved across the predicted β -strand region, figure 3.4. This makes the conservation of the β -strand motif within all the sequences all the more remarkable, and along with the conservation of the length of the inter-domain region strongly supports the hypothesis that the inter-domain region of the type-1 and type-2 sequences performs a specific function within plants.

Profile fed secondary structure prediction

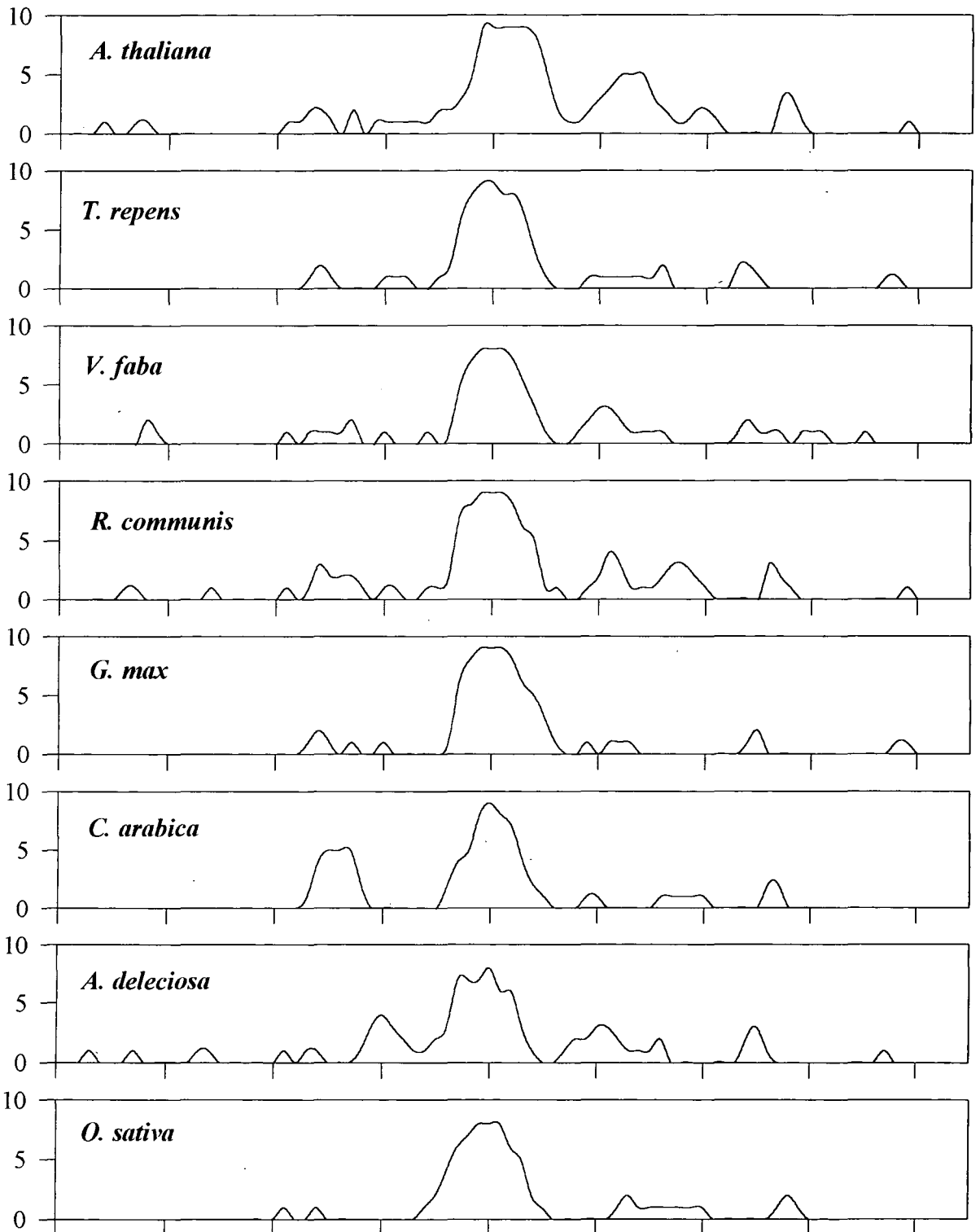
	10	20	30	40	50	60	70
prediction	<u>MSGCGCGSSCNCGDSCKCNKRSSGLSYSEMETTETVILGVGPAKIQFEGAEMSAASEDGGCKCGDNCTCDPCNCK</u> LLLLLLLLLLLLLLLLLLLLLLLL L L LLL EEEEE LLL LL LLLLL LLLLLLLLLLLLLLL						
α -helix	00000010111021210010101011110000000000000011111122222122111111110010000100						
β -strand	00120000000000002110012121211134789898541100222111122100000121100000000000						
loop	9987888987787777778776766677755110001348887566766554677788756788888998889						
prediction	EEEEEEE						
reliability	997688898778676757687646454657326899983187873446544324766886357889988998789						

Figure 3.5 Secondary structure prediction for the PsMT_A amino acid sequence from the program PHDsec. The numbers are scores from 0 to 9, on the basis of which an assignment is made for helix (H), strand (E) or loop (L). The reliability index is calculated from the relative values of the three predictions, a high score represents a high probability of the prediction being correct.

Figure 3.6 Graphical representation of the predicted probability of formation of a β -strand structure for all known plant type-1 and type-2 metallothionein-like gene products. The data was taken from the profile fed neural network secondary structure prediction program PHDsec (Rost and Sander 1993). The tick marks on the x-axis of each graph are at 10 amino acid intervals. The schematic diagram at the top of each set of graphs represents the arrangement of cysteines, and predicted β -strand in the two types of structure.



CC CxC CxC CxxC  GV  CxC CxC CxC



3.4 Conclusions

cDNA's encoding peptides with sequence similarity to metallothionein have been isolated from a wide range of higher plant species (section 3.1.1 and table 3.1). At this stage it seems likely that this class of gene may be common to all higher plants. The basic feature of the putative products of these genes remains the same for the genes reported to date, that is two cysteine rich domains separated by a cysteine free region. Two genes have been reported with a truncated interdomain region (Zhou and Goldsbrough 1994, Buchanan-Wollaston 1994). The information regarding tissue specificity and the effect of transition metals on gene transcription in different species does not present a clear picture as to the function of the gene products. To date there has been no report of the isolation of the translational product of the gene from a higher plant.

Comparison of the putative product of the *PsMT_A* gene with the protein databases suggest that this is a novel class of protein most closely related to metallothionein (section 3.3.1). A unique property of the gene is the interdomain region which, uncharacteristically for a metallothionein, contains aromatic residues. The product of the *MT1* gene from *A. thaliana* scores better in sequence comparisons with other metallothionein because the interdomain region in this predicted peptide is shortened. The plant metallothionein-like gene products can be placed into different categories according to features in the predicted primary structure (section 3.3.2). The most numerous category reported to date are the type-1 and type-2 gene products. The putative products differ consistently only in the arrangement of cysteine residues in the amino terminal domain (figure 3.1) but in addition a pattern of tissue specificity has emerged in which the type-1 genes are expressed in root tissue whilst the type-2 genes are expressed in leaf tissue.

There is a very high degree of sequence conservation between the gene products within the different categories (figure 3.2). The predicted structural characteristics of the gene products are also conserved (table 3.1). A phylogenetic tree constructed in the basis of amino acid substitutions between the different sequences within the type-1 and type-2 categories is basically as would be predicted from the phylogenetic relationship between the species represented (figure 3.3). The type-1 and type-2 categorisation of the products is preserved using the phylogenetic algorithm (section 3.3.5). If the conservation of amino acids between sequences is examined more closely it can be seen that the most conserved

sequences lie within the cysteine rich domains and towards the centre of the interdomain region (figure 3.4).

A region of β -strand is predicted to occur in the centre of the interdomain region of the *PsMT_A* gene product (figure 3.5). This structure is conserved throughout the type-1 and type-2 gene products (figure 3.6). Even though the structure is preserved there is not complete sequence conservation apart from a Gly-Val motif immediately following the β -strand (figure 3.4 and 3.6). This region could be of importance to the role of the interdomain region and speculation on this will be presented in section 8.1.

CHAPTER 4
CHARACTERISATION OF THE PRODUCT OF THE *PsMT_A* GENE
AND AN ANTI GST-*PsMT_A* IMMUNE SERUM

4.1 Introduction and objectives

In order to assign a function to the metallothionein-like gene products, for example the putative *PsMT_A* protein, data is required relating to the activity of the protein *in planta*. The protein needs to be identified in, and isolated from, plant tissue and then sequenced to determine if it has undergone post-translational modification. Which, if any, metals the protein binds *in planta* and the localisation of the protein within the cell will need to be determined. In the absence of this data, an insight into the role of the protein can be gained by studying the properties of a recombinant protein produced by expression of the gene in *E. coli*.

4.1.1 Characterisation of the product of the *PsMT_A* gene

It has been proposed that metal binding to the *PsMT_A* protein involves the formation of a metal-thiolate cluster analogous to that observed in metallothionein (Kille *et al.* 1991). Metal chelation, attributable to the *PsMT_A* moiety, has been demonstrated following overexpression of the GST-*PsMT_A* fusion protein in *E. coli*, for the metals copper, zinc and cadmium (Tommy *et al.* 1991). No evidence was obtained to support the chelation of iron by the GST-*PsMT_A* fusion protein *in vitro* (Robinson *et al.* 1992). However, *PsMT_A* may be unable to take up an appropriate conformation for iron binding in the fusion protein due to steric hindrance by the GST moiety, iron may not have been available in an appropriate oxidation state in *E. coli*, or the metal may have been lost during purification. An initial aim of this project was to characterise the metal binding site of the metallothionein-like protein from *P. sativum* by [¹¹³Cd] NMR. The suggested stoichiometry of 6 cadmium atoms and 12 potential thiol ligands may represent a unique mode of metal binding (Kille *et al.* 1991). Whether or not the linking region between the two cysteine rich domains are involved in metal binding could also be addressed in such a study.

The pGPMT3 plasmid, described in section 2.1.3 and Tommy *et al.* (1991), was used for the expression of the product of the *PsMT_A* gene in *E. coli*. In preliminary experiments prior to the start of this project it had been established that a low yield of the *PsMT_A* moiety

from the GST-PsMT_A fusion protein was obtained by factor Xa cleavage. (N.J. Robinson, unpublished results). Consequently production of preparative quantities of the PsMT_A protein by cleavage of the GST-PsMT_A fusion protein is prohibitively time consuming (and expensive). Since the metal binding property of the PsMT_A protein is conserved in the fusion protein, indicating that GST might not interfere with PsMT_A, it was hypothesized that the [¹¹³Cd] NMR spectra of GST-(Cd₆)-PsMT_A could have the same features as (Cd₆)-PsMT_A allowing the structural study of metal binding in the plant metallothionein-like gene product. For [¹¹³Cd] NMR spectroscopic analysis it was estimated that a 2 mM solution of protein would be required (at least 1 ml but preferably 3 ml) (P. Sadler personal communication). An aliquot (1 ml) of a 2 mM solution of the GST-PsMT_A fusion protein is equivalent to approximately 80 mg protein.

4.1.2 Characterisation of a rabbit anti GST-PsMT_A fusion protein immune serum

An immune serum to GST-PsMT_A was isolated from rabbit following inoculation with the purified fusion protein, isolated from *E. coli* grown in the presence of exogenous zinc using the glutathione affinity matrix and on acrylamide gels (A.M. Tommey unpublished). GST has low antigenicity and the GST fusion system has been used successfully to raise antibodies to the non GST portion of the fusion protein (Toye *et al.* 1990). Prior to the start of this project it had been demonstrated on western blots that the immune serum recognized the fusion protein and bound to it specifically in lysates of *E. coli* expressing the pGPMT3 plasmid (A.M. Tommey unpublished results).

An anti-PsMT_A immune serum would allow the identification of the product of the *P. sativum* metallothionein-like protein in plant tissue and could be used in the isolation of the protein. An ability to identify the protein in plant extracts would allow further characterisation of the protein with respect to, for example, metal binding. Further information leading to an elucidation of the function of the protein could be obtained by immunolocalisation techniques.

4.2 Methods

4.2.1 Expression of PsMT_A in *E. coli*

The GST-PsMT_A fusion protein was expressed in *E. coli* and purified from a crude cell lysate as described in sections 2.3.1 and 2.3.2. As a control GST protein was obtained from a strain

of *E. coli* JM101 transformed with the pGEX3X vector without an insert. To test the purification system electrophoresis of aliquots (5 μ l) of the crude lysates and pure proteins was performed on a 12.5 % (w/v) polyacrylamide gel as described in section 2.3.6.1. To investigate degradation of the purified fusion protein an aliquot of the protein in 50 mM Tris-HCl buffer was stored at room temperature for 5 days and then analysed by polyacrylamide gel electrophoresis as above.

4.2.2 The association of metal with the PsMT_A portion of the fusion protein

The GST-PsMT_A fusion protein was expressed in *E. coli* supplemented with 500 μ M ZnSO₄ (as described in section 2.3.1). A crude protein extract was prepared and the recombinant protein isolated on a glutathione-Sepharose matrix. The bridge between the GST moiety and PsMT_A was cleaved with activated factor Xa as described in section 2.3.4. The sample was desalted by loading it onto PD-10 column and eluted in 50 mM Tris, pH 8.0 (final total sample 7 ml). The enzyme and cleaved product were separated by gel filtration chromatography on Sephadex G-50 (as described in section 2.3.11.2) The column flow rate was approximately 1 ml min⁻¹ and fractions of 3.5 ml were collected. The fractions were assayed for zinc by atomic absorption spectrophotometry (section 2.3.13) and protein was identified using the dye binding assay (section 2.3.3)

An aliquot (400 μ l) of fractions 8, 17 and 25 (corresponding to peaks A, B and C on figure 4.4) were vacuum blotted onto PVDF membrane and were subjected to automated amino terminal sequence analysis.

4.2.3 Preparation of bulk quantities of GST-PsMT_A fusion protein for structural studies

In order to perform [¹¹³Cd] NMR on the GST-PsMT_A fusion protein at least 80 mg of purified fusion protein was required (section 4.1.1). As a fermenter was not available the largest practical culture volume was 1.5 l. From this a yield of 5 to 8 mg of fusion protein in 8 ml of buffer could be obtained by the method described in sections 2.3.1 and 2.3.2. The culture was supplemented with 500 μ M ZnSO₄, it was proposed that [¹¹³Cd] enriched cadmium could be exchanged into the protein at a later date. Each batch of protein was stored at -80 °C immediately following elution from the glutathione affinity matrix. The

method yielded protein extracts at a concentration of approximately 1 mg ml⁻¹ which required concentration to obtain a solution of 2 mM (equivalent to approximately 80 mg ml⁻¹).

4.2.4 Characterisation of an anti GST-PsMT_A immune serum by western blotting

A 12 % polyacrylamide gel was loaded with crude extracts of *E. coli* expressing the pGEX3X and pGPMT3 plasmids, glutathione affinity purified GST and GST-PsMT_A fusion protein (prepared as described in section 2.3.1 and 2.3.2) and a crude extract from the root of *P. sativum* (prepared as described in section 2.3.10.1). Following electrophoresis the protein was transferred to nitrocellulose by electroblotting (section 2.3.8). Cross reactivity with the anti GST-PsMT_A fusion protein immune serum was performed as described in section 2.3.9.

4.2.4.1 Purification of the immune serum on a GST affinity matrix

In order to remove any anti-GST specific antibody contamination from the immune serum a GST affinity matrix was constructed. A batch of GST was prepared from *E. coli* expressing the pGEX3X plasmid (section 2.3.1). The GST was immobilised on glutathione-Sepharose matrix and an aliquot of the immune serum mixed with the matrix and the eluent collected. Theoretically the anti-GST antibody should bind to the GST on the matrix and be immobilised. The eluent from the column would then contain a reduced quotient of anti-GST antibody.

4.2.4.2 Further refinement of the immune serum characterisation

Aliquots (400 µl) of the fractions from the gel chromatography of products of the cleavage of the GST-PsMT_A fusion protein with factor Xa (section 4.2.2) were vacuum blotted onto a nitrocellulose membrane using dot blot apparatus. The membrane was incubated with the anti-GST-PsMT_A immune serum and processed as described in section 2.3.9.

4.2.5 Characterisation of an anti-PsMT_A antibody

Independently, an antibody to (Cd₆)-PsMT_A was raised in mice (P. Kille unpublished). An aliquot of this antibody, and an aliquot of (Cd₆)-PsMT_A prepared by the method cited in Kille *et al.* (1991), was a generous gift. An Enzyme Linked Immunoabsorbent Assay (ELISA) was performed essentially as described by Norey *et al.* (1990). Both antibodies and the (Cd₆)-PsMT_A and GST-PsMT_A proteins were used. BSA was used as a negative control.

The wells of a 96 well Falcon 'Pro-bind' ELISA plate were coated with 500 ng of protein in 0.1 M carbonate-bicarbonate buffer (pH 9.6) by incubation overnight at 4 °C as illustrated in figure 4.9. The wells were washed repeatedly with TBS containing Tween-20 (0.05 %) and then incubated for 2 hours at room temperature with a 1:500 dilution of the appropriate antibody. The wells were washed and then incubated for a further 2 hours with either anti-mouse or anti-rabbit IgG conjugated to alkaline phosphatase. The wells were thoroughly washed and developed. After 45 minutes the reaction was photographed

4.3 Results and discussion

4.3.1 Expression of the GST-PsMT_A fusion protein in *E. coli*

Figure 4.1 confirms the presence of the GST-PsMT_A fusion protein in *E. coli* extracts. The crude extracts, tracks 1 and 3, illustrate that in extracts from cells containing the pGEX3X and pGPMT3 plasmids respectively the recombinant protein is highly abundant. The single bands detected in tracks 2 and 4 correspond with the predicted molecular weights of GST and the GST-PsMT_A fusion protein respectively (Smith and Johnson 1988 and Tommey *et al.* 1991 respectively). The resolution of samples in a single band following electrophoresis illustrates the effectiveness with which the glutathione affinity purification system isolates GST containing protein from the *E. coli* proteins.

Additional low molecular weight bands were observed on PAGE gels containing the fusion protein following storage of the protein at 4 °C for even a few hours or at -20 °C over several days. Degradation was halted completely at -80 °C. Figure 4.2 shows samples of fusion protein after one and five days incubation at room temperature respectively. As an equivalent degradation of GST is not observed the observed bands can be attributed to degradation of the PsMT_A protein. The relative mobility, R_f , of the marker bands and those of the degradation products were calculated. A calibration curve was plotted and a linear regression calculated for the best fit, figure 4.3. The apparent molecular weights of the degradation products on the gel estimated from this curve are presented in table 4.1;

The calculated molecular weights of the recombinant GST and GST-PsMT_A proteins from the amino acid sequences are 27 500 and 35 100 respectively. Taking into account the projected 95 % confidence limits of the regression line the 5 bands fall within the range of GST and the fusion protein. As the smallest band could correlate to GST alone this indicates

that proteolysis of PsMT_A forms four discrete degradation products and implies that PsMT_A is most susceptible to proteolysis at four specific sites.

Band	Relative molecular mass
1	37 900
2	34 700
3	32 600
4	29 900
5	27 900

Table 4.1 Estimated relative molecular masses of the GST-PsMT_A degradation products in figure 4.2

If the size of GST is subtracted from band 4, a molecular weight of 2400 is obtained. This is roughly equivalent to 20 amino acids and could speculatively be attributed to the amino terminal cysteine rich domain. Band 3 could be this peptide plus the next 20 or so amino acids and so on. The molecular weights of the degradation products cannot be determined accurately enough to precisely define the residues at which cleavage occurs.

4.3.2 Metal association with the PsMT_A protein

Analysis of the fractions obtained from gel filtration chromatography of the cleavage products of the GST-PsMT_A fusion protein with factor Xa are presented in figure 4.4. Sequencing of the fractions forming the three major peaks, labelled A (fraction 8), B (fraction 17) and C (fraction 25), gave the following result;

Peak A - the major protein peak. No amino acid sequence was obtained. The most probable assignment for this peak is the factor Xa enzyme. The failure to obtain sequence data can be attributed to the protein being N-terminally blocked thus preventing the Edman degradation reaction.

Peak B - Two peptide sequences were obtained; GIPGNSS... and GVGPAKIQ... These sequences are identical to those reported previously by Tommey *et al.* (1991), following cleavage of the GST-PsMT_A fusion protein by factor Xa. The first sequence corresponds to the region immediately following the site of factor Xa cleavage in the pGPMT3 plasmid and

the start of the PsMT_A protein, figure 4.5a. The second peptide sequence is located within the interdomain region of PsMT_A, figure 4.5b. The proceeding sequence is not similar to the factor Xa cleavage site and is therefore unlikely to be due to specific proteolysis by factor Xa. A possible assignment of band 3, figure 4.2, could be GST moiety plus the PsMT_A moiety up to Leu³⁸. An internal cleavage at the same site was one of four reported by Kille *et al.* 1991 after purification of recombinant PsMT_A from *E. coli*. It has been suggested that *in planta* the region may be removed after the formation of a metal cluster (Kille *et al.* 1991, Robinson 1992).

Peak C - No peptide sequence was obtained from this fraction. This peak is close to the predicted total volume of the G-50 column and may correspond to zinc which has dissociated from the fusion protein after the desalting step.

4.3.3 Preparative protein purification for [¹¹³Cd] NMR

After obtaining about 80 mg of protein at a concentration of approximately 1 mg ml⁻¹ it was necessary to concentrate this 80-fold to obtain a solution suitable for NMR. The initial approach was acetone precipitation (described in section 2.3.5.1). The protein was resuspended in a minimal volume of distilled deionised water. Initially a 10 fold concentration by this method was attempted. A fusion protein batch (3.5 ml) with an estimated concentration of 1.06 µg µl⁻¹ was precipitated and resuspended in 370 µl water. A 5 µl aliquot of the original solution and the concentrated solution was resolved on a polyacrylamide gel (as described in section 2.3.6) to check the integrity of the protein, figure 4.6. There was only minor degradation of the protein following the concentration procedure. The concentration of the protein solution was estimated by the modified Bradford technique (described in section 2.3.3). An average value of 3.6 mg of protein was obtained which indicated a yield of approximately 97.3 % (± 12 %).

It proved impossible to resuspend protein in volumes of water small enough to produce a concentration greater than 10 mg ml⁻¹. Increasing the salt concentration of the water used for resuspension up to 0.1 M Tris (pH 8.0), heating to 40 °C, stirring for 30 minutes or freezing -80 °C and thawing, had no significant effect on solubility. Batches of protein were expressed with and without exogenous zinc to investigate if zinc loading was effecting the solubility of the protein, there was no discernible difference in the solubility of the two batches.

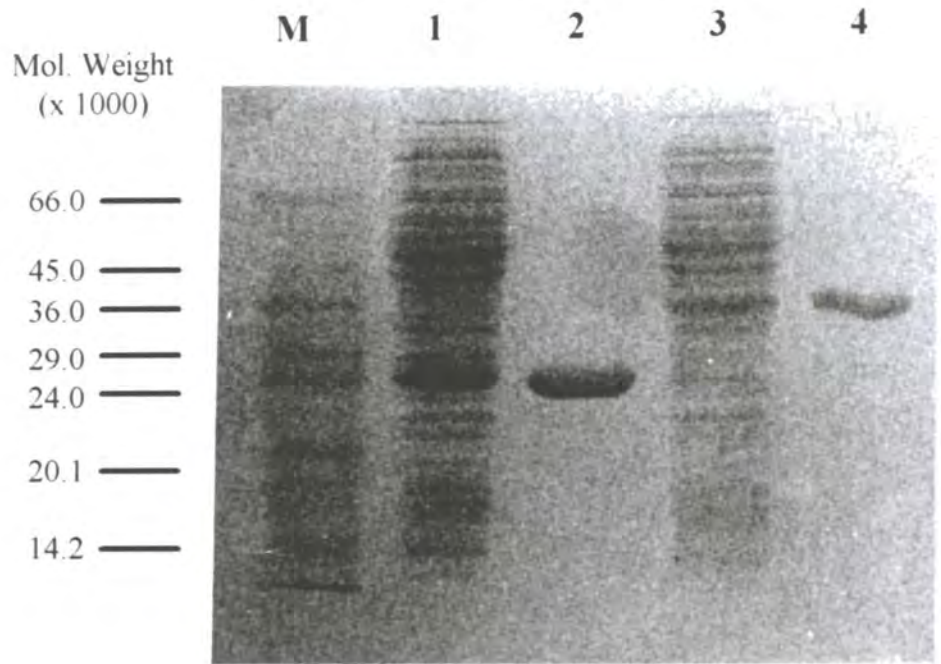


Figure 4.1 Polyacrylamide gel electrophoresis of crude cell extracts and purified protein obtained from *E. coli* containing the pGEX3X and pGPMT3 plasmids.

Track M - Molecular weight markers.

Track 1 - Crude extract of *E. coli* containing the pGEX3X plasmid.

Track 2 - GST protein following purification on glutathione affinity matrix.

Track 3 - Crude extract of *E. coli* containing the pGPMT3 plasmid.

Track 4 - GST-PsMT_A fusion protein following purification on glutathione affinity matrix.

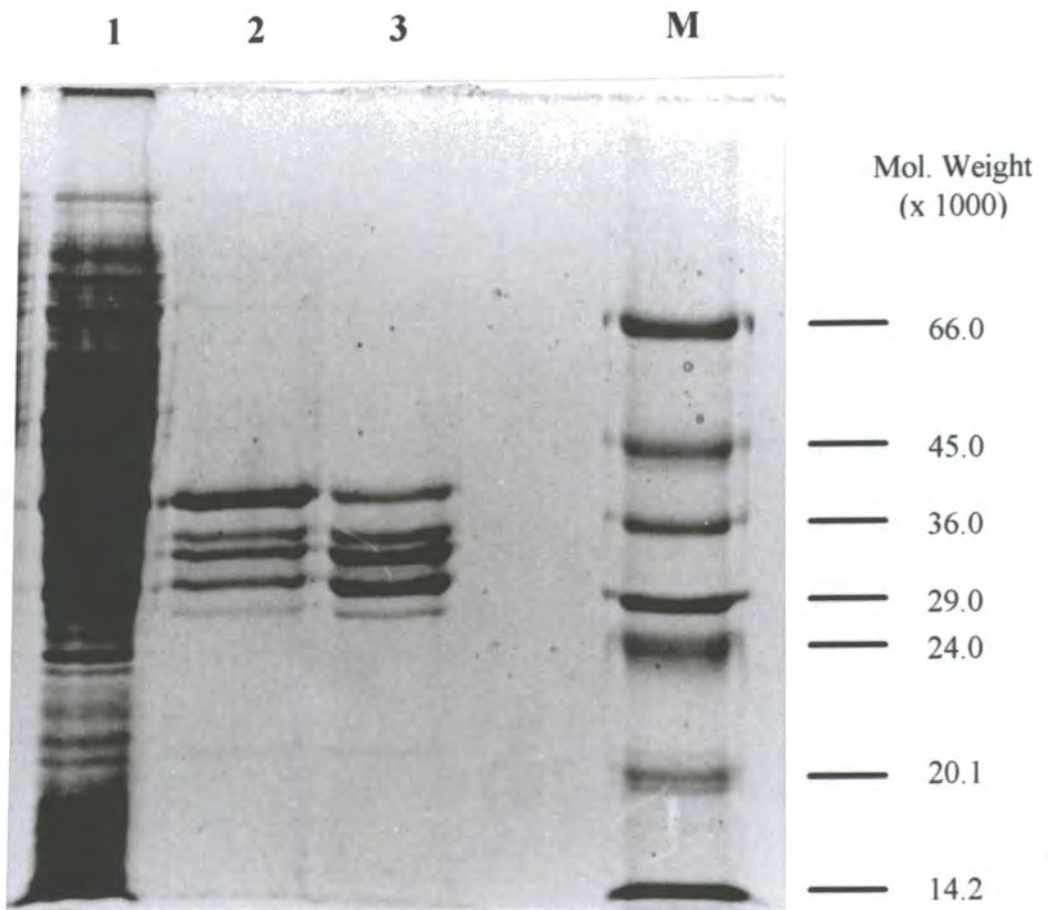


Figure 4.2 Polyacrylamide gel electrophoresis of the GST-PsMT_A fusion protein showing the susceptibility of the protein to proteolysis.

Track 1 - Crude extract of *E. coli* containing the pGPMT3 plasmid.

Track 2 - Purified fusion protein after storage at room temperature for 1 day

Track 3 - The same sample after further storage for 5 days

Track M - Molecular weight markers

Calibration curve

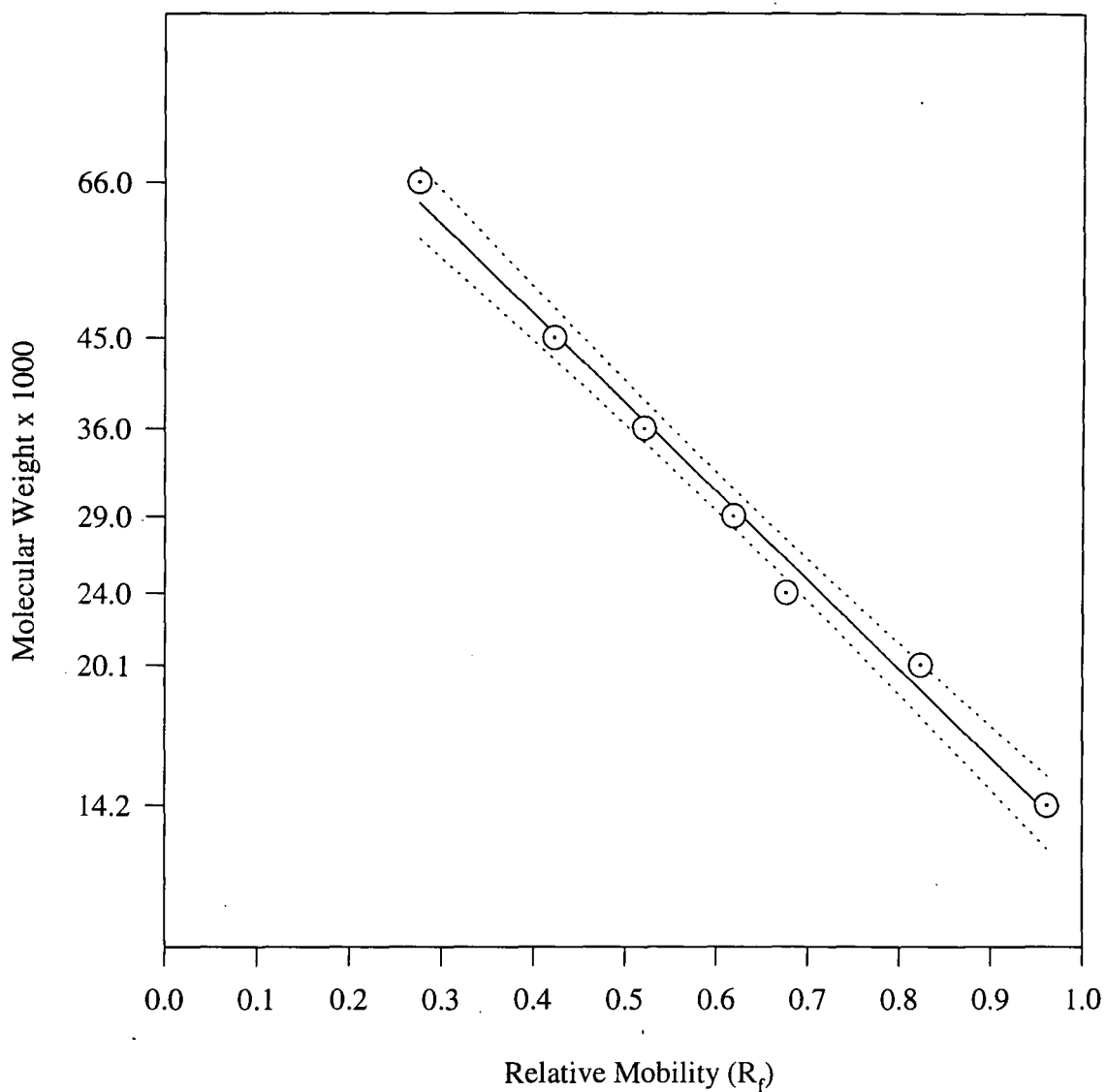


Figure 4.3 Calibration curve for molecular weight markers for polyacrylamide gel, figure 4.2.

($\text{Log}[\text{Mol. Wt.}] \propto R_f$) Dotted line represents 95 % confidence limits.

Gel filtration chromatography of factor Xa cleavage products

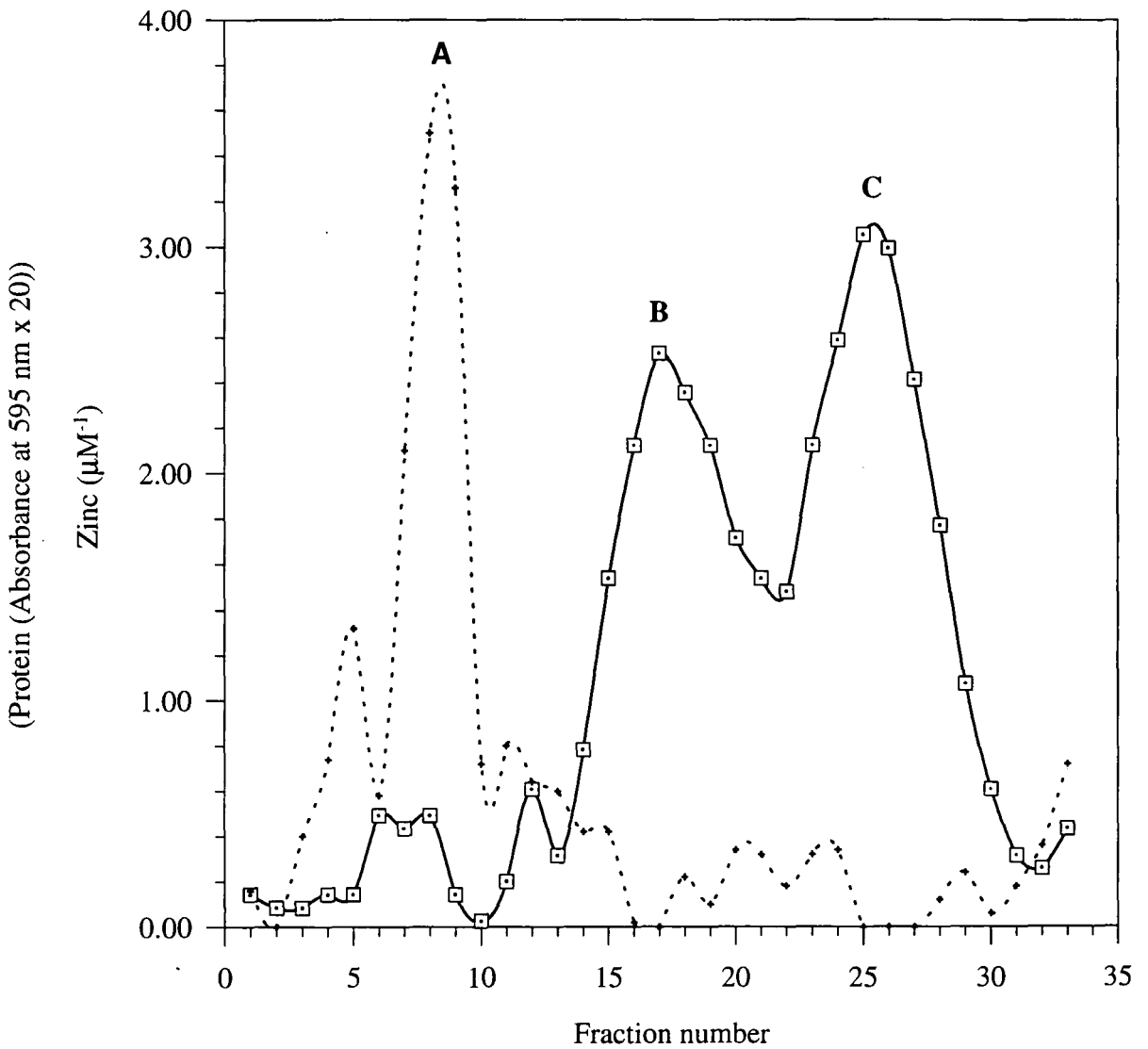


Figure 4.4 Gel filtration chromatography of factor Xa enzyme and cleavage products eluted from glutathione Sepharose matrix. Assayed for zinc (—, \square) and protein (\cdots , +).

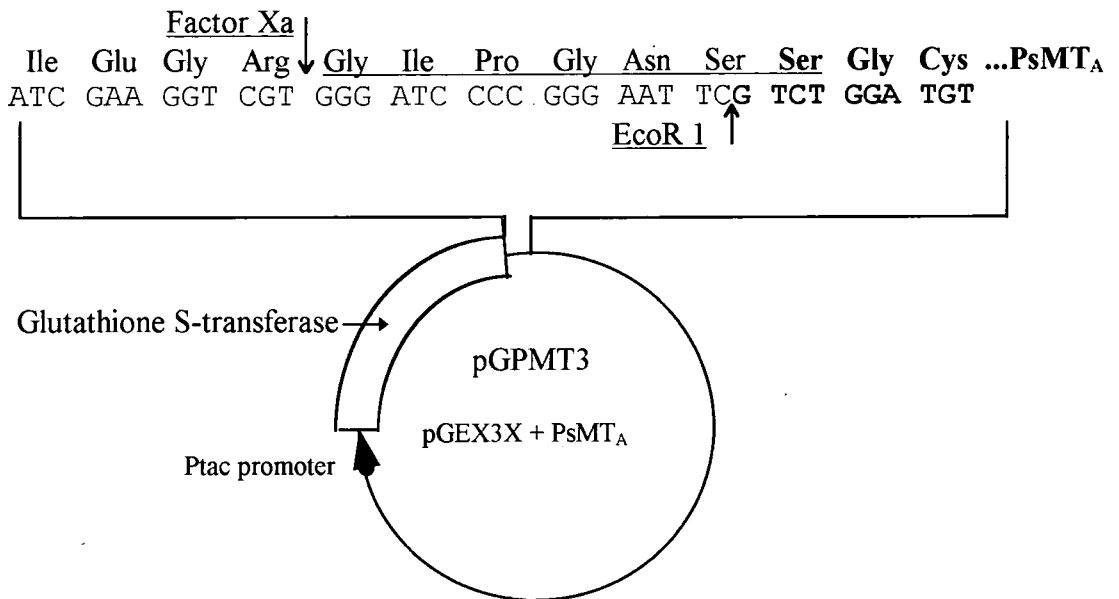


Figure 4.5a Nucleotide sequence and translation of the GST to PsMT_A linking region in the pGPMT3 plasmid. PsMT_A sequence is shown in bold and the amino acids obtained by sequencing are underlined.

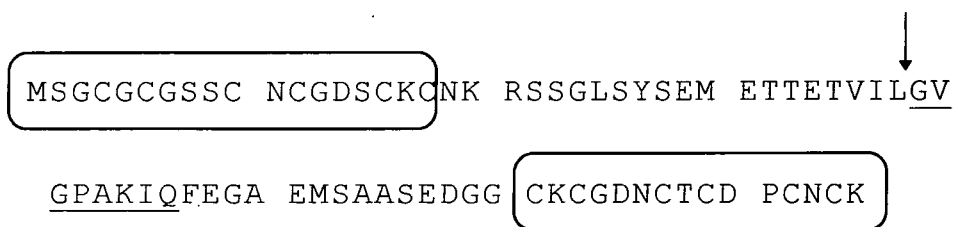


Figure 4.5b Primary structure of the PsMT_A gene product. The cysteine rich domains are boxed. The arrow indicates the position at which the protein has been cleaved and the amino acids obtained by sequencing are underlined.

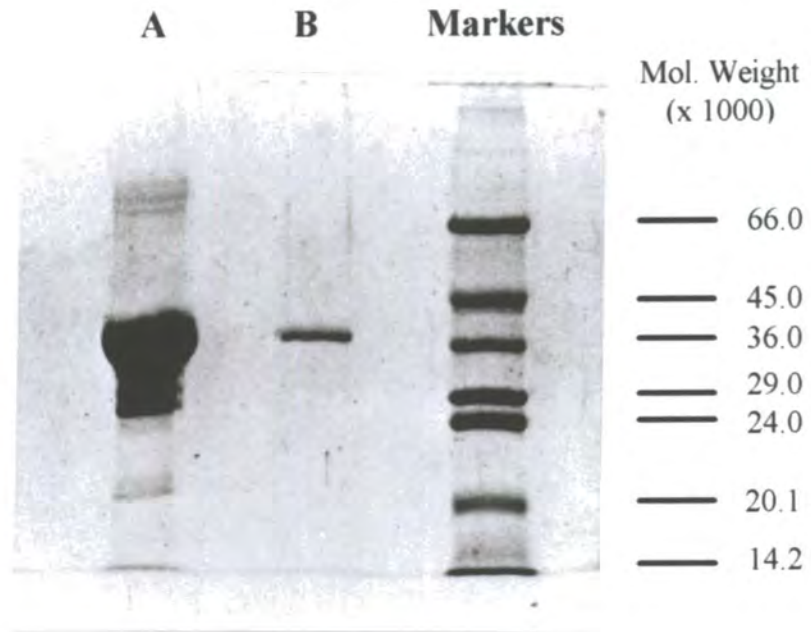


Figure 4.6 Polyacrylamide gel electrophoresis of 5 μ l of a solution of GST-PsMT_A fusion protein before (B) and after (A) concentration by acetone precipitation.

An alternative method of concentration was adopted using microconcentrator centrifuge vials (described in section 2.3.5.2). A fresh batch of protein was prepared with an estimated protein concentration of 11.2 mg in 12.2 ml (estimated by dye binding assay described in section 2.3.3). The solution was equally distributed between six microconcentrator vials. Following centrifugation for 30 minutes the volume was reduced to a total of 870 μl . The protein concentration was estimated to be $9.3 \mu\text{g } \mu\text{l}^{-1}$ which is equivalent to 8.09 mg total protein indicating a loss of approximately 3 mg of protein. This concentration was still inadequate for the structural study and so the solution was added to a single vial and subjected to centrifugation for a further 20 minutes resulting in a final volume of 210 μl . The protein concentration was estimated to be $17.8 \mu\text{g } \mu\text{l}^{-1}$ a total of only 3.75 mg of protein. The centricon used for this final concentration was washed with water and 1 mg of protein was recovered.

The procedure was repeated with fresh protein solutions a further two times and concentration limits of approximately $17 \mu\text{g } \mu\text{l}^{-1}$ and $21 \mu\text{g } \mu\text{l}^{-1}$ of protein were obtained. The three concentrated samples were pooled and centrifuged in centricons, periodically the concentration was checked. It failed to exceed $17 \mu\text{g } \mu\text{l}^{-1}$. A visible precipitate was observed on the filter of the centricons, this could be resuspended at a concentration of $10 \mu\text{g } \mu\text{l}^{-1}$. GST-PsMT_A is a protein of molecular weight 35 000. It is predicted that the size of the fusion protein is the limiting factor in obtaining solubility above approximately $20 \mu\text{g } \mu\text{l}^{-1}$. This concentration was approximately a fifth of that required for the structural study by [¹¹³Cd] NMR. The fusion protein is therefore an unsuitable subject for study by NMR. This structural study will require the production of a large quantity of purified PsMT_A protein. The facilities for the preparation of large batches (10 to 50 l) of *E. coli* for protein isolation were not available. This aspect of the project was not pursued any further.



4.3.4 Characterisation of a rabbit anti GST-PsMT_A fusion protein immune serum

The Ponceau S stained nitrocellulose filter and western blot produced by the method described in section 2.3.9 and section 4.2.4 is presented in figure 4.7. The immune serum cross-reacted with the GST protein, the GST-PsMT_A fusion protein and the degradation products from that protein. The immune serum did not cross-react with the other *E. coli* proteins or with any proteins in the crude pea extract. The cross reaction with degradation products both within the crude pGPMT3 track and the purified tracks suggests that either the degradation of the PsMT_A protein occurred before purification or that degradation occurs independently of the *E. coli* proteolytic machinery. The continuing degradation of the protein *in vitro*, as demonstrated in figure 4.2, supports the latter hypothesis. The intensity of the colour change on the western blot is approximately in proportion with the amount of protein loaded on the gel (figure 4.7A), within the bounds of sensitivity of detection method. This indicates that this is a specific response. The western blot strongly indicates that the epitope for the antibody lies within the GST moiety of the fusion protein. Equivalent data was obtained on four occasions.

4.3.4.1 Purification of the immune serum on a GST affinity matrix

It was speculated that any specific anti-PsMT_A signal in the western blot could be masked by an anti-GST signal. An aliquot of the immune serum was purified as described in section 4.2.1. Two polyacrylamide gels, equivalent to figure 4.7, with equal loading were prepared and blotted onto nitrocellulose. The blots were incubated with either the original immune serum or with the immune serum collected after passing through the GST-glutathione-Sepharose matrix. The blots were developed together. There was no difference in relative intensity of the GST to GST-PsMT_A signals between the blot incubated with the original immune serum and the blot incubated with the immune serum exposed to GST (result not shown). This indicates that either there is no specific anti-PsMT_A in the antibody or that if there is it is a very minor component.

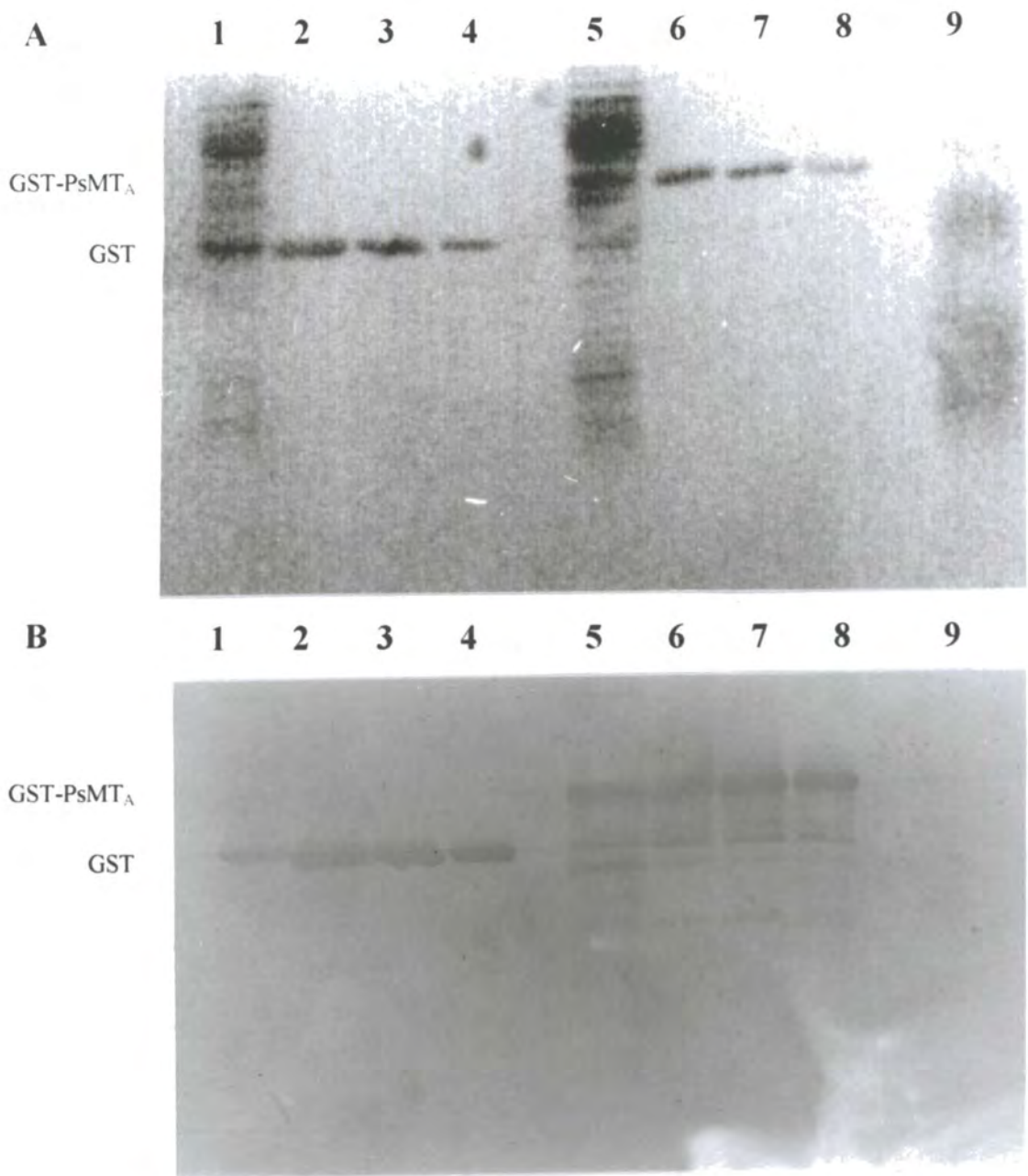


Figure 4.7 A - Ponceau S stained nitrocellulose filter.

B - Filter probed with anti-GST-PsMT_A immune sera.

Track 1 - Crude extract *E. coli* containing the pGEX3X plasmid.

Tracks 2 to 4 - Purified GST protein.

Track 5 - Crude extract *E. coli* containing pGPMT3 plasmid.

Tracks 6 to 8 - Purified GST-PsMT_A protein.

Track 9 - Crude protein extract from plant roots.

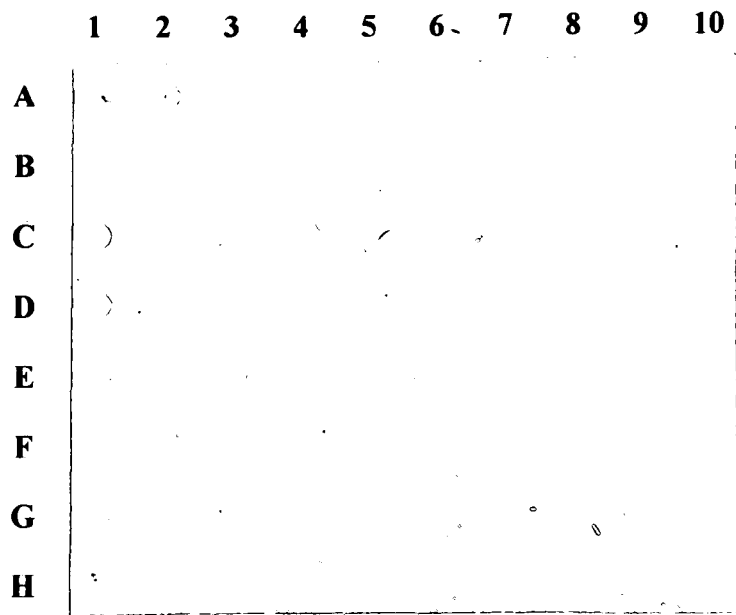
4.3.4.2 Further refinement of the immune serum characterisation

The question of whether the immune serum possessed any anti-PsMT_A activity was addressed directly. A dot blot of chromatography fractions which had been demonstrated to contain PsMT_A (section 4.3.2), incubated with the immune serum is presented in figure 4.8. The zinc profile and amino acid analysis indicate that fractions 16 to 19 contain the PsMT_A peptide (figures 4.4 and 4.5). However the immune serum cross-reacts most strongly with fractions 7 to 10. From figure 4.4 it can be seen that these fractions correspond to the abundant protein peak, designated factor Xa. The strong signal associated with the proposed factor Xa fraction may be due to nonspecific binding which becomes visible due to over development of the blot. Even with this over development there is no signal associated with the PsMT_A containing fractions. The procedure was repeated using half the concentration of immune serum to reduce the non specific binding, the result was identical, not shown.

From this result it can be concluded that the immune serum does not cross-react with PsMT_A. Alternatively it could be argued that the strong signal due to non-specific binding with factor Xa was "swamping" the specific signal. To investigate this possibility aliquots of fractions 6 to 24 were added to centricon C-10 microconcentrator tubes and centrifuged until all the liquid had passed through the membrane. The molecular weight cut-off of 10 000 should allow the PsMT_A protein to pass through (molecular weight 7500) whilst blocking the larger factor Xa protein. The samples were then vacuum blotted onto a nitrocellulose filter, using a slot blot apparatus, and processed as above. After incubation with the secondary antibody the blot was developed for a full 30 minutes. No positive signal was detected (data not shown).

4.3.5 Characterisation of an anti-PsMT_A antibody

The fully developed ELISA plate described in section 4.2.5 is presented in figure 4.9. The only observed colour change was due to the anti-GST-PsMT_A fusion protein immune serum cross-reacting with the GST-PsMT_A coated wells. The anti-GST-PsMT_A immune serum did not cross-react with the (Cd₆) PsMT_A protein or with BSA. The anti-PsMT_A immune serum was ineffective against all three proteins.



	1	2	3	4	5	6	7	8	9	10
A	1	9	17	25	33					
B	2	10	18	26						
C	3	11	19	27						
D	4	12	20	28						
E	5	13	21	29						
F	6	14	22	30						
G	7	15	23	31						
H	8	16	24	32						

Figure 4.8 Dot blot of fractions collected following gel filtration chromatography of eluent collected after factor Xa cleavage of the GST-PsMT_A fusion protein immobilised on glutathione affinity matrix probed with anti-GST-PsMT_A immune sera. The second grid provides a key to the numbers

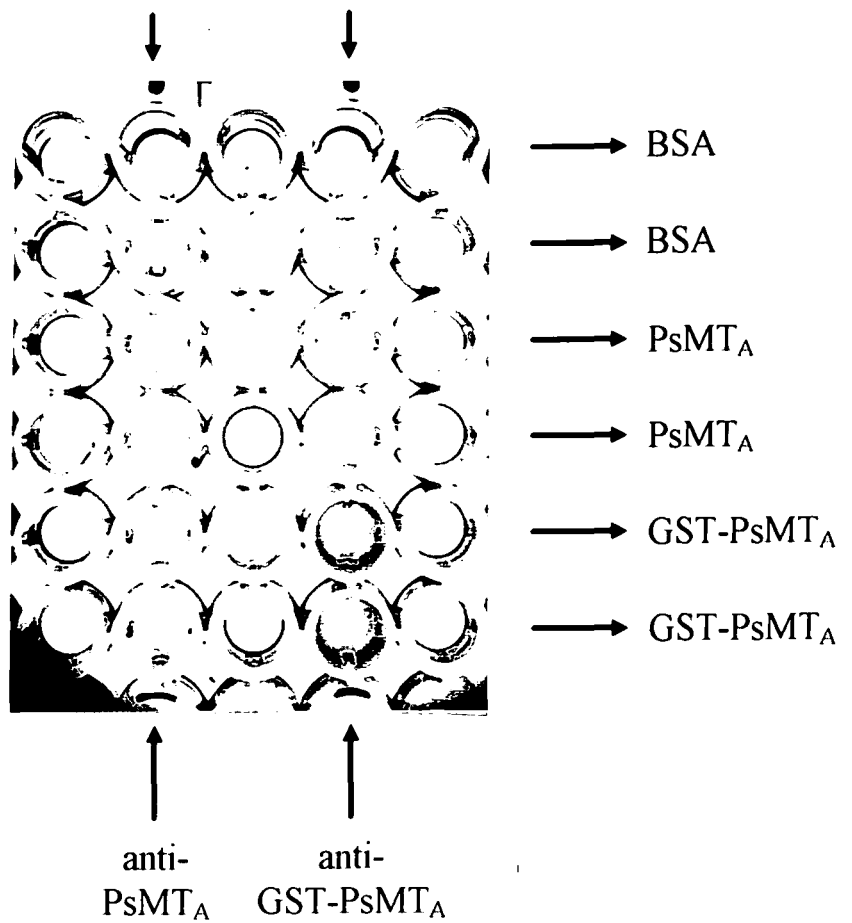


Figure 4.9 ELISA of BSA, GST-PsMT_A and PsMT_A probed with anti-(Cd₆)-PsMT_A and anti anti-GST-PsMT_A immune sera. The protein in each well is indicated by the horizontal arrows and the immune sera used to probe each column by the vertical arrows.

4.4 Conclusions

The product of the *PsMT_A* gene can be expressed in *E. coli* as a carboxyl terminal extension of GST protein (figure 4.1). The gene product functions as a metal chelator with respect to zinc (figures 4.4 and 4.5). The GST-*PsMT_A* fusion protein had a solubility limit of approximately 20 µg ml⁻¹ which was inadequate to allow the structural characterisation of metal binding in the *PsMT_A* protein (section 4.3.3). The limiting factor in achieving an adequately concentrated solution for study by [¹¹³Cd] NMR is the size of the GST moiety of the fusion protein. It is predicted that it should be possible to achieve an adequate concentration of the *PsMT_A* protein alone for such a study. Adequate quantities of the protein could be produced either by cleavage of the GST fusion protein or by expressing *PsMT_A* alone (not as a fusion protein) in *E. coli*. In both cases it would be necessary to employ a large scale purification strategy. The *PsMT_A* gene product is susceptible to proteolysis in solution at discrete sites with the region between the two cysteine rich domains being the most likely location of those sites (figure 4.2). This observation is in accord with previous observations made during the isolation of the recombinant *PsMT_A* protein from *E. coli* (Kille *et al.* 1991).

The epitope of the anti-GST-*PsMT_A* immune serum lies within the GST moiety of the fusion protein (section 4.3.4). The immune serum therefore cannot be used to identify the product of the *PsMT_A* gene in extracts from *P. sativum*. The immune serum has been used successfully as an anti-GST antibody as a control in western blots in subsequent experiments (D. Fairweather PhD thesis).

In archetypal mammalian metallothionein a major antigenic determinant is the amino terminal 5 residues (AcMDPNC) (Kikuchi *et al.* 1990). The amino terminal methionine in metallothionein is acetylated and the loss of this acetylated group leads to a loss of antigenicity. The amino terminal region of animal metallothionein is not conserved in the plant metallothionein-like proteins. There has been a report of cross-reactivity between an anti-rat metallothionein antibody (OAL-JI) with an unidentified protein in soybean (Nakajima *et al.* 1992). However the antigenic molecule has not been purified and hence positively identified as a metallothionein.

The low antigenicity of the *PsMT_A* protein complicates the production of antibodies to it. If this problem could be overcome there would be further complications in using such an antibody to identify the active protein in plant tissue. The possibility of post translational

modification of the protein *in planta* could destroy an epitope present in a recombinant protein. The metal specificity of PsMT_A should also be considered as the binding of metal ions with different oxidation states and different ionic radii will effect the conformation of the protein and could destroy an epitope found in one species. However, if such an antibody could be generated, a functional anti-PsMT_A antibody would be a useful tool for the elucidation of the function of the metallothionein-like protein.

CHAPTER 5

CLONING AND CHARACTERISATION OF THE TYPE-2 METALLOTHIONEIN-LIKE GENE FROM *ARABIDOPSIS THALIANA*

5.1 Introduction and objectives

The amino terminal plant metallothionein-like type-1 domain has some similarity to the β -domain of mammalian metallothionein as both contain predominantly Cys-Xaa-Cys motifs whilst the type-2 amino terminal domain and α -domains have a more heterologous nature, see figure 4.1. Studies on the different domains of mammalian metallothionein have revealed that they have different metal preferences (section 1.4.4). The α -domain has a preference for the divalent metal ions cadmium and zinc compared to the β -domain which conversely has a higher preference for monovalent copper ions. This implies that the number and arrangement of the cysteine residues within metallothionein may have a direct consequence for metal preference and stoichiometry. The aim of this section of research was to investigate the effect of the different arrangement of cysteines within the type-1 and type-2 plant metallothionein-like gene products on metal affinity. Specifically the pH of half dissociation with respect to zinc will be compared for a candidate type-1 and type-2 recombinant protein using the pGEX3X expression system in *E. coli*. A type-1 gene product was already available for this study from the expression of the *PsMT_A* gene in the pGPMT3 plasmid (section 4.3.1). A metallothionein-like gene from *A. thaliana* (from here on referred to as *AtMT-t2*) was selected to represent the type-2 gene products for this experiment because of the availability of the cDNA sequence on the EMBL database, the availability of an *A. thaliana* cDNA library and the increasing use of *A. thaliana* as a model plant for biochemical and genetic studies.

A mutant strain of the cyanobacteria *Synechococcus* PCC 7942 (R2-PIM8 (*smt*-)) deficient in the metallothionein locus, *smt*, is hypersensitive to elevated zinc (Turner *et al.* 1993). Zinc tolerance was restored to wild type levels by reintroducing the *Synechococcus* metallothionein locus. To further examine the potential zinc chelating properties of the product of the *A. thaliana* plant metallothionein-like gene (*AtMT-t2*) a complementation experiment was designed, in which a modified *smt* locus was introduced into *smt* deficient cells in which the *AtMT-t2* gene was substituted for the *Synechococcus* metallothionein, *smtA*

(cyanobacterial work in collaboration with Dr. J.S. Turner). The phenotype of these cells with respect to zinc could then be studied. To date, plant metallothionein-like genes have been used to complement a copper metallothionein deficient, copper hypersensitive, mutant of yeast (Zhou and Goldsbrough 1994). The complementation of *smtΔ* *Synechococcus* with a plant metallothionein-like gene provides an opportunity to study the effect of expression of these genes in a zinc hypersensitive mutant to assess the possible role of this class of gene in the metabolism of zinc.

5.2 Methods

5.2.1 Design of primers for the Polymerase Chain Reaction

The cDNA sequence for the type-2 gene from *A. thaliana* (*AtMT-t2*) was obtained from the EMBL nucleotide sequence database (accession number X62818). The design for the homologous primers is presented in figure 5.1A. These were a 5' primer matching the initial 6 codons of the *AtMT-t2* gene and a 3' primer matching the inverse complement of the final 7 codons of the coding sequence, figure 5.1B. In order to facilitate direct cloning into the polylinker of the pGEX3X vector a *Bam*H1 restriction enzyme recognition site was incorporated into the 5' primer design and an *Eco*R1 recognition site was incorporated into the 3' primer, figure 5.1B. The extra 'CC' between the *AtMT-t2* ATG and the *Bam*H1 recognition site places the *AtMT-t2* sequence in frame for expression as a carboxyl terminal extension of GST. The 3' primer includes the *AtMT-t2* stop codon, but two stop codons in the pGEX3X polylinker will also be in frame. The expected size of a PCR product produced from these primers is 265 nucleotides.

The oligonucleotides were synthesized as described in section 2.5.7. The concentration of the oligonucleotides was estimated by UV spectroscopy at 260 nm and adjusted to a final concentration of 60 pM.

5.2.2 PCR of the coding sequence of the *AtMT-t2* gene

A PCR reaction was carried out on a range of *A. thaliana* and *P. sativum* DNA sources, detailed in figure 5.2 by the method described in section 2.5.8. In addition to the primers for *AtMT-t2* described in section 5.2.1 a set of primers homologous to the 5' and 3' regions of the *PsMT_A* gene were available, described in Evans *et al.* (1992). An aliquot (50 µl) of each

reaction was visualized by agarose gel electrophoresis on a 1.5 % (w/v) agarose gel as described in section 2.5.2.1.

5.2.3 Cloning of *AtMT-t2* into pGEX3X

The *Eco*R1 and *Bam*H1 sites designed into the PCR primers were used to clone the PCR product directly into pGEX3X. For a preparative sample of the putative *AtMT-t2* DNA fragment, five samples of the DNA equivalent to lane 5 in figure 5.2, were amplified by PCR as described in section 2.5.8. Aliquots (80 µl) were run on a 1.5 % agarose gel and the single band of approximately 260 nucleotides (not shown) was cut from each lane. There were no other bands on the gel. The DNA was extracted from each lane by the silica fines method described in section 2.5.3. The DNA was further purified by the phenol:chloroform extraction method (section 2.5.4.1) and stored at -20 °C.

An aliquot of the DNA sample was restricted with the enzymes *Eco*R1 and *Bam*H1 as described in section 2.5.5. The DNA was removed by addition of silica fines (section 2.3.5) and cleaned with phenol:chloroform (2.5.4.1). An aliquot of the pGEX3X vector (2 µg) was restricted with the enzymes, *Eco*R1 and *Bam*H1 (section 2.5.5). The DNA was removed by addition of silica fines (2.5.3) and cleaned with phenol:chloroform (2.5.4.1). The DNA and vector were ligated in a reaction mixture containing vector (1 µg) and DNA (100 ng) and DNA-T4 ligase which was incubated overnight at 16 °C. Competent *E. coli* cells (SURE) were transformed with this plasmid as described in section 2.5.6.

The pGEX3X vector system does not allow blue/white selection. To select colonies containing the *AtMT-t2* insert, individual colonies (24) were picked, and plasmids recovered as described in section 2.5.1.1. The recovered DNA was restricted with *Bam*H1 and *Eco*R1 and separated on a 1.5 % (w/v) agarose gel (not shown). Cultures yielding plasmids with inserts of the anticipated size were transferred to 50 % (v/v) glycerol.

5.2.4 Genomic analysis

The *P. sativum* and *A. thaliana* genomes were examined for the presence of sequences which cross hybridized with the *AtMT-t2* clone and with the *PsMT_A* clone. Restriction digests of genomic DNA from *A. thaliana* (Columbia) and *P. sativum* (Feltham First) were produced by incubating DNA with the enzymes *Eco*RV, *Eco*RI, *Bam*HI, *Hind*III and *Bgl*II, and separating the fragments on a 0.8 % (w/v) agarose gel, figure 5.4a. The DNA was transferred to a

membrane as described in section 2.5.11.1. After fixing the filter was probed with [α - 32 P] dCTP labelled *AtMT-t2* DNA, released from the pJWNR1.1 plasmid by restriction with *Bam*H1 and *Eco*R1, as described in section 2.5.11.2. The *AtMT-t2* probe was stripped from the filter by washing with boiling 0.1 % SDS and the filter was re-probed with [α - 32 P] dCTP labelled *PsMT_A* DNA released from the pGPMT3 plasmid by restriction with *Eco*RI by the same method.

5.2.5 Overexpression of *AtMT-t2* in *E. coli*

The *AtMT-t2* gene was expressed in *E. coli* from the pJWNR1.1 plasmid as a carboxyl terminal extension of GST, as described in section 2.3.1. Expression from the plasmid was induced in the presence of 500 μ M zinc and the GST-*AtMT-t2* fusion protein was isolated from a crude *E. coli* lysate using the glutathione affinity matrix, described in section 2.3.2. To confirm expression of the fusion protein an aliquot of the purified protein was run on a 12.5 % (w/v) acrylamide gel along with an aliquot of the crude extract, as described in section 2.3.6.1.

5.2.6 Confirmation of zinc association with the *AtMT-t2* protein

Cell lysates, of *E. coli* grown in 500 μ M exogenous zinc, containing recombinant GST-*AtMT-t2* fusion protein were applied to glutathione affinity matrix and the fusion protein cleaved with activated bovine factor Xa (as described in section 2.3.4). The column wash, containing cleaved protein and factor Xa was desalted (PD-10 column) and subjected to gel filtration chromatography (as described in section 2.3.11.2). The column was equilibrated in 50 mM Tris pH 7.2 + 1 % (v/v) 2-ME. The flow rate was 0.4 ml min⁻¹ in that buffer. Fractions of 3 ml were collected and assayed for zinc (section 2.3.13) and protein (section 2.3.3).

5.2.7 Measurement of zinc affinity of recombinant plant metallothionein-like peptides

To investigate the hypothesis that the recombinant *AtMT-t2* protein might have a higher affinity for zinc than the recombinant *PsMT_A* protein proton displacement experiments in which the proportion of bound to free zinc is estimated over a range of pH values were performed essentially as described in Tommey *et al.* (1991). A batch of each GST fusion protein was prepared as described in sections 2.3.1 and 2.3.2. The protein was eluted from

the glutathione affinity matrix in a total of 5 ml, and desalted on PD-10 columns equilibrated in 0.05 M K₂HPO₄. The protein was eluted in a total of 7 ml of that buffer and assayed for zinc. Fifteen PD-10 columns were equilibrated in buffers covering a range of pH values from approximately 1.5 to 9.0 (described in section 2.2.4).

To 2.15 ml of each buffer 350 µl protein solution (in 0.05 M K₂HPO₄) was added and incubated at room temperature for 1 h. To take account of the change in pH that the addition of the potassium phosphate buffer causes two sets of the fifteen buffers were prepared, the extra set contained a proportional quantity of 0.05 M K₂HPO₄, referred to as buffer-P, and the working pH of buffers selected accordingly.

Each PD-10 column was equilibrated with the appropriate buffer-P (25 ml). The sample in the complementary buffer was loaded onto the column (2.5 ml). The sample was eluted in the appropriate buffer-P (3.5 ml), this is the total volume. The column was washed in a further 6 ml of buffer to collect metal which has dissociated from the sample, the void volume. The zinc content of buffer-P (BP), and total and void volumes was estimated by atomic absorption spectrophotometry. The values of the void and total volumes were corrected for the zinc content of the buffers by subtracting BP. The total number of moles of metal in the void volume (V_d) and total (V_t) volumes was calculated and the proportion of metal associated with the protein, that is in the void volume, calculated as follows;

$$\text{proportion of bound metal} = \frac{V_d}{V_d + V_t}$$

This value was calculated for each buffer and then normalised for the proportion of bound metal at pH 9. The data was plotted and the pH at which 50 % of the metal was displaced estimated.

5.2.8 Expression of *AtMT-12* in *Synechococcus*

5.2.8.1 Design of PCR primers

A modified 5' primer was designed to facilitate the cloning of the *AtMT-12* coding sequence into the *Synechococcus smt* locus (figure 5.1C). The PCR product generated from this primer, the 3' primer described in figure 5.1B and *AtMT-12* template DNA will replace *smtA*

in the *smt* locus (described in Huckle *et al.* 1993). When the *Bam*H1 site reforms it will form the Shine-Delgarno sequence (AGGA). To maintain the optimum spacing between the Shine-Delgarno sequence and the ATG of *AtMT-t2* nine bases have been introduced between the *Bam*H1 site and the ATG in the primer. Six of these bases are homologous to the equivalent sequence in the *smtA* promoter (single underlined, figure 5.1C).

5.2.8.2 PCR and initial cloning of *AtMT-t2*, for the expression of *AtMT-t2* in *Synechococcus*

PCR was performed, using the 5' primer described in figure 5.1C and the 3' primer described in 5.1B and the plasmid pJWNR1.1 (section 5.3.2) as template DNA, according to the method described in section 2.5.8. The product of this PCR reaction was cloned into pGEX3X and transformed into *E. coli* (SURE) cells as described in section 5.2.3.

5.2.8.3 Transformation of *Synechococcus* and examination of the zinc phenotype

Subsequent sub-cloning of the *AtMT-t2* gene to create an *smt* locus containing the *AtMT-t2* gene, transformation of *Synechococcus* PCC 7942 (R2-PIM8(*smt*-)) with this construct and examination of the zinc phenotype of the transformed cells was carried out by Dr. J.S. Turner essentially as described in Turner *et al.* 1993.

Figure 5.1 AtMT-t2 primer design

A: Published nucleotide sequence of the type-2 metallothionein-like gene from *Arabidopsis thaliana* (Takahashi, K., EMBL accession number X62818, submitted Nov. 1991). The coding sequence is underlined and the sequence homologous to the primers is in bold.

B: Primers for PCR of *AtMT-t2*. Oligonucleotide sequence is in capitals and complementary sequence is in lower case. The *Bam*H1 and *Eco*R1 recognition sequences, and their cleavage sites incorporated into the 5' and 3' primer design respectively are indicated. The sequence homologous to the *AtMT-t2* gene is in bold.

C: Primer for PCR of *AtMT-t2* for subsequent transformation into a mutant line of *Synechococcus* PCC 7942 (R2-PIM8) deficient in metallothionein. The *Bam*H1 recognition sequence and cleavage site are indicated. The double underlined bases are required to reform the Shine-Delgarno sequence when the PCR product is introduced into the *smt* locus. The single underlined bases are homologous to the equivalent sequence in the promoter of *smtA* and are required to maintain an optimum distance between the Shine-Delgarno sequence and the ATG of the expressed gene.

A

1 CATTCAATAA TTTTCTTCA ATTTGAATTT TCTCGAGAAA AATGTCTTGC
 51 TGTGGAGGAA ACTGCGGATG TGGATCTGGC TGCAAGTGCG GCAACGGTTG
 101 TGGAGGTTGC AAAATGTACC CTGACTTGGG ATTCTCCGGC GAGACAACCA
 151 CAACTGAGAC TTTTGTCTTG GGCGTTGCAC CGGCGATGAA GAATCAGTAC
 201 GAGGCTTCAG GGGAGAGTAA CAACGCTGAG AGCGATGCTT GCAAGTGTGG
 251 ATCTGACTGC AAGTGTGATC CTTGACCTG CAAGTGAAGA AGCCTTTTTA
 301 AATAAGCAGA GATAATCGAG TCTCTTTAAT NTAATTAAGT TATTCAATAA
 351 GTAAACCATA TATAGGATGG TGTTTTTAGG TTTGGTTTAT GTGTAATAAT
 401 GGCTTCAGCT TATCTTTTAG CCGATCATTG TCTTTTGTGT TTGTTTTGAT
 451 CATATCTTTT AGATGTCTAG CAAATCTGCC ATGTGATGAG TTTGTACTTC
 501 CAGTGGAATG ATAATAATAT TATAGTTTTA AATCAAAAAA AAAAA

B**5' primer (#519)**

↓
 5' - CGT GGG ATC CCC ATG TCT TGC TGT GGA GGA -3'
 gca ccc tag ggg tac aga acg aca cct cct
 ↑
*Bam*H1 site

3' primer (#518)

↓
 5' - G GCG AAT TCA CTT GCA GGT GCA AGG ATC -3'
 c cgc tta agt gaa cgt cca cgt tcc tag
 ↑
*Eco*R1 site

C**5' primer (#861)**

↓
 5' - C GTG GGA TCC GCT GTC ATG TCT TGC TGT GGA GGA -3'
 g cac cct agg cga cag tac aga acg aca cct cct
 ↑
*Bam*H1 site

5.3 Results and discussion

5.3.1 PCR

The result of PCR with the *AtMT-t2* and *PsMT_A* primers and a number of DNA samples is presented in figure 5.2. The details of the primer and DNA combinations for each lane are detailed in the legend and labels on figure 5.2.

5.3.1.1 *AtMT-t2* primers No PCR product was detected with the three *A. thaliana* root cDNA samples, lanes 1 to 3, indicating that the *AtMT-t2* gene was not represented in any of these samples. The lack of product in lane 4 indicates that there is insufficient homology between the *AtMT-t2* primer sequences and the corresponding region of the *PsMT_A* gene for the primers to anneal to it. The single product of approximately 260 base pairs from the *A. thaliana* leaf cDNA library, lane 5, corresponds to the predicted size of the *AtMT-t2* coding sequence (section 5.3.2). There was no detectable product from the *P. sativum* root cDNA, lane 6, using the *A. thaliana* primers.

5.3.1.2 *PsMT_A* primers The low molecular weight products in lanes 7,8 and 11 were not positively identified. There are several possibilities; they could be primer multimers (this may be unlikely because the same primer concentrations were used in all 12 PCR reactions), they could be a *P. sativum* homolog to a type-3 metallothionein-like gene potentially with a type-2 like amino terminal domain. (The type-3 sequences had not been reported at the time of this experiment), or they could represent mispriming or hybridisation to some sequence only distantly related to metallothionein-like genes. There was no PCR product from *A. thaliana* root cDNA, lane 9, which could indicate that if the product in lanes 7,8 and 11 is genuine then it is not expressed in this sample. The product of approximately 260 base pairs in lanes 10 and 12 coincides with the predicted size of the fragment of the *PsMT_A* gene which could be amplified using these primers. The larger product in lane 11 could correspond to an *A. thaliana* type-1 gene or it could be contaminating carry over from either of the two adjacent lanes where a product of that size is abundant. An investigation of the unidentified products in lanes 7,8 and 10 would be interesting, however to keep within the time constraints of this project only the proposed *AtMT-t2* product, lane 5, was pursued any further.

5.3.2 Cloning of the *AtMT-t2* coding sequence

The PCR reaction equivalent to lane 5, figure 5.2, was repeated and the product cloned into the pGEX3X vector as described in section 5.2.3. Of the 24 colonies picked, plasmid DNA was recovered from 19 of which 16 had an insert of the correct size. Four of these original cultures were stored at -80 °C (designated pJWNR1.1 to 1.4). Plasmid pJWNR1.1 was selected for sequencing (as described in section 2.5.7). The resulting sequence corresponds to the *AtMT-t2* sequence reported on the EMBL database and the pGEX3X polylinker sequence as indicated, figure 5.3. There is a single base substitution giving a codon change AGC to AAC, which results in an amino acid substitution of Ser⁶⁴ to Asn⁶⁴. This conservative change has subsequently been reported in another *AtMT-t2* clone (Zhou and Goldsbrough 1994). It is therefore likely to be genuine and there may be an error in the original database submission or it could arise due to variation within strains of *A. thaliana*.

5.3.3 Genomic analysis

Figure 5.4a is a photograph of a gel stained with ethidium bromide of restriction digests of *A. thaliana* and *P. sativum* genomic DNA, which were subsequently transferred to a nylon membrane filter. The results of probing this filter with *AtMT-t2* and *PsMT_A* DNA are presented in figures 5.4b and 5.4c respectively. In the *A. thaliana* genomic DNA lanes 1, 2, 3 and 4 (figure 5.4c) a single band is visible corresponding to a fragment containing DNA which hybridises to the *AtMT-t2* coding sequence which suggests that there may be a single copy of the *AtMT-t2* gene. The hybridisation signal was too weak to detect a band in lane 5. In a similar experiment a single strong band corresponding to hybridisation with *AtMT-t2* was seen in digests of *A. thaliana* genomic DNA (Zhou and Goldsbrough 1994). The cause of the strong, apparently unspecific signal in the *P. sativum* genomic DNA tracks with the *AtMT-t2* DNA probe was not determined. It is most likely to be an artifact due to 5 fold excess of DNA in the pea tracks compared to the *A. thaliana* tracks coupled with partial digestion of the DNA and therefore may not represent any significant sequence homology. More stringent washing of the filter did not result in clarification of this signal (data not presented).

The pattern of multiple bands in the pea genomic DNA tracks probed with *PsMT_A* DNA (figure 5.4c) is analogous to that reported in Evans *et al.* (1990). These multiple bands are indicative of a multi-gene family. There is no signal, either specific or otherwise, in the lanes

containing *A. thaliana* DNA which suggests there is no strong homology between the *P. sativum* coding sequence and any *A. thaliana* homologs.

5.3.4 Expression of *AtMT-t2* in *E. coli*

Polyacrylamide gel electrophoresis analysis of protein extracts isolated from *E. coli* cells (SURE) containing the pJWNR1.1 plasmid (section 5.3.2) is presented in figure 5.5. Adjacent lanes contained crude and purified GST recovered from *E. coli* cells (JM101) containing the pGEX3X plasmid alone. A protein with the predicted molecular weight for the GST-*AtMT-t2* fusion protein (approximately 37 000) was very abundant in crude extracts (lane 3). The gel was slightly overloaded but there was little indication of the same degree of degradation observed with the GST-PsMT_A fusion protein. There is a faint band of the same apparent molecular weight of GST and possibly a band of intermediate molecular weight. It is not clear if these are degradation products or contaminants.

5.3.5 Confirmation of zinc binding with the *AtMT-t2* peptide

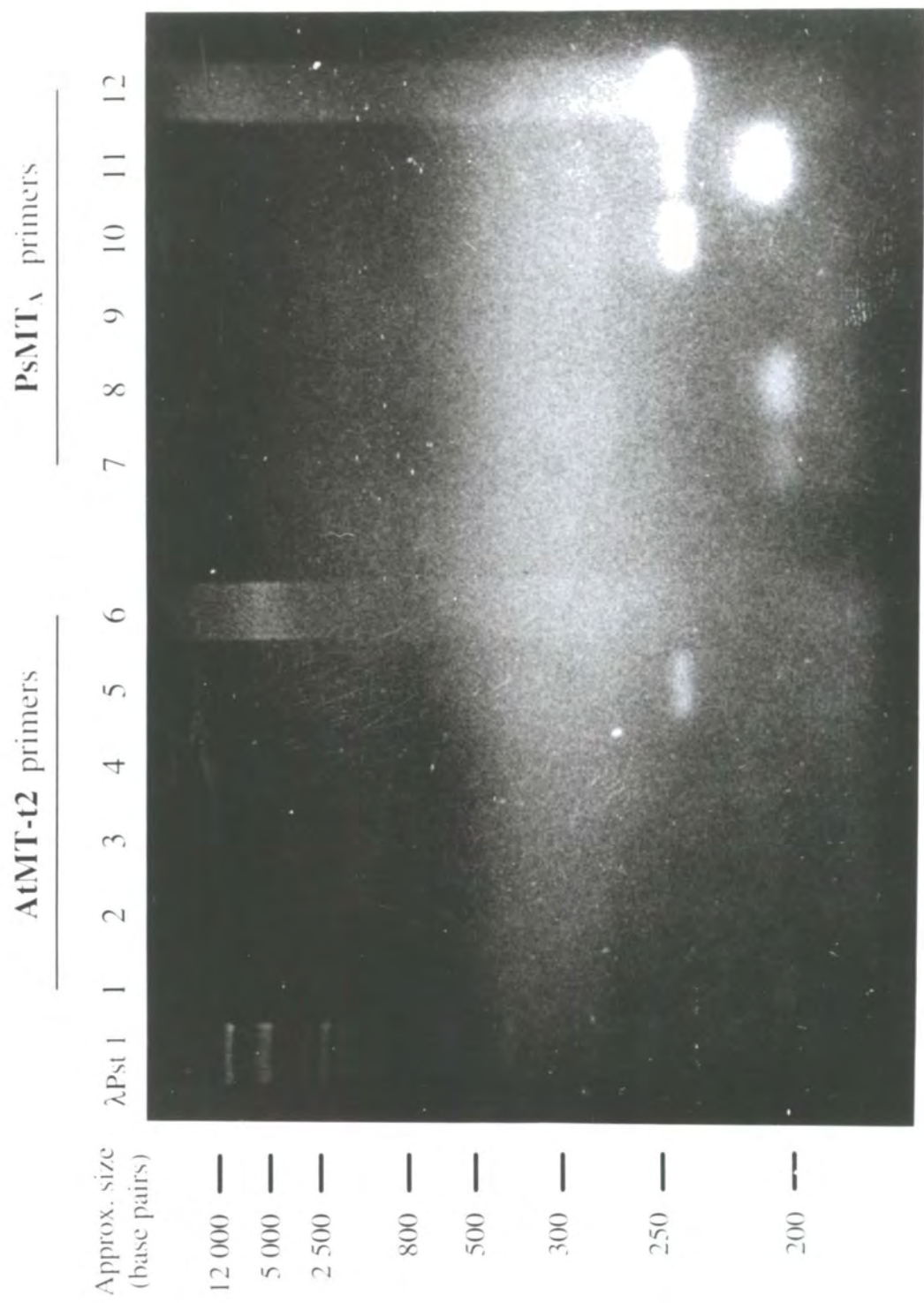
Gel filtration chromatography of the *AtMT-t2* peptide produced in *E. coli* in the presence of zinc and separated from the GST moiety of the fusion protein by cleavage with factor Xa is presented in figure 5.6. The presence of the zinc peaks, marked B and C, indicates the presence of a zinc binding component. The initial concentration of fusion protein was similar to that in the equivalent experiment with the GST-PsMT_A fusion protein, figure 4.3. On the basis of the size of the zinc peaks the yield from this experiment is very low. Aliquots from fractions from peaks B and C were subjected to microsequencing (as described in section 2.2.12) but this did not yield an amino acid sequence. A combination of a very low concentration of material and problems with the automatic sequencer at this time may account for the lack of sequence. As with the previous experiment with PsMT_A (described in section 4.3.2) the putative peptide containing peak B corresponds to a trough in the protein curve. The PsMT_A and *AtMT-t2* peptides share this anomalous activity with the dye binding assay. Despite the failure to produce definitive conformation by sequence analysis of the zinc peaks the similarity of this chromatogram (figure 5.6) with that produced by the same method for PsMT_A (figure 4.3) strongly indicates that the *AtMT-t2* peptide also is capable of zinc chelation.

Figure 5.2 PCR of *P. sativum* and *A. thaliana* DNA samples with primers homologous to the metallothionein-like gene coding sequences from those organisms. The colleagues who supplied the DNA samples, to whom many thanks are owed, are in parenthesis following the sample description.

Lane

M- λ DNA cut with *Pst*I

- 1,7 - *A. thaliana* root cDNA (K. Evans)
- 2, 8 - *A. thaliana* root cDNA (K. Evans)
- 3, 9 - *A. thaliana* root cDNA (K. Evans)
- 4, 10 - pGPMT3 vector
- 5, 11 - *A. thaliana* leaf cDNA library (L. Edwards)
- 6, 12 - *P. sativum* root cDNA (I.M. Evans)



...	AAC	TGC	GGA	TGT	GGA	TCT	GGC	TGC	AAG
						Asn	Cys	Gly	Cys	Gly	Ser	Gly	Cys	Lys
TGC	GGC	AAC	GGT	TGT	GGA	GGT	TGC	AAA	ATG	TAC	CCT	GAC	TTG	GGA
Cys	Gly	Asn	Gly	Cys	Gly	Gly	Cys	Lys	Met	Tyr	Pro	Asp	Leu	Gly
TTC	TCC	GGC	GAG	ACA	ACC	ACA	ACT	GAG	ACT	TTT	GTC	TTG	GGC	GTT
Phe	Ser	Gly	Glu	Thr	Thr	Thr	Thr	Glu	Thr	Phe	Val	Leu	Gly	Val
GCA	CCG	GCG	ATG	AAG	AAT	CAG	TAC	GAG	GCT	TCA	GGG	GAG	AGT	AAC
Ala	Pro	Ala	Met	Lys	Asn	Gln	Tyr	Glu	Ala	Ser	Gly	Glu	Ser	Asn
AAC	GCT	GAG	AAC	GAT	GCT	TGC	AAG	TGT	GGA	TCT	GAC	TGC	AAG	TGT
Asn	Ala	Glu	<u>Asn</u>	Asp	Ala	Cys	Lys	Cys	Gly	Ser	Asp	Cys	Lys	Cys
GAT	CCT	TGC	ACC	TGC	AAG	TGA	<u>ATTCATCGTGACTGACTGACG</u>							
Asp	Pro	Cys	Thr	Cys	Lys	*								

Figure 5.3 Nucleotide sequence of insertion into pGEX3X from clone pJWNR1.1, including translation. Original primer sequence (bold). pGEX3X polylinker sequence (underlined). Double underlined amino acid is a single conservative substitution from published database sequence resulting from single base change (bold).

Figure 5.4 Analysis of *A. thaliana* and *P. sativum* genomic DNA by probing with the *PsMT_A* and *AtMT-t2* coding sequences.

a. Gel photograph of ethidium bromide stained gel of restriction digest of *A. thaliana* (lanes 1 to 5) and pea (lanes 6 to 10) genomic DNA.

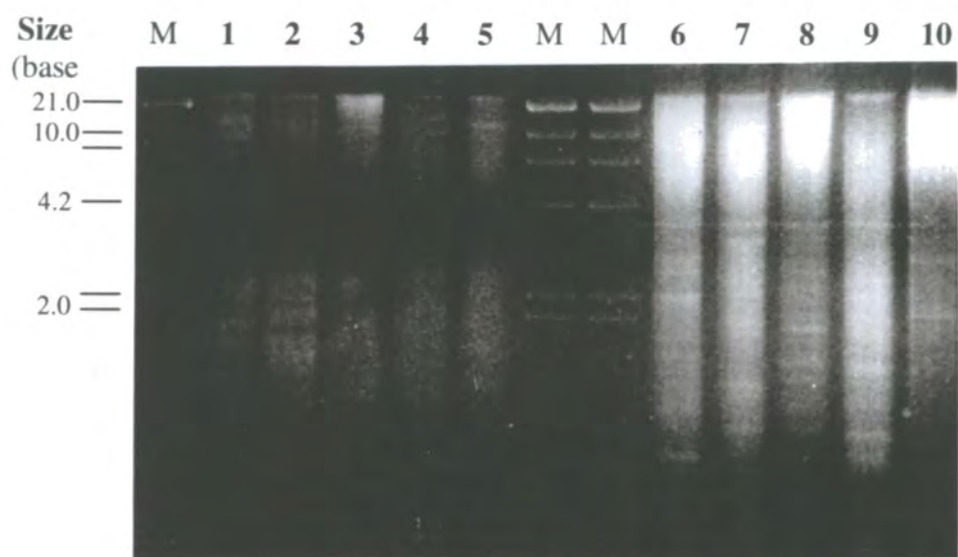
Lane
M - size markers, λ *Hind*III
1, 6 - *EcoRV* digest
2, 7 - *EcoR1* digest
3, 8 - *Bam*H1 digest
4, 9 - *Hind*III digest
5, 10- *Bgl*II digest

b Southern blot of digests probed with [α -³²P] labelled *AtMT-t2* DNA.

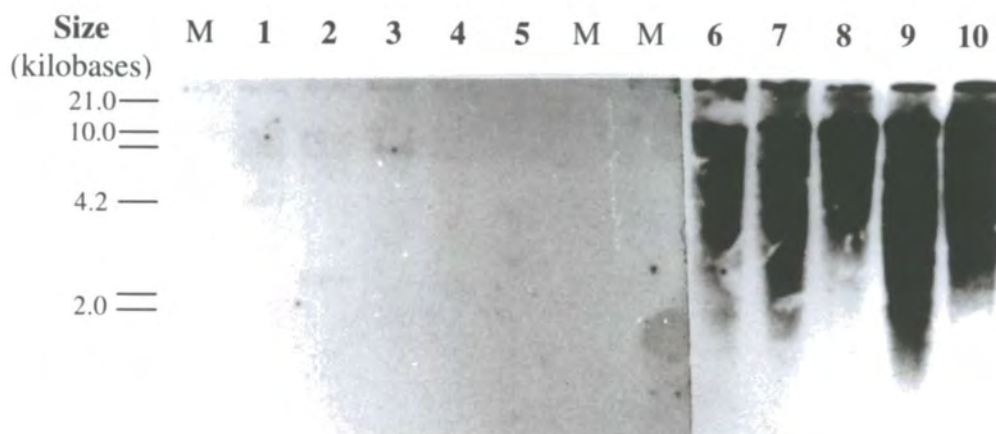
Development of the *P. sativum* DNA portion of the autorad was stopped after 2 minutes. Development of the *A. thaliana* portion was continued for a further 15 minutes,

c Southern blot of digests probed with [α -³²P] labelled *PsMT_A* DNA. developed for 15 minutes.

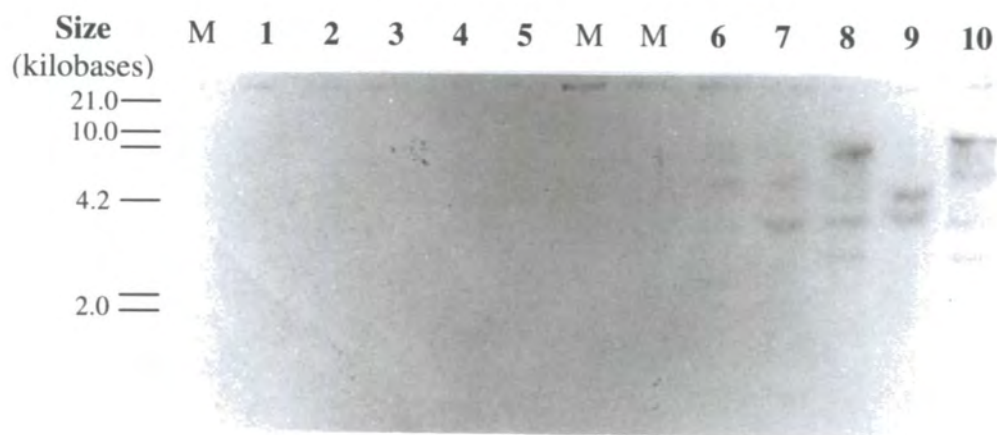
a



b



c



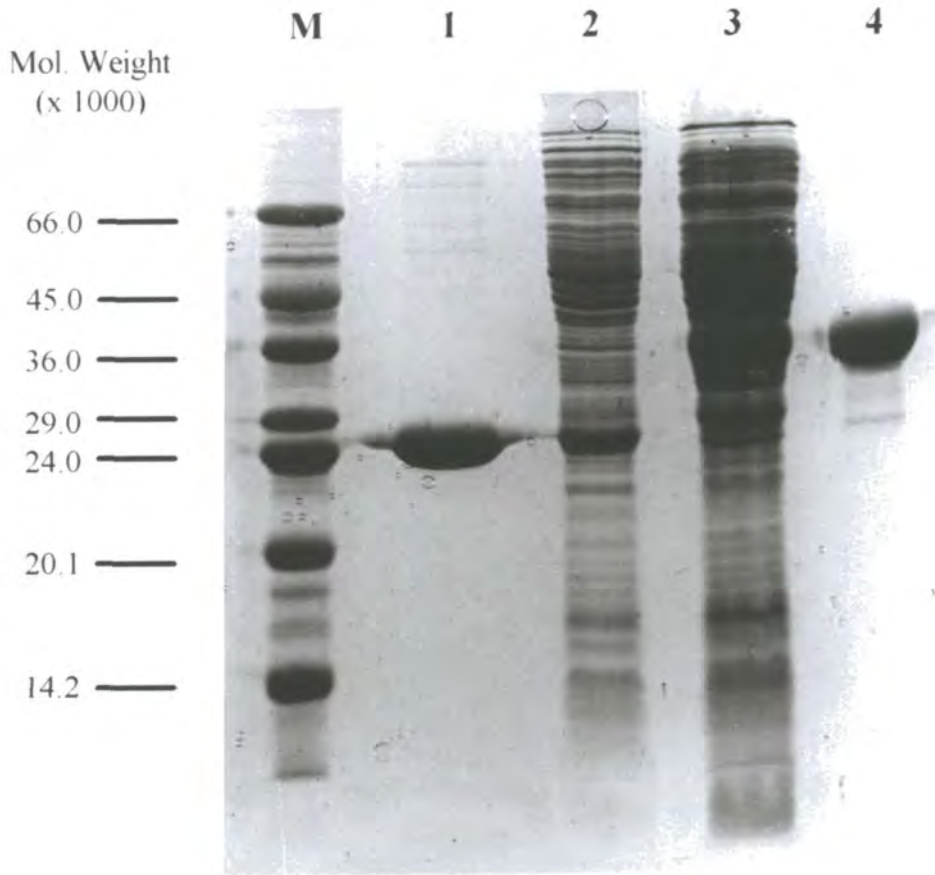


Figure 5.5 Polyacrylamide gel confirming the production of the GST-AtMT-t2 fusion protein in *E. coli* containing pJWNR1.1.

Lane

M - Molecular weight markers

1 - glutathione affinity purified GST

2 - crude protein extract from *E. coli* containing pGEX3X

3 - crude protein extract from *E. coli* containing pJWNR1.1

4 - glutathione affinity purified GST-AtMT-t2 fusion protein

Gel filtration chromatography of factor Xa cleavage products

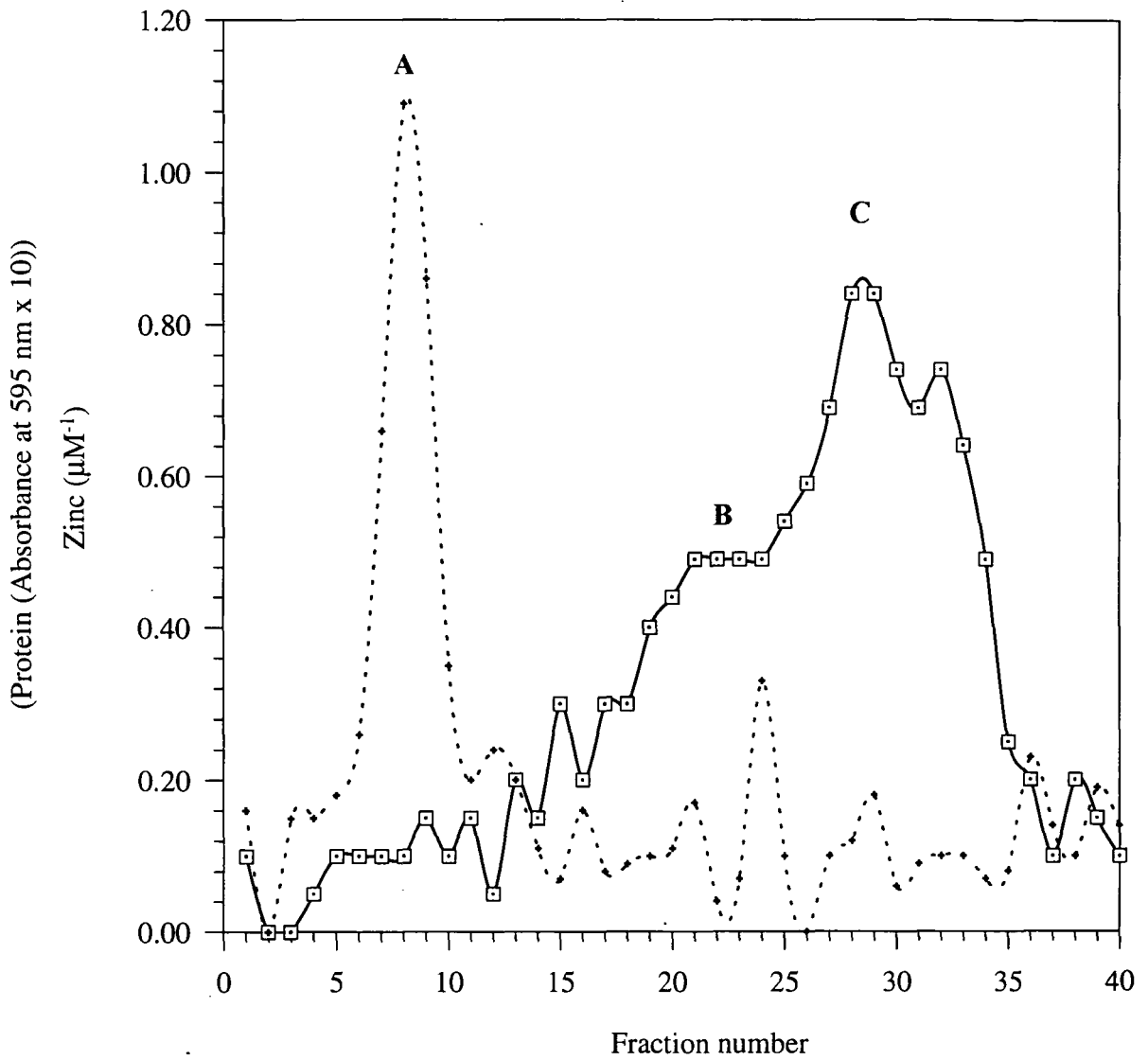


Figure 5.6 Gel filtration chromatography of factor Xa enzyme and cleavage products eluted from glutathione Sepharose matrix loaded with GST-AtMT-t2. Assayed for zinc (—, \square) and protein (\cdots , +).

5.3.6 Comparison of the zinc affinity of AtMT-t2 and PsMT_A GST fusion proteins

Proton displacement curves representing the proportional zinc loading of the AtMT-t2 and PsMT_A peptides over a pH range are presented in figure 5.7a and b. From these curves the pH at which 50 % of bound metal was displaced was estimated to be 5.0 for the GST-AtMT-t2 fusion protein and 5.25 for the GST-PsMT_A fusion protein. The value for the GST-PsMT_A fusion protein is in agreement with the previously determined value of pH 5.25 (Tommeey *et al.* 1991). In a replicate experiment a value for pH of half displacement of 5.1 was determined for the GST-AtMT-t2 fusion protein. From this data it appears that there may be a slight increase in the affinity of the AtMT-t2 peptide for zinc compared to the PsMT_A peptide. Such a change may arise from the variation in the arrangement of cysteines in the amino terminal domain, as predicted.

In this series of experiments with the recombinant fusion proteins a reduction in metal stoichiometry was observed compared to experiments performed previously. A reduction in zinc loading of approximately 4 to 5 times for the GST-PsMT_A fusion protein compared to the average value of about 6 gram atoms of zinc per mole of protein reported by Robinson *et al.* (1992). The stoichiometry for GST-AtMT-t2 fusion protein was equivalent to the GST-PsMT_A fusion protein. The reason for this discrepancy in stoichiometry is not clear as the method and conditions of isolation were identical to those used previously. Coincident with the start of this experiment the probe on the laboratory sonicator was replaced as the previous sonicator probe had been badly corroded and was as a result inefficient. However, as a consequence the sonication action of this probe was more gentle than the replacement.

A number of approaches were followed to obtain protein preparations with better zinc loading: Samples were sonicated for different time periods and at different amplitudes to investigate the effect on zinc yield. Alternative methods of cell lysis were employed, freeze thaw, incorporating lysozyme, grinding under liquid nitrogen and the use of an X-press pressure cell. None of these techniques resulted in an improvement in zinc loading of the fusion proteins (data not presented). In addition different batches of glutathione Sepharose and as an alternative glutathione agarose (Sigma Chemical Company) were used and the zinc concentration at different stages of the purification were monitored. The zinc levels again did not return to the levels required. It was not possible to determine and therefore correct the cause of the loss of zinc binding.

1 The apparent reduction in zinc loading, between the two sets of experiments, may be the result of a mixed population of GST-PsMT_A proteins. A population loaded with zinc as reported previously (Tommey *et al.* 1991 and Robinson *et al.* 1992) and a population in which the zinc binding activity has been lost. This could account not only for the problems presented in section 5.3.6 but also for previous difficulties in determining the metal binding capacity of the GST-PsMT_A fusion protein (described in section 1.9.3).

5.3.7 Expression of *AtMT-t2* in a zinc metallothionein deficient mutant of *Synechococcus*

Following PCR a single band was observed, with the predicted size of the *AtMT-t2* coding region, on an ethidium bromide stained agarose gel following electrophoresis of an aliquot of the reaction mixture (not presented). The fragment was successfully isolated from the gel, ligated into pGEX3X, and *E. coli* cells (SURE) transformed with the resulting plasmid. Subsequent sequence analysis confirmed that the fragment was the coding sequence of *AtMT-t2*, with the additional bases incorporated into the design of the primers (not presented). The sequence contained the single base substitution giving the codon change AGC to AAC and resulting in Ser⁶⁴ to Asn⁶⁴, as observed in the previous cloning of *AtMT-t2* (section 5.3.2).

Following a series of subcloning steps cells a construct of the *smt* locus, in which the *smtA* gene had been replaced by *AtMT-t2*, was created in the vector pGEM3Z. This plasmid was introduced into metallothionein deficient *Synechococcus* (R2-PIM8 (*smt*-)) (all steps performed by Dr. J.S. Turner). The pGEM3Z plasmid cannot autonomously replicate in *Synechococcus* as it lacks a suitable origin of replication. However the R2-PIM8 strain contains a recombination platform which allows integration of the plasmid by homologous recombination with concomitant restoration of ampicillin resistance allowing antibiotic selection of transformed cells. A control strain, in which the unaltered *smt* locus (including *smtA*) was introduced into R2-PIM8 by the same method was also created. Zinc dependent expression of *AtMT-t2* was confirmed by northern analysis (J.S. Turner, unpublished). Growth curves showing the response of wild type *Synechococcus* (R2-PIM8), R2-PIM8 (*smt*-), R2-PIM8(*AtMT-t2*) and R2-PIM8(*smtA*) cells are presented in figure 5.8 (data courtesy of Dr. J.S. Turner).

When grown in media containing up to 3.0 μ M zinc the R2-PIM8 (*AtMT-t2*) and R2-PIM8 (*smt*-) cells grew normally compared to the wild type. Growth of the R2-PIM8

(*AtMT-t2*) cells in media containing 4.0 μM zinc was slightly impaired compared to the wild type or R2-PIM8 (*smtA*) cells whereas there was no detectable growth of the R2-PIM8(*smt-*) cells. The R2-PIM8 (*AtMT-t2*) cells did not grown in media containing 5.0 μM zinc. Wild type and R2-PIM8 (*smtA*) cells were viable in media containing up to 10 μM zinc. These results imply zinc binding by *AtMT-t2 in vivo* and shows that the product of this *A. thaliana* metallothionein-like gene can effect zinc metabolism / detoxification *in vivo*.

Proton dissociation curves for GST fusion proteins

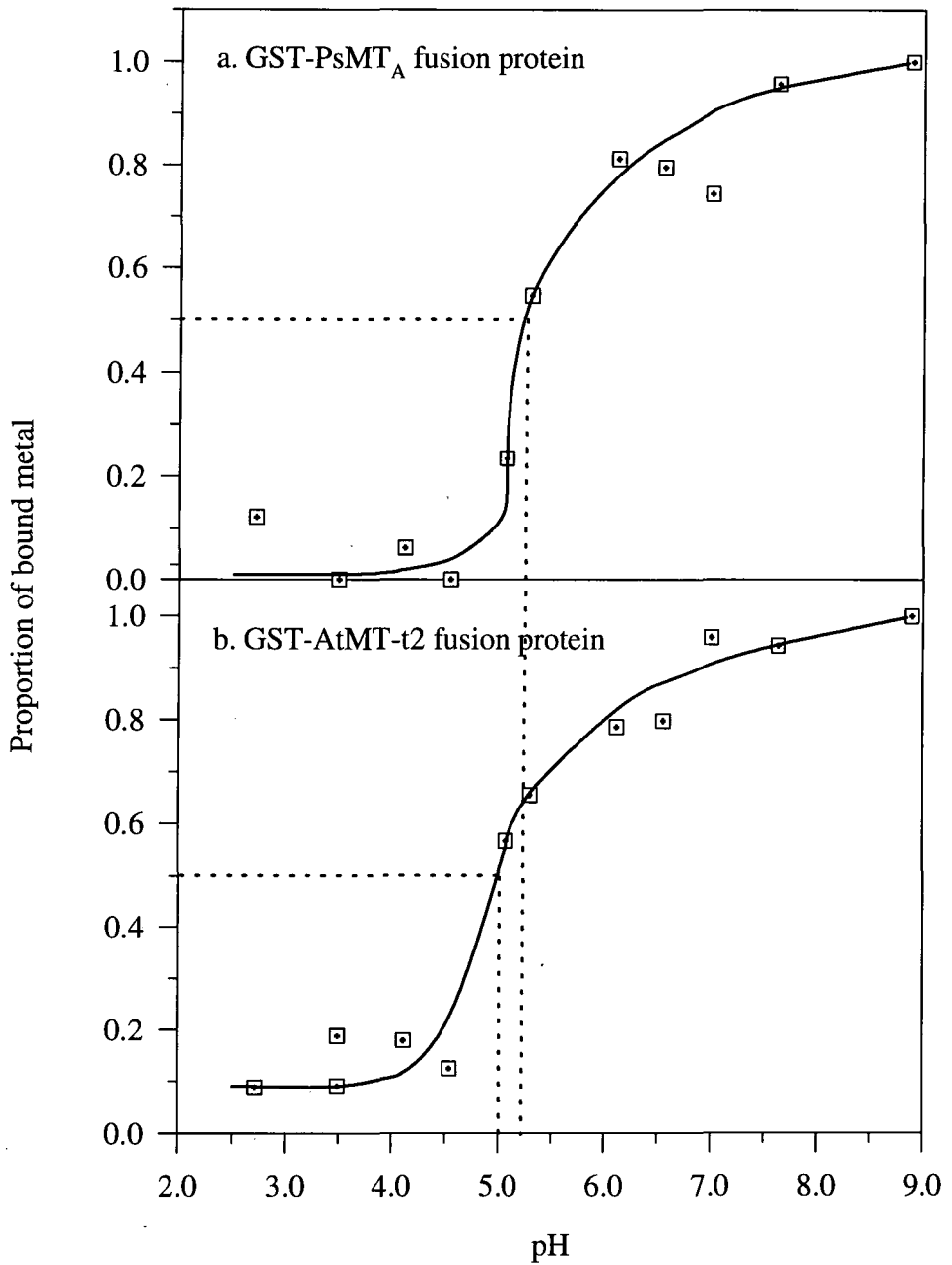


Figure 5.7 Proton dissociation curves with respect to zinc for;
a. GST-PsMT_A fusion protein
b. GST-AtMT-t2 fusion protein
the pH of 50 % displacement is indicated for each curve.

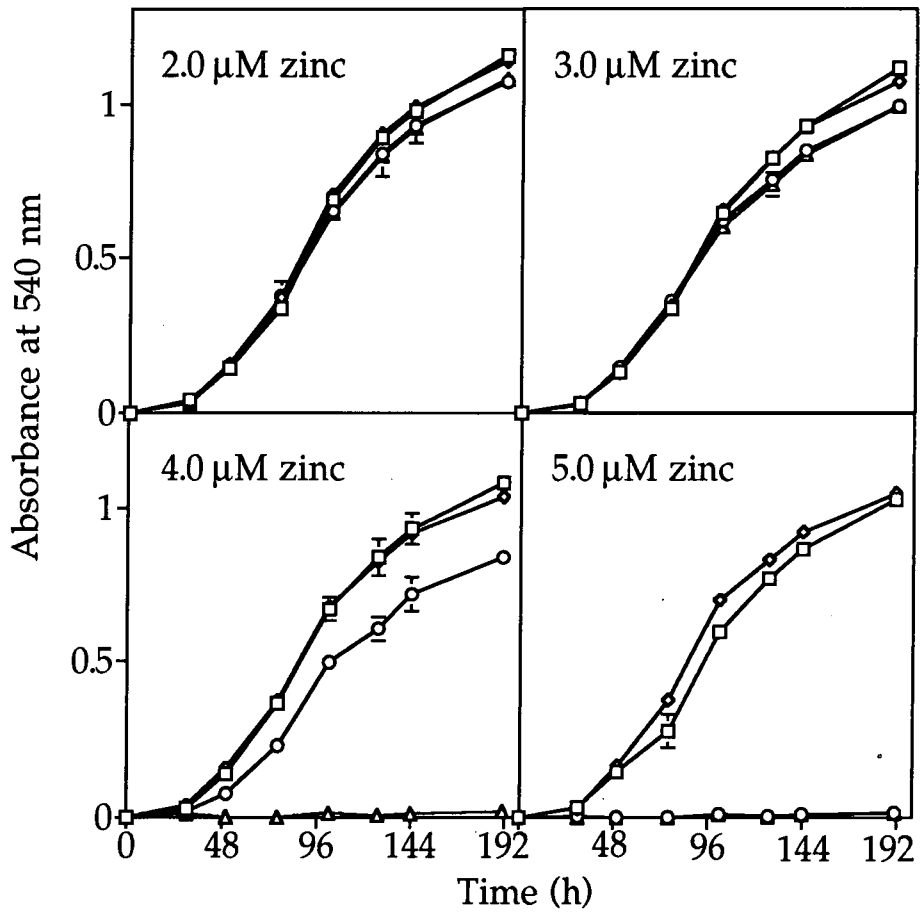


Figure 5.8 Growth of *Synechococcus* R2-PIM8 (□), R2-PIM8 (*smt*-) (Δ), R2-PIM8 (*smtA*) (◇) and R2-PIM8 (*AtMT-t2*) (○) in Allen's medium (Allen 1968) supplemented with 2.0, 3.0, 4.0 or 5.0 μM ZnCl₂. The data points represent the mean values from three separate cultures, with standard deviation. Growth was measured by measuring the optical density at 595 nm. (Data courtesy of Dr. J.S. Turner)

5.4 Conclusions

The coding sequence of the plant metallothionein-like gene from *A. thaliana*, first reported in the EMBL nucleotide database (accession number X2818), was successfully amplified from an *A. thaliana* leaf cDNA library and cloned into the pGEX3X vector (sections 5.3.1 and 5.3.2). The single base change from the originally reported sequence was subsequently observed independently by Zhou and Goldsbrough (1994). Genomic analysis suggests that there may be a single copy of the *AtMT-t2* gene in the *A. thaliana* genome in contrast to the *PsMT_A* gene which appears to be a member of a multi-gene family (section 5.3.3). This difference is consistent with the difference in size between the *A. thaliana* and *P. sativum* genomes. These are estimated to be approximately 100 Mbp and 4500 Mbp respectively (Arumuganathan and Earle 1991). However, analysis of the recently reported sequences on the NCBI GenBank nucleotide database suggests that there may be at least two closely related type-2 metallothionein-like genes in *A. thaliana* (strain Columbia) (section 3.3.2). The observation of only a single band on the Southern blot may indicate that there is insufficient homology between the two genes for hybridisation or that the genes are located on the same restriction fragment. The latter possibility may indicate close spacial proximity of the two genes. Further genetic analysis, for example isolation of genomic clones for both genes, will be required to examine these possibilities.

The *AtMT-t2* gene was expressed in *E. coli* as part of the pGEX3X fusion system producing a product migrating on polyacrylamide gels with a size consistent with the predicted size of the fusion protein. Evidence was produced that zinc binding in the protein could be attributed to the *AtMT-t2* moiety (section 5.3.5). Zinc affinity studies suggest that the GST-*AtMT-t2* protein has a slightly higher affinity for zinc than the GST-*PsMT_A* protein. The major difference in the two predicted primary structures of the *AtMT-t2* and *PsMT_A* gene products is the arrangement of cysteines in the amino terminal domain (section 5.1).

Although the change in affinity is small, in the region of 0.2 pH units, it may be of biological significance. Reese and Wagner (1987a) determined pH of half displacement values for cadmium binding peptides in *N. tabacum* of pH 5.0 to 5.8. They proposed that these values would allow the complexes to have a physiological role in cadmium detoxification. However they inferred from previous work on mammalian metallothionein that the pH of half displacement of these complexes for zinc would be 1 or more pH units greater and that as such zinc binding would be very weak and of little value in a zinc

sequestration or homeostatic role. In the case of the type-1 and type-2 recombinant proteins pH of half displacement values for zinc in the region 5.0 to 5.3 would by the criteria of Reese and Wagner allow for a physiological role in the metabolism of this metal. The small decrease in the pH of half displacement for the type-2 protein, relative to the type-1 protein, implies it may potentially form a more stable complex with zinc which may have a bearing on metal binding *in planta*.

A second *AtMT-t2* clone with a modified 5' region was successfully cloned into pGEX3X and the resulting plasmid used to transform *E. coli* (SURE) cells (section 5.3.7). Zinc dependent expression of the *AtMT-t2* gene in zinc metallothionein deficient *Synechococcus* was observed and this partially restored tolerance to zinc (figure 5.8). The *AtMT-t2* gene was not as effective in restoring zinc tolerance as the *Synechococcus* zinc metallothionein (*smtA*). The determined pH of half displacement of a GST-*smtA* fusion protein was 4.10 (Shi *et al.* 1992). Therefore the *smtA* protein has a higher affinity for zinc than *AtMT-t2*. This is likely to effect the degree of zinc tolerance conferred by the two proteins *in vivo*. Other factors may be less efficient transcription / translation of the *smt* + *AtMT-t2* construct compared to *smt* + *smtA* or impaired folding or stability of the translated product. However the restoration of a degree of zinc tolerance to the metallothionein deficient cell line does indicate that *AtMT-t2* may be capable of binding zinc *in vivo*. This suggests that involvement of the products of the metallothionein-like genes in zinc metabolism in higher plants cannot be ruled out.

CHAPTER 6

REGULATION OF THE EXPRESSION OF *PsMT_A* IN THE ROOTS OF *PISUM SATIVUM* IN RESPONSE TO TRACE METALS

6.1 Introduction

At the start of this project in 1991 there was very little published data relating to the regulation of expression of plant metallothionein-like genes in response to varying concentrations of trace metals. In *M. guttatus* expression of the plant metallothionein-like gene in roots was repressed in response to elevated copper concentrations (de Miranda *et al.* 1990). Subsequently as more genes have been reported the information on the regulation of metallothionein-like genes by different metal stimuli has increased but a clear pattern has not emerged (3.1.2). For example in *G. max*, like *M. guttatus*, expression of the metallothionein-like gene is repressed in response to elevated copper concentrations (Kawashima *et al.* 1991), in others, for example *A. thaliana* and *T. aestivum*, transcripts accumulate in response to elevated metal concentrations (Zhou and Goldsbrough 1994, Snowden and Gardner 1993). In *H. vulgare* the *ids1* gene is expressed in response to growth in iron depleted conditions (Okumura *et al.* 1992).

It has been demonstrated that expression of *PsMT_A* in roots of *P. sativum* can be repressed by the addition of iron-EDDHA to the growth media and that expression can be restored by the addition of elevated concentrations of copper (Robinson *et al.* 1993). Northern analysis was undertaken to investigate more fully the effect of different concentrations of copper, iron and zinc on the expression of *PsMT_A* in roots of *P. sativum*.

6.2 Methods

6.2.1 Growth conditions

Seedlings of *P. sativum* were prepared and treated as described in section 2.4. Changes in the concentration of iron, copper and zinc in the growth media are detailed in section 6.2.3.

6.2.2 Extraction of RNA from *P. sativum* roots and northern analysis

On day 15 of growth (unless otherwise stated) *P. sativum* roots were harvested, rinsed in distilled water, blotted dry and flash frozen in liquid nitrogen. Frozen roots were stored at -80 °C until required. RNA was extracted from roots as described in section 2.5.10. Aliquots

(approximately 15 μg) of the RNA samples were separated on a denaturing agarose gel as described in section 2.5.2.2. Northern blotting was performed as described in sections 2.5.11.3. Blots were probed with DNA corresponding to the coding region of *PsMT_A* released from the pGPMT3 and labelled with [α - ^{32}P] as described in section 2.5.9. Hybridisation conditions are described in section 2.5.11.4.

6.2.3 Metal treatments used in the study the expression of *PsMT_A*

6.2.3.1 The response of *PsMT_A* to different exogenous copper concentrations with and without added iron

In order to determine the response of *PsMT_A* gene expression to different exogenous levels of copper, in the presence and absence of iron two sets of treatments were prepared, as described in table 6.1. One set of plants was grown without iron (treatments 1 to 6) and one set was supplemented with iron (treatments 7 to 12), as in section 2.2.3. Both treatments contained 2 μM ZnSO_4 .

Treatment	Copper concentration (nM)
1, 7	0
2, 8	50
3, 9	100
4, 10	500
5, 11	1000
6, 12	1500

Table 6.1 Hydroponic solution copper concentrations for copper response experiment, figures 6.1A and 6.1 B.

The experiment was also repeated with the same copper and iron treatments but the hydroponic media was not supplemented with zinc.

6.2.3.2 The response of *PsMT_A* to different exogenous iron concentrations with and without added copper

In order to determine the effect of varying the concentration of iron in the hydroponic media on the expression of *PsMT_A*, two sets of *P. sativum* seedlings were grown in media containing a range of iron concentrations, as described in table 6.2a. Treatments 1-6 were not supplemented with copper, treatments 7-12 were supplemented with 0.5 μM CuSO_4 . In all treatments ZnSO_4 was not added to the hydroponic solution.

Treatment	Iron concentration (nM)
1, 7	0
2, 8	50
3, 9	100
4, 10	500
5, 11	1000
6, 12	5000

Table 6.2a Hydroponic solution iron concentrations for iron response experiment, figure 6.2A

The treatments were repeated with a similar iron concentration range (table 6.2b) but with either no added copper or 1 μM CuSO_4 in the hydroponic solution;

Treatment	Iron concentration (nM)
1, 6	0
2, 7	100
3, 8	500
4, 9	1000
5, 10	5000

Table 6.2b Hydroponic solution iron concentrations for iron response experiments, figure 6.2B

6.2.3.3 The response of *PsMT_A* to different exogenous zinc concentrations with and without added iron

To determine the effect of varying exogenous zinc concentrations on the expression of *PsMT_A* two sets of *P. sativum* seedlings were grown in media containing a range of zinc concentrations, described in table 6.3a. Treatments 1-6 were not supplemented with iron, treatments 7-12 were supplemented with iron as in section 2.2.3. In all treatments CuSO_4 was not added to the hydroponic solution.

Treatment	Zinc concentration (nM)
1, 7	0
2, 8	100
3, 9	500
4, 10	1000
5, 11	5000
6, 12	10000

Table 6.3a Hydroponic solution zinc concentrations for zinc response experiment, figure 6.3A.

The treatments were repeated with a similar, but smaller range of zinc concentrations as indicated table 6.3b.

Treatment	Zinc concentration (nM)
1, 4	0
2, 5	500
3, 6	5000

Table 6.3b Hydroponic solution zinc concentration for zinc response experiment, figure 6.3A

6.2.4 Time course experiments to study the response of *PsMT_A* gene expression to changes in copper and iron concentrations

The conditions detailed in section 6.2.3 were used to investigate *PsMT_A* gene expression in response to different metal ion concentrations under steady state conditions. In order to investigate the response of the gene to changes in the exogenous metal conditions time course experiments were performed

6.2.4.1 Conditions for time course experiment 1

P. sativum seedlings were grown for 14 days under continuous conditions as described in section 2.4, but on day 15 the metal treatment was changed. The *P. sativum* roots were then harvested, and the roots frozen in liquid nitrogen, at time intervals following this change. There were no further media changes. Media contained 2.0 μM ZnSO_4 .

Treatment	Metal supplement day 3 to 14	Metal supplement day 15	Time of harvest
1			1 h
2	0.5 μM CuSO_4	0.5 μM CuSO_4	7 h
3	no iron	no iron	24 h
4			48 h
5			1 h
6	0.5 μM CuSO_4	1.0 μM CuSO_4	7 h
7	no iron	+ 2.0 μM iron-	24 h
8		EDDHA	48 h
9	0.5 μM CuSO_4	2.0 μM iron-	1 h
10	no iron	EDDHA	7 h
11		no CuSO_4	48 h

Table 6.4 Conditions for time course experiment 1, figure 6.4

[Note: roots grown in 0.5 μM CuSO_4 / no iron-EDDHA and transferred to no copper / 2.0 μM iron-EDDHA were harvested after 24 hours but due to problems during the extraction procedure no RNA was obtained for this sample]

RNA was extracted from the *P. sativum* roots and $PsMT_A$ expression investigated by northern analysis, described in section 6.2.2.

6.2.4.2 Conditions for time course experiment 2

P. sativum seedlings were grown for 14 days under continuous conditions as described in section 2.4, but on day 15 the metal treatment was changed. The *P. sativum* roots were then harvested, and the roots frozen in liquid nitrogen, at time intervals following this change. There were no further media changes. Media contained 2.0 μM ZnSO_4 .

Treatment	Metal supplement day 3 to 14	Metal supplement day 15	Time of harvest
1	1.5 μM CuSO_4	1.5 μM CuSO_4	1 h
2	no iron	no iron	7 h
3			48 h
4	2.0 μM iron-	2.0 μM iron-	1 h
5	EDDHA	EDDHA	7 h
6	no copper	no copper	48 h
7	1.5 μM CuSO_4	2.0 μM iron-	1 h
8	no iron	EDDHA	7 h
9		no copper	48 h
10	2.0 μM iron-	1.5 μM CuSO_4	1 h
11	EDDHA	no iron	7 h
12	no copper		48 h

Table 6.5 Conditions for time course experiment 2, figures 6.5A and 6.5B.

RNA was extracted from the *P. sativum* roots and $PsMT_A$ expression investigated by northern analysis as described in section 6.2.2.

6.3 Results and Discussion

6.3.1 The response of *PsMT_A* to different exogenous copper concentrations with and without added iron

Northern analysis of the effect of varying concentrations of copper in the growth media on expression of the *PsMT_A* gene in roots of *P. sativum* is presented in figures 6.1A and B. In both figures data is presented for seedlings grown without added iron and with added iron in the growth media. In figure 6.1B data is presented for seedlings grown under the same conditions as in 6.1A except without the addition of zinc to the growth media.

In both sets of data expression of the gene is consistently higher in the extracts from seedlings grown without added iron in the growth media for any given concentration of copper. In all four sets of treatments the lowest expression is observed in seedlings grown in 100 nM CuSO₄. There is no clear pattern of expression above 100 nM CuSO₄ in these blots. However, expression is consistently higher than at the 100 nM copper level. In a previous report (Robinson *et al.* 1993) induction of expression of *PsMT_A* was observed with the addition of elevated levels of copper to *P. sativum* seedlings grown in the presence of 2.0 μM iron-EDDHA.

Comparison of figures 6.1A and 6.1B, to ascertain the effects of micronutrient levels of zinc on gene expression, is complicated because of the difference in signal strength between the two northern blots. The effect of not adding ZnSO₄ to the hydroponic growth media appears to have accentuated the effects of iron on expression of the *PsMT_A* gene. The difference in transcript levels between the plus and minus iron samples at any given copper concentration is greater in figure 6.1B than 6.1A. An exception may be tracks relating to 1000 nM CuSO₄ in figure 6.1B as expression in the 2.0 μM iron / 1000 nM CuSO₄ track is particularly high.

Another effect which may be due to the omission of ZnSO₄ from the hydroponic media is the observed reduction of *PsMT_A* transcripts in roots of seedlings grown in 1500 nM CuSO₄ compared to 1000 nM CuSO₄. If this effect is due to zinc it may indicate that the seedlings grown without the addition of this metal to the media were more susceptible to copper toxicity, perhaps because trace metal scavenging mechanisms were active due to a deficiency in zinc. The roots of seedlings grown in 1500 nM CuSO₄ in both sets of experiments appeared necrotic compared to the roots of seedlings grown in lower copper concentrations.

In seedlings grown in copper concentrations lower than 100 nM expression increased with decreasing copper concentration. Figure 6.1C is compiled from figures 6.1A and 6.1B and is intended to highlight this response. This response contrasts with metallothionein in other species where induction of expression in response to an increase in the concentration of trace metal is a defining characteristic (Hamer 1986). In a study of expression driven from yeast copper metallothionein promoters, in response to a series of copper concentrations, stimulation of expression required the addition of copper to the growth medium (Thorvaldsen *et al.* 1993). The level of expression then increased to a maximum as the copper concentration in the media was increased. The expression of *PsMT_A* in response to the exogenous copper concentration does not follow this pattern (figures 6.1A and B). The pattern of expression may indicate the *PsMT_A* gene is induced by growth in low copper conditions, perhaps as part of an enhanced copper uptake mechanism. Alternatively, it may be an indirect response to changes in metabolism induced by growth in these conditions, for example a stress response.

6.3.2 The response of *PsMT_A* to different exogenous iron concentrations with and without added copper

Northern analysis of the effect of growth in media containing a range of concentrations of iron, with and without added copper, on the expression of the *PsMT_A* gene in roots of *P. sativum* is presented in figures 6.2A and 6.2B. For any given iron concentration *PsMT_A* transcript levels in total RNA extracted from roots grown in the presence of exogenous 0.5 μM or 1.0 μM CuSO_4 are higher than levels in roots grown in the absence of copper. This increase in the level of expression of *PsMT_A* in the presence of elevated copper concentrations is consistent with a previously reported observation (Robinson *et al.* 1993).

In the northern analysis of the series of treatments containing 0.5 μM CuSO_4 in figure 6.2A and 1.0 μM CuSO_4 in figure 6.2B the level of *PsMT_A* transcripts is very low in seedlings grown in media not supplemented with iron. It has previously been observed that expression was higher in roots of seedlings grown in media not supplemented with iron compared to media supplemented with 2.0 μM iron (Robinson *et al.* 1993, and figures 6.1A and B). The low level of expression observed in the extracts from non iron supplemented seedlings in figures 6.2A and B appears to contradict these earlier observations. The transcript abundance increased with iron concentration up to a maximum at 500 nM iron-

EDDHA in the treatments containing 0.5 μM CuSO_4 (in 6.2A) and a maximum at 1000 nM iron-EDDHA in the treatments containing 1.0 μM CuSO_4 (in 6.2B). In seedlings grown in media containing iron concentrations above these values transcript abundance decreased. The repression of the *PsMT_A* gene by growth in iron-EDDHA concentrations of 2.0 μM is consistent with previous observations (Robinson *et al.* 1993, and figures 6.1A and B). The apparent increase in the iron concentration required to repress gene expression observed by growth in 1.0 μM as opposed to 0.5 μM CuSO_4 is also consistent with these earlier findings. The lower level of gene expression observed in the seedlings grown without added iron, and the induction of gene expression by growth of seedlings in iron concentrations less than those causing repression, would not have been predicted from these earlier observations.

The effect of different iron concentrations on expression of the *PsMT_A* gene in seedlings grown in media without added copper is less consistent between the two sets of data (figures 6.2 A and B). In both, very low expression is observed at the highest iron concentration, which is consistent with the repression of *PsMT_A* gene expression by iron concentrations above 2.0 μM . In figure 6.2B very low expression was observed in the extract from seedlings grown in 0 nM iron and induction of gene expression was observed by growth of seedlings in media containing non repressing iron concentrations. The low level of expression in the minus copper treated seedlings in figure 6.2A shows less consistent trends with respect to iron concentration compared to the other sets of treatments in figure 6.2A and B. There appears to be an inconsistency between the level of expression in the minus copper / minus iron tracks in figures 6.2A and 6.2B (tracks 1 in both figures) and the tracks containing RNA extracted from seedlings grown in the same conditions (track 1, figures 6.1A and B). This inconsistency may arise because it is not possible to directly compare signal strengths between blots due to variation in RNA concentrations on gels, efficiency of transfer to membrane and in the specific activity of the probe.

6.3.3 The response of *PsMT_A* to different exogenous zinc concentrations with and without added iron

Northern analysis of the effect of growth in media containing different concentrations of zinc, with and without added iron-EDDHA, on the expression of the *PsMT_A* gene roots of *P. sativum* is presented in figures 6.3A and 6.3B. The response of *PsMT_A* gene expression to exogenous zinc seems to be dependent on the level of exogenous iron. When 2.0 μM iron-

EDDHA is included in the hydroponic media P_sMT_A transcript abundance is low, as observed in previous experiments. Repression by this level of iron is overcome by growth of seedlings in media containing 5000 nM $ZnSO_4$ (figure 6.3A and 6.3B) and also by 10000 nM (10 μ M) $ZnSO_4$ (figure 6.3A)

In figure 6.3A, in the tracks containing extracts from seedlings grown in media not supplemented with iron, there is no obvious effect on P_sMT_A transcript abundance over the range of 0 to 5000 nM $ZnSO_4$. The reduction in signal at 1000 nM $ZnSO_4$ appears to be due to RNA loading. Transcript abundance is very low in the extract from seedlings grown in media containing 10000 nM (10 μ M) $ZnSO_4$. In the non iron supplemented samples in figure 6.3B expression is highest in the extract from seedlings grown without the addition of zinc to the hydroponic media. The main trend in figures 6.3A and B is induction of P_sMT_A in roots of seedlings in response to elevated zinc concentrations in media containing 2.0 μ M iron and repression by higher zinc concentrations in media not supplemented with iron.

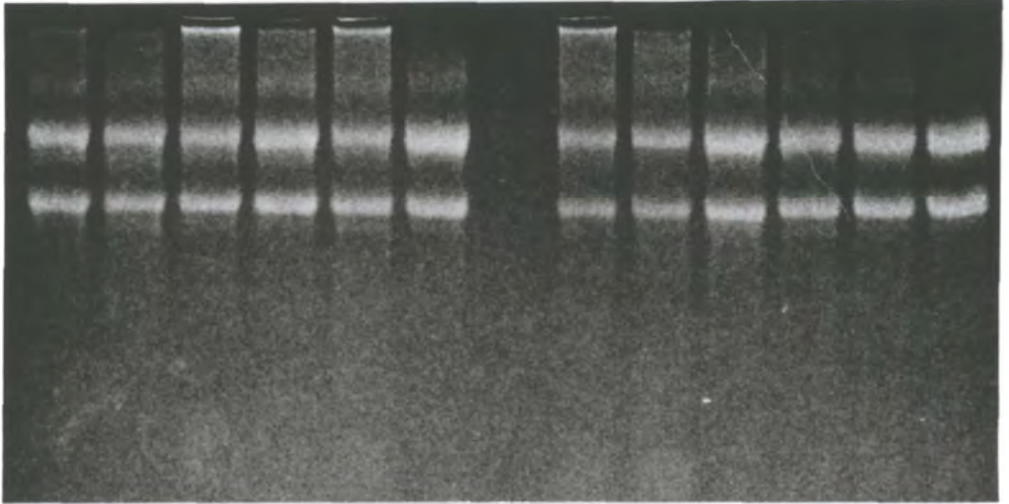
It is also noted that where the growth conditions replicate the minus copper / minus iron treatment, where an apparent inconsistency was noted between figures 6.1A and B and 6.2A and B, the relative level of expression in figures 6.3A and B is higher.

Figure 6. 1 A Northern analysis of total RNA extracted from *P. sativum* roots from plants grown in media containing a range of copper concentrations, probed with *PsMT_A*. Photograph of agarose gel stained with ethidium bromide and autoradiograph.

- Plants grown with and without 2.0 μM Fe-EDDHA
- Plants grown in media supplemented with 2.0 μM ZnSO₄

A

1 2 3 4 5 6 7 8 9 10 11 12



- Iron

+ Iron

[Copper]
(nM)

0 50 100 500 1000 1500

0 50 100 500 1000 1500

←
Origin



Figure 6.1 B Northern analysis of total RNA extracted from *P. sativum* roots from plants grown in media containing a range of copper concentrations, probed with *PsMT_A*. Photograph of agarose gel stained with ethidium bromide and autoradiograph.

- Plants grown with and without 2.0 μ M Fe-EDDHA
- Plants grown in media not supplemented with zinc

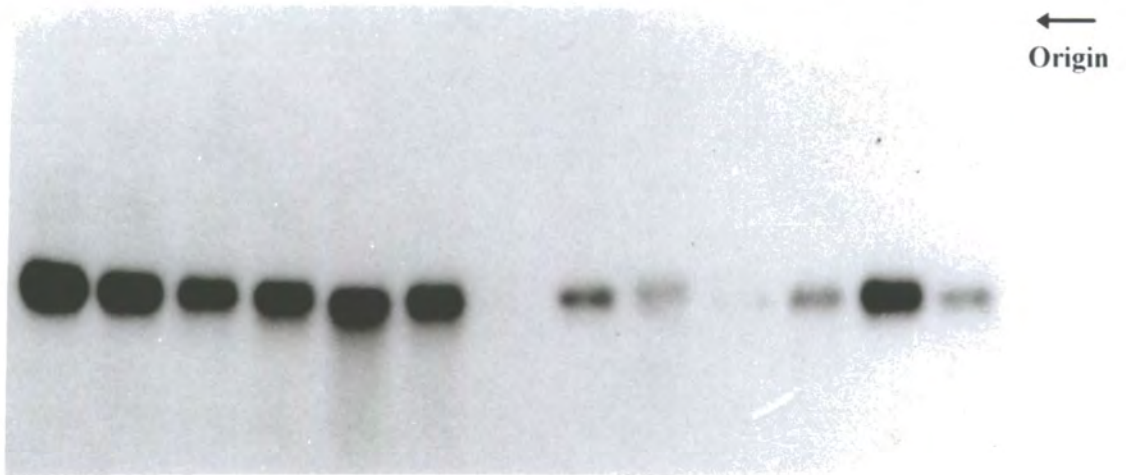
B

1 2 3 4 5 6 7 8 9 10 11 12



- Iron **+ Iron**

[Copper] (nM) 0 50 100 500 1000 1500 0 50 100 500 1000 1500



C

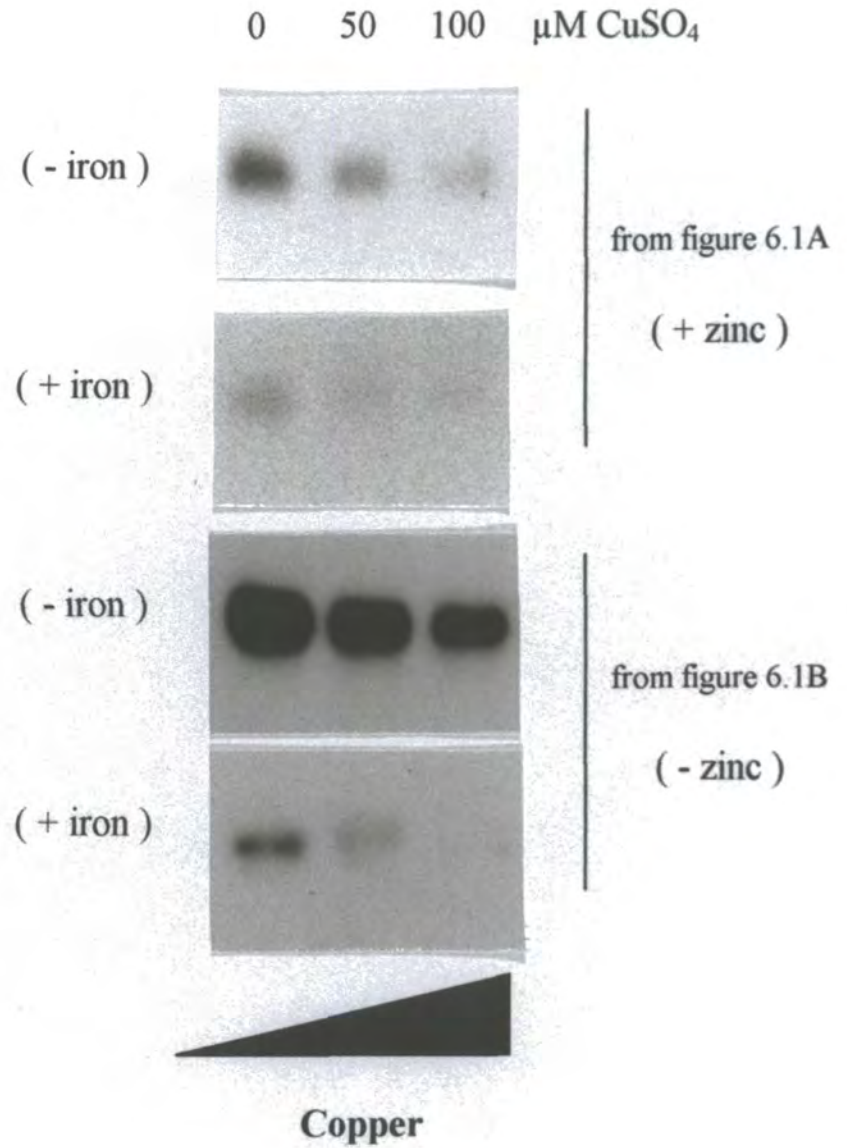


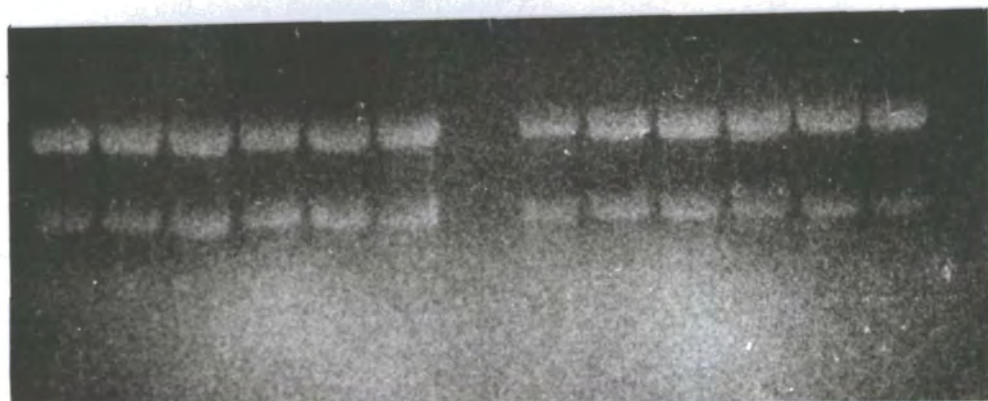
Figure 6.1C Northern analysis of the effect of growth in low copper media (0 to 100 nM CuSO_4) on expression of *PsMT_A* in roots of *P. sativum* seedlings. Compiled from figures 6.1A and 6.1B.

Figure 6.2 A Northern analysis of total RNA extracted from *P. sativum* roots from plants grown in media containing a range of iron concentrations, probed with *PsMT_A*. Photograph of agarose gel stained with ethidium bromide and autoradiograph.

- Plants grown with and without 0.5 μM CuSO_4 .
- Media not supplemented with zinc

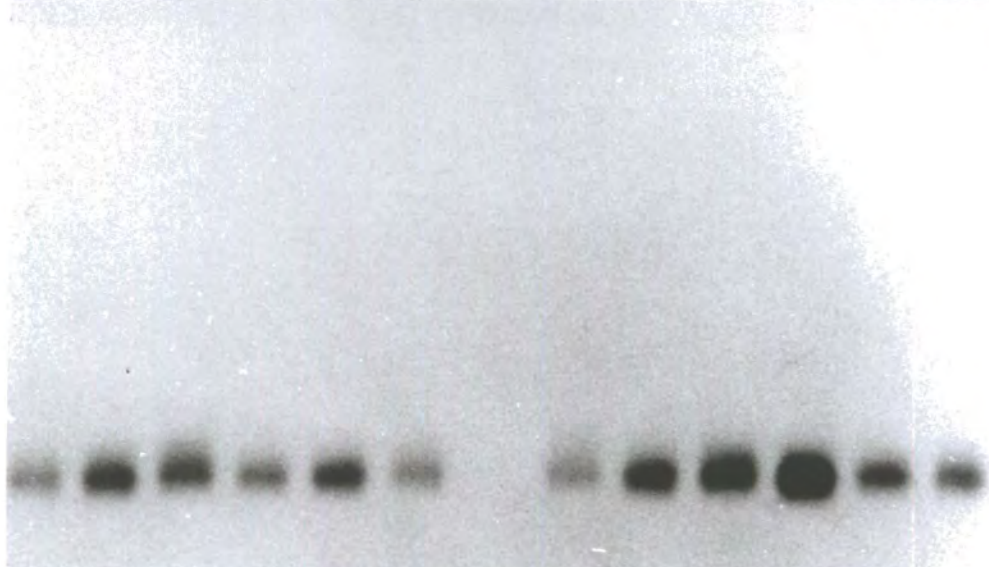
A

1 2 3 4 5 6 7 8 9 10 11 12



[Iron] (nM)

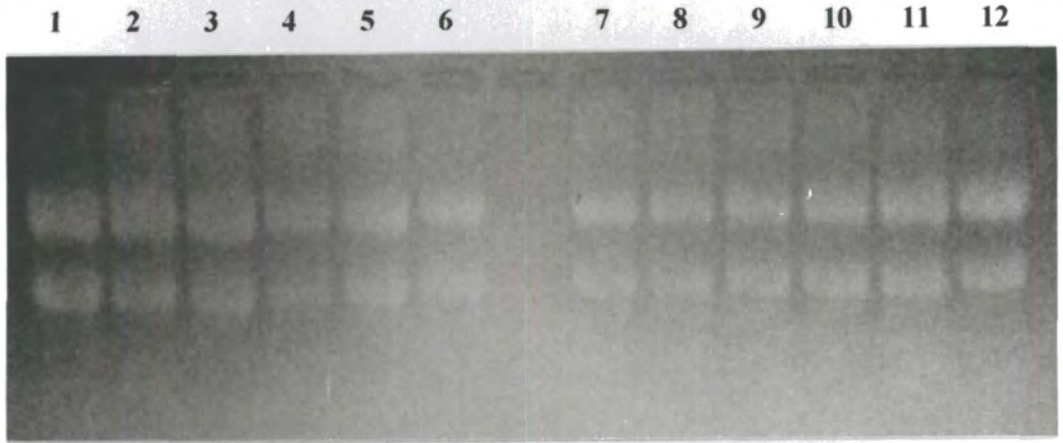
- Copper						+ 0.5 μ M CuSO ₄					
0	50	100	500	1000	5000	0	50	100	500	1000	5000



←
Origin

Figure 6.3 B Northern analysis of total RNA extracted from *P. sativum* roots from plants grown in media containing a range of zinc concentrations, probed with *PsMT_A*. Photograph of agarose gel stained with ethidium bromide and autoradiograph.

- Plants grown with and without 2.0 μ M iron-EDDHA
- Media not supplemented with copper



- Iron

[Zinc] (nM) 0 100 500 1000 5000 10000

+ Iron

0 100 500 1000 5000 10000

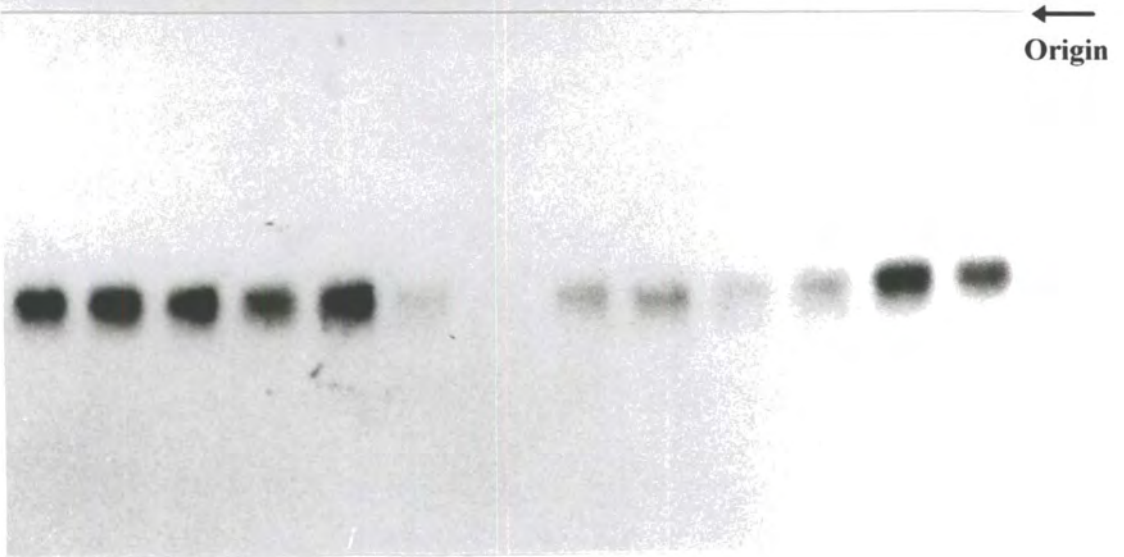
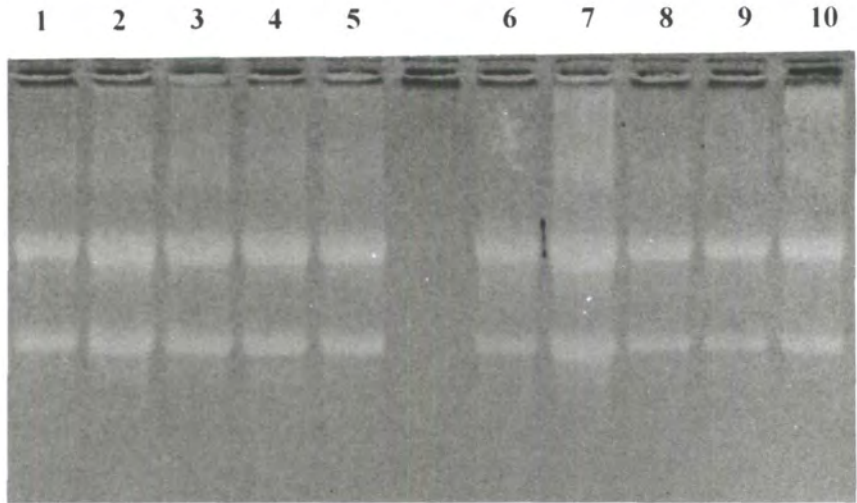


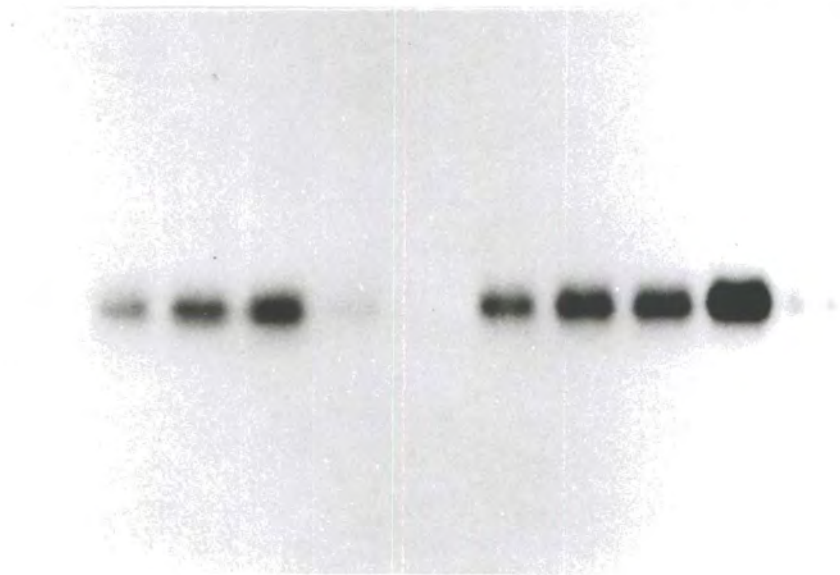
Figure 6.3 A Northern analysis of total RNA extracted from *P. sativum* roots from plants grown in media containing a range of zinc concentrations, probed with *PsMT_A*. Photograph of agarose gel stained with ethidium bromide and autoradiograph.

- Plants grown with and without 2.0 μ M iron-EDDHA
- Media not supplemented with copper

B



	- Copper					+ 1.0 μM CuSO_4				
[Iron] (nM)	0	100	500	1000	5000	0	100	500	1000	5000



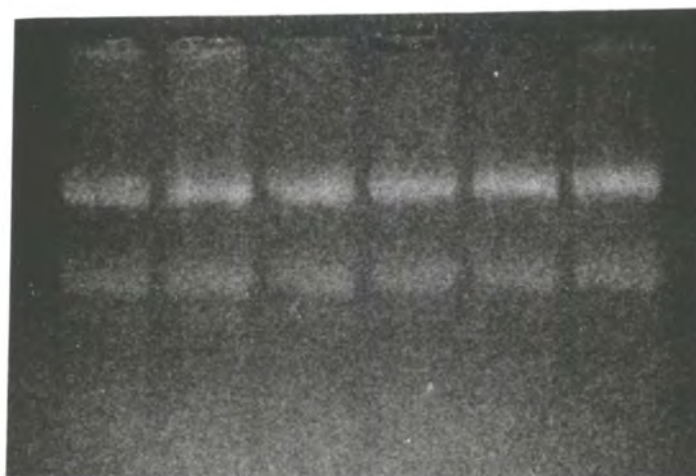
←
Origin

Figure 6.2 B Northern analysis of total RNA extracted from *P. sativum* roots from plants grown in media containing a range of iron concentrations, probed with *PsMT_A*. Photograph of agarose gel stained with ethidium bromide and autoradiograph.

- Plants grown with and without 1.0 μM CuSO_4 .
- Media not supplemented with zinc

B

1 2 3 4 5 6



	+ Iron			- Iron		
[Zinc] (nM)	0	500	5000	0	500	5000



←
Origin

6.3.4 Time course experiments to study the response of *PsMT_A* gene expression to changes in copper and iron concentrations

6.3.4.1 Time course experiment 1

Northern analysis of *PsMT_A* expression in roots of *P. sativum* seedlings harvested at different times following a final change in growth media are presented in figure 6.4. All seedlings were grown in media containing 0.5 μM CuSO_4 / no added iron for days 3 to 14, on day 15 the copper and iron content of the growth media and the time of harvest following this last media change was as indicated.

Lanes 1 to 4 contain RNA from seedlings in which the media in the final change was 0.5 μM CuSO_4 / no added iron, that is the same as days 3 to 14. The transcript level was initially high but decreased significantly over the 48 h period. From figure 6.1A and 6.1B it was established that the minimum expression of *PsMT_A* (in response to copper) was observed in seedlings grown in media containing 100 nM CuSO_4 . If the reduction in transcript levels, in tracks 1 to 4 in figure 6.4, is due to a direct response to copper concentration in the media this implies that significant depletion of copper in the media by the seedlings has occurred. There was no circulation of the media in these experiments. It may be possible that a micro-environment formed around the root mass. If this was the case then depletion of the copper concentration in this micro-environment could occur at a faster rate than in the solution as a whole. The effect of a reduction of exogenous copper concentration could be accentuated if the fresh media contained contaminating iron salts. Figures 6.2A and 6.2B suggest that reduction of the iron concentration in the growth media would reduce the levels of *PsMT_A* transcripts.

In the second set of treatments (figure 6.4 lanes 5 to 8) on day 15 the media was changed from 0.5 μM CuSO_4 / no added iron to 1.0 μM CuSO_4 / 2.0 μM iron-EDDHA. Previous results (figures 6.1 and 6.2 A and B) suggest that this concentration of iron would reduce *PsMT_A* expression but that this effect could be counteracted by the higher copper levels. After 1 h transcript levels were high. By 7 h they had decreased markedly to a similar level or slightly lower than that observed after 7 h in the previous treatment. At 24 h the transcript levels had increased but by 48 h they had decreased to very low levels. Figure 6.2B shows that depletion of the iron in the hydroponic media would lead to an increase in the expression of *PsMT_A*. This effect in addition to the higher concentration of copper in the

growth media compared to the first set of treatments may account for the high level of transcripts at 24 h.

In the third set of treatments (figure 6.4 lanes 9 to 11) on day 15 the media was changed from 0.5 μM CuSO_4 / no added iron to no added copper / 2.0 μM iron-EDDHA. The very low level of transcripts after 1 h suggests that *PsMT_A* responds rapidly to the exogenous metal concentration. At the equivalent time in the second set of treatments the high transcript level may indicate that the presence of 1.0 μM copper reduced iron uptake or that the copper concentration counteracted the repressing effect of iron. The increase of transcript abundance over the time course of the experiment, in the third set of treatments, may indicate the depletion of iron in the media.

6.3.4.2 Time course experiment 2

Northern analysis of *PsMT_A* expression in roots of *P. sativum* seedlings harvested over a range of times following the final growth media change are presented in figure 6.5A and B. The initial treatment refers to the iron and copper concentrations in the growth media from day 3 to 14 and the final treatment to the growth media on day 15. The times refer to the time of harvest following the final solution change.

In the first set of treatments (lanes 1 to 3 figure 6.5A) the final media was as for days 3 to 14, that is 1.5 μM CuSO_4 / no added iron. Transcript levels were high at 1 h and had increased slightly by 7 h. By 48 h transcript abundance had decreased markedly. When grown in media containing 1.5 μM CuSO_4 roots exhibit necrosis indicating that this concentration of copper is toxic and may have a detrimental effect on gene expression. This may account for the slight increase in transcript levels from 1 h to 7h as the copper in the media becomes depleted. By 48 h the level of transcripts decreases markedly as observed in figure 6.4 and may be due to further copper depletion. The rate of decrease in transcript levels is less than that observed in lanes 1 to 4 in figure 6.4 which may be due to the higher copper concentration requiring longer to become depleted by the root in time course experiment 2.

In the second set of treatments (lanes 4 to 6, figure 6.5A) the media in the final change was no added copper / 2.0 μM iron-EDDHA, that is the same as days 3 to 14. Transcript levels were low after 1 h, increased slightly by 7 h and had not changed from this level by 48 h. The result is similar to that observed upon changing the treatment from 0.5 μM CuSO_4 /

no iron to no copper / 2.0 μM iron-EDDHA in time course experiment 1 (lanes 9 to 11, figure 6.4). This again highlights the speed of the response to the change in growth conditions in experiment 1. In the experiment 1 transcript abundance did increase slightly from 7 to 48 h.

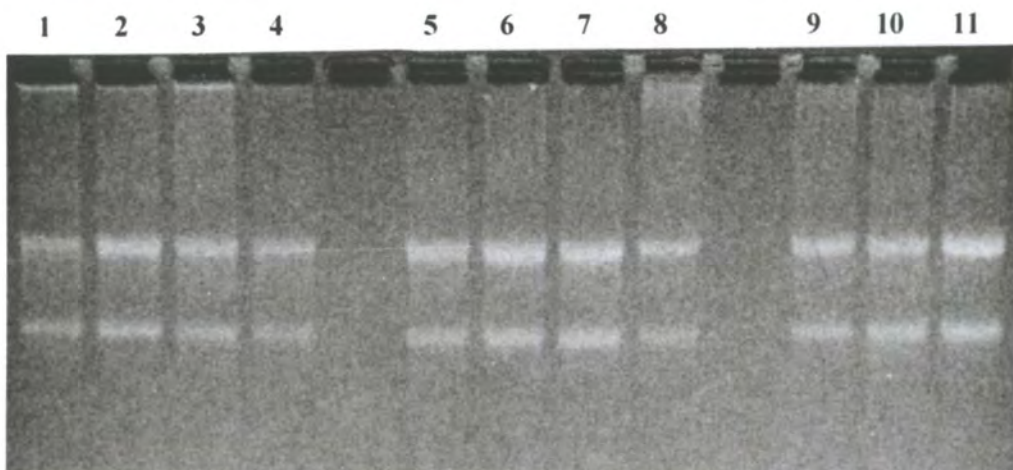
In the third set of treatments (lanes 7 to 9, figure 6.5B) on day 15 the media was changed from 1.5 μM CuSO_4 / no added iron to no added copper / 2.0 μM iron-EDDHA. Transcript levels after 1 h are lower than after the equivalent time in seedlings whose growth conditions were not changed (lane 1 figure 6.5A). At 7 h transcript abundance is lower and at 48 h decreases further. This reduction of *PsMT_A* expression over time may be due to the slow accumulation of iron by the roots. This result contrasts to that obtained lanes 9 to 11 (figure 6.4) in which a very low level of transcripts was observed after 1 h of exposure to iron and then increased over time. The difference between the two experiments was the copper concentration in the growth media over days 3 to 14. The result may indicate that iron uptake or sensing has been effected by growth in very high copper concentrations. These high copper concentrations cause necrosis and the reduction in the rate of response to iron may be due to root damage.

In the fourth set of treatments (lanes 10 to 12, figure 6.5B) on day 15 the media was changed from no added copper / 2.0 μM iron-EDDHA to 1.5 μM CuSO_4 / no added iron. The level of transcripts was low after 1 h and remained at this level after 7 h. By 48 h the transcript level had increased significantly. This may be due to the depletion of iron stores in the cell and uptake of copper. The response to the change in metal concentration is again slower than observed for responses in experiment 1. This may be an effect of growth for days 3 to 14 in media not supplemented with copper.

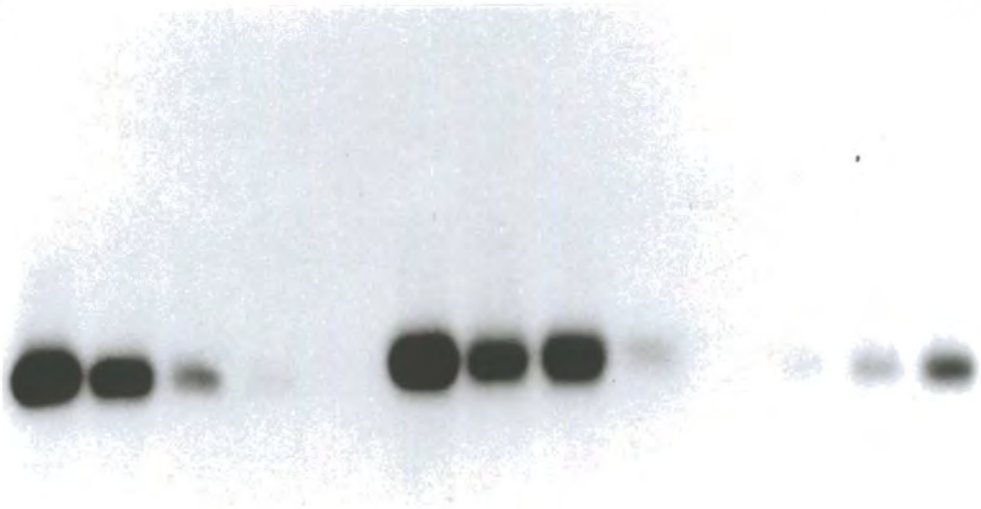
Figure 6.4 Northern analysis of total RNA extracted from *P. sativum* roots, harvested over a range of times following the final solution change, probed with *PsMT_A*.

Photograph of agarose.gel stained with ethidium bromide and autoradiograph.

- Initial media contained 0.5 μM CuSO_4 , 2.0 μM ZnSO_4 , no added iron



Final treatment	0.5 μM CuSO_4 no iron				1.0 μM CuSO_4 2.0 μM iron				no CuSO_4 2.0 μM iron		
	1	7	24	48	1	7	24	48	1	7	48
Time (hours)											



←
Origin

Figure 6.5 A Northern analysis of total RNA extracted from *P. sativum* roots, harvested over a range of times following the final solution change, probed with *PsMT_A*. Photograph of agarose gel stained with ethidium bromide and autoradiograph.
- Media contained 2.0 μM ZnSO_4

A

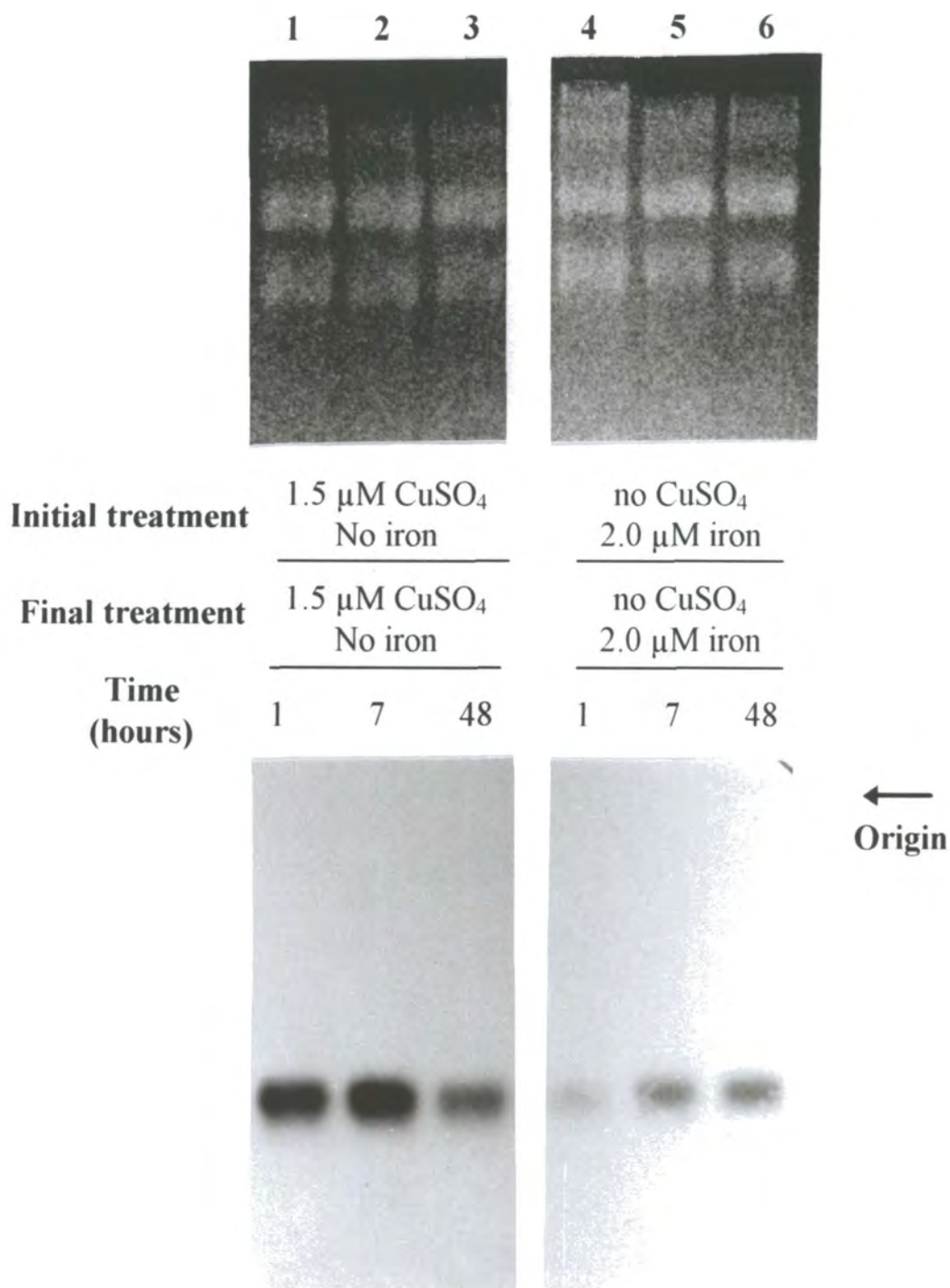
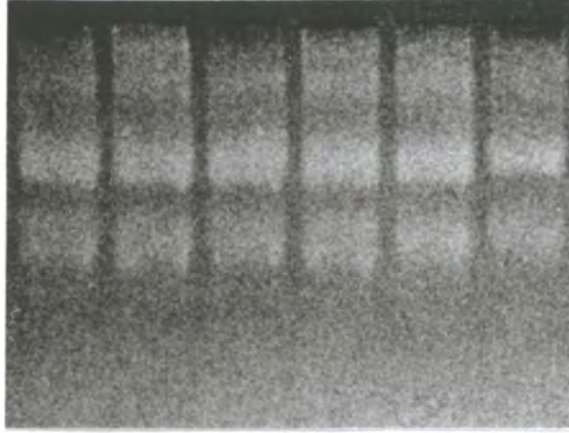


Figure 6.5 B Northern analysis of total RNA extracted from *P. sativum* roots, harvested over a range of times following the final solution change, probed with *PsMT_A*.
Photograph of agarose gel stained with ethidium bromide and autoradiograph.
- Media contained 2.0 μM ZnSO_4

B

7 8 9 10 11 12



Initial treatment

1.5 μ M CuSO₄
No iron

no CuSO₄
2.0 uM iron

Final treatment

no CuSO₄
2.0 uM iron

1.5 μ M CuSO₄
No iron

**Time
(hours)**

1

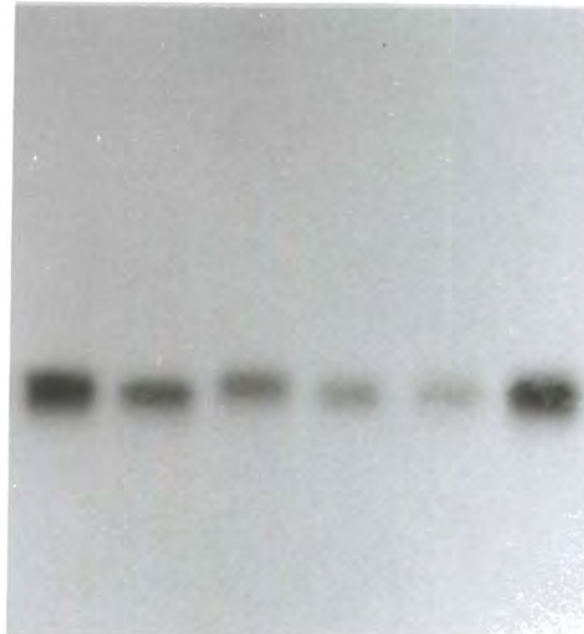
7

48

1

7

48



←
Origin

6.4 Conclusions

Minimal expression of *PsMT_A* was observed in roots of seedlings grown in media containing 100 nM CuSO₄ (figures 6.1A and B). Expression of the gene in roots is reduced by growing seedlings in media supplemented with iron chelate in excess of 2.0 μM (figures 6.1A and B and 6.2A and B). Maximal expression of the gene was observed in the roots of seedlings grown in media containing 500 nM to 1000 nM iron chelate (figures 6.2A and B). The iron concentration giving maximal expression of the gene is likely to lie somewhere between these values and on the evidence of figures 6.2A and B may be effected by copper concentration. The basal level of expression of *PsMT_A* in roots of seedlings grown in solution containing 0.5 μM and 1.0 μM CuSO₄ was increased relative to expression in roots grown in media containing no added copper (figures 6.2A and B). Depressed expression of the *PsMT_A* gene was observed in roots of seedlings grown in media containing both high and low iron concentrations. It is not clear if in both extremes of exogenous iron concentration the reduction in *PsMT_A* expression is a specific iron response or an indirect response of *PsMT_A* expression due to other aspects of root metabolism.

Elevated expression of the *PsMT_A* gene was observed in roots of seedlings grown in media containing both high and low copper concentrations (figures 6.1a and B). This observation suggests that expression of *PsMT_A* is unlike known metallothionein genes in other organisms where expression has only been reported to increase with increasing trace metal concentrations (Hamer *et al.* 1986). This could imply that *PsMT_A* has functions specific to both extremes of copper status. Growth in media containing a low copper concentration may cause fluctuations in aspects of metabolism such that the level of other factors in the cell are increased and these could effect the expression of *PsMT_A*. This could be part of, for example, a stress response. It is not clear if the *PsMT_A* protein may itself have an important role in cellular metabolism under such conditions.

Further speculation on the possible significance of this data for *PsMT_A* function will be presented in chapter 8. The interdependence of iron and copper accumulation in yeast demonstrates that responses to iron and copper cannot necessarily be considered independently (section 1.5.3.1). If such interactions occur in higher plants then this could be a further factor leading to the complex response of *PsMT_A* expression to the iron and copper treatments. This will also be considered in chapter 8.

A feature of the time course experiments, sections 6.3.4 and 6.3.5, was that in conditions where media copper was either 0.5 μM or 1.0 μM or unchanged from 1.5 μM , *PsMT_A* transcript abundance was observed to decrease markedly following the final media change over the 48 hour period studied. This effect could be due to gradual depletion in the copper concentration of the media, or possibly in the micro-environment of the root. Effects other than trace metal concentration may have caused or contributed to this repression (de-induction ?) of the *PsMT_A* gene. For example, the hydroponic media was not aerated over the time course of the experiment.

The repression of *PsMT_A* expression by an exogenous iron concentration of 2.0 μM occurred within 1 hour of exposure to the metal (lane 9, figure 6.4). This response is rapid and may indicate that gene expression is responding directly to the exogenous metal concentration, via a metal sensor on the root surface, rather than the cellular concentration of metal. It may again be speculated that this is not a specific response to metal concentration but part of a more generalised response, such as for example a stress response. The rapid response might not be expected for a gene responding to cellular metal concentrations as these would be expected change more slowly due to homeostatic effects. This rapid response was absent if 1.0 μM CuSO_4 was included in the hydroponic media (lane 5, figure 6.4) or if the seedlings had been grown in 1.5 μM CuSO_4 prior to exposure to iron (lane 7, figure 6.4B).

Induction of *PsMT_A* by exogenous ZnSO_4 in excess of 5 μM was observed in seedlings grown in media containing 2.0 μM iron-EDDHA but the response was not observed in seedlings grown in media not supplemented with iron (figure 6.3A and B). This could indicate that iron availability may effect zinc metabolism, perhaps uptake or cellular availability. Alternatively iron availability may merely effect the response of *PsMT_A* to zinc. It is possible that that induction of *PsMT_A* in response to environmental factors, such as elevated zinc, occurs via an iron dependent transcription factor. The induction of *PsMT_A* expression by elevated zinc concentrations may imply a role for the putative protein in zinc detoxification.

CHAPTER 7
COPPER AND ZINC LIGANDS IN *PISUM SATIVUM*:
EVIDENCE FOR THE PsMT_A PROTEIN IN ROOT EXTRACTS

7.1 Introduction

With the notable exception of the E_c protein from *T. aestivum*, there have, to date, been no reports of the isolation of the translational product of a metallothionein-like gene from plant tissue. The search for a plant metallothionein predates the discovery of the plant metallothionein-like genes and lead to the discovery and characterisation of phytochelatins (reviewed Rauser 1990). In common with phytochelatins the predicted products of plant metallothionein-like genes are small cysteine rich metal binding polypeptides and therefore it might be expected that they would have similar spectroscopic and chromatographic properties to phytochelatin and so be isolated from plant tissue by similar techniques.

The predicted products of plant metallothionein-like genes are charged, therefore, the first step in the purification strategy was to separate charged material from the bulk protein using an anion exchange matrix (section 7.3.1). The suitability of such a strategy to purify the product of the *PsMT_A* gene from plant tissue can be verified by experiments with the recombinant protein. From the properties of the product of the *PsMT_A* gene discussed elsewhere in this thesis it seems possible that the putative protein binds trace metal *in planta*. The copper and zinc ligands of root extracts were therefore investigated with the long term aim of designing a purification strategy to isolate the *PsMT_A* protein from plant tissue. Following the discovery that the expression of the *PsMT_A* gene could be reduced by the addition of exogenous iron chelate to the growth media (Robinson *et al.* 1993), the experimental strategy was altered to exploit this (section 7.3.2 to 7.3.4 and 7.3.7).

An alternative approach to identify the translational product of the *PsMT_A* gene was to exploit the high cysteine content of the putative proteins. *In vivo* labelling was performed with [³⁵S] SO₄ and [³⁵S] cysteine (sections 7.3.6 and 7.3.9). The recombinant *PsMT_A* from *E. coli* was labelled, added to a root extract and followed through the ligand purification strategy (section 7.3.8). Finally, one and two dimensional electrophoresis was applied to the analysis of labelled extracts (7.3.9).

7.2 Methods

7.2.1 Basic strategy for the isolation of ligands from roots of *P. sativum*

P. sativum seedlings were grown in hydroponic conditions as described in section 2.4, but without the addition of iron to the media. A crude soluble extract (40 ml) was obtained from roots of *P. sativum* as described in section 2.3.10.1. Following acetone precipitation the pellet was resuspended in 10 mM Tris-HCl / 1 % (v/v) 2-mercaptoethanol (2-ME) (12 ml). Charged material was separated from the bulk material using DEAE Sephadex anion exchange matrix as described in section 2.3.11.1. This weakly basic matrix has a high capacity for proteins with molecular weights up to 20 000. Charged material was released from the column by increasing salt concentrations using the following sequence of buffers;

1. 10 mM Tris-HCl / 1 % (v/v) 2-ME, pH 7.2 - 75 ml
2. 100 mM Tris-HCl / 1 % (v/v) 2-ME, pH 7.2 - 75 ml
3. 300 mM Tris-HCl / 1 % (v/v) 2-ME, pH 7.2 - 150 ml

The flow rate of the column was 1.0 ml min⁻¹ and fractions of 4 ml were collected and assayed for copper and zinc by atomic absorption spectrophotometry (section 2.3.13). A crude indication of the protein content of fractions was obtained by using the dye binding assay (2.3.3). An aliquot (400 µl) of the major copper/zinc fraction (figure 7.1 no. 37) was transferred to PVDF membrane by vacuum blotting and microsequenced (section 2.3.12).

7.2.2 Copper and zinc ligands from *P. sativum* seedlings grown in media with and without added iron-EDDHA

Two sets of *P. sativum* seedlings (12 seedlings of each treatment) were grown in parallel one set with added iron and one set without (as described in section 2.4). A fresh weight of approximately 15 g was obtained from each set of roots. A crude extract was obtained from the roots as described in section 2.3.10.1. The heat denaturing step was not included in the extraction procedure to avoid possible damage to metal binding components by oxidation. Following acetone precipitation the pellets were resuspended in 10 mM Tris pH 7.2 / 1 % (v/v) 2-ME (12 mls). The samples were desalted on PD-10 columns (final volume to 17.5 mls). The crude extract from the non iron supplemented seedlings was loaded onto a fresh ion exchange column. The crude extract from the iron supplemented seedlings was stored at -80 °C for 24 hours before being thawed on ice loaded onto the anion exchange matrix. Charged material was eluted from the column with the following buffers;

1. 10 mM Tris-HCl / 1 % (v/v) 2-ME, pH 7.2 - 100 ml
2. 100 mM Tris-HCl / 1 % (v/v) 2-ME, pH 7.2 - 100 ml
3. 300 mM Tris-HCl / 1 % (v/v) 2-ME, pH 7.2 - 100 ml

The column flow rate was approximately 1 ml min⁻¹ and fractions (3.5 ml) were collected and assayed for copper and zinc, figures 7.2a and b. The total copper and zinc content represented by the peaks was calculated from the volume and metal concentration of the fractions comprising the peak.

The 300 mM copper / zinc peak (figure 7.2a fractions 77 to 81) from non iron supplemented and iron supplemented (figure 7.2b fractions 73 to 77) treatments, and from the 100 mM zinc peak (figure 7.2a fractions 46 to 49) from non iron supplemented treatments, were collected. The fractions were pooled and aliquots (2.5 ml) desalted using a PD-10 column and eluted in 50 mM Tris-HCl, pH 8.0. The samples were separated by gel filtration chromatography as described in section 2.3.11.2. The column had been equilibrated in 50 mM Tris-HCl, pH 8.0. The column flow rate was 0.5 ml min⁻¹, fractions (3 ml) were collected and assayed for copper and zinc (figure 7.2 c, d and e).

7.2.3 Revised protocol for the isolation of ligands from *P. sativum* seedlings

To allow more consistent comparison of the gel filtration profiles from different treatments a single step salt concentration increase from 10 mM Tris-HCl to 400 mM Tris-HCl was adopted. This sharp salt gradient should remove all the previously observed ligands from the matrix. To increase the amount of starting material, and therefore the quantity of ligands extracted, two sets of 30 seedlings were grown in 20 l basins. This yielded between 40 and 50 g fresh weight of root material. The maximum variation in the fresh weight of harvested root material between seedlings grown in iron supplemented and non supplemented media was 10 %. After harvest roots were rinsed in distilled water, blotted dry and flash frozen in liquid nitrogen after which they were stored at -80 °C until required.

The roots were ground to a fine powder under liquid nitrogen and allowed to thaw slightly. One volume (approximately 30 ml) of 10 mM Tris-HCl / 1 % (v/v) 2-ME, pH 7.2 was added and the resulting pulp mixed thoroughly with a glass rod. As a further measure to prevent oxidation of the ligands during the purification procedure the buffers were saturated with O₂ free nitrogen. The pulp was squeezed through two layers of sterilised muslin and remaining debris removed by centrifugation (900 g, 5 min). The crude extract was then

loaded directly onto the ion exchange matrix. Ion exchange chromatography was performed as described in section 2.3.11.1 with the following buffers;

1. 10 mM Tris-HCl / 1 % (v/v) 2-ME, pH 7.2 - 200 ml
2. 400 mM Tris-HCl / 1 % (v/v) 2-ME, pH 7.2 - 100 ml

The column flow rate was 1 ml min⁻¹, fractions (3.5 ml) were collected and assayed for copper, zinc and protein.

For further analysis fractions were pooled and desalted on a PD-10 column prior to gel filtration chromatography as described in section 2.1.11.2. The buffer throughout was changed to 10 mM Tris-HCl / 1 % (v/v) 2-ME, pH 7.2 which had been pretreated with gaseous nitrogen. A column rate was 0.5 to 0.8 ml min⁻¹ was used, fractions (3 to 5 ml) were collected and assayed for copper, zinc and protein.

7.2.4 Purification of a putative copper ligand by thiol affinity chromatography

A putative copper ligand obtained following gel filtration chromatography (Cu-X, figure 7.5c) was purified using thiopropyl Sepharose-6B affinity matrix. The sample (2.5 ml) was desalted twice using a PD-10 column to remove 2-ME. The eluting buffer in both cases was 300 mM ammonium acetate, pH 5.5. Thiopropyl Sepharose (1g) was equilibrated overnight in this buffer and placed in a small glass column. The sample was loaded onto the matrix and washed twice with 300 mM ammonium acetate / 1 M NaCl, pH 5.5 (3 ml), once with 50 mM Tris-HCl / 1 M NaCl, pH 8.0 (3 ml) and twice with 50 mM Tris-HCl, pH 8.0 (3 ml). Bound material was eluted with 50 mM Tris-HCl / 50 mM 2-ME, pH 8.0 (3 ml). An aliquot (1.5 ml) of the sample was transferred to PVDF membrane by centrifugation for automated microsequencing (as described in section 2.3.12).

7.2.5 Copper and zinc ligands from the leaves of *P. sativum* seedlings

To investigate if similar copper and zinc ligands are present in the leaves of *P. sativum* seedlings an analogous extraction protocol (section 7.2.3) was performed with non iron supplemented seedlings. Seedlings of *P. sativum* (30) were grown as in section 7.2.3. On day 15 the leaves were cut from the stems of the seedlings and flash frozen in liquid nitrogen. A crude extract was prepared from the leaves by grinding the leaves to a powder in liquid nitrogen, thawing and mixing with one volume of 10 mM Tris-HCl / 1 % (v/v) 2-ME, pH 7.2. The extract was mixed thoroughly and debris removed by straining through muslin and

centrifugation as described for the root preparation. The extract was loaded onto a fresh sephadex DEAE ion exchange matrix and ion exchange chromatography performed as described in section 2.3.11.1. The column flow rate was 0.7 ml min^{-1} and fractions (3.5 ml) were collected and assayed for copper, zinc and protein, figure 7.6a.

Fractions corresponding to the copper peak Cu-1 (62/63) and the initial zinc peak Zn-1 (69/70) were desalted on PD-10 columns and resolved using gel filtration chromatography. The flow rate was 0.5 ml min^{-1} and fractions (4 ml) were collected and assayed for copper, zinc and protein (figures 7.6b and 7.6c respectively).

7.2.6 *In vivo* labelling of plant material with [^{35}S] SO_4

A batch of 30 seedlings was grown as described in section 2.4 without added iron. In parallel a further 3 seedlings were grown in a separate 2 l pot. Both sets of seedlings were grown as described previously until day 12. From day 12 to 15 the batch of 30 *P. sativum* seedlings was treated as before. On day 13 the hydroponic solution of the batch of 3 seedlings was supplemented with $750 \mu\text{Ci } [^{35}\text{S}] \text{SO}_4$. The roots of the labelled seedlings were harvested into liquid nitrogen on day 15.

Both sets of roots were ground to a fine powder in liquid nitrogen and combined. The root extract was then prepared as described in section 7.2.3. Ion exchange chromatography was performed as described in section 7.2.3. The flow rate was 0.7 ml min^{-1} and fractions (3.5 ml) collected and assayed for protein as described in section 2.3.3. An aliquot (200 μl) of each fraction was mixed with scintillation cocktail (6 ml) and incorporation measured as counts per minute (CPM) on a Packard scintillation counter using the manufacturers protocol (figure 7.7a).

Two pools of the radioactive material eluted from the ion exchange matrix were desalted on PD-10 columns and further analysed by gel filtration chromatography as described in section 2.3.11.2. The flow rate was 0.5 ml min^{-1} and fractions (3.5 ml) were collected. All fractions were assayed for protein and radiolabel, and non radiolabelled fractions were assayed for copper and zinc as described in section 2.3.13. The radiolabelled fractions were not assayed by atomic absorption spectrophotometry due to the risk of radioactive contamination.

7.2.7 Labelling of the recombinant PsMT_A peptide with [³⁵S] cysteine and spiking of a crude extract from *P. sativum* roots

The PsMT_A protein was expressed in *E. coli* as a GST-PsMT_A fusion protein as described in section 2.3.1 with the following amendments. After growing for 45 minutes at 37 °C the culture was inoculated with CuSO₄ to 500 μM and with 40 μCi [³⁵S] L-cysteine. Expression from the pGPMT3 plasmid was induced with IPTG and a crude protein extract was prepared as before. The extract was loaded onto glutathione Sepharose matrix and *E. coli* proteins and other cell components removed by washing with PBS. The GST-PsMT_A protein was cleaved by incubation with activated factor Xa as described in section 2.3.4. The cleavage solution (3 ml) was eluted from the column and collected (eluent 1), the column was washed twice more with cleavage buffer (3 ml) (eluent 2 and eluent 3).

The incorporation of radiolabel into the sample was measured by adding 100 μl of each sample to 6 ml of liquid scintillant and measuring the counts per minute (CPM) on a Packard scintillation counter, table 7.2. As the purification strategy is effective (section 4.3.1) and the factor Xa protein was not labelled the radiolabel must be associated with the PsMT_A alone. Eluents 1 and 2 were combined giving a total of 5.8 ml (13 000 CPM).

Seedlings of *P. sativum* were grown as described in section 2.4 without the addition of exogenous copper, iron or zinc. A crude extract was prepared, as described in section 7.2.3, but before loading onto the ion exchange matrix the extract was mixed with the labelled PsMT_A sample. The flow rate was 0.5 ml min⁻¹ and fractions (3 ml) were collected. Aliquots (500 μl) were assayed for radiolabel (figure 7.10a).

7.2.8 Electrophoresis of *P. sativum* root extracts labelled with [³⁵S] cysteine

Two sets of *P. sativum* seedlings were grown in hydroponic media, as described in section 2.4, which did not contain added copper or zinc. One set of seedlings was supplemented with iron-EDDHA as described in section 2.4.1. On day 15 individual seedlings were transferred to a test tube (masked with silver foil) containing the appropriate hydroponic media (8 ml) to which 40 μCi [³⁵S] cysteine had been added. *P. sativum* plants were grown (on the bench) for a further 6 hours and roots were harvested into liquid nitrogen.

Protein samples were prepared as described in section 2.3.10.1. Incorporation of radiolabel was estimated as follows; An aliquot of sample (5 μl) was spotted onto a cellulose acetate disk (approximately 1 cm diameter) and air dried. The disk was washed in 10 %

(w/v) TCA (10 min), 95 % (v/v) ethanol (10 min), di-ethyl ether (1 min) and air dried. The disk was placed in a scintillation vial with liquid scintillant and incorporation measured on a Packard scintillation counter.

Following electrophoresis the protein was transferred to PVDF membrane as described in section 2.3.8. The filter was stained with Coomassie blue, destained, air dried and photographed. The filter was placed in an autoradiographic cassette and stored at room temperature for 2 to 7 days before being developed by normal photographic techniques.

7.2.8.1 Carboxymethylation of protein samples

Samples were reconstituted in normal sample buffer (section 2.3.6) and incubated in boiling water for 5 min following which iodoacetic acid was added to 20 mM. The sample was incubated for 15 min at 50 °C.

7.3 Results and discussion

7.3.1 Basic ligand isolation procedure

An early example of the results of this procedure is shown in figure 7.1. A large proportion of the protein was eluted from the column in the initial wash with 10 mM Tris-HCl along with a smaller proportion of the copper and zinc. In this experiment the major copper (Cu-1) and zinc (Zn-1) components eluted from the matrix upon the introduction of the 300 mM Tris-HCl buffer along with the remaining major protein components. In some experiments these components eluted in part or in total in the 100 mM Tris-HCl washes (not presented). Attempted sequence analysis of fraction 37 yielded a complex mixture of peptides indicating that the copper and zinc fractions obtained from ion exchange chromatography consist of many components requiring further purification.

7.3.2 Copper and zinc ligands from *P. sativum* seedlings grown with and without added exogenous iron

Ion exchange chromatography profiles of root extracts from seedlings grown in media to which no iron had been added and media containing 2.0 μ M iron-EDDHA are presented in figure 7.2a and b. The most obvious difference between the two plots is the reduction of both the zinc and copper peak in 300 mM Tris-HCl. The total copper content in the fractions comprising peak Cu-1 in figure 7.2a was 350 nmol, compared to 140 nmol in figure 7.2b.

The total zinc content in the fractions comprising peak Zn-1 in figure 7.2a was 1200 nmol, compared to 600 nmol in figure 7.2b. A zinc component (Zn-2) was eluted from the column in 100 mM Tris-HCl in non iron supplemented root extract. The distribution of copper and zinc components between the 100 mM Tris-HCl buffer wash and 300 mM Tris-HCl buffer wash varied in replicate experiments (not presented). The effect of freezing and then thawing the iron supplemented crude extract prior to loading onto the column may have effected the integrity of copper and zinc components in the sample.

In both gel filtration profiles (figure 7.2c and d) copper and zinc components have separated into species with slightly different apparent molecular weights (Cu-A and Zn-A), with the copper species having the slightly higher molecular weight. The Sephadex G-50 matrix separates globular proteins, in the molecular weight range 1500 to 30000 (according to the manufacturers specifications). The column has not been calibrated. However, the position of the copper peaks (Cu-A on both profiles) would suggest a molecular weight below 10000. The copper species from the iron supplemented sample (figure 7.2d) appears to be closer to the apparent molecular weight of the zinc species in this sample than the copper species in the non iron supplemented sample (figure 7.2c). However this slight difference could simply indicate that greater separation was obtained on the column for the non iron supplemented sample, perhaps due to a slight difference in loading volume, or in flow rate.

Figure 7.2e is the gel filtration profile of the Zn-2 peak (figure 7.2a). The zinc species is of similar molecular weight to the species eluted in both the 300 mM samples. Despite there being no measurable copper content in the fractions pooled for this sample there is a copper species of very low molecular weight on the gel filtration profile (Cu-B). There is also an indication that there may be a copper species represented similar to that found in the samples eluted in 300 mM Tris-HCl. The very low molecular weight copper species (Cu-B) is similar to that observed previously (Robinson *et al.* 1992). The observation of a reduction in the overall concentration of copper and zinc associated with ligands detected in roots from *P. sativum* seedlings grown in the presence of iron was repeated in three subsequent extractions using the same procedure (data not shown).

The isolation protocol described in section 7.2.1 and 7.2.2 had a number of limitations. The position of the major copper and zinc peak observed on ion exchange chromatography profiles varied between 100 mM Tris-HCl and 300 mM Tris-HCl washes in different

extractions (not shown), with apparently the same species being observed on subsequent gel filtration profiles. A consequence of this was that differences in the amount of metal in the fractions comprising the observed peaks eluted from the ion exchange matrix for the two metal treatments could differ due to an apparently arbitrary distribution between the 100 mM Tris-HCl and 300 mM Tris-HCl washes. Further deficiencies in the original extraction procedure were identified. The blender caused frothing of the extract and was not an efficient method for homogenisation of the *P. sativum* roots. The method required the freeze / thaw of one sample, which may cause degradation of ligands in one sample and not the other. The acetone precipitation step could potentially lead to loss of metal binding capacity of components because it involved solvent extraction, freezing, centrifugation and resuspension. To eradicate these problems an alternative extraction procedure was adopted section 7.2.3.

Ion exchange chromatography of extract from roots of *P. sativum* seedlings

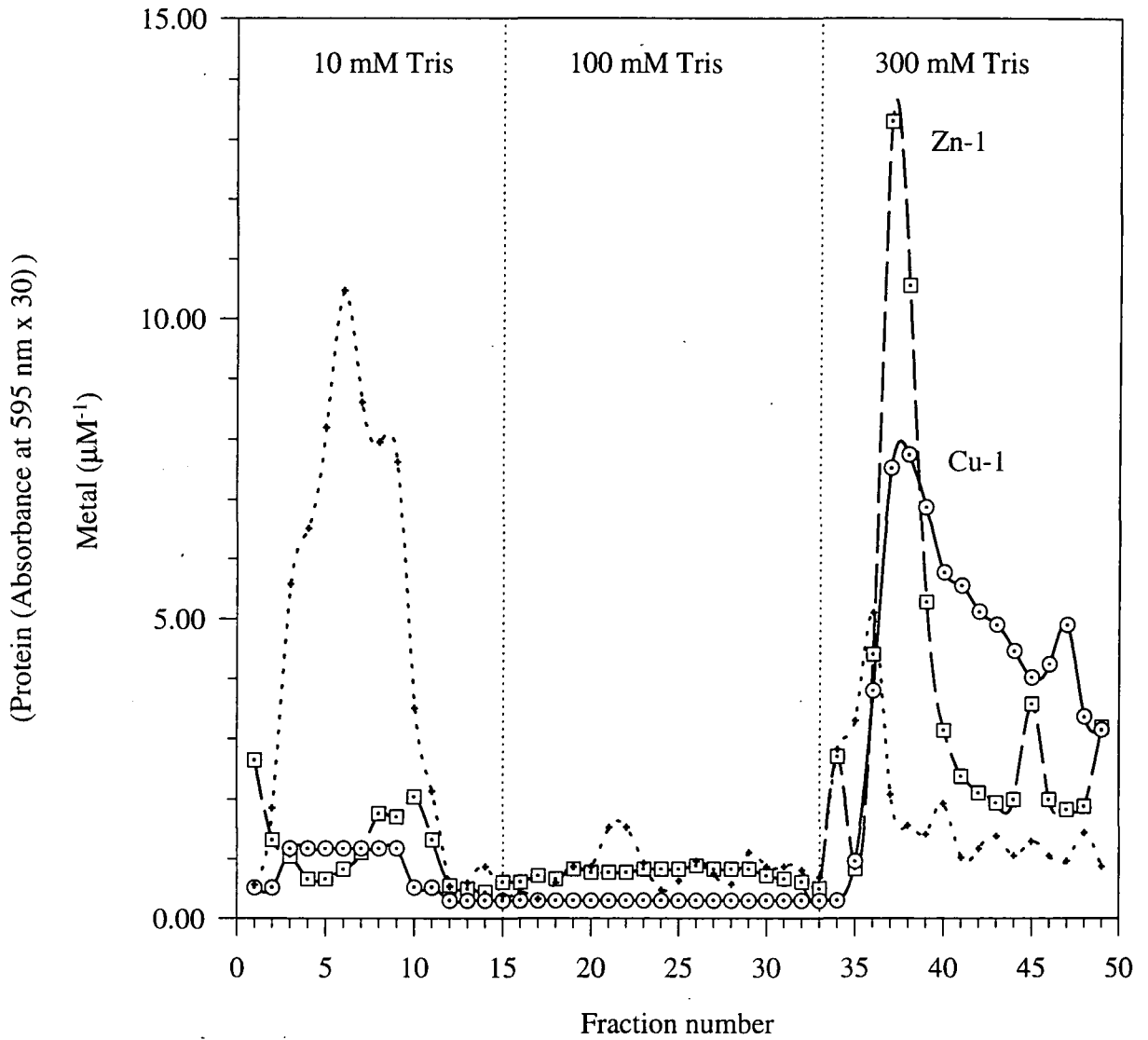
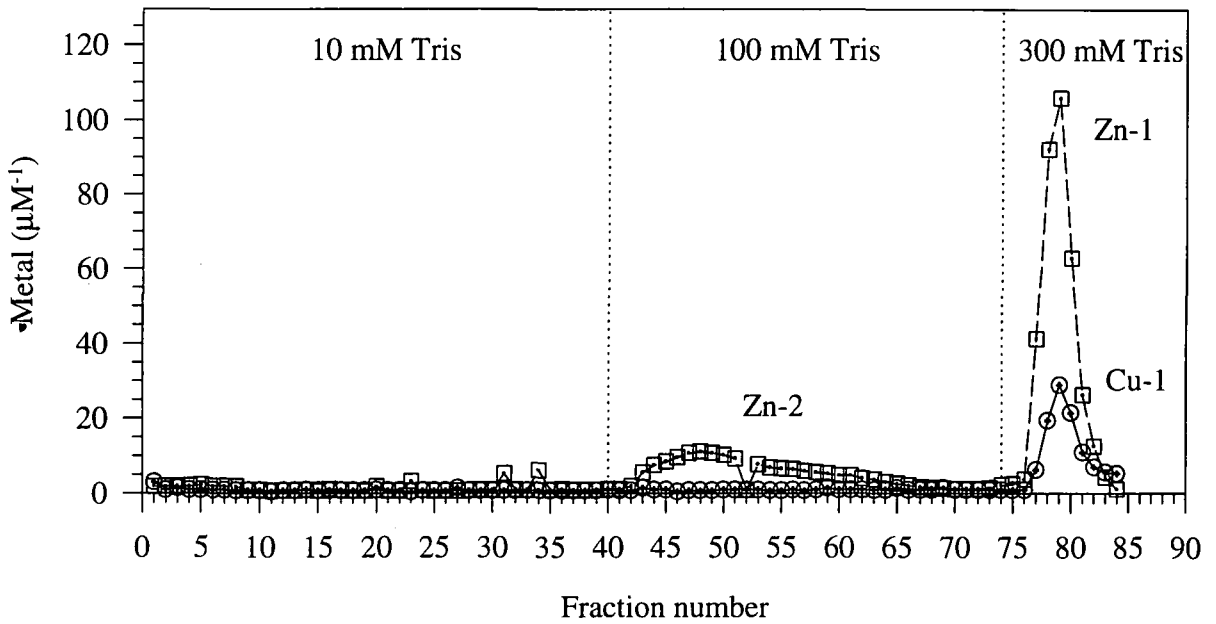


Figure 7.1 Chromatography profile of a crude soluble extract from the roots of *P. sativum* on DEAE anion exchange matrix. Assayed for copper (—, \odot), zinc (- - -, \square) and protein (\cdots , +).

a. Ion exchange chromatography of extract from non iron supplemented seedlings



b. Ion exchange chromatography of extract from iron supplemented seedlings

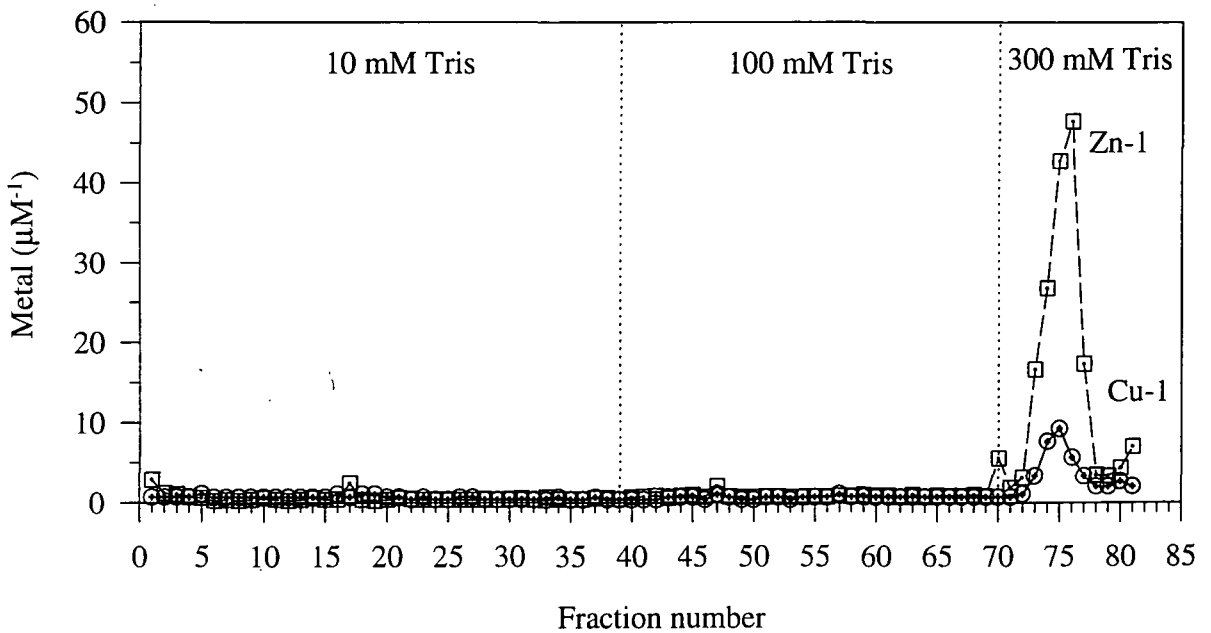
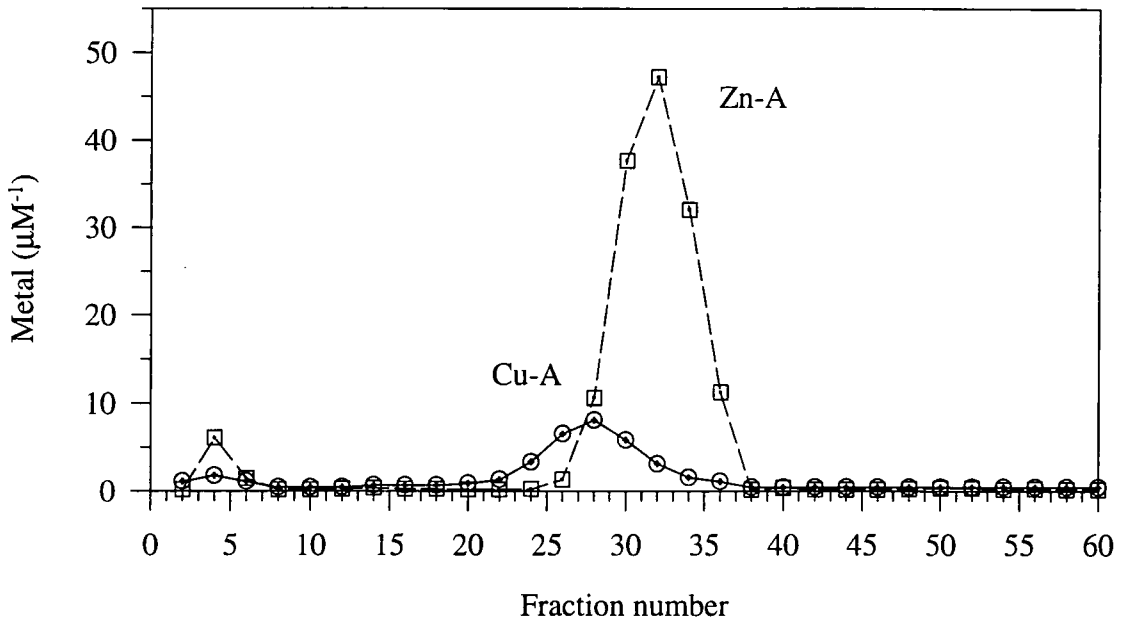


Figure 7.2 a., b. Chromatography profiles of crude soluble extracts from the roots of *P. sativum* on DEAE anion exchange matrix. Assayed for copper (—, \odot) and for zinc (- - -, \square).

c. Gel filtration chromatography of peak Zn-1 / Cu-1 from figure 7.2a



d. Gel filtration chromatography of peak Zn-1 / Cu-1 from figure 7.2b

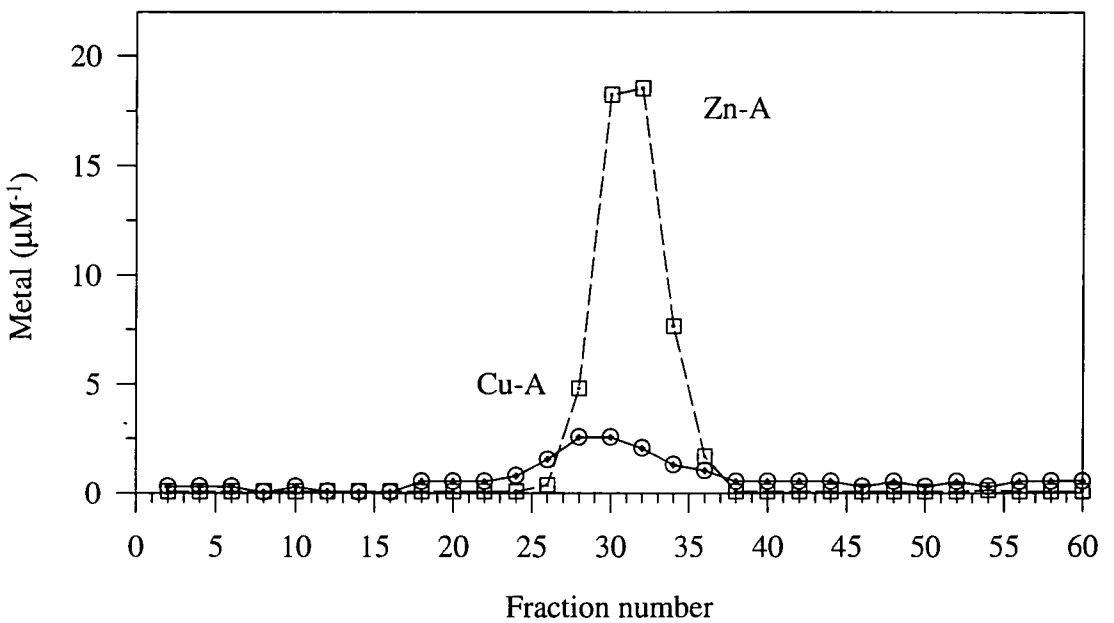


Figure 7.2 c., d. Gel filtration chromatography profiles of representative metal containing fractions from the ion exchange chromatography profiles, figures 7.2a and b respectively. Assayed for copper (—, ○) and for zinc (- - -, □).

e. Gel filtration chromatography of peak Zn-2 from figure 7.2a

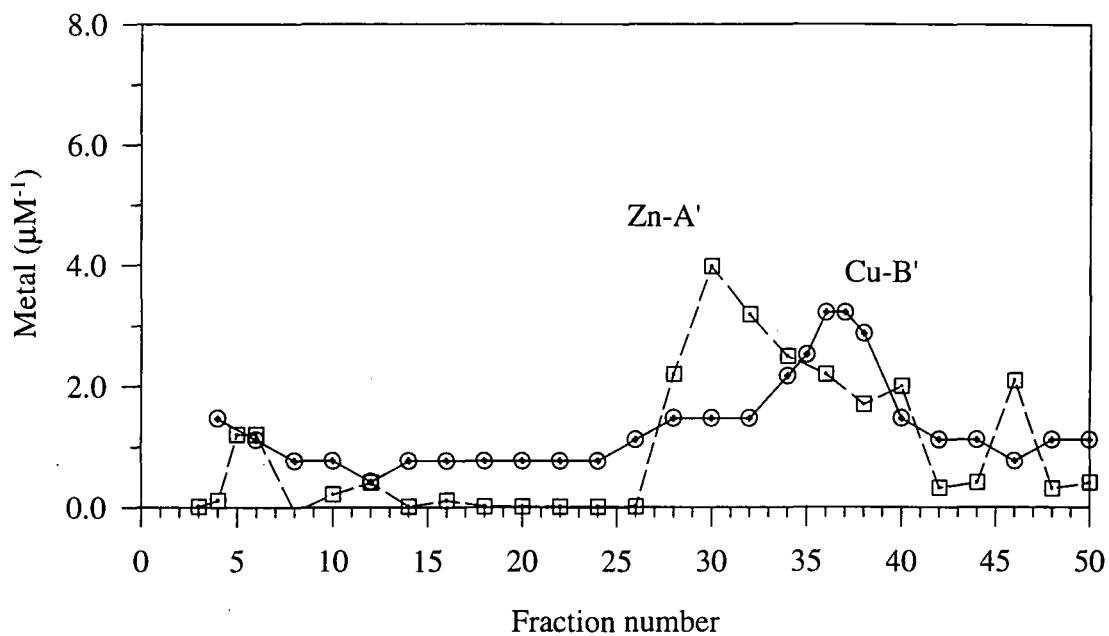


Figure 7.2 e. Gel filtration chromatography profile of representative metal containing fractions from the ion exchange chromatography profile, figure 7.2a. Assayed for copper (—, \odot) and for zinc (- - -, \square).

7.3.3 Extraction of copper and zinc ligands from *P. sativum* seedlings, grown with and without added iron, using the revised protocol (7.2.3)

Approximately 50 g fresh weight of root material was obtained for each of the treatments. This method reduced considerably the time between root homogenisation and loading the crude extract onto the matrix and the separation of the bulk material, which will include phenolics and proteases, from the charged species. Ion exchange chromatography profiles from non iron supplemented and iron supplemented seedlings are presented in figures 7.3a and 7.3b. There is a notable increase in the amount of free zinc washed from the matrix by the 10 mM Tris-HCl wash. This is probably attributable to the removal of the PD-10 desalting step prior to loading the sample. This step was impractical due to the increase in sample volume. A further feature of the ion exchange profiles using the revised protocol is the appearance of a shoulder to the major zinc peak (Zn-1' figure 7.3a). The reduction in the quantity of zinc eluted in the 400 mM Tris-HCl wash between the non iron supplemented (figure 7.3a) and iron supplemented extract (figure 7.3b) is very dramatic in this extract (2000 nmol zinc compared to only 80 nmol). The amount of zinc in the 400 μ M Tris-HCl wash for this non iron supplemented extract was considerably greater than that observed in replicate experiments, a contributing factor to this anomaly may have been that unbound zinc had not been fully washed off the matrix in the 100 mM Tris-HCl wash. The amount of copper in peak Cu-1 was 750 nmol in the non iron supplemented extract compared to 360 nmol in the iron supplemented extract.

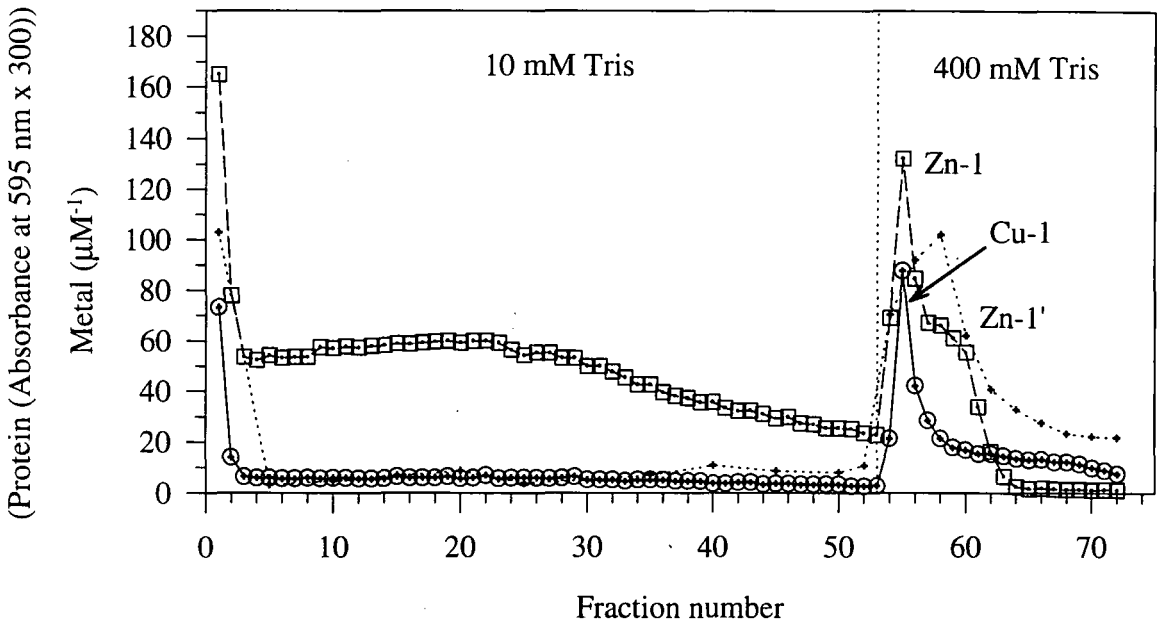
The copper/zinc fractions (numbers 56 and 57) overlapping peak Zn-1' on the ion exchange chromatography profile (figure 7.3a) were pooled and separated by gel filtration chromatography as described in section 7.2.3, figure 7.3c. The profile contains only one zinc species (Zn-A) which is similar to that observed previously. There are two copper species. Cu-A has a slightly higher apparent molecular weight than the zinc species and appears to be similar in size to the copper ligand observed previously. Cu-B co-eluted with the zinc species. This may indicate that it is the same molecular species but binding copper instead of zinc or a single heterogeneous species. It is possible that in the previous extraction method the copper had dissociated from this species due to oxidation.

Ion exchange chromatography profiles of another example of an extraction using the revised technique (section 7.2.3) are presented in figure 7.4a and 7.4b. There was no significant difference in the amount of copper in the fractions comprising the copper peak,

Cu-1 (2500 nmol in figure 7.4a and 2700 nmol in figure 7.4b). The total amount of zinc in the fractions comprising peak Zn-1 was 790 nmol in the extract from non iron supplemented seedlings (figure 7.4a) and 240 nmol in the extract from iron supplemented seedlings (figure 7.4b).

Figure 7.4c is a gel filtration chromatography profile obtained from the main copper / zinc peak Cu-1 / Zn-1 (figure 7.4a, fractions 58/59) from the extract from non iron supplemented seedlings by the method described in section 2.3.11.2. The ligands obtained are a low apparent molecular weight zinc species (Zn-A) and a single copper species of slightly larger apparent molecular weight (Cu-A). The relative magnitude of the two peaks is slightly surprising when the difference in magnitude of the original ion exchange peaks (Cu-1 and Zn-1) is considered. More specifically the ratio of Cu-1 : Zn-1 in the ion exchange profile (figure 7.4a) is approximately 3 : 1 (2500 nmol copper to 790 nmol zinc) whereas the ratio of the Cu-A : Zn-A peaks in figure 7.4c is approximately 1 : 1 (376 nmol copper to 368 nmol zinc). (The estimated ratio of copper : zinc in fractions 58 and 59 is actually 4 : 1). This suggests that a considerable amount of copper has been lost from the sample prior to loading onto the gel filtration column, probably during desalting on the PD-10 column. The implication is that either a large proportion of the copper observed on the ion exchange profile is only loosely associated with cellular components in the extract or that the copper associated with these components is becoming dissociated from the cellular components due to oxidation during further manipulation. The latter case is likely and may indicate that working under inert gas may be required if the copper and zinc ligands of roots of *P. sativum* seedlings are to be investigated in more detail, especially if less abundant ligands are to be investigated.

a. Ion exchange chromatography of extract from non iron supplemented seedlings



b. Ion exchange chromatography of extract from iron supplemented seedlings

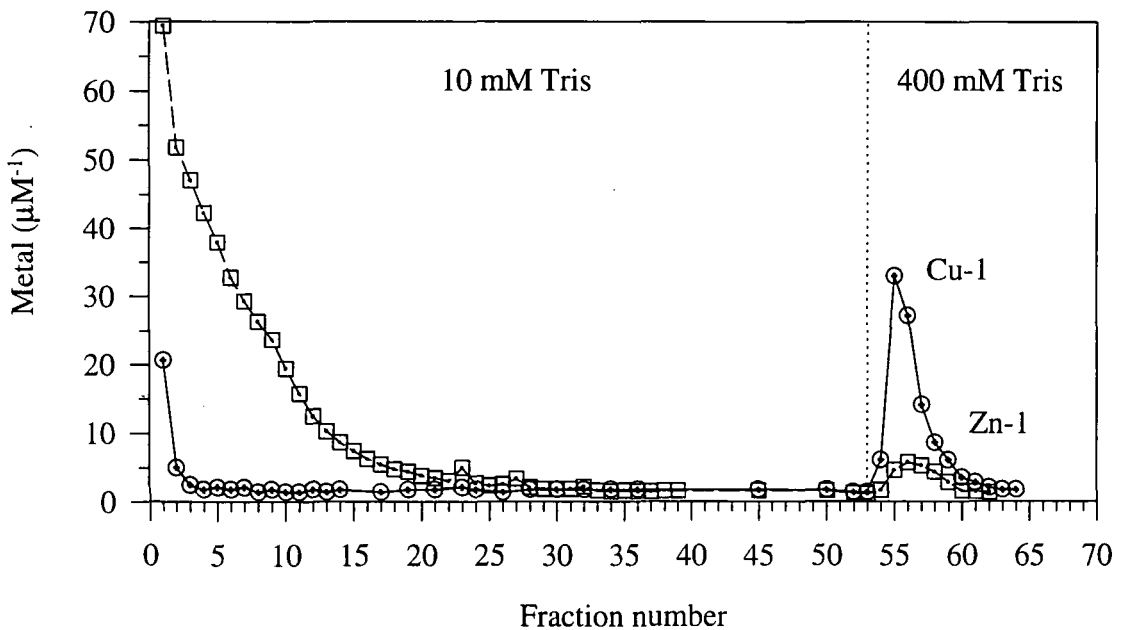


Figure 7.3 a., b. Chromatography profiles of crude soluble extracts from the roots of *P. sativum* on DEAE anion exchange matrix. Assayed for copper (—, \odot) and for zinc (- - -, \square) (and protein (\cdots , +), figure 7.3a).

c. Gel filtration chromatography of peak Zn-1 figure 7.3a

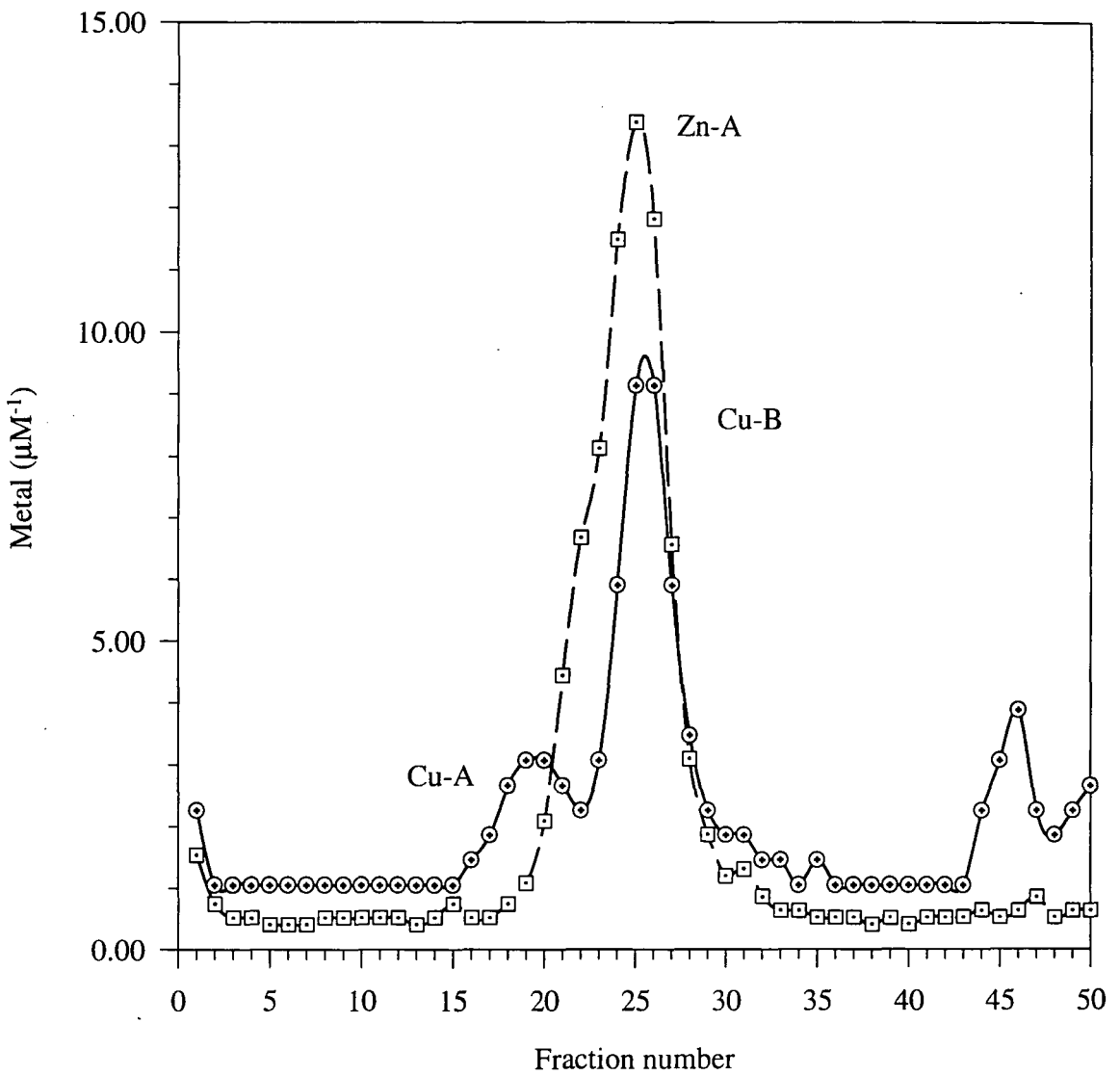
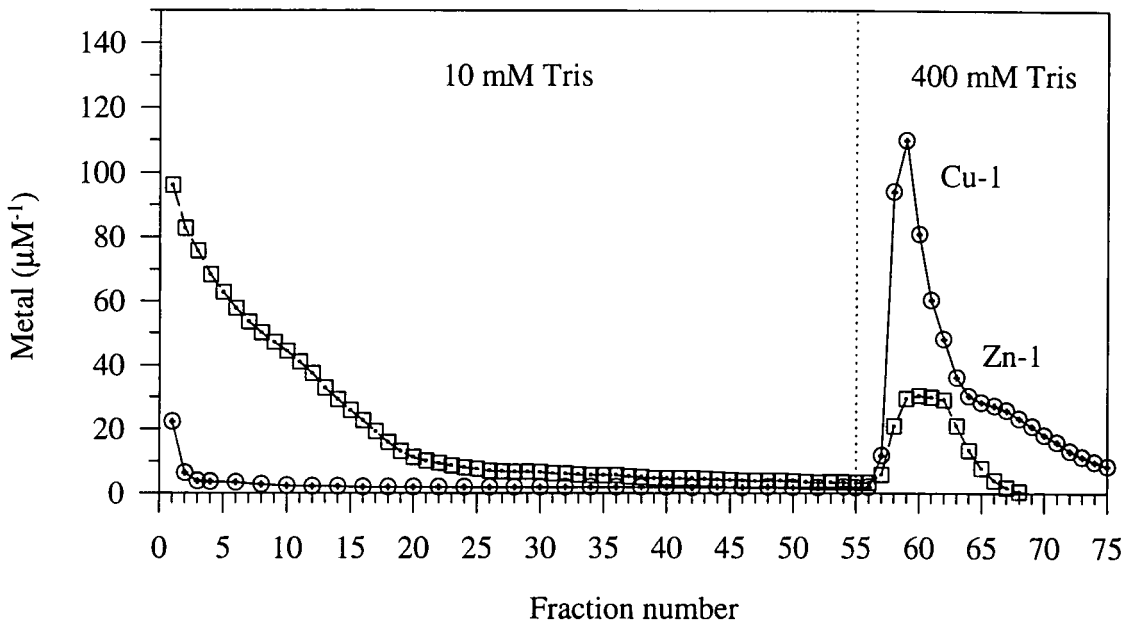


Figure 7.3 c. Gel filtration chromatography profile of representative metal containing fractions from the ion exchange chromatography profile, figure 7.3a. Assayed for copper (—, \odot) and for zinc (- - -, \square).

a. Ion exchange chromatography of extract from non iron supplemented seedlings



b. Ion exchange chromatography of extract from iron supplemented seedlings

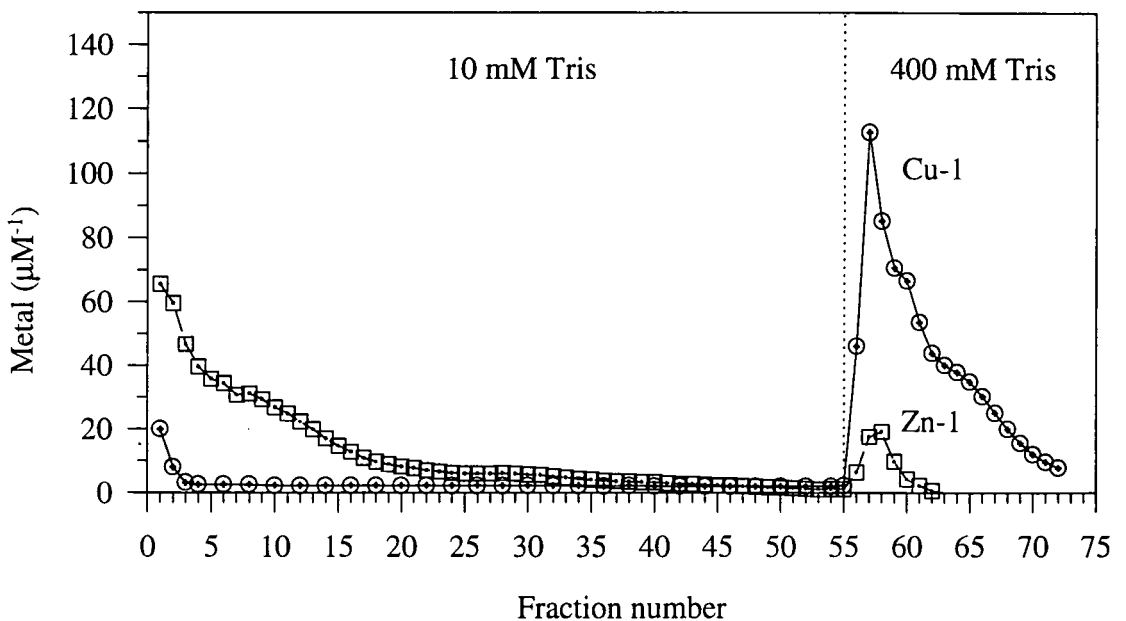


Figure 7.4 a., b. Chromatography profiles of crude soluble extracts from the roots of *P. sativum* on DEAE anion exchange matrix. Assayed for copper (—, \odot) and for zinc (- - -, \square).

c. Gel filtration chromatography of peak Zn-1 / Cu-1 figure 7.4a

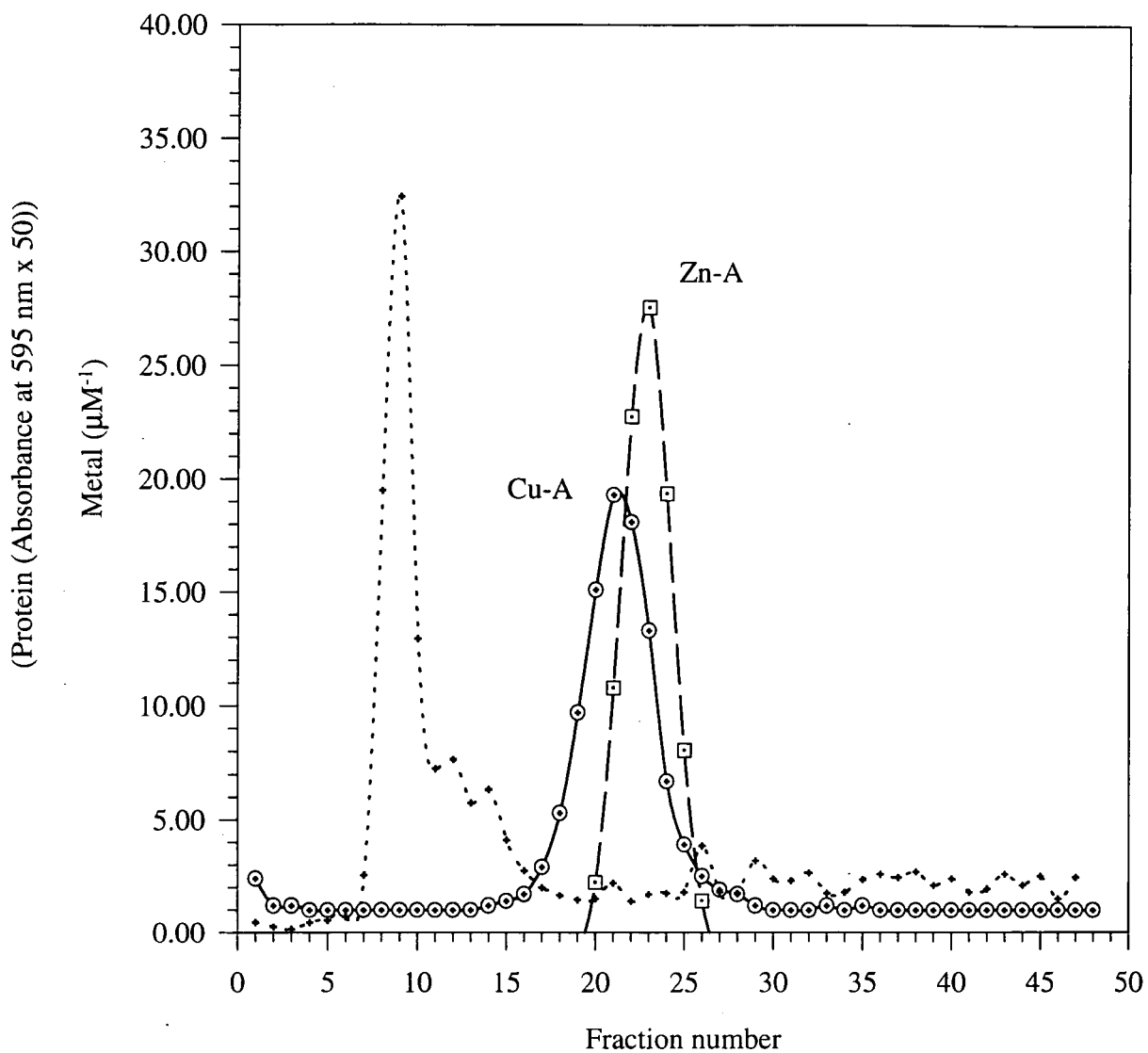


Figure 7.4 c. Gel filtration chromatography profile of representative metal containing fractions from the ion exchange chromatography profile, figure 7.4a. Assayed for copper (—, \odot), zinc (- - -, \square) and protein (\cdots , +).

7.3.4 Identification of a high apparent molecular weight copper species and purification of the putative copper ligand by thiol affinity chromatography

Root extracts of non iron supplemented and iron supplemented seedlings were prepared as described in section 7.2.3 and subjected to ion exchange chromatography as described in that section with a flow rate of 0.8 ml min^{-1} and fractions of 4 ml were collected (figure 7.5a and 7.5b). In these profiles the copper shoulder observed in previous extracts has resolved into a distinct peak (Cu-2) in both extracts. The estimated copper content of the fractions comprising both Cu-1 and Cu-2 was approximately 1000 nmol in the extract from both the iron supplemented and non supplemented seedlings. The zinc content of the fractions comprising peak Zn-1 was approximately 200 nmol in the extract from non iron supplemented seedlings and 100 nmol in the extract from iron supplemented seedlings.

Gel filtration chromatography profiles obtained from the major copper peak (Cu-1) from the non iron supplemented and the iron supplemented extracts respectively (in both cases fractions 55 and 56 were pooled) are presented in figure 7.5c and 7.5d (as in section 2.3.11.2 with 4 ml fractions). Both profiles contain the zinc species and the slightly higher molecular weight copper species, although the apparent size difference is greater in the case of the extract from the iron supplemented seedlings. The most striking feature of the non iron supplemented profile is an even higher molecular weight copper species (Cu-X) in a single fraction. This was the second occurrence of this feature in non iron supplemented data (previous data not shown) which encouraged the view that it was not an artifact, although in the previous case the copper species was also apparently in a single fraction in the same position.

The high molecular weight species was purified further by thiol affinity chromatography as described in section 7.2.4. Initial sequencing yielded no useful data but a putative sequence of **WGWGGGYR** was determined following cleavage with CNBr, table 7.1. However the amino acid yields are very low and this sequence cannot be considered reliable. This peptide does not match a fragment of any published sequence on the OWL database.

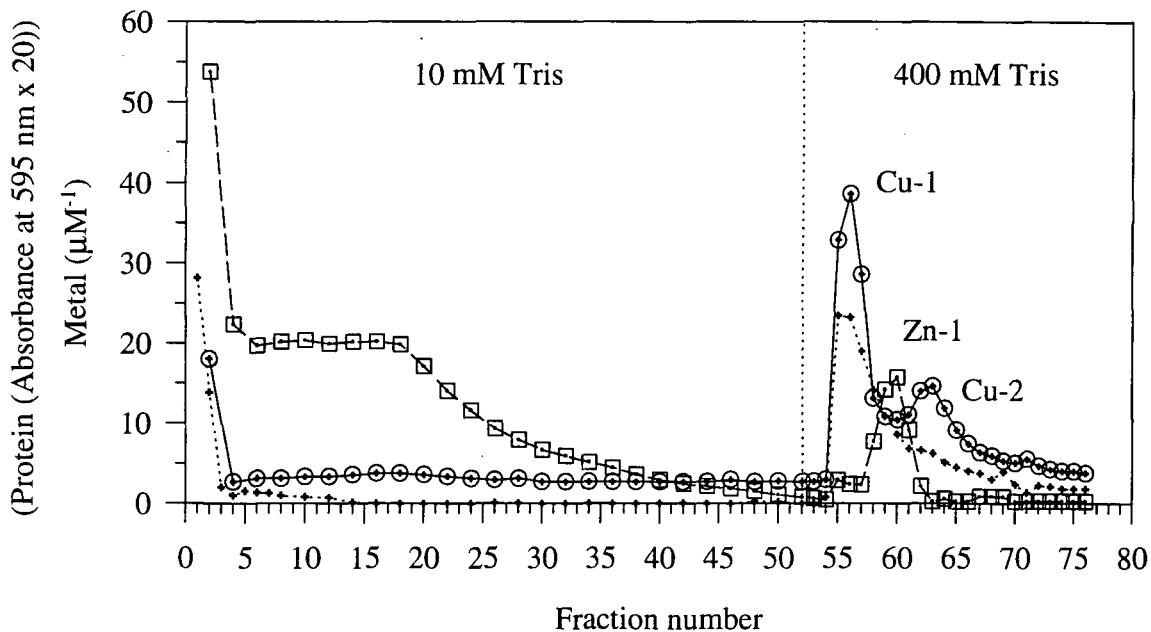
Fractions 60 and 61 from the non iron supplemented ion exchange profile (figure 7.5a), corresponding to the zinc peak (Zn-1) and leading edge of the second copper peak (Cu-2) were pooled, desalted on a PD-10 column and resolved by gel filtration chromatography, as described in section 2.3.11.2. The flow rate was 0.6 ml min^{-1} and fractions (4 ml) were collected and assayed for copper, zinc and protein, figure 7.5e. The single zinc peak lies in

approximately the same position as observed previously despite having a slightly longer retention time on the ion exchange column. Eluting with the same apparent molecular weight is a copper species (Cu-B). This corresponds to the peak Cu-B observed in figure 7.3c. If this copper species is the same ligand as the zinc species then the implication is that the component is more negatively charged when copper is bound. On the copper trace in figure 7.5e there is an indication of the higher apparent molecular weight copper species.

Cycle	1	2	3	4	5	6	7	8	9
Ala	3.8	-2.1	2.5	0.0	-1.4	2.7	-9.5	-5.0	3.1
Arg	0.1	-0.0	-0.4	0.6	-0.0	0.1	-0.9	0.5	3.2
Asn	0.4	-0.3	0.0	0.3	-0.1	-0.4	-0.1	-0.1	-0.1
Asp	0.8	-0.8	1.1	-0.1	0.9	0.5	-0.4	-0.3	-0.1
Cys	-1.0	-1.0	-1.0	-1.0	-1.0	-1.0	-1.0	-1.0	-1.0
Glu	-0.4	-0.1	0.7	0.1	-0.2	0.5	-0.3	-0.4	0.5
Gln	-0.9	0.7	1.1	0.5	1.0	0.8	-0.1	0.2	-0.1
Gly	-11.7	5.2	4.4	5.3	4.8	3.6	-9.6	-2.2	-0.3
His	-0.0	-0.1	-0.1	0.1	0.2	0.1	-0.2	-0.0	-0.2
Ile	1.3	0.2	0.0	-0.1	-0.2	-0.4	0.4	-0.3	2.1
Leu	0.5	0.1	-0.2	-0.0	-0.3	0.2	-0.9	-0.3	0.2
Lys	0.4	-0.2	-0.1	-0.1	-0.1	-0.0	-0.2	-0.1	0.2
Met	1.3	0.0	-0.3	0.3	1.4	0.3	-0.2	-0.3	1.6
Phe	0.4	0.2	-0.2	-0.2	-0.2	-0.2	2.3	-0.2	-0.2
Pro	-0.8	0.7	0.4	0.0	0.1	-0.1	-0.4	-0.1	0.5
Ser	5.7	2.4	0.3	-0.5	-0.6	-0.1	0.3	0.6	-0.3
Thr	5.6	2.9	0.4	-0.6	1.4	0.1	-0.4	1.1	1.4
Trp	18.0	-0.4	5.2	-0.4	2.4	-0.4	2.2	0.8	-0.4
Tyr	-0.2	0.5	-0.2	-0.2	-0.2	-0.2	10.0	4.5	-0.2
Val	2.0	-0.1	-0.2	0.0	0.6	2.0	0.0	-0.7	0.2

Table 7.1 Yield (pM) of each amino acid at each cycle from automated microsequencing of copper species Cu-X figure 7.5c following cleavage with CNBr. The most abundant amino acid at each cycle of N-terminal degradation is in bold.

a. Ion exchange chromatography of extract from non iron supplemented seedling



b. Ion exchange chromatography of extract from iron supplemented seedlings

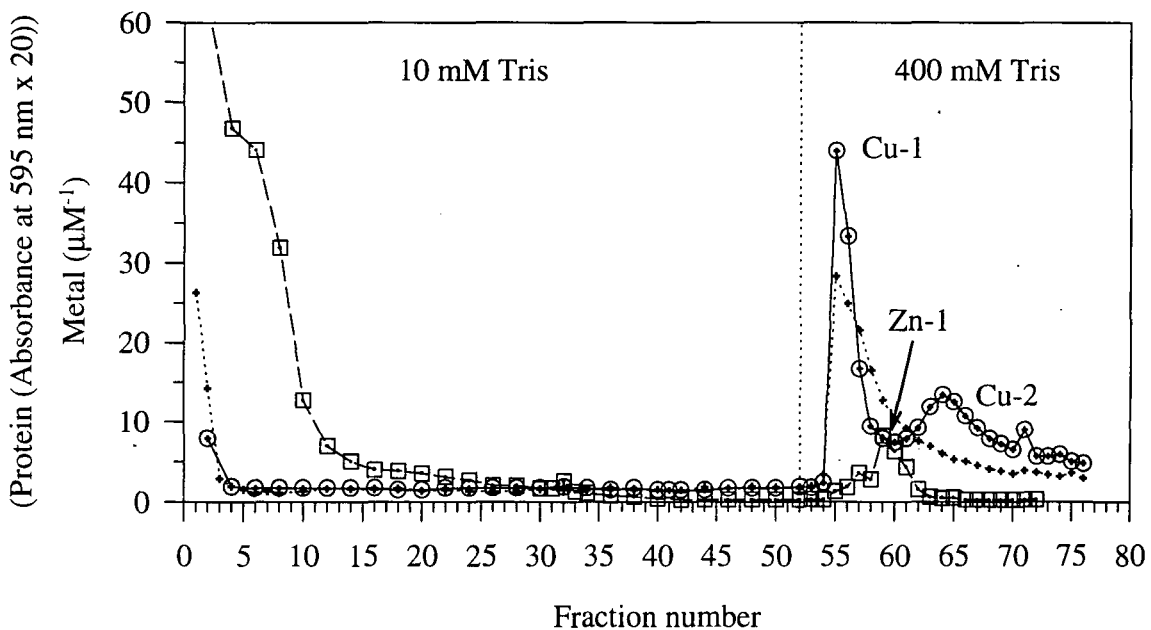
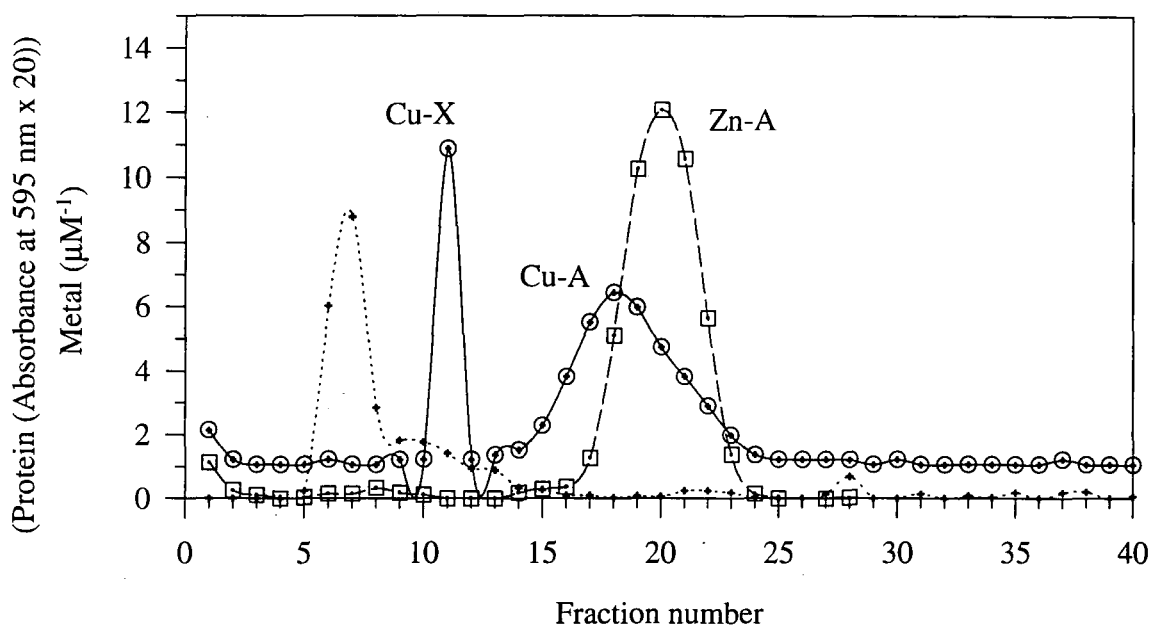


Figure 7.5 a., b. Chromatography profiles of crude soluble extracts from the roots of *P. sativum* on DEAE anion exchange matrix. Assayed for copper (—, ○), zinc (---, □) and protein (···, +).

c. Gel filtration chromatography of peak Cu-1 figure 7.5a



d. Gel filtration chromatography of peak Cu-1 figure 7.5b

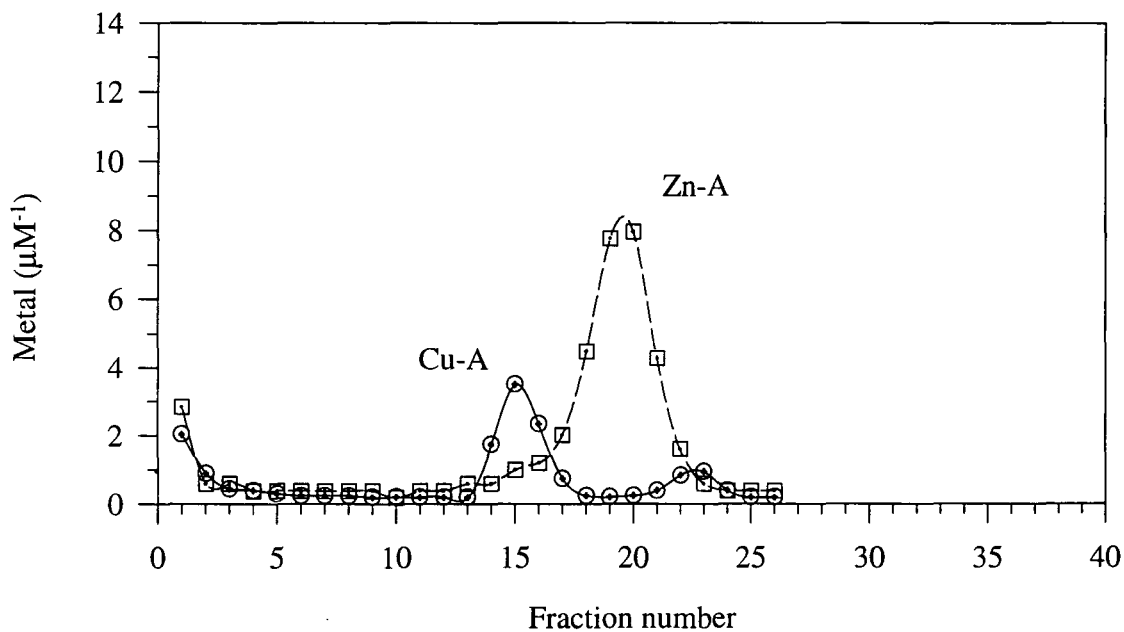


Figure 7.5 c., d. Gel filtration chromatography profiles of representative metal containing fractions from the ion exchange chromatography profiles, figure 7.5a and 7.5b. Assayed for copper (—, \odot), zinc (- - -, \square) (and protein (· · ·, +), figure 7.5c).

e. Gel filtration chromatography of peak Zn-1 / Cu-2 figure 7.5a

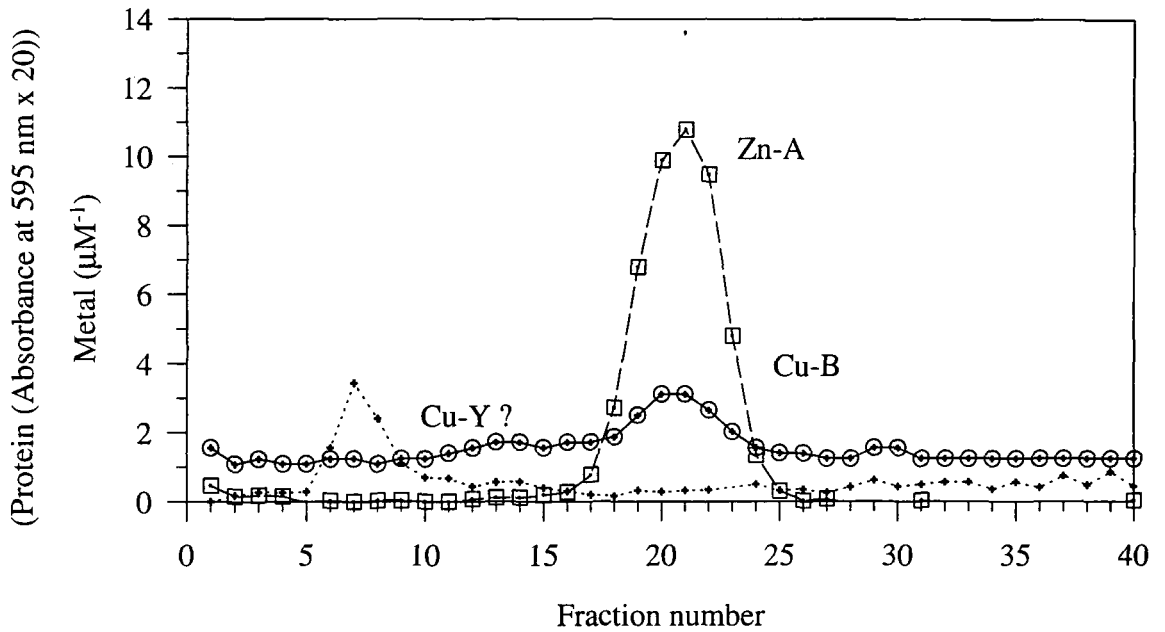


Figure 7.5 e. Gel filtration chromatography profile of representative metal containing fractions from the ion exchange chromatography profile, figure 7.5a. Assayed for copper (—, \odot), zinc (- - -, \square) and protein ($\cdot \cdot \cdot$, +).

7.3.5 Copper and zinc ligands from the leaves of *P. sativum* seedlings

Ion exchange profiles of extracts from leaves of *P. sativum* are presented in figures 7.6a. In 400 mM Tris-HCl a copper species (Cu-1) was eluted first followed by a zinc species (Zn-1) with a slightly longer retention time and then a second potential zinc species. The gel filtration profiles of the copper peak (fractions 62/63) and the initial zinc peak (fractions 69/70) are presented in figures 7.6b and 7.6c respectively.

In both profiles there is a zinc peak (Zn-A) in a similar relative position to that observed in gel filtration profiles of the root extracts. In figure 7.6b, the extract from Cu-1, there is an apparent shoulder to this peak which could indicate that there is a second zinc species present. However at such low metal concentrations, approaching the limit of the sensitivity of the atomic absorption spectrophotometer, this could be an artifact. In both traces there is a copper species of slightly higher molecular weight than the zinc species (Cu-A) and the indication of a less abundant second species of smaller molecular weight (Cu-B). The major copper and zinc ligands in *P. sativum* roots and leaves have similar chromatographic properties. Whether or not they are identical molecular species will require further investigation.

7.3.6 Extraction of ligands from *P. sativum* roots labelled with [³⁵S] SO₄

A different approach was to identify sulphur rich ligands, and by inference cysteine rich compounds such as the putative product of the *PsMT_A* gene, by labelling the seedling with the radioisotope of sulphur. This was achieved by the introduction of [³⁵S] SO₄ to the plant media. Ion exchange chromatography of a radiolabelled plant extract is presented in figure 7.7a. The [³⁵S] peak was eluted in the same position in the 400 mM Tris-HCl buffer as the major copper and zinc fractions in the previous experiments. *

Gel filtration chromatography of pool 1 and pool 2 (figure 7.7a) is presented in figures 7.7b and 7.7c. A copper species, Cu-A, present in both pools is not labelled with [³⁵S]. This implies either that this species does not contain sulphur (and therefore cysteine) or that the [³⁵S] has not been incorporated into the this ligand. If this copper ligand (Cu-A) is the same copper component seen in previous root extracts then a zinc ligand species, observed in the previous root extracts would be expected. The [³⁵S] label appears to be associated with, or at least co-elutes with, the zinc species in pool 1. Alternatively the radiolabel could be eluting as free sulphate, however it would be expected that most of any free sulphate present

would be removed from the sample during the desalting step prior to loading the sample onto the G-50 matrix. If it is assumed the elution of ligands from the ion exchange matrix followed the pattern observed in, for example figure 7.5a, then this pool should contain more copper and less zinc than pool 2. This assumption is supported by the reduction of the copper peak in pool 2 and the appearance of what appears to be the leading edge of a zinc peak before the radiolabelled fractions and the trailing edge of both a zinc and copper peak following the radiolabelled fractions. These implied peaks suggest that the [³⁵S] may be associated with the zinc species and possibly the copper species of the same apparent size seen in previous experiments. It is possible that the [³⁵S] has not been incorporated into protein but is associated with these species as free sulphur compounds. This could be analogous to the association of free sulphur compounds with phytochelatin (for example Plocke and Kägi 1992).

a. Ion exchange chromatography of an extract from leaves of *P. sativum*

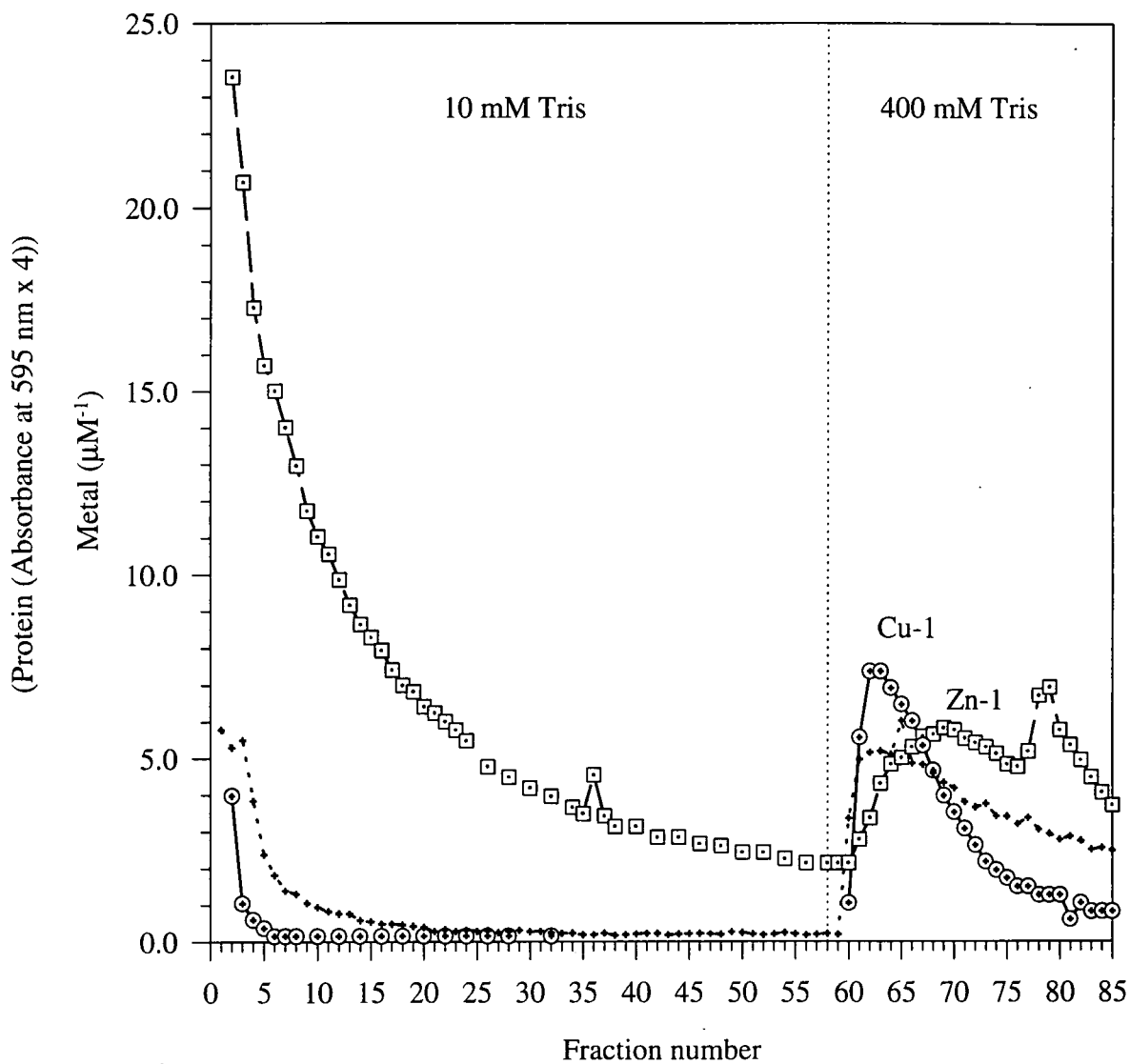
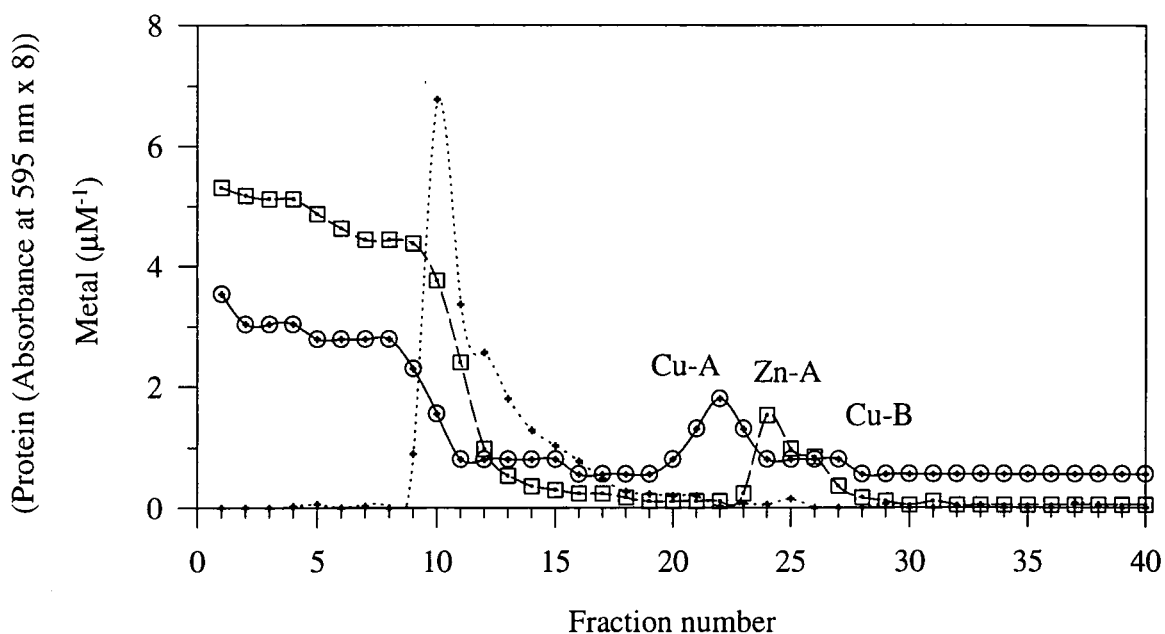


Figure 7.6 a. Chromatography profile of crude soluble extracts from the leaves of *P. sativum* on DEAE anion exchange matrix. Assayed for copper (—, \odot), zinc (- - -, \square) and protein (\cdots , +).

b. Gel filtration chromatography of peak Cu-1 figure 7.6a



c. Gel filtration chromatography of peak Zn-1 figure 7.6a

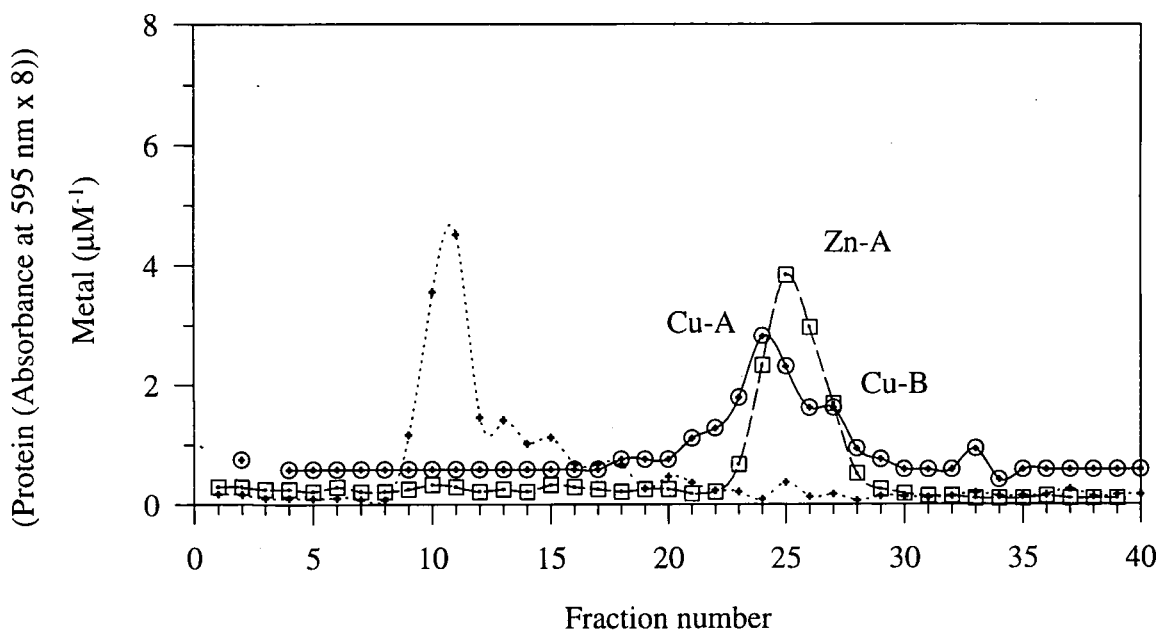


Figure 7.6 b., c. Gel filtration chromatography profiles of representative metal containing fractions from the ion exchange chromatography profile, figure 7.6a. Assayed for copper (—, \odot), zinc (- - -, \square) and protein (\cdots , $+$).

a. Ion exchange chromatography of [³⁵S] SO₄ labelled *P. sativum* roots

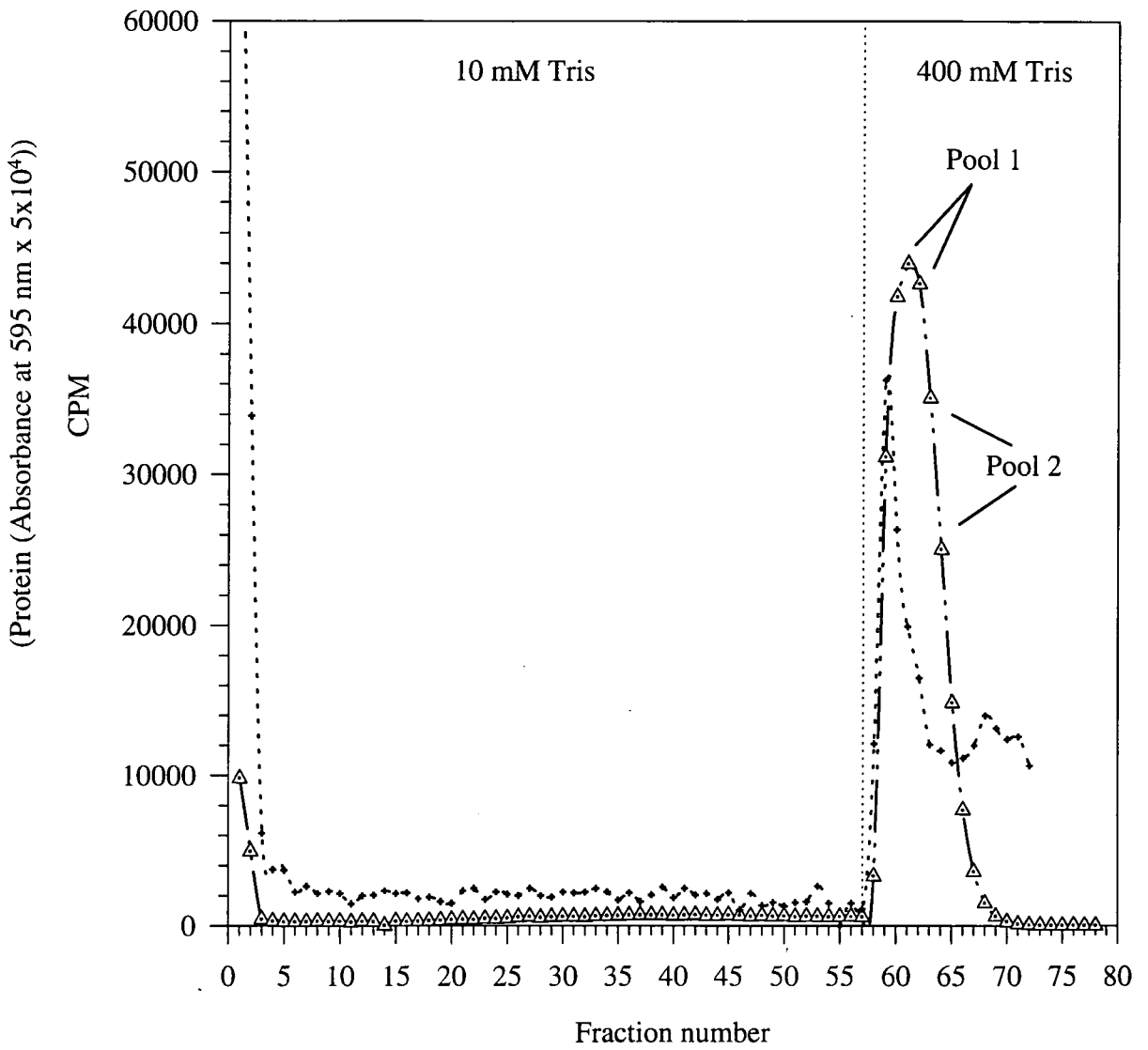
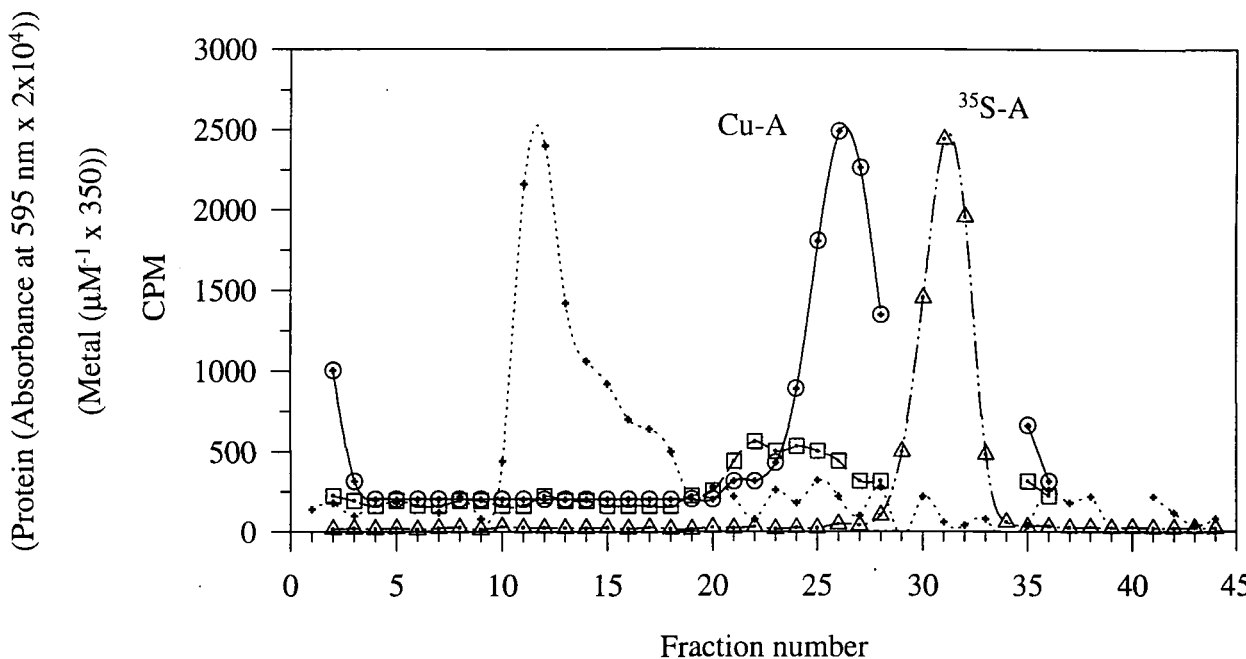


Figure 7.7 a. Chromatography profile of crude soluble extract from the roots of *P. sativum* seedlings, labelled with [³⁵S] SO₄, on DEAE anion exchange matrix. Assayed for protein (· · · , +) and radioactivity (· · - , Δ).

b. Gel filtration chromatography of [³⁵S] pool 1, figure 7.7a



c. Gel filtration chromatography of [³⁵S] pool 2, figure 7.7a

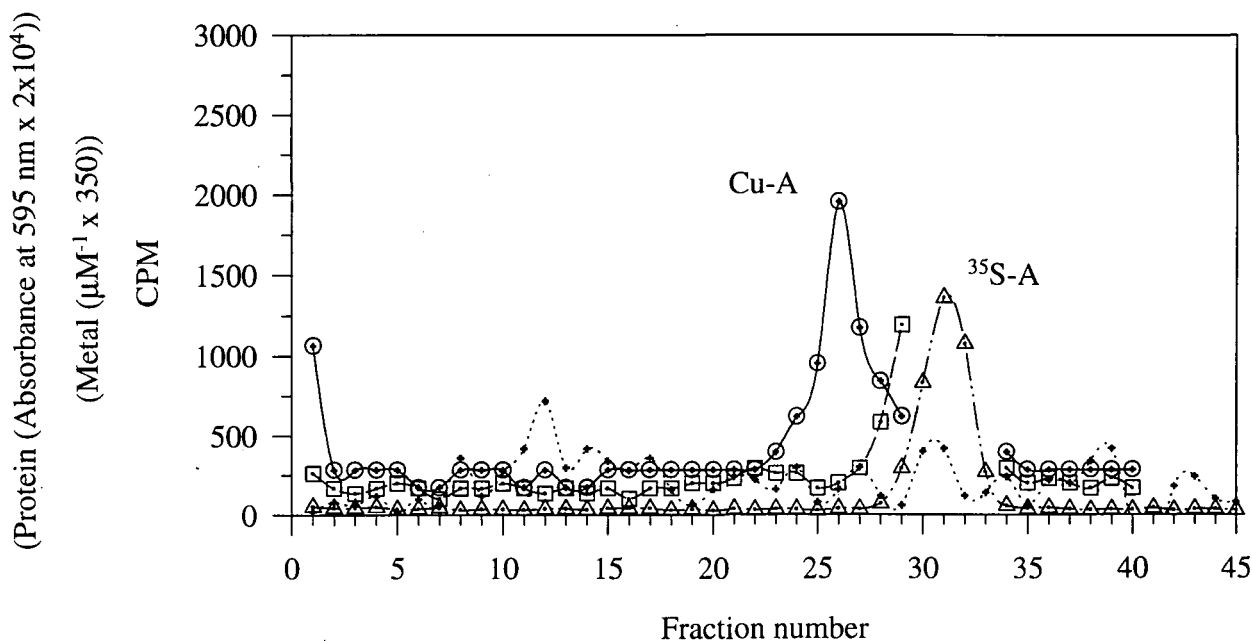


Figure 7.7 b., c. Gel filtration chromatography profiles of representative [³⁵S] containing fractions from the ion exchange chromatography profile, figure 7.7a. Assayed for copper (—, ⊙), zinc (- - -, ⊠), protein (· · ·, +) and radioactivity (· · -, Δ).

7.3.7 Copper and zinc ligands in roots of *P. sativum* seedlings grown in media without added copper and zinc

The chromatographic properties of the ligands identified in root extracts in sections 7.3.1 to 7.3.4 are similar to those which have previously been observed for phytochelatin (for example, refer to Tomsett *et al.* 1989). The copper and zinc concentrations (0.5 μM and 2.0 μM respectively) in the hydroponic medium may be sufficiently high to induce the biosynthesis of phytochelatins. It is possible that these phytochelatins could mask a putative metallothionein-like protein. The quantity of BSO required to inhibit production of phytochelatins in a sufficiently large sample of *P. sativum* seedlings, grown in hydroponic solution by the method described in section 2.4, in order to make comparisons of seedlings grown in different metal treatments was prohibitively expensive. Preliminary data suggested that $PsMT_A$ was expressed at low exogenous copper and zinc concentrations provided the iron concentration is low (as detailed in chapter 6). The putative $PsMT_A$ ligand would therefore be predicted to be in root extracts from seedlings grown in low iron in the presence of low copper and zinc conditions which may minimise the biosynthesis of phytochelatin like compounds.

Two sets of *P. sativum* seedlings were grown as described in section 2.4 but without the addition of copper or zinc to the hydroponic medium. One set was supplemented with iron-EDDHA as described in section 2.4. The fresh weight of roots obtained by growing seedlings with this media was similar to that obtained with previous growth conditions, that is approximately 40 g. The crude extract was prepared as above and loaded onto the ion exchange matrix. The flow rate was 0.6 mls min^{-1} and fractions (3 ml) were collected and assayed for copper, zinc and protein, figure 7.8a and b.

The estimated copper content of the fractions comprising the peak Cu-1 was 190 nmol for the extract from non iron supplemented seedlings (figure 7.8a) and 65 nmol for the extract from iron supplemented seedlings (figure 7.8b). For both extracts this represents a considerable reduction in the copper species eluted from the ion exchange matrix compared to that obtained with the previous growth conditions. The estimated zinc content of fractions comprising peak Zn-1 was 60 nmol for the extract from non iron supplemented seedlings (figure 7.8a) and 160 nmol for the extract from iron supplemented seedlings (figure 7.8b). The reduction of the amount of zinc eluted from the ion exchange matrix in conditions of

low iron is the reverse of the effect observed with seedlings grown in media supplemented with copper and zinc.

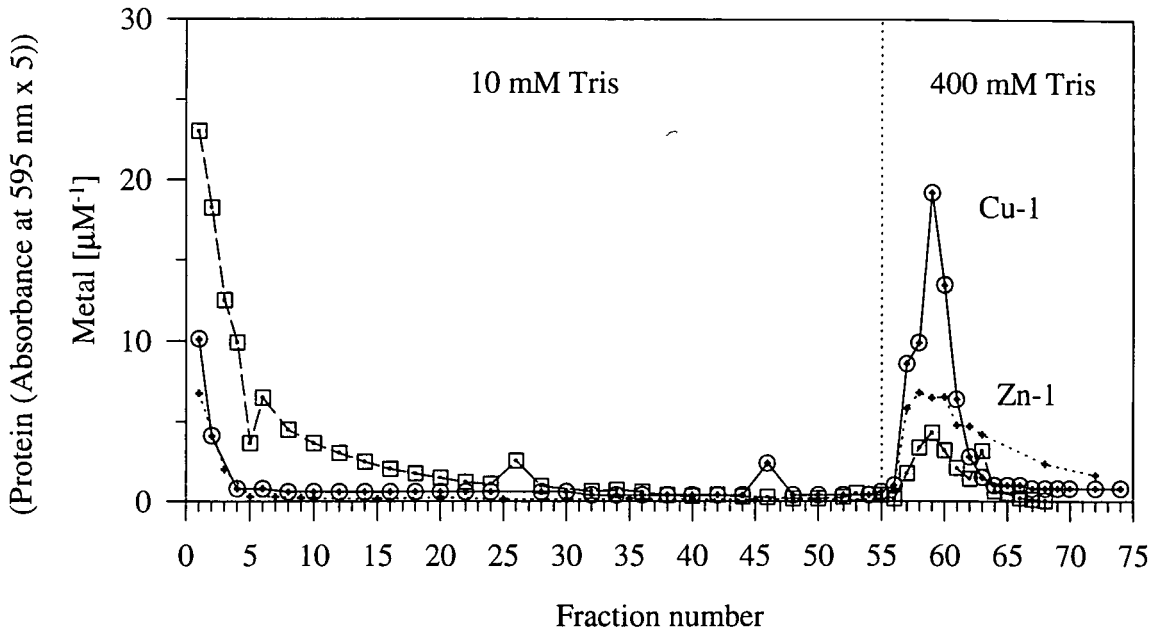
The metal containing fractions (59 and 60 from both extracts) were desalted on PD-10 columns and separated by gel filtration chromatography as described in section 2.4 and 7.2.3. The flow rate was 0.4 ml min^{-1} and fractions (3 ml) were collected and assayed for copper, zinc and protein, figure 7.8c and d. The non iron supplemented chromatography profile is dominated by a wide zinc peak (Zn- α). Surprisingly there is not an analogous peak in the profile of the iron supplemented extract. A second zinc peak (Zn- β) has co-eluted with the bulk protein peak in the profile of the non iron supplemented seedlings, again this peak is absent in the profile of the iron supplemented extract. In the profile of the non iron supplemented extract there is a peak (Cu- β) which co-elutes with Zn- β and is the most obvious copper feature. There may also be a small and widely dispersed copper peak (Cu- α) coincident with the peak Zn- α . There are no features in the copper profile of the non iron supplemented extract. The lack of ligands in the iron supplemented extract complicates the interpretation of these profiles. Copper and zinc components were eluted from the ion exchange matrix and the differences in the gel filtration profiles from the two treatments may due to degradation or oxidation of the copper/zinc ligands.

The experiment was repeated with the same growth conditions and the same extraction procedure. The ion exchange profiles, figures 7.9a and b, are similar to the previous extract although the difference in the copper peaks is less marked. The estimated copper content of the fractions comprising the peak Cu-1 was 150 nmol for the extract from non iron supplemented seedlings (figure 7.9a) and 140 nmol for the extract from iron supplemented seedlings (figure 7.9b). Once again the magnitude of the zinc peak in the iron supplemented extract is greater than that in the extract from seedlings grown without iron. The fractions comprising Zn-1 contain 33 nmol zinc in figure 7.9a and 100 nmol zinc in figure 7.9b. The metal containing fractions (62 and 63 from the non iron supplemented root extract and fractions 61 and 62 from the iron supplemented extract) were desalted on PD-10 columns and separated by gel filtration chromatography as described in section 2.4 and 7.2.3. The flow rate was 0.5 ml min^{-1} and fractions (3 ml) were collected and assayed for copper, zinc and protein, figures 7.9c and d. There is an indication of the zinc peak (Zn- α) and a copper peak (Cu- α) on the profile from the non iron supplemented sample but this is not as clear as

figure 7.8c. There is no indication of any copper or zinc ligands co-eluting with the main protein peak. There is no obvious interpretation of the copper and zinc profiles in figure 7.9d except that the sensitivity limit of the atomic absorption spectrophotometer had been reached.

The metal concentration of extracts from *P. sativum* seedlings grown without any added copper or zinc in the media are too low for reliable detection by atomic absorption spectrophotometry. The ion exchange data implies that, with low exogenous copper and zinc, an increase in the availability of exogenous iron decreases the amount of available copper in the cell but increases the amount of available zinc.

a. Ion exchange chromatography of non iron supplemented seedlings



b. Ion exchange chromatography of extract from iron supplemented seedlings

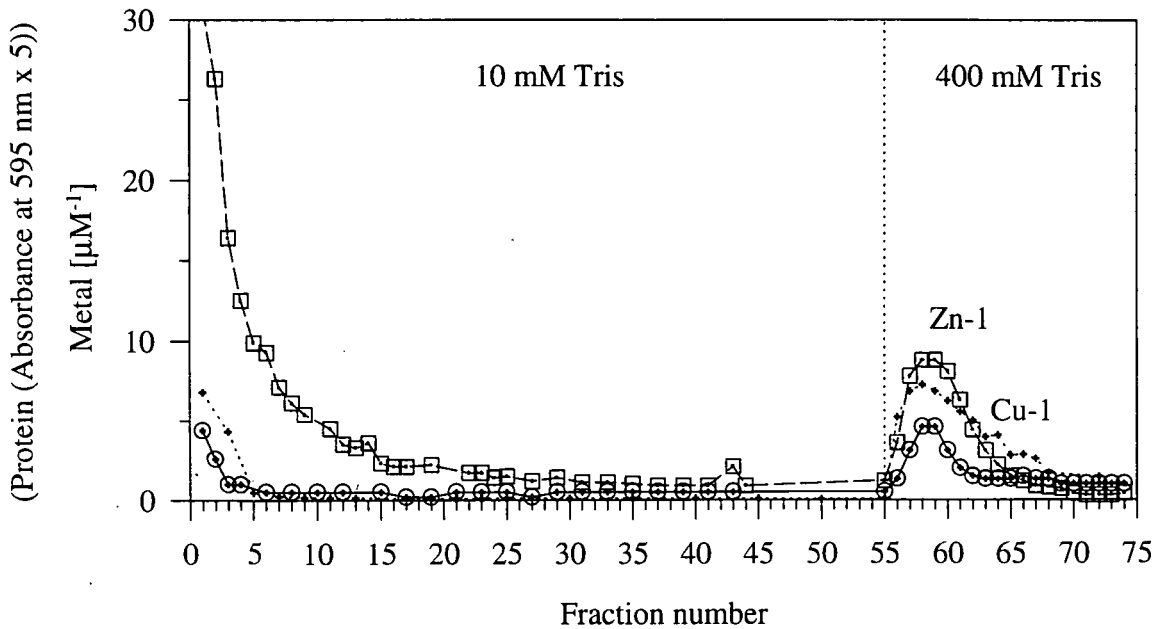
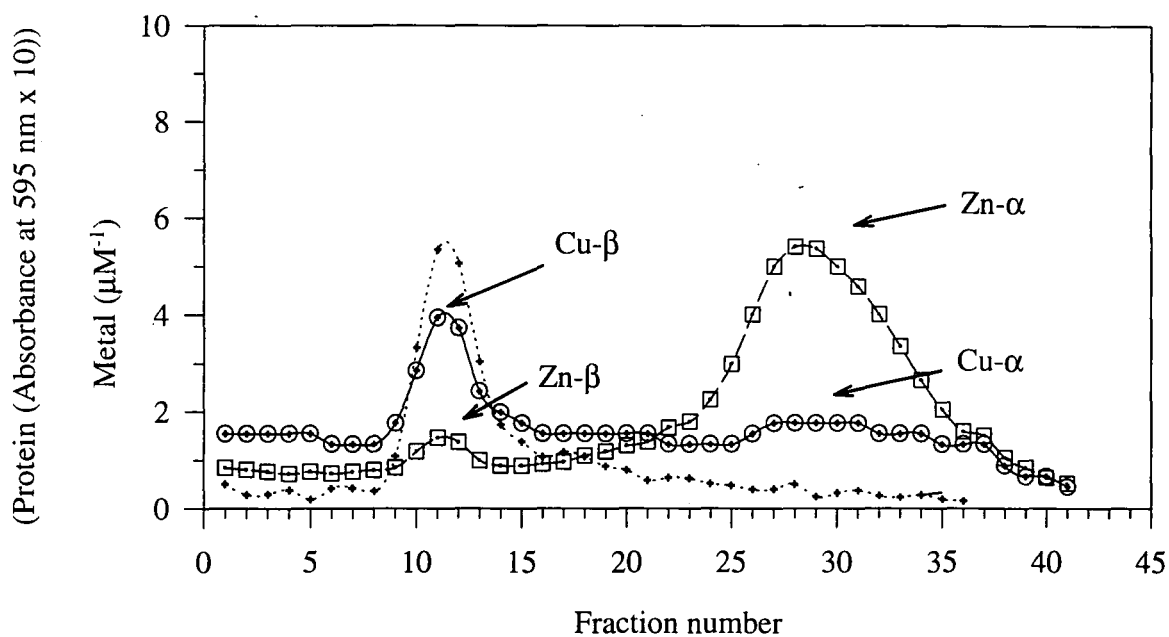


Figure 7.8 a., b. Chromatography profiles of crude soluble extract from the roots of *P. sativum* seedlings, not supplemented with copper and zinc, on DEAE anion exchange matrix. Assayed for copper (—, ○), zinc (- - -, □) and protein (· · ·, +).

c. Gel filtration chromatography of peak Zn-1 / Cu-1 from figure 7.8a



d. Gel filtration chromatography of peak Zn-1 / Cu-1 from figure 7.8b

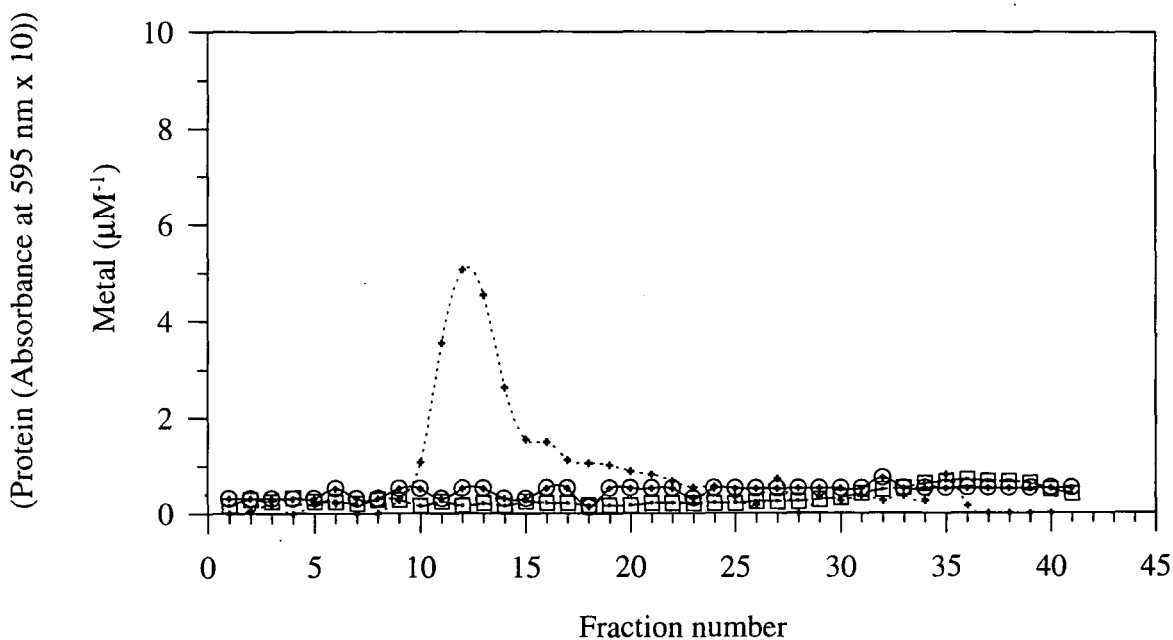
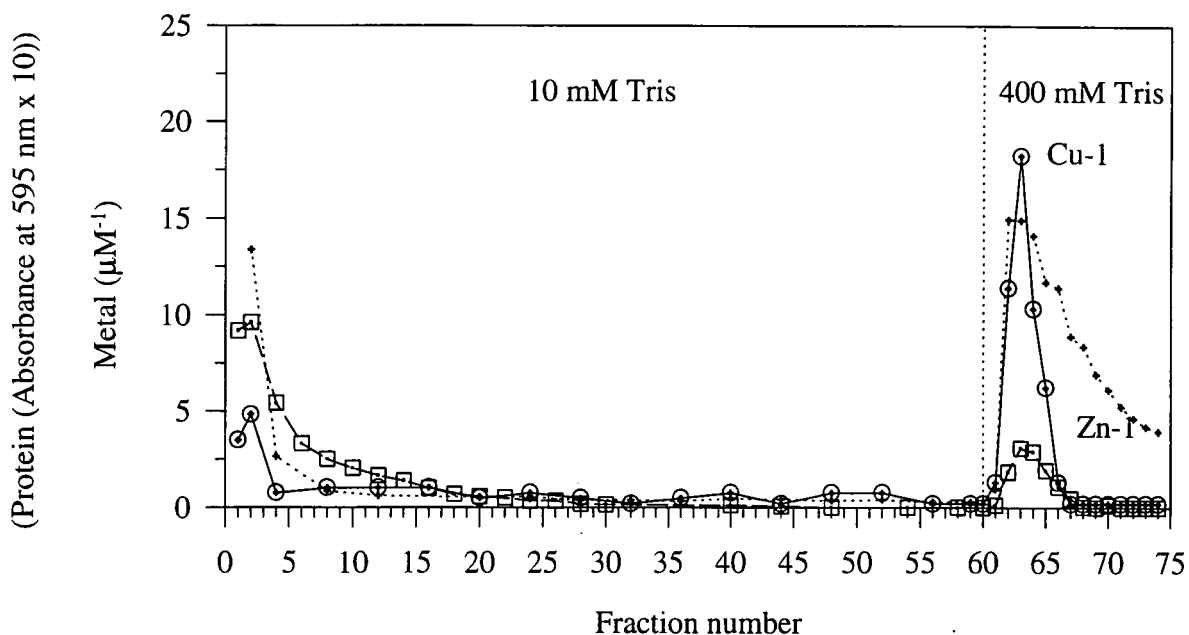


Figure 7.8 c., d. Gel filtration chromatography profiles of representative metal containing fractions from the ion exchange chromatography profile, figures 7.8a and 7.8b. Assayed for copper (—, \odot), zinc (- - -, \square) and protein (\cdots , +).

a. Ion exchange chromatography of extract from non iron supplemented seedlings



b. Ion exchange chromatography of extract from iron supplemented seedlings

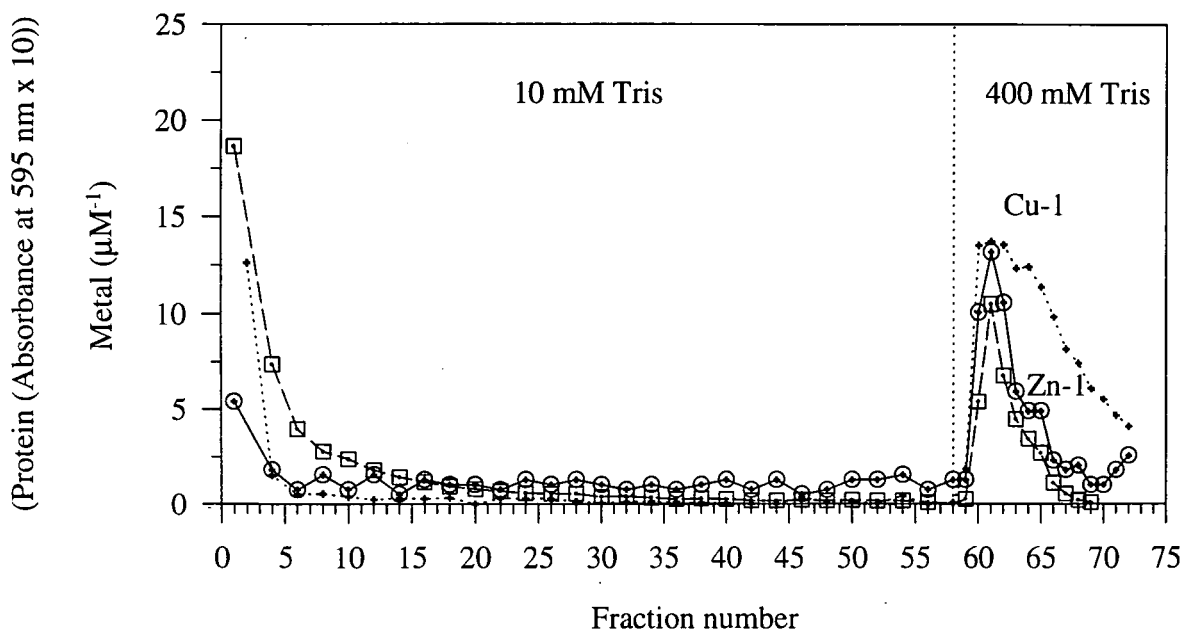
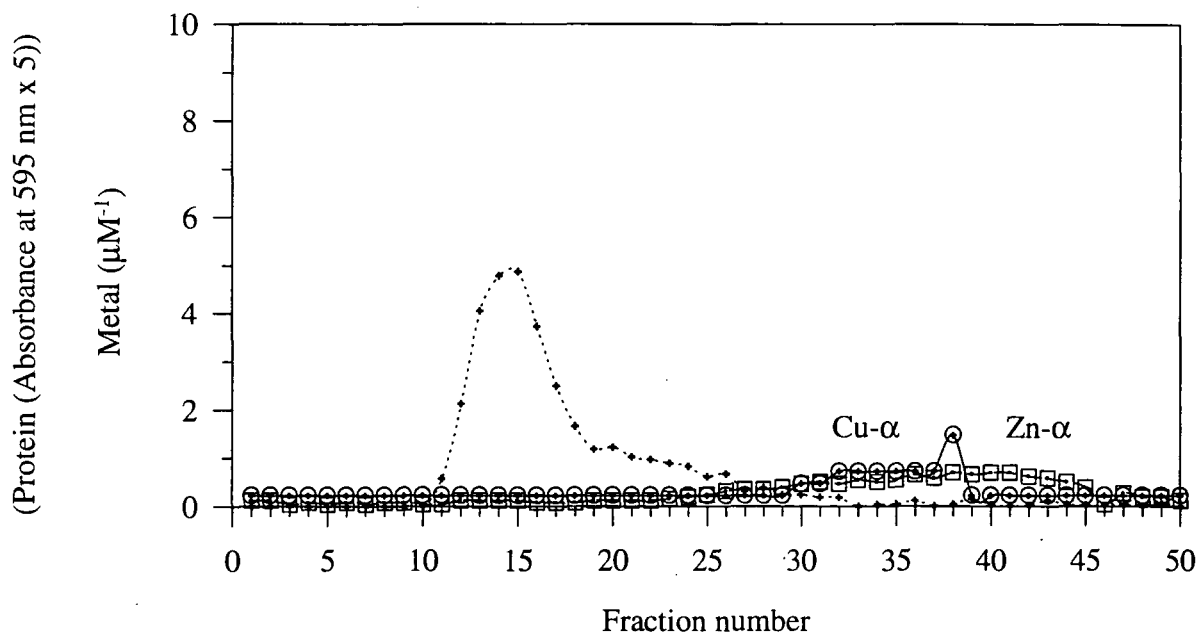


Figure 7.9 a., b. Chromatography profiles of crude soluble extract from the roots of *P. sativum* seedlings, not supplemented with copper and zinc, on DEAE anion exchange matrix. Assayed for copper (—, \odot), zinc (- - -, \square) and protein (\cdots , +).

c. Gel filtration chromatography of peak Zn-1 / Cu-1 figure 7.9a



d. Gel filtration chromatography of peak Zn-1 / Cu-1 figure 7.9b

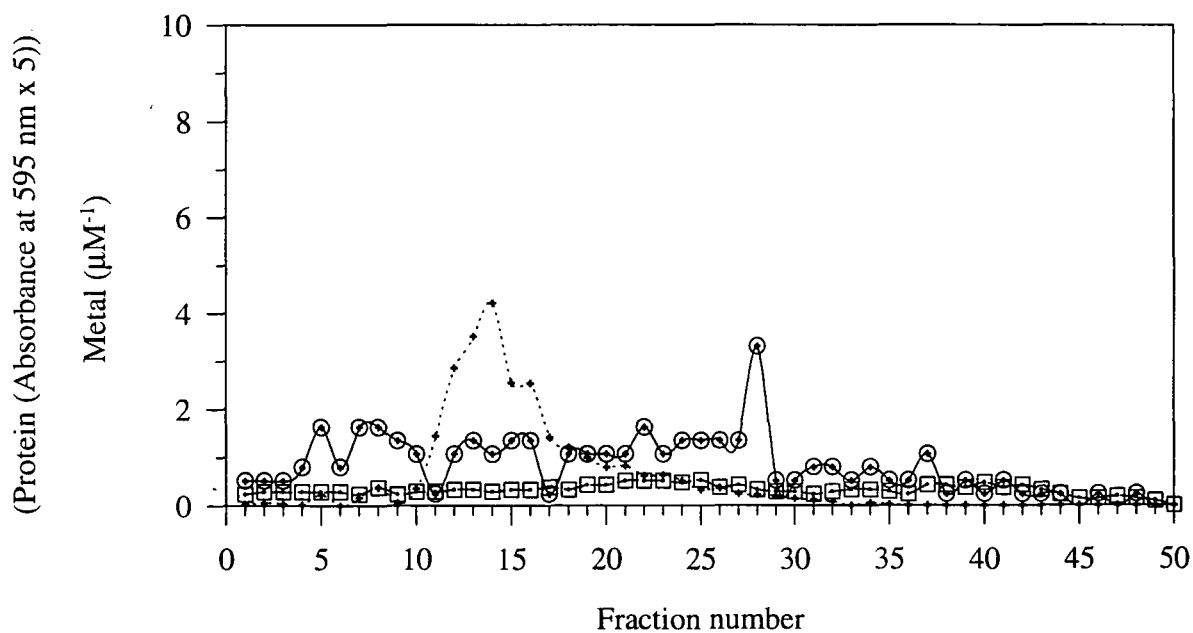


Figure 7.9 c., d. Gel filtration chromatography profiles of representative metal containing fractions from the ion exchange chromatography profile, figures 7.9a and 7.9b. Assayed for copper (—, ○), zinc (- - -, □) and protein (· · · , +).

7.3.8 Chromatographic properties of PsMT_A

A radiolabelled sample of the recombinant PsMT_A protein was prepared from *E. coli* and added to a crude root extract to determine the chromatographic properties of PsMT_A and hence if the ligand purification procedures were compatible with the recovery of the PsMT_A protein. A sample of recombinant PsMT_A was labelled with [³⁵S] cysteine and this was used to “spike” a crude root extract, as described in section 7.2.7. The seedlings were grown without the addition of copper, iron or zinc to the hydroponic media.

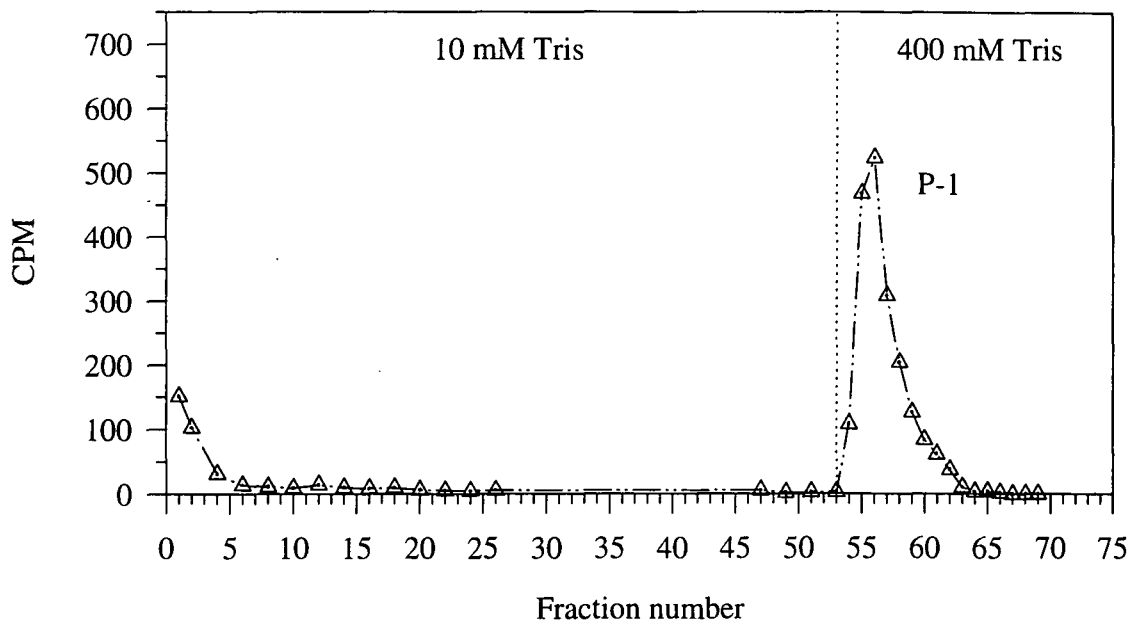
Sample	CPM
eluent 1	290.0
eluent 2	156.0
eluent 3	59.0

Table 7.2 Incorporation of [³⁵S] cysteine into PsMT_A protein. Measured in a 100 µl aliquot of eluents from glutathione affinity matrix following expression of GST-PsMT_A fusion protein in *E. coli* and cleavage by factor Xa (as described in section 7.2.7).

On the ion exchange profile, figure 7.10a the radiolabelled material eluted at a similar position on ion exchange chromatography to the main copper peak in the previous experiments (for example figure 7.4a). This suggests that PsMT_A produced *in planta* would have been recovered on the DEAE ion exchange matrix. The total counts per minute (CPM) for all the fractions eluted in the 400 mM Tris-HCl is 11600. Accepting that the different buffers may affect the accuracy of any direct comparison this figure (or other factors that could effect quenching) suggests that around 80 to 90 % of the labelled material was recovered following ion exchange chromatography.

Fractions 55 and 56 were pooled, desalted on a PD-10 column and subjected to gel filtration chromatography as described in section 2.3.11.2. The flow rate was 0.5 ml min⁻¹ and fractions (3 ml) were collected and assayed for copper, zinc and protein and aliquots of 500 µl were assayed for radiolabel, figure 7.10b.

a. Ion exchange chromatography of extract 'spiked' with labelled PsMT_A



b. Gel filtration chromatography of peak P-1 figure 7.10a

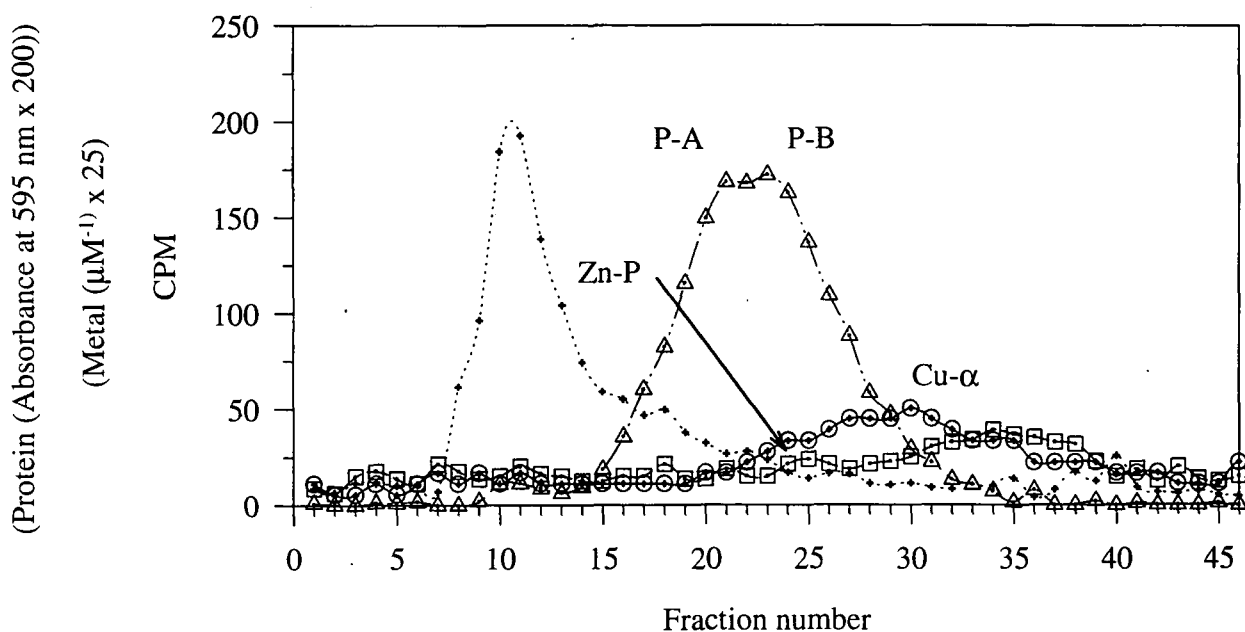


Figure 7.10 a. Chromatography profiles of crude soluble extract from the roots of *P. sativum* seedlings, not supplemented with copper and zinc, spiked with labelled PsMT_A on DEAE anion exchange matrix. Assayed for radioactivity (· · -, Δ)

b. Gel filtration chromatography profile of representative labelled fractions from figure 7.10. Assayed for copper (—, ○), zinc (- - -, □), (· · ·, +) and radioactivity (· · -, Δ).

The radiolabel was resolved into two major peaks of similar molecular weight (figure 7.10b P1 and P2). These peaks correspond to PsMT_A and confirm the validity of the method for recovering metallothionein-like protein from root extracts. A very small amount of radiolabel has co-eluted with the bulk protein. Potentially some of the PsMT_A may have associated with a larger protein. The major radiolabelled peaks are on the shoulder of the large copper peak (Cu- α) which dominates the profile. However this leading edge of Cu- α has two shoulders the peak of each is one fraction above the putative PsMT_A peaks. Copper associated with PsMT_A may contribute to these peaks. Coincident with the copper shoulder and the edge of the radiolabel peak is a small zinc peak (Zn-P). In relation to the gel chromatograms of extracts from root extracts grown in the presence of exogenous copper and zinc, the PsMT_A has eluted in a similar position to the observed copper species, for example Cu-A in figure 7.3c.

7.3.9 Polyacrylamide gel electrophoresis of root extracts from *P. sativum*

Gel electrophoresis of copper and zinc species identified by gel filtration chromatography did not yield any bands, either with conventional Coomassie staining or with silver staining (data not presented). This can be attributed to the very low concentration of the ligands after the second purification step. In order to investigate differences in protein expression in plants, grown with and without the addition of iron to the exogenous media, seedlings were radiolabelled with [³⁵S]. Early attempts to run conventional and radiolabelled protein gels with root extracts prepared by grinding roots in an extraction buffer (buffer described in section 2.3.6) produced gels with badly smeared and poorly resolved protein bands (not shown). Subsequently a phenol extraction method was adopted, described in section 2.3.10.2 and section 7.2.8.

7.3.9.1 One dimensional polyacrylamide gel electrophoresis of *P. sativum* root extracts labelled with [³⁵S] cysteine

Pea seedlings and crude protein extracts were prepared as described in section 7.2.8. The incorporation of radiolabel into the iron supplemented and non supplemented sample was as described in table 7.3.

Sample	CPM
+ iron	86000
- iron	99500

Table 7.3 Incorporation of [³⁵S] cysteine into non iron supplemented and iron supplemented root extract. Measured in a 5 µl aliquot of crude protein extract from roots of *P. sativum* spotted onto cellulose acetate (as described in section 7.2.8).

The two sets of samples (aliquots equivalent to approximately 200 000 counts of each sample) were loaded onto a 15 % (w/v) acrylamide gel, and electrophoresis was performed as described in section 2.3.6.2. A duplicate set of samples was carboxymethylated to derivatise cysteine residues (as described in section 7.2.8.1). The Coomassie blue stained membrane and autoradiograph are presented in figure 7.11.

There are no obvious differences between the tracks in the Coomassie blue stained membrane, figure 7.11A. In the autoradiograph, figure 7.11B, there are major cysteine rich protein bands of apparent molecular weights 70000, 50000, 34000, 21000 and 17000. These bands are not equivalent to the major Coomassie blue stained bands. The most notable feature of the autoradiograph is a band represented strongly only in the non iron supplemented extract, this is highlighted with an arrow, figure 7.11B. The intensity of the band relative to other proteins was increased by carboxymethylation. The band is not visible in the conventionally stained gel indicating that it is produced from a protein with a high proportion of cysteine.

R_f values were calculated for the two sets of molecular weight markers on the gel and a calibration curve plotted, figure 7.12. The R_f value for the differentially expressed protein is 0.65 giving an apparent molecular weight of approximately 11 500, although the 95 % confidence intervals plotted on the graph suggest that there may be a potential error of 1000 in that calculation (10 500 to 12 500). In rod gels at pH 6.9 the cadmium binding peptide from *L. esculentum* (cadmium phytochelatin) migrated with an R_f of 0.7 to 0.8 following electrophoresis (Bartolf and Rauser 1986). Furthermore, metallothioneins from other sources are noted for giving spurious molecular weights on acrylamide gels. On 20 % SDS gels produced during the purification of PsMT_A from *E. coli* three bands of apparent molecular weight 4500, 14000 and 17000 were attributed to PsMT_A (Kille *et al.* 1991). The

band of 11500 on the gel which has differential intensity in the two metal treatments could potentially be the metallothionein-like protein. Northern analysis was used to confirm that the *PsMT_A* gene is differentially expressed in the two extracts total RNA was extracted from roots grown in the same pots as those labelled with [³⁵S] cysteine (method as described in sections 2.5.10 and 2.5.11. The gel photograph and northern blot are presented in figure 7.13A and B. The *PsMT_A* gene is expressed more highly in the non iron supplemented roots in which there is a low molecular weight cysteine rich protein.

7.3.9.2 One dimensional polyacrylamide electrophoresis of *P. sativum* root extracts labelled with [³⁵S] methionine

Differential protein expression in *P. sativum* roots, grown in media supplemented and non supplemented with iron, was further investigated by repeating the *in planta* labelling experiment as described in section 7.2.8 but using [³⁵S] methionine instead of cysteine. The incorporation of [³⁵S] methionine was measured as estimated as described in section 7.2.8.

Sample	CPM
+ iron	15300
- iron	10000

Table 7.4 Incorporation of [³⁵S] methionine into non iron supplemented and iron supplemented root extract. Measured in a 5 µl aliquot of crude protein extract from roots of *P. sativum* spotted onto cellulose acetate (as described in section 7.2.8).

Aliquots equivalent to approximately 60 000 counts were loaded onto a 15 % tricine gel following carboxymethylation. The protein was transferred to PVDF membrane, stained with Coomassie, air dried and photographic film exposed, figure 7.14A and B.

Figure 7.11 One dimensional polyacrylamide gel electrophoresis of a crude root extract

A - PVDF membrane stained with Coomassie.

M - molecular weight markers.

1 - +Fe protein extract, conventional sample buffer.

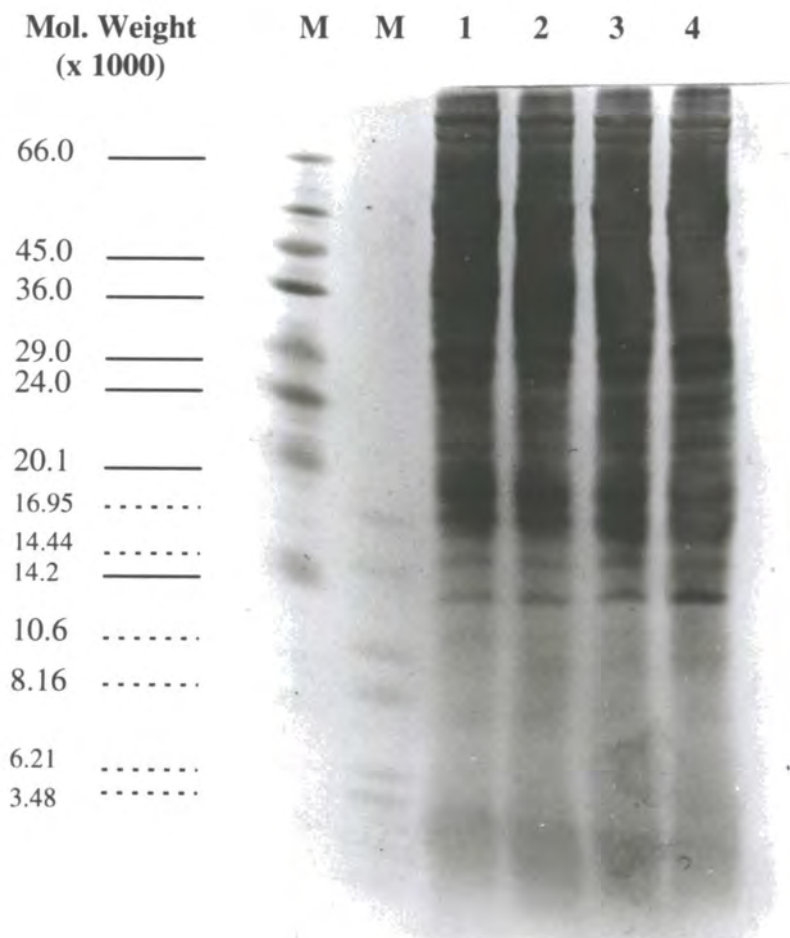
2 - - Fe protein extract, conventional sample buffer.

3 - +Fe protein extract, carboxymethylated.

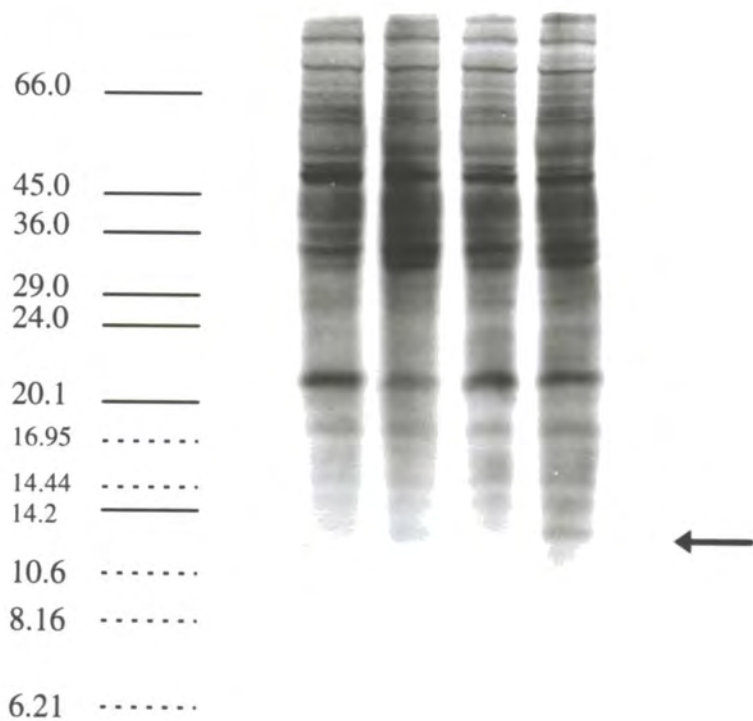
4 - - Fe protein extract, carboxymethylated.

B - Autorad developed to display [³⁵S] cysteine labelled protein. The putative metallothionein-like protein is indicated with an arrow.

A



B



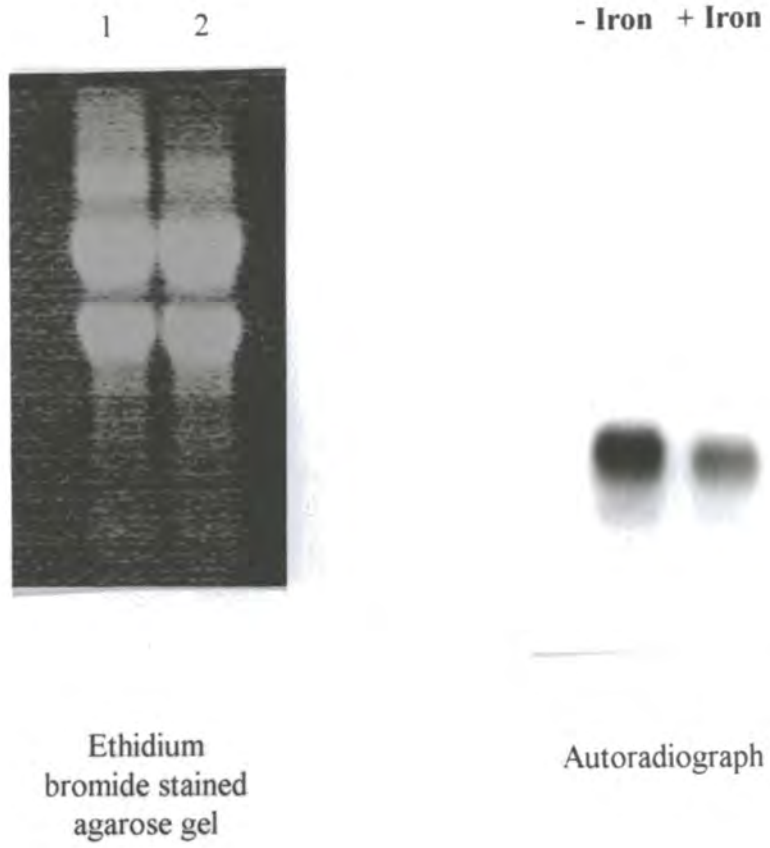


Figure 7.13 Photograph of agarose gel stained with ethidium bromide and autoradiograph of RNA extracted from root material treated identically to the material labelled with [35 S] cysteine, probed with *PsMT_A* DNA.

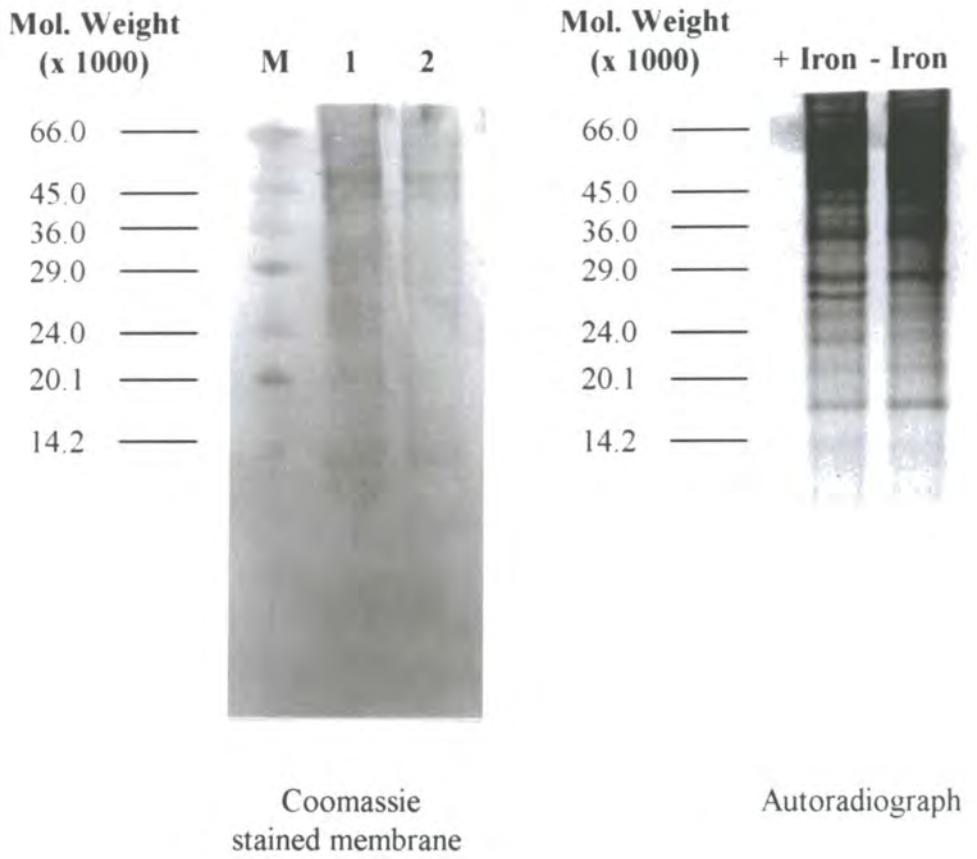


Figure 7.14 Polyacrylamide gel electrophoresis of [^{35}S] methionine labelled root extract from seedlings grown with and without iron supplement

The poor resolution of bands in the Coomassie blue stained gel is improved in the autoradiograph. As would be predicted from the distribution of methionine amongst proteins the higher molecular weight proteins are more intensely labelled, although there are several major bands below 30 000. The most notable feature is an approximately 28 000 molecular weight band which is much more intense in the iron supplemented root extract compared to the non iron supplemented extract. There are some other bands which may be slightly stronger in the non iron supplemented extract. For example, the major band at approximately 18 000. If the relative protein loadings, as represented on the Coomassie blue stained membrane, are taken into account then this band must be better represented in the non iron supplemented extract. The band does not appear to be particularly strong in the Coomassie blue stained membrane and must therefore correspond to a methionine rich protein.

7.3.9.3 Two dimensional polyacrylamide gel electrophoresis of [³⁵S] cysteine labelled protein

Root extracts were prepared as in section 7.2.8 except that the final pellet was resuspended in isoelectrofocusing sample buffer (9M urea, 5 % 2-ME, 2 % pharmalyte (ampholine mixture), 2 % nonidet P-40). The incorporation of [³⁵S] cysteine in the sample was estimated and is presented in table 7.5.

Sample	CPM
+ iron	110000
- iron	63000

Table 7.5 Incorporation of [³⁵S] cysteine into non iron supplemented and iron supplemented root extract. Measured in a 5 µl aliquot of crude protein extract from roots of *P. sativum* spotted onto cellulose acetate (as described in section 7.2.8).

Aliquots equivalent to approximately 1 000 000 counts (approx. 100 µl) were loaded onto 5 % (w/v) acrylamide rod gels and two-dimensional electrophoresis was performed as described in section 2.3.7. Protein was transferred to PVDF membrane by electroblotting (as described in section 2.3.8), stained with Coomassie blue, air dried and photographic film exposed figures 7.15a, b, c and d.

Comparing the Coomassie blue stained gels, the loading on the iron supplemented gel is slightly greater than the non iron supplemented gel. However, the variations are small and on the [³⁵S] labelled autoradiographs a very similar pattern of spots are observed. The reason for the vertical banding pattern on the autoradiograph of the iron supplemented gel is not known. Many minor differences can be seen but most are probably attributable to differences in resolution. It was difficult to assign the molecular weight markers for these gels as the markers were next to the acid end of the first phase rod gel and this resulted considerable distortion of the bands. The major difference between the iron supplemented and non iron supplemented extracts is a very low molecular weight doublet of spots in the pH 4.3 section at an apparent molecular weight below 20 000 in the non iron supplemented autoradiograph (figure 7.15c). This doublet has migrated to a pH which is consistent with the predicted properties of the putative metallothionein-like protein (table 3.1). It should be noted that phytochelatin also migrate to less than pH 5.0 on isoelectric focusing gels (Wagner 1984, Reese and Wagner 1987a). Although the extracts, in both the one-dimensional (section 7.3.9.1) and the two-dimensional gels, were from *P. sativum* seedlings grown in conditions which were likely to minimise the production of phytochelatin, the possibility that these bands could be phytochelatin cannot be precluded. There is a spot on the iron supplemented gel at a similar molecular weight but in the pH 7.8 section which is much reduced in the radiograph of the non iron supplemented extract.

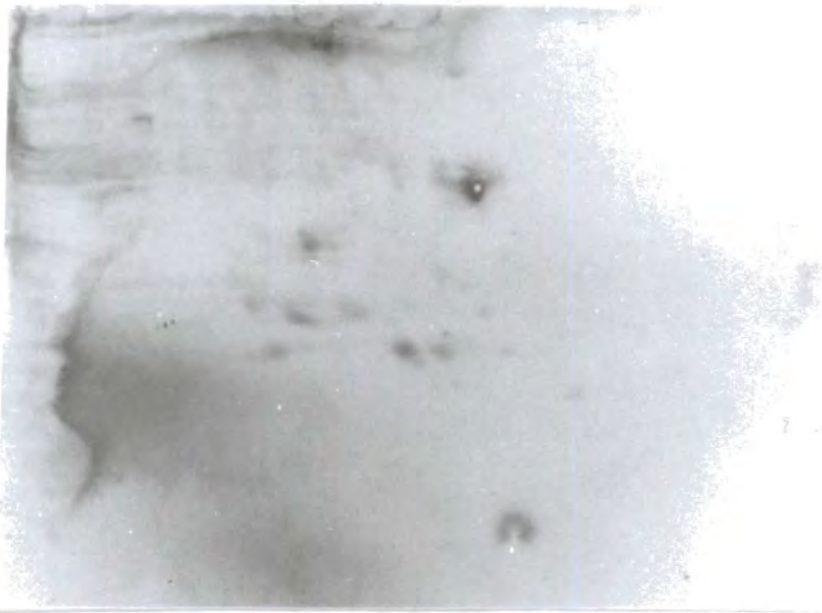
Figures 7.16a, b, c and d are replicates of the above experiment. The resolution on these gels is not as clear as figure 7.15 making comparison difficult. The resolution of the non iron supplemented extract is better than the iron supplemented extract. The pattern of spots is very similar to the previous autoradiographs. The doublet of spots in the low pH section of the autoradiograph described for figure 7.15c may be present but very much less intense. The feature is absent on the iron supplemented extract but the very poor resolution of this extract makes comparison of this autoradiograph with the others difficult.

Figure 7.15 a. Two dimensional PAGE of crude root extract from seedlings grown without the addition of iron to the hydroponic media.

b. Two dimensional PAGE of crude root extract from seedlings grown with the addition of iron to the hydroponic media.

Membranes are stained with Coomassie blue. The positions of molecular weights and gel pH values are approximate only due to the difficult in resolving the markers on these gels. The were diffuse and severe 'smiling' towards the acid side of the rod gel increased the ambiguity of the assignments.

pH	7.7	7.6	7.5	7.1	6.3	5.5	4.8	4.5	4.0	Mol. Weight (x 1000)
----	-----	-----	-----	-----	-----	-----	-----	-----	-----	-------------------------



—	66.0
—	45.0
—	36.0
—	29.0
—	24.0
—	20.1
—	14.2

a. Extract from non iron supplemented seedlings

pH	7.7	7.6	7.5	7.1	6.3	5.5	4.8	4.5	4.0	Mol. Weight (x 1000)
----	-----	-----	-----	-----	-----	-----	-----	-----	-----	-------------------------

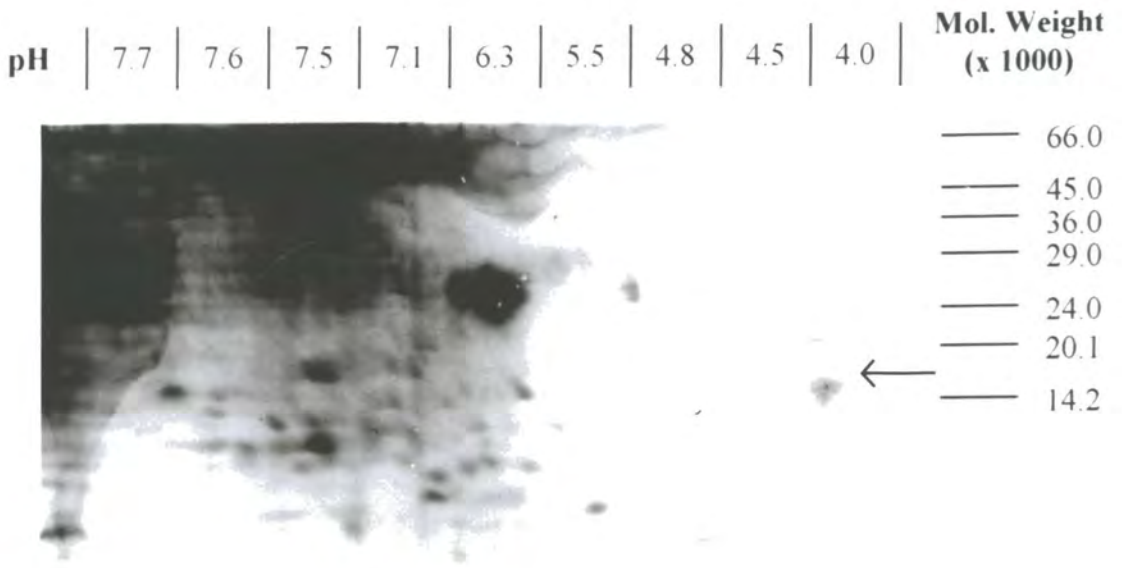


—	66.0
—	45.0
—	36.0
—	29.0
—	24.0
—	20.1
—	14.2

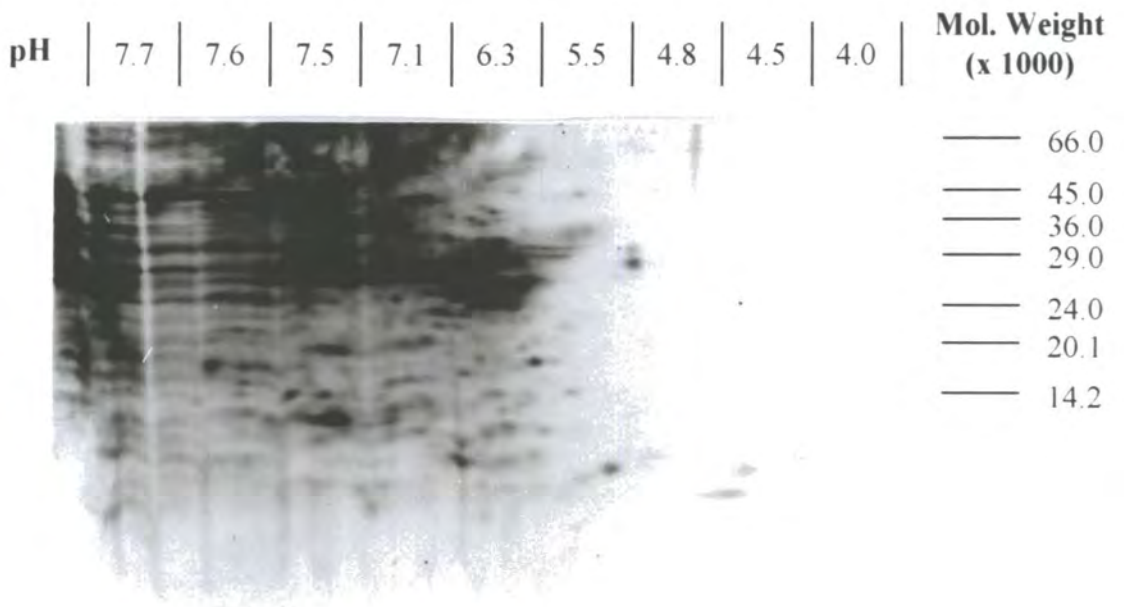
b. Extract from iron supplemented seedlings

Figure 7.15 c. Two dimensional PAGE of crude root extract from seedlings grown without the addition of iron to the hydroponic media. [³⁵S] cysteine label.

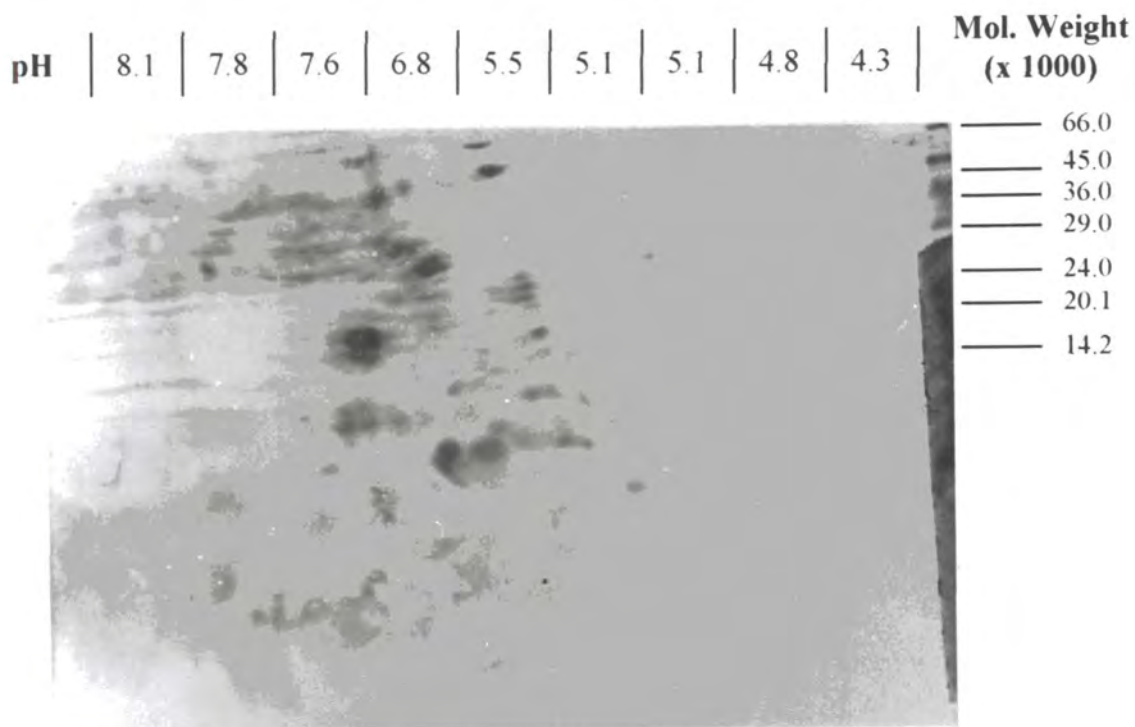
d. Two dimensional PAGE of crude root extract from seedlings grown with the addition of iron to the hydroponic media. [³⁵S] cysteine label.



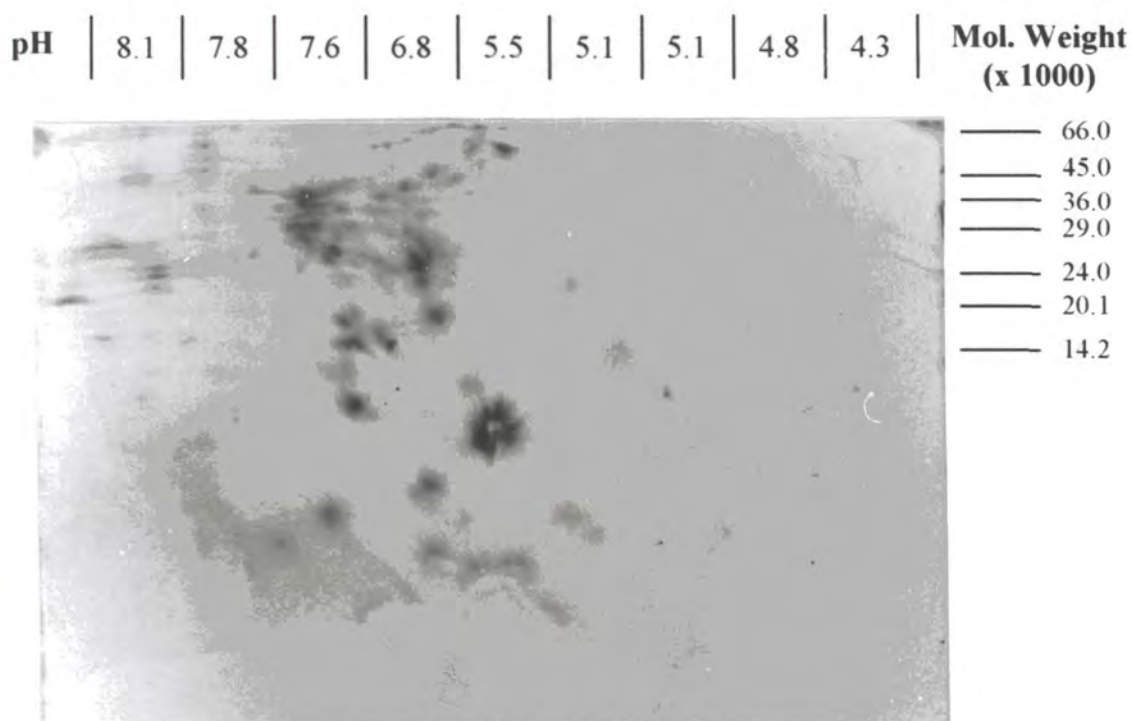
c. Extract from non iron supplemented seedlings



d. Extract from iron supplemented seedlings



a. Extract from non iron supplemented seedlings



b. Extract from iron supplemented seedlings

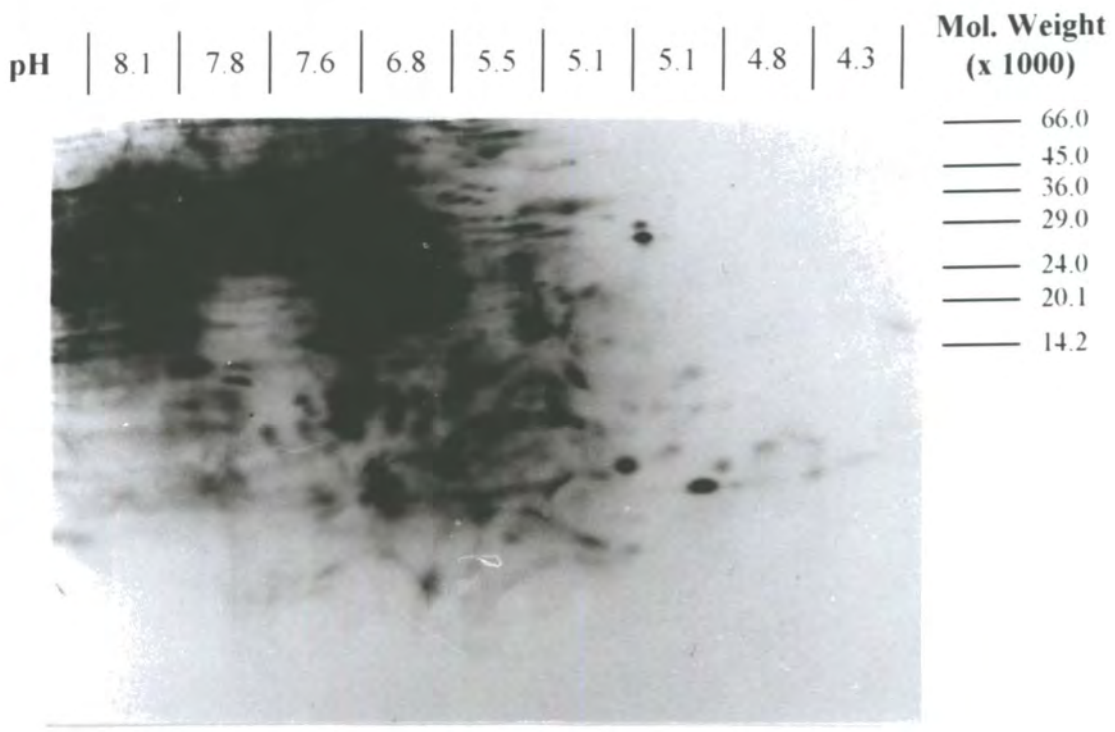
Figure 7.16 a. Two dimensional PAGE of crude root extract from seedlings grown without the addition of iron to the hydroponic media.

b. Two dimensional PAGE of crude root extract from seedlings grown with the addition of iron to the hydroponic media.

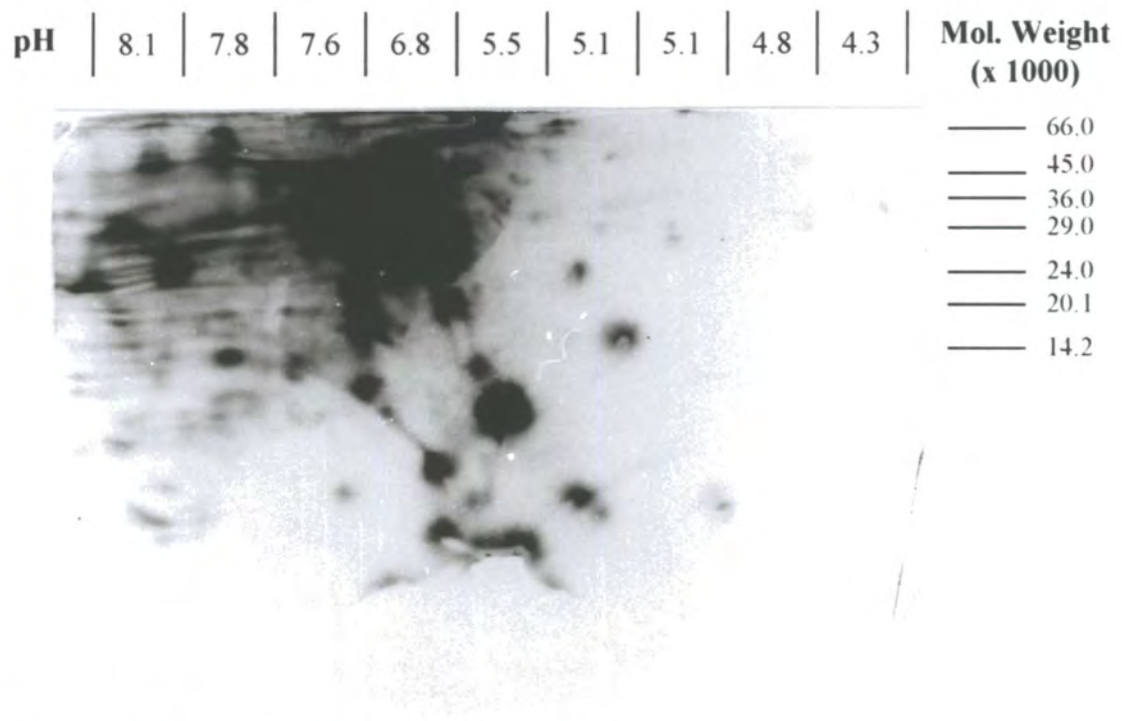
Membranes are stained with Coomassie blue. The ambiguity in the assignment of molecular weights and pH applies as in figure 7.15.

Figure 7.16c Two dimensional PAGE of crude root extract from seedlings grown without the addition of iron to the hydroponic media. [³⁵S] cysteine label.

d. Two dimensional PAGE of crude root extract from seedlings grown without the addition of iron to the hydroponic media. [³⁵S] cysteine label.



c. Extract from non iron supplemented seedlings



d. Extract from iron supplemented seedlings

7.4 Conclusions

In extracts from roots of *P. sativum* seedlings grown in hydroponic media copper and zinc containing cellular components could be isolated from the bulk extract by ion exchange chromatography (sections 7.3.1 to 7.3.4). These components were eluted from the ion exchange matrix by washing with 300 mM or 400 mM Tris-HCl (peaks Cu-1 and Zn-1 on ion exchange profiles). A low molecular weight zinc component (Zn-A) and a copper component of slightly higher apparent molecular weight (Cu-A) were reproducibly identified on gel filtration chromatography profiles of the fractions containing these components (sections 7.3.2 to 7.3.4). A second copper component (Cu-B) was observed in some extracts with very similar chromatographic properties to the zinc component (Zn-A) (figures 7.3c and 7.5e). The elution characteristics of the components Cu-A, Cu-B and Zn-A following chromatography on G-50 Sephadex are similar to those reported for copper and cadmium phytochelatin on the same matrix (for example Salt *et al.* 1989 and Howden *et al.* 1995a respectively). In the ion exchange profiles presented in figure 7.5a and b the peaks Cu-1 and Zn-1 were resolved into different peaks and a component Cu-2 was identified. In subsequent gel chromatography profiles (figures 7.5c and e) there was some evidence that Cu-A may be the major component of Cu-1 and that Cu-B may be the major component of Cu-2. If this is the case then it the components Cu-A, Cu-B and Zn-A may have different charge characteristics. The components Cu-A, Cu-B and Zn-A were not further characterised.

Expression of the metallothionein-like gene *PsMT_A* was expected to be higher in seedlings grown in media not supplemented with iron and by inference levels of the putative translational product of the gene was expected to be higher in extracts of these seedlings (Robinson *et al.* 1993). A summary of the estimated copper and zinc content of peaks obtained on chromatograms following ion exchange chromatography is presented in table 7.2. The ratio of zinc to copper is presented for each extract. The ratio of metals observed in equivalent peaks obtained from pairs of extracts from iron supplemented and non supplemented seedlings is also presented.

In experiments, labelled 1, 2 and 3 in table 7.5, the ratio of zinc to copper contained in the fractions comprising the peaks observed in the ion exchange chromatography profiles is consistently higher in the extracts from seedlings grown in media not supplemented with iron. The effect of growing seedlings in media not supplemented with iron was to increase the amount of zinc ligand relative to copper ligand which can be isolated from soluble root

extracts by ion exchange chromatography. In all three experiments the ratio of zinc in plus iron to zinc in minus iron conditions is less than 0.5 indicating the accumulation of the zinc ligand(s) comprising this peak. The copper species did not consistently increase or decrease in response to the availability of iron in the growth media.

Experiment		Iron supplemented			Non iron supplemented			Zinc ratio (+Fe : -Fe)	Copper ratio (+Fe : -Fe)
		Zn peak (nmol)	Cu peak (nmol)	ratio Zn:Cu	Zn peak (nmol)	Cu peak (nmol)	ratio Zn:Cu		
1	figure 7.3	80	360	0.2	2000	750	2.7	0.04	0.5
2	figure 7.4	240	2700	0.1	790	2500	0.3	0.3	1.1
3	figure 7.5	100	990	0.1	205	990	0.2	0.5	1.0
a	figure 7.8	160	65	3	60	190	0.3	2.7	0.3
b	figure 7.9	100	140	0.7	33	140	0.2	3.0	1.0

Table 7.6 Summary of estimated metal contents of fractions corresponding to chromatogram peaks following ion exchange chromatography of root extracts from seedlings of *P. sativum*. In experiments 1, 2 and 3 the growth media was supplemented with copper and zinc. In experiments a and b the growth media was not supplemented with zinc.

In experiments, labelled a and b in table 7.6, in which no copper or zinc was added to the growth media, the ratio of zinc to copper contained in the fractions comprising the metal peaks is lower in the extracts from seedlings not supplemented with iron. It was not established if the copper and zinc components identified in experiments a and b were synonymous with the copper and zinc components observed in experiments 1, 2 and 3. It should be noted that the amount of zinc recovered following ion exchange chromatography of extracts in experiments a and b was less than in experiments 1, 2 and 3 and may effect the significance of this data. The ratio of zinc in extracts from iron supplemented compared to non iron supplemented seedlings in experiments a and b is 3, indicating that growth of seedlings in media not supplemented with iron leads to a decrease in the accumulation of zinc associated with these ligand(s) under these conditions. This is the reverse of the situation

observed when seedlings are grown in media supplemented with copper and zinc. There was again no consistent change in the copper ligands due to the growth conditions.

It was demonstrated that the recombinant PsMT_A protein could be recovered from a root extract using the ion exchange and gel chromatography purification techniques used to identify copper and zinc ligands (figure 7.10). Providing the recombinant PsMT_A protein from *E. coli* retains similar properties to the native protein in the roots of *P. sativum* (and the native protein is found in the soluble extract), then the chromatographic techniques used should isolate the putative metallothionein-like protein. Although the zinc component Zn-1, identified following ion exchange chromatography, was reduced in extracts from seedlings grown in conditions known to reduce expression of *PsMT_A* it could not be positively attributed to PsMT_A. The PsMT_A protein may not represent a particularly abundant zinc or copper pool in extracts of *P. sativum* root tissue and therefore may require more sensitive assay techniques to identify it following gel filtration chromatography.

Copper and zinc components (Cu-1 and Zn-1) were isolated from an extract from leaves of *P. sativum* seedlings grown in hydroponic media supplemented with copper and zinc, but not iron, by ion exchange chromatography (figure 6.6a). The ion exchange profile suggests that Cu-1 and Zn-1 have different charge characteristics. In subsequent gel filtration chromatography of the fractions comprising Cu-1 and Zn-1, two copper components Cu-A and Cu-B were identified and a single zinc component Zn-A (figures 6.b and c). The position of Cu-A and Zn-A on the profile is similar to the position of Cu-A and Zn-A on profiles obtained from root extracts. In the leaf extract Cu-B has an apparent molecular weight which is slightly lower than Zn-A. Transcripts of the metallothionein-like gene *PsMT_A* do not accumulate at high levels in the leaves of *P. sativum* seedlings (Robinson *et al.* 1992). It is therefore unlikely that copper or zinc complexes identified in leaves of *P. sativum* seedlings would be the translational product of that gene. However, similar genes analogous to the type-2 genes identified in other species (for example *A. thaliana*, Zhou and Goldsbrough (1994)) may be found in *P. sativum*. It is possible that ligands identified in leaves could represent the product of such a gene.

In a one dimensional polyacrylamide gel a [³⁵S] labelled band, with a molecular weight of approximately 11 500, was identified in a [³⁵S] cysteine labelled root extract (figure 7.11). The band was only visible in the root extract from seedlings grown in hydroponic media not supplemented with iron. Expression of the *PsMT_A* gene in the same batch of seedlings was

demonstrated by northern analysis to be higher in the non iron supplemented seedlings (figure 7.13). The recombinant PsMT_A protein has been reported to migrate with a higher apparent molecular weight than it's true weight on polyacrylamide gels (Kille *et al.* 1991). It is possible that the band of molecular weight 11 500 in the tracks containing the non iron supplemented extract in figure 7.11 could be the translational product of the *PsMT_A* gene.

A doublet of [³⁵S] labelled spots was identified in the low pH region following two-dimensional polyacrylamide gel electrophoresis of an extract from roots of seedlings grown in the same conditions as in figure 7.11 (figure 7.15c). From the predicted primary structure of the predicted PsMT_A protein an isoelectric point of 4.3 is estimated and therefore the PsMT_A protein would be expected to migrate to a low pH following isoelectric focusing. However, as the band in figure 7.11 and the spots in figure 7.15c have not been identified by sequencing other possible assignments for these bands must be considered. In the context of a discussion of copper ligands in plant roots phytochelatin may be considered. Phytochelatins have been reported to migrate to the low pH region of isoelectric focusing gels (Reese and Wagner 1987a). However, in the results reported here the extracts were from seedlings grown in media which were not supplemented with copper and therefore were not likely to synthesise large quantities of phytochelatin. Differential production of phytochelatin has not been reported in response to exogenous iron concentrations.

A highly [³⁵S] labelled band, with a molecular weight of approximately 28 000, was also identified which was much more intense following electrophoresis of non iron supplemented root extracts labelled with [³⁵S] methionine (figure 7.14). The band was not positively identified but it may be a protein involved in iron or copper metabolism.

CHAPTER 8

GENERAL DISCUSSION

Sequence analysis (section 3.3.2) of the predicted primary structures of the plant metallothionein-like genes lead to the proposal of different structural categories. The significance of sequence conservation within the cysteine rich domains of the different categories and of the predicted secondary structure motif (β -strand) within the region linking the cysteine rich domains (section 3.3.7) will be discussed in section 8.1.

The translational product of the *PsMT_A* protein was produced in *E. coli* as a GST fusion protein (section 4.3.1). Specific degradation products were observed following the electrophoresis of the purified protein on polyacrylamide gels (section 4.3.1).

Characterisation of an antiserum raised to the fusion protein established that the epitope of the fusion protein was within the GST moiety (section 4.3.4). The type-2 metallothionein-like gene from *A. thaliana* was amplified from a leaf cDNA library (section 5.3.1) and cloned into pGEX3X (section 5.3.2) to allow expression of the putative protein in *E. coli* as a GST fusion protein (section 5.3.4). Comparison of proton dissociation curves with respect to zinc indicated that the type-2 gene product may have a slightly higher affinity for zinc than the type-1 gene product (section 5.3.6). In addition to the *in vitro* studies the *AtMT-t2* gene was expressed in *Synechococcus* where it partially restored zinc tolerance to a zinc metallothionein deficient mutant (section 5.3.7). The implications of these observations for the function of these proteins which will be discussed in section 8.2.

A complex pattern of expression of *PsMT_A* was observed in roots of *PsMT_A* in response to different concentrations of copper, iron and zinc (chapter 6) and the implications of this will be discussed in section 8.3. A zinc complex isolated from the roots of *P. sativum* by ion exchange chromatography responded to changes in the concentration of iron in the growth media (section 7.4). The implications of this observation and other aspects of the extraction of copper and zinc ligands from *P. sativum* will be discussed in section 8.4. A cysteine rich protein band has been identified on acrylamide gels following electrophoresis, with the same characteristics as those predicted for the *PsMT_A* protein (section 7.3.10.1). The possibility that this band could represent the *PsMT_A* protein will be discussed in section 8.5.

Concluding remarks are given in section 8.6, and prospects for future work in this field will be briefly discussed in section 8.7.

8.1 Plant metallothionein-like genes

Metallothionein-like cDNA's have been isolated from different plants because of their differential expression in response to a range of factors, table 4.1. These factors include, different developmental stages, tissue specificity, aluminium tolerance, copper sensitivity, iron deficiency and ethylene regulation. A range of factors are known to influence the expression of metallothionein genes in mammalian systems (reviewed Hamer 1986). It is not known whether the metallothionein-like higher plant genes respond directly to each of these different stimuli or to changes in some other factor(s) which are themselves effected by the stimuli.

For example, the type-3 gene from *A. thaliana* was isolated because it was induced by ethylene (Zhou and Goldsbrough 1994). The type-3 gene from *B. napus* was isolated because of its expression during leaf senescence (Buchanan-Wollaston 1994). Expression of the type-2 gene from *A. deleciosa* reaches a maximum during fruit development (Ledger and Gardner 1994). The *ids1* gene from *H. vulgare* was isolated because it was expressed as part of an iron deficiency response (Okumura *et al.* 1991). The phytohormone ethylene is involved in both leaf senescence and fruit development (though specifically the ripening response) where it induces the synthesis of cell wall degrading enzymes. In cucumber roots there is evidence to suggest that the iron deficiency response, including ferric reductase activity, is mediated by ethylene (Romera and Alcántara 1994). It may therefore be formally possible that plant metallothionein-like genes are regulated by plant hormones such as ethylene. Regulation of mammalian metallothionein by hormones has been reported (Hamer 1986).

However, during fruit development in *A. deleciosa* cellular copper levels also fluctuate, the maximum accumulation coinciding with one of the peaks in the expression of the metallothionein-like gene (Ledger and Gardner 1994). The metallothionein-like genes may not be responding directly therefore to ethylene. One of the effects of ethylene during fruit ripening may be to alter cellular trace metal levels perhaps through the breakdown of cellular components due to degradation by enzymes such as cellulase and pectinase which are known to be induced by ethylene.

The type-1 metallothionein-like gene from *T. aestivum*, *wali1*, was identified because it was expressed during aluminium stress (Snowden and Gardner 1993). Expression of the gene was greater with identical treatments in an aluminium sensitive strain than in a more tolerant strain. This could be consistent with previous reports that the exclusion from the

root tissue is the main aluminium tolerance mechanism in many plants (Delhaize *et al.* 1993). Delhaize *et al.* (1993) report that in the tolerant *T. aestivum* cultivar there is a lower aluminium concentration in root tissues relative to the sensitive strain for the same exogenous concentration. The expression of the metallothionein-like gene would appear to correlate with an elevation in cellular aluminium concentration (Snowden and Gardner 1993). However, the plants in which the *wali* clones were identified were grown in acidic medium, pH 4.3, a key factor in aluminium toxicity (Snowden and Gardner 1993). The binding of the mugineic acid-iron complex to the plasma membrane is favoured by low pH conditions (Mihashi *et al.* 1991). This prevents the uptake and transport of iron in plant roots. It may be that the low pH conditions used to study aluminum toxicity may effect the iron status of strategy 2 plants such as *T. aestivum*. It is also noted that many stress responses in higher plants are mediated by ethylene (cited in Itzhaki *et al.* 1994). The expression of the metallothionein-like gene, *wali1*, in aluminium stressed *T. aestivum* roots may not necessarily be a direct response to increased aluminium levels.

Another important aspect of the regulation of metallothionein-like gene expression is tissue specificity. The genes from *P. sativum* and *Z. mays* were isolated on the basis of root specific expression (Evans *et al.* 1990, de Frammond 1991), whilst the gene from *V. faba* was isolated on the basis of leaf specific expression. A tissue specific pattern of expression has been observed in the other metallothionein-like genes, with the type-1 genes predominantly being expressed highly in root tissue and the type-2 genes being expressed highly in leaf tissue. *T. repens* is an unusual example as both type-1 and type-2 cDNA's have been identified in the same tissue, the stolon node (see table 4.1). This is an unusual tissue type having both leaf and root characteristics. By analogy to metallothionein-like genes in plants, tissue specific expression of different metallothionein isoforms is observed in mammals. For example the isoform MT-III is expressed only in brain tissue (Palmiter *et al.* 1992). As with other metallothionein the full function of MT-III is not known but it is thought to be a growth factor required for the normal development of neurones and deficiency in the protein has been implicated in Alzheimer's disease. Unlike other mammalian metallothioneins it is not inducible by cadmium or zinc. The regulation of metallothionein-like genes by trace metals will be discussed in more detail in section 8.3.

Comparison of the predicted primary structures of the plant metallothionein-like genes with databases of protein sequences suggests that they represent a discreet group of novel

proteins related to metallothionein (section 3.3.3). Within this group a system of categorisation has been proposed based on salient features of the primary structure (section 3.3.2). These are the arrangement of cysteine residues within the amino terminal domain and the length of the region separating the cysteine rich domains. The sequence alignments, figure 3.2, strongly support the categorisation. There is a high degree of sequence conservation between the sequences especially within the cysteine rich domains and at the centre of the interdomain region (figure 3.4). The apparent tissue specificity of the genes such that the type-1 category is expressed in root tissue and the type-2 category is expressed in leaf tissue appears to support this categorisation. Additional data on the tissue specificity of the categories of gene in a wider range of plant species and on the presence of more than one gene type within single species will be required to fully justify the categorisation of the products on this basis. The phylogenetic prediction program DISTANCES gave a higher score to the arrangement of cysteines within the amino terminal domain in terms of sequence relatedness than other species specific similarities (section 3.3.5). The type-3 category has an abridged interdomain region and an extra cysteine residue preceding the carboxyl terminal cysteine rich domain (figure 3.1). The significance of these features is not yet known. To date there are only two examples of this structure, in *A. thaliana* (expressed in roots, Zhou and Goldsbrough 1994) and in *B. napus* (expressed in leaf, Buchanan-Wollaston 1994). A putative type-4 category is presented in figure 3.2. This group of sequences have superficial similarity to the other metallothionein-like sequences but have a different amino terminal domain with notably fewer cysteines and a different interdomain region. As little information is available on these sequences they will not be discussed further.

The discovery of the type-3 gene category encoding products lacking the internal linking region has obvious implications for the function of this region in the type-1 and type-2 proteins. When the type-3 metallothionein-like gene from *A. thaliana* is expressed in *cup1Δ* yeast it confers copper resistance to the cells implying that it is acting as a functional metallothionein (in terms of metal detoxification) and actively chelating copper (Zhou and Goldsbrough 1994). This implies that the interdomain region is not essential for metal binding. However, the 10 amino acids, including one cysteine, which replace the long interdomain region in the type-3 structure may perform a similar function to the longer linking region. It may fold in such a way as to bring the two cysteine rich domains together and facilitate metal binding. Potentially this folding could be initiated by the formation of a

metal-thiolate bond involving the extra cysteine residue. It is also possible that the two interdomain arrangements perform specific and separate functions *in planta*. For example, the extended interdomain region could be required for interaction with other cellular components, interactions which do not occur in the type-3 species. The type-3 structure may represent a form of the plant metallothionein-like protein which is a mobile metal chelator while other sequences may be associated with other cell components. It will be interesting to see if a type-1 metallothionein-like gene is expressed in the roots of *A. thaliana* and *B. napus* and a type-3 metallothionein-like gene expressed in the roots of plants currently known to possess the type-1 gene.

The secondary structure prediction for PsMT_A, figure 3.5, provides supporting evidence for structural order within the interdomain region of the putative type-1 and type-2 proteins. The structural motif, β -strandGV, is conserved throughout the type-1 and type-2 categories (figure 3.6). The presence of a glycine residue immediately following a section of β -strand is commonly found in secondary structure motifs known as 'reverse turns' (Phillips and North 1978). These allow the protein chain to turn sharply and reverse direction. The implication is that far from being a random loop, as has been proposed previously (Kille *et al.* 1991, Robinson *et al.* 1993), the interdomain region may in fact be highly folded. Possible functions of such a structure may be to aid the formation of the metal-thiolate cluster during initial protein folding or to stabilise the metal cluster to allow exchange of metal ions without disruption of the conformation of the cysteine rich domains. Alternatively an ordered interdomain region may be the site of interaction with other cellular components. For example, as part of a multicomponent complex or as the point of contact between the protein and an integral membrane protein. If the linking region is a point of contact with other cell components then this suggests that type-3 and type-4 proteins would have alternative functions.

Irrespective of function the β -strandGV motif appears to be unique to the plant metallothionein-like gene products. A search of the OWL protein database with the interdomain region yielded no particularly significant matches. Four of the highest non plant metallothionein-like matches to the region were a diverse group of proteins; a GTP binding protein from mouse (35 % identity over 26 amino acids) (Swissprot JC1349), cannabinoid receptors from rat and human (38.5 % identity over 26 amino acids) (Swissprot P20272 and P21554) and yeast RNA polymerase (45 % identity over 20 amino acids) (Swissprot

S10340). The common sequence fragment had not been given any structural or functional significance in reports of these proteins. It is not likely that any of these matches will prove significant.

8.2 Characterisation of the translational products of the *PsMT_A* and *AtMT-t2* genes

A salient feature of the metal-thiolate cluster of metallothionein is that it is refractory to proteolysis (Nielson and Winge 1983). In contrast the random protein chain of apometallothionein is highly susceptible to proteolytic degradation. The recombinant zinc-*PsMT_A* protein, isolated from *E. coli* as the cleavage product of factor Xa and the GST fusion protein, had been specifically cleaved between leucine³⁸ and glycine³⁹ (section 4.3.2). This is within the region linking the two cysteine rich regions which could combine to form the putative metal-thiolate cluster, figure 3.5b. When a recombinant cadmium-*PsMT_A* protein was isolated from *E. coli* by gel filtration and ion exchange chromatography this interdomain region had undergone multiple proteolytic cleavages, at leucine²⁵, leucine³⁸, alanine⁴³, glutamine⁴⁶ and serine⁵³ (Kille *et al.* 1991).

This data is consistent with the cysteine rich regions of the protein forming a refractory thiolate cluster leaving the interdomain region susceptible to proteolysis. Interestingly the Leu³⁸ residue immediately precedes the GV motif conserved at the end of the predicted β -strand in all the type-1 and type-2 metallothionein-like gene products supporting the view that these residues may have particular functional significance. The continued degradation of the purified recombinant protein *in vitro* was visualized on a polyacrylamide gel (figure 3.2). The appearance of discreet breakdown products on the gel indicates that proteolysis occurs at specific sites. It is possible that these sites could be the same sites reported in the proteolysis of the cadmium peptide during purification (Kille *et al.* 1991). If the interdomain region does form an ordered structure potentially these residues could be exposed leaving them susceptible to proteolysis.

The recombinant *PsMT_A* protein expressed in *E. coli* is associated with zinc (section 4.3.2). The cysteine residues grouped in the amino and carboxyl domains are likely to act as metal ligands. The arrangement of the cysteines in Cys-Xaa-Cys motifs suggests that metal binding is analogous to mammalian metallothionein, that is via thiolate bonds. The type-1 and type-2 categories (described in section 3.3.2), which include the products of the majority of cDNA's so far reported, differ significantly only in the arrangement of cysteine residues in

the amino terminal domain. This, and the apparent tissue specificity, implies that the two types of gene product may perform different but related functions. The study of mammalian metallothionein has highlighted the importance of cysteine arrangement to metal specificity (Winge and Miklossy 1982). The differences in the arrangement of cysteines in the amino terminal domains of the plant metallothionein-like gene products are similar to the α and β domains of the mammalian metallothionein which implies there may be similarities in the relative preferences for metal ions. The primary structures of the metallothionein from *S. cerevisiae* and *N. crassa* are shown in figure 3.2. Both proteins are known to bind copper *in vivo* (Butt *et al.* 1984 and Lerch 1980). The predominant cysteine arrangement in these proteins is the Cys-Xaa-Cys motif.

The proton displacement curves for AtMT-t2 and PsMT_A GST fusion proteins (figure 5.7) are consistent with the hypothesis that the primary structure of the type-2 gene products favour zinc binding relative to the type-1 gene products. However only a small difference in affinity, measured by a shift in the pH of half displacement of 0.25 pH units, was observed. The significance of this small change in affinity for the function of the putative proteins *in planta* remains to be investigated. Reese and Wagner (1987a) obtained pH of half displacement values for cadmium peptides (phytochelatin) in *N. tabacum* in the range 5.0 to 5.8. They reasoned that pH of half displacement for zinc phytochelatin would be a pH unit above this (on the basis of values for different metals obtained for mammalian metallothionein) and as such, unlike cadmium phytochelatin, would be of little physiological significance. Based on these criteria the predicted products of plant metallothionein-like genes could be involved in zinc homeostasis *in planta*. A small difference in pH of half displacement within the pH 5.0 to 6.0 range may be significant for the involvement of a protein in zinc metabolism at physiological pH. Speculation that there may be significant differences in protein function due to the cysteine arrangement is supported by experiments with *cup1* Δ mutant of *S. cerevisiae* (Zhou and Goldsbrough 1994). Cells expressing AtMT-t2 were tolerant to cadmium concentrations up to 100 μ M whereas cells expressing the type-3 *A. thaliana* metallothionein-like gene were tolerant up to only 10 μ M cadmium (Zhou and Goldsbrough 1994). However this is significant for the comparison of the type-1 and type-2 products only if metal specificity is independent of the interdomain region. A degree of zinc tolerance was restored to metallothionein deficient *Synechococcus* by the zinc regulated expression of the AtMT-t2 gene (section 5.3.7). This indicates an ability of the recombinant

protein to bind zinc *in vivo* and a potential involvement of the putative metallothionein-like gene products in zinc metabolism *in planta*.

It is possible that the difference in cysteine arrangements between different categories of putative plant metallothionein-like gene products may effect other aspects of protein properties, such as, metal binding capacity, the lability of the bound metal and therefore the ability to donate metal to metalloenzymes or even an aspect of function not related to metal binding. These possibilities were not addressed in this study and will require further study.

The instability of the putative metal binding complex in the recombinant system was an obstacle preventing a more complete comparison of the type-1 and type-2 fusion proteins (section 5.3.6). The susceptibility of the putative metallothionein-like proteins to degradation may contribute to the difficulty in isolating products of the metallothionein-like genes from plant tissue.

Metal may be lost from metallothionein by direct transfer to a higher affinity ligand, proteolysis of the polypeptide chain releasing low molecular weight metal chelates or by oxidization of the metal thiolate bond. *In vitro* studies indicate that the copper-thiolate cluster, though more resistant to proteolytic degradation than cadmium or zinc metallothionein, is more susceptible to oxidation (Weser *et al.* 1986). As a consequence copper thionein is degraded faster *in vivo* than cadmium or zinc species. The half life of rat [³⁵S] labelled MT-1 and MT-2 was 15 and 18 hours respectively for copper thionein and 19 hours and up to 4 days for cadmium and zinc (Weser *et al.* 1986). Oxidation during the extraction procedure is likely to be another factor which may contribute to the difficulty of extracting copper loaded metallothionein from plant tissue.

8.3 The regulation of expression of *PsMT_A* in response to trace metals

From the published data the response of the plant metallothionein-like genes to trace metals is ambiguous. Expression of the *P. sativum* gene was reported to be inhibited by elevated exogenous iron concentrations and induced or derepressed by high exogenous copper (Robinson *et al.* 1993). Expression of the *M. guttatus* gene was inhibited by copper shock but unaffected by continuous growth in 5 µM copper, whilst it was inhibited by continuous growth in cadmium and zinc (de Miranda *et al.* 1991). The *ids1* gene from *H. vulgare* was induced during iron deficient growth (Okumura *et al.* 1992). The *T. aestivum* gene was induced by high aluminium concentrations but slightly inhibited by cadmium (Snowden and

Gardner 1993). In the type-2 category of genes expression of the *G. max* gene was unaffected by growth in 3 μM copper but expression was slightly reduced in 6 μM copper (Kawashima *et al.* 1991). The gene from *V. faba* did not respond to elevated concentrations of copper, zinc or cadmium (Foley and Singh 1994). Expression of the *AtMT-t2* gene from *A. thaliana* was induced by treatment with high levels of copper, slightly increased with cadmium treatment and was not effected by zinc (Zhou and Goldsbrough 1994). In a published abstract it has been reported that the upstream regulatory sequence of the gene fused to a *gus* reporter gene was induced by metal in root tips (Fujiwara *et al.* 1994). The type-3 gene from *A. thaliana* was induced slightly by copper in leaves and repressed by zinc (Zhou and Goldsbrough 1994).

The observations from the northern analysis in this thesis were that a minimum in expression of *PsMT_A* in the roots of *P. sativum* seedlings was found in media containing 100 nM CuSO_4 (figures 6.1A and B). Higher expression was observed in seedlings grown in media containing a higher or a lower copper concentration. An increase in the basal level of expression of *PsMT_A* was observed in seedlings grown in media containing 0.5 μM or 1.0 μM CuSO_4 compared to media not supplemented with copper (figures 6.2A and B). In response to different concentrations of iron-EDDHA in the growth media, minimal expression of the *PsMT_A* gene was observed at very low exogenous iron concentrations and at concentrations above 2.0 μM (figures 6.2A and B). A maximal level of expression was observed for iron concentrations between 500 to 100 nM (figures 6.2A and 6.2B respectively). A reduction of *PsMT_A* expression by iron concentrations above 2.0 μM was observed for seedlings in all copper concentrations studied (figures 6.1A and B). The gene was induced by exogenous zinc concentrations above 5.0 μM but only in iron replete media (figures 6.3A and B).

The metal concentrations quoted in the northern analyses (chapter 6) refer to the metal added to the hydroponic solution. There are two other sources of metal which should be considered. Firstly, the hydroponic solutions will contain copper, zinc and iron present as contaminants in the other minerals which comprise the hydroponic solution. The concentration of these contaminants should be very low, but it is not likely that in any of the treatments any given metal concentrations would have been 0 nM. For example, the copper concentration in a micronutrient solution containing no added copper was estimated to be 9 nM by atomic absorption spectroscopy. A second, and significant source of trace metals will

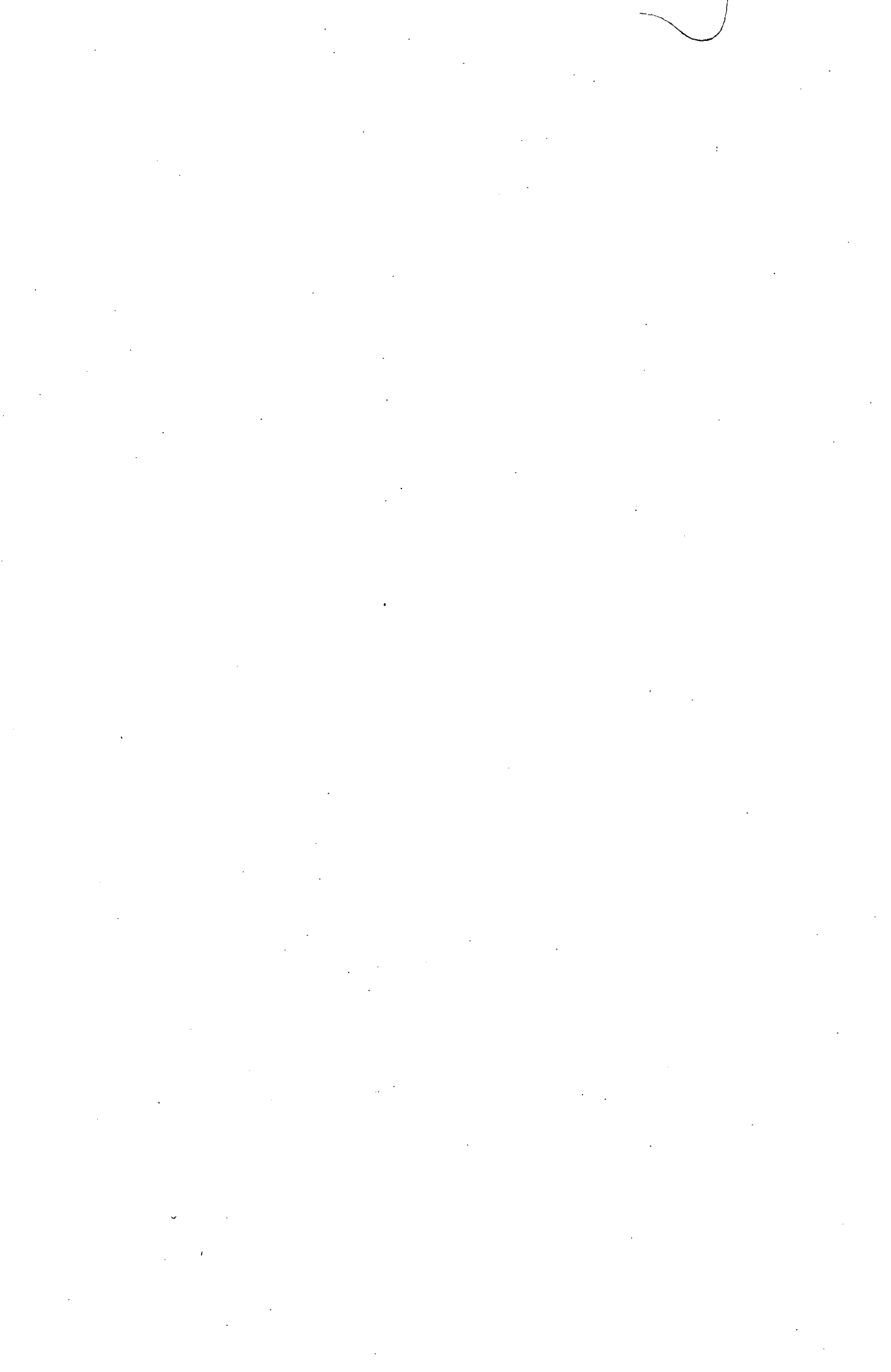
be metal stores in the seed. In a study of the effect of copper deficiency on the mineral content of seedlings of *P. sativum* grown in the absence of copper, it was found that it was not possible to induce copper deficiency in 14 day old plants (Welch *et al.* 1993). It was concluded that to obtain true copper deficiency would required prolonged growth in copper depleted media. A reduction in the intracellular copper concentration of seedlings and induction of iron and copper reductase activity was not observed until day 18 (Welch *et al.* 1993). Growth in copper depleted media was not considered to have effected the concentration of other elements in the seedlings in this study. Growth in iron deficient conditions however caused an increase in the shoot concentrations of copper, magnesium, manganese and potassium. The copper concentration being doubled. Both copper and iron reductase activity was induced by growth in iron deficient conditions by day 14 (Welch *et al.* 1993). The nutrient solution and other growth conditions used in this thesis were based on the conditions reported by Grusak *et al.* (1990), as were those used by Welch *et al.* (1993). However, whereas by day 14 Welch *et al.* (1993) reported that all seedlings exhibited chlorosis due to iron deficiency when grown in the absence of iron-EDDHA supplement, chlorosis was not observed in the leaves of seedlings harvested on day 15 in any of the experiments in this thesis.

Lower *PsMT_A* expression was observed at 50 nM compared to no added copper, and a further reduction was observed at 100 nM (figures 6.1C). It has not been established if this is a direct effect of the exogenous copper concentration or if different levels of expression are due to the perturbation of some other cellular factor at these copper concentrations. A correlation between iron and copper uptake has been proposed for yeast (Dancis *et al.* 1994). It is possible that at very low exogenous copper concentrations iron uptake and perhaps the increase of iron from cellular stores, such as ferritin, may occur and *PsMT_A* expression does respond to iron (figures 6.2A and B). However two observations seem to oppose the possibility that the response of the gene at low copper concentrations is due to changes in iron status; the relative levels of *PsMT_A* expression for 0, 50 and 100 nM copper was replicated in seedlings grown in media containing both no added iron and 2.0 μ M iron-EDDHA (figures 7.1A and B), and in similar growth conditions to those used in this study by day 14 there was no observed change in the iron content of *P. sativum* seedlings due to growth in media to which no copper had been added (Welch *et al.* 1993). Increased accumulation of copper was observed in seedlings grown in media to which no iron had been

added (Robinson *et al.* 1993). This might be expected to effect the pattern of expression at different copper concentrations in seedlings grown in iron deficient and iron replete media, but this was not observed in figures 6.1C, apparently only the basal level of *PsMT_A* expression was effected. This could be because at the low exogenous copper concentrations the copper uptake systems of the roots were already maximised and therefore not effected by iron status.

However, recently a putative ethylene regulatory element (TTTGAAAT) has been identified in the *PsMT_A* promoter sequence, at position -460 to -467 relative to the putative translational start site (Robinson and co-workers unpublished). The element is next to a partial reverse repeat (AAAGTTT). The element is identical to an ethylene regulatory element, which is also associated with a partial reverse repeat, that was identified in the senescence related glutathione-S-transferase gene in the carnation (*Dianthus caryophyllus*) (Itzhaki *et al.* 1994). A similar element (ATTTCAA) is also present in the promoter of the type-3 *A. thaliana* gene (at position -418 to -411 relative to the putative translational start site), based on genomic clone sequenced by J. Bartley, MSc. thesis (1994). The identification of these elements is in keeping with the link between plant metallothionein-like gene regulation and ethylene discussed in section 8.2. It is possible that the induction of *PsMT_A* expression in response to low levels of copper in the hydroponic medium may be an ethylene mediated stress response, caused by the low copper levels. The function of the putative *PsMT_A* protein under such conditions remains unknown.

An increase in the basal level of expression of *PsMT_A* was observed in the roots of seedlings grown in media containing 0.5 μ M and 1.0 μ M CuSO_4 (figures 6.2A and 6.2B) and is consistent with the observed increase of expression of *PsMT_A* in response to copper concentrations above 100 nM (figures 6.1A and B). A clear pattern of expression of *PsMT_A* in response to different copper concentrations above 100 nM was not observed (figures 6.1A and B) and the response was independent of the iron concentration of the growth media. The difference in the basal level of expression of *PsMT_A* observed in the seedlings grown in iron supplemented and non supplemented media (figures 6.1A and B) might be enhanced by the influx of copper into the roots in the non iron supplemented seedlings (Robinson *et al.* 1993). The observed response of *PsMT_A* to copper was complex and this may reflect transcriptional control by a range of factors, ethylene being a prime candidate, some of which may themselves be sensitive to exogenous copper concentrations.



The relationship between *PsMT_A* expression and variation in exogenous iron concentration was also more complex than previous work suggested (Robinson *et al.* 1993). As with copper the response is different at high and low exogenous concentrations. Growth in iron deficient conditions induces the plasmamembrane ferric reductase (Welch *et al.* 1993). In addition to facilitating the uptake of iron this causes an influx of a number of ions including copper into the *P. sativum* seedling. The amount of copper in the roots of pea seedlings grown in media containing iron-EDDHA was half that found in roots from seedlings grown in its absence (Robinson *et al.* 1993). In conditions where copper was freely available, as the exogenous iron concentration decreased so did the observed levels of *PsMT_A* transcripts even though increased copper uptake might be expected from these conditions (figures 6.2A and B). This suggests that either the expression of *PsMT_A* is being repressed by the accumulation of copper (contradictory to the observed response to copper concentrations above 100 nM) or that the response of gene expression to different levels of iron is a specific response to iron and independent of, and opposing to the effects of copper. There seem to be contradictions in the observed effects of different concentrations of exogenous copper and iron on gene expression which have not been resolved. Ethylene has also been implicated in the iron deficiency response in *C. sativus* (Romero and Alcántara 1994). In addition, an enzyme in the ethylene biosynthetic pathway, ACC oxidase requires iron for activity. It is possible that some of the apparently confusing aspects of the response of the *PsMT_A* to iron and copper may be due to the involvement of ethylene in the regulation of this gene. It is also noted that the sensor is thought to be a zinc metalloprotein (Zarembinski and Theologis 1994).

Regulation of expression by iron has also been examined for the *ids1* gene from *H. vulgare* (Okumura *et al.* 1992). If the response of the type-1 genes from *H. vulgare* and *P. sativum* to iron are to be compared there are several factors to consider. These two plants employ different strategies for iron uptake. *P. sativum* employs a plasmalemma oxireductase (Grusak *et al.* 1990) whereas *H. vulgare* secretes phytosiderophores to sequester and solubilise ferrous iron (Shojima *et al.* 1990). Differences in the growth conditions should also be considered. The *H. vulgare* plants had been grown in iron replete conditions until the fourth leaf had emerged and then grown in iron deficient conditions for 1 month before the root tips were harvested (Okumura *et al.* 1994). The *P. sativum* seedlings were grown in iron deficient conditions for 12 days from germination and the entire root system was harvested. The difference in growing conditions, in iron uptake strategies and the effects of

localisation, may make the comparison of the effect of iron on the expression of the respective metallothionein-like genes more difficult to compare. However induction of *ids1* gene expression by growth in iron deficient conditions was observed after 15 days of iron deficiency treatment in *H. vulgare*.

An exogenous zinc concentration above 5.0 μM overcame suppression of *PsMT_A* expression by iron, figure 6.3A and B. Under these conditions the response of the *PsMT_A* gene is analogous to the response of mammalian metallothionein, that is it is induced by high levels of zinc. However the response to zinc was dependent on the exogenous iron concentration. The failure to induce *PsMT_A* with zinc under iron deficient growth conditions may be a feature of the iron deficiency response. Whether regulation of *PsMT_A* expression is direct response to zinc remains to be established. However the response of the gene to zinc would support the hypothesis that the products of metallothionein-like genes have a role in tolerance to elevated levels of trace metals.

The complex response of *PsMT_A* to different exogenous trace metal concentrations may indicate that the gene is regulated by multiple transcriptional factors. Whether these factors are directly controlled by iron, zinc or copper ions or other aspects of cellular metabolism which are effected by these metals, such as the change in the redox state of the membrane due to induction of the oxireductase, remains to be established. Although in light of recent evidence regulation by ethylene is likely to play a key role in the development of this field. The interdependence of copper and iron metabolism has been observed in *S. cerevisiae* (section 1.5.3.1) and in higher plants a highly complex relationship is likely to exist between the exogenous concentrations, uptake, metabolism and homeostatic regulation of trace metals. It may therefore be difficult to predict the intracellular consequences small change in the exogenous concentration of a trace metal. The response of genes such as *PsMT_A* to extremely high concentrations of trace metals may be more easily described. It would be illuminating to study the pattern of expression of *PsMT_A* in varying metal concentrations in a pea mutant such as E107 which is phenotypically iron deficient irrespective of the availability of iron (Grusak *et al.* 1990). Preliminary data confirms the constitutive expression of *PsMT_A* in this mutant (N.J. Robinson unpublished).

Regulation of metallothionein by a range of factors other than trace metals has been reported in other species. For example, the induction of metallothionein in mouse Hepa cells by hydrogen peroxide involves an antioxidant response element (Dalton *et al.* 1994). In

higher plants ethylene has been implicated in a range of “stress” responses including stress caused by mechanical wounding, infection, herbicides, metal, ozone, chilling, flooding and drought (cited in Yang and Hoffman 1984). The stimulation of ethylene biosynthesis by stress can occur rapidly, 10 to 30 minutes, and after reaching a peak it subsides over several hours (Yang and Hoffman 1984). It is possible that the rapid response of the *PsMT_A* gene observed in the time course experiments 6.3.4 may be a stress response mediated by ethylene caused by changes in the exogenous metal concentration. The speed of the response may indicate that it is a reaction to the metal concentration in the media rather than the cellular metal concentration.

The trace metal ions copper, iron and zinc have been demonstrated to effect the expression of *PsMT_A* but it is not yet clear if the gene is directly regulated by these metals. If ethylene is the major factor controlling the regulation of the gene then a more complex role than the detoxification of trace metals may be implied for *PsMT_A* and the other plant metallothionein-like gene products. However, the role of the putative *PsMT_A* protein in an ethylene mediated response needs to be established and it is still possible that such a role may involve the regulation of the endogenous concentration of trace metals, in particular copper and / or zinc.

8.4 Copper and zinc ligands in *P. sativum*

Previous investigations of ligands of trace metals in plant roots have concentrated on ligands induced by elevated concentrations of those metals (for example Wagner 1984, Salt *et al.* 1989, Meuwly *et al.* 1993, Chen and Goldsbrough 1994). In this project the isolation of the translational product of a metallothionein-like gene was a long term goal. During most of the time when the ligands were isolated the complex response of the *PsMT_A* gene to exogenous copper and iron concentrations, as presented in chapter 6, and the potential regulation of the gene by ethylene was not known. On the basis of the information regarding the repression of the *PsMT_A* gene by exogenous iron-EDDHA (Robinson *et al.* 1993), extracts from the roots of seedlings grown in non iron supplemented and iron supplemented conditions were compared.

Copper and zinc containing components bound to the DEAE anion exchange matrix were eluted when the concentration of Tris-HCl in the wash buffer was increased from 10 to 400 μ M. In extracts, from seedlings grown in media supplemented with 0.5 μ M CuSO_4 and

2.0 μM ZnSO_4 , the quantity of zinc in fractions obtained by this method was consistently greater, by a factor of at least 2, in seedlings grown in media not supplemented with iron compared to seedlings grown in media containing 2.0 μM iron-EDDHA (section 7.3.8). The zinc content in the young leaves and shoots of *P. sativum* seedlings grown in iron deficient conditions has been reported to decrease (Welch *et al.* 1993). This suggests that in iron deficient conditions this zinc ligand becomes particularly enriched in the roots of *P. sativum* seedlings. The amount of copper in fractions isolated on the ion exchange matrix, using extracts from seedlings grown in media supplemented and not supplemented with iron, did not change consistently (section 7.3.8). In seedlings grown without the addition of copper and zinc to the hydroponic media the fractions comprising the zinc peak, Zn-1', on ion exchange chromatograms decreased in response to growth in media not supplemented with iron (section 7.3.8).

The fractions comprising the zinc peak (Zn-1) from ion exchange chromatograms were resolved into a single zinc binding component of low apparent molecular weight by gel filtration chromatography (figures 7.2c and, 7.3c, 7.4c and 7.5c and d). The fractions comprising the copper peak (Cu-1) on ion exchange profiles were resolved into a copper binding component of slightly higher molecular weight than the zinc component (Zn-A) (figures 7.2c and, 7.3c, 7.4c and 7.5c and d) following gel filtration chromatography. A second copper binding component (Cu-B), with the same apparent molecular weight as Zn-A, was observed on some chromatograms (figures 7.3c, 7.5e). The variation in the recovery of Cu-B could be due to variations in oxidation of the component during the extraction method between different extractions. There was some evidence that Cu-B may be more highly charged than Cu-A as it was of higher abundance in the copper containing fractions which had a longer retention time on the DEAE matrix (figure 7.5a, c and e).

The putative zinc ligand Zn-1 (and by inference Zn-A), isolated from extracts from seedlings grown in media supplemented with copper and zinc, decreased in abundance in response to elevated iron which correlates with the predicted response of the *PsMT_A* gene. However, the putative zinc ligand Zn-1', observed in extracts from seedlings grown in media not supplemented with iron and copper, increased in response to elevated iron, whilst under these conditions the *PsMT_A* gene was still down regulated (figure 7.13). It remains to be established if Zn-1 and Zn-1' represent the same ligand or under what conditions, if any, the putative *PsMT_A* protein might bind zinc in *P. sativum* roots. The chromatographic properties

of the copper and zinc ligands observed in these experiments are similar to those observed in other investigations of copper ligands in plant roots (for example in *M. guttatus*, Robinson and Thurman 1986, Salt *et al.* 1989). In these cases further investigation identified these copper ligands as phytochelatin. It is possible that the copper ligands observed in gel filtration chromatograms in this investigation may be phytochelatin. Induction of phytochelatin biosynthesis has been observed in response to elevated exogenous zinc (Grill *et al.* 1987) and phytochelatin synthase activity is activated by zinc *in vitro* (Grill *et al.* 1989). However on the basis of predictions of phytochelatin affinity for zinc, Reese and Wagner (1987a) discounted a role for phytochelatin in the homeostasis of zinc. Furthermore, cadmium sensitive *A. thaliana* mutants, unable to synthesise phytochelatin, showed no significant difference in sensitivity to elevated zinc concentrations than the wild type (Howden *et al.* 1995a and b).

The recombinant *PsMT_A* protein, isolated from *E. coli* and mixed with an extract from the roots of *P. sativum*, was eluted from DEAE ion exchange matrix in the 400 mM Tris-HCl wash (section 7.3.9). The protein was resolved by subsequent gel filtration chromatography into a doublet of peaks (figure 7.10b). The radiolabelled *PsMT_A* protein was mixed with a root extract from seedlings grown in media not supplemented with copper or zinc and so it was not possible to correlate the position of these peaks with the position of any copper or zinc components on previous profiles. The possibility that *PsMT_A* may co-elute with either the Zn-A, Cu-A or Cu-B components seen on previous profiles cannot be precluded. It is possible that the putative native *PsMT_A* protein may only form a small proportion of the copper and zinc components isolated by ion exchange chromatography making its detection by subsequent gel filtration chromatography more difficult. The position of [³⁵S] cysteine labelled *PsMT_A* on the chromatogram in figure 7.10b suggests that even in low copper conditions *PsMT_A* is not a major copper binding component in roots of *P. sativum*, although the copper could have been lost from *PsMT_A* during purification. The sensitivity of the metal detection method may be insufficient to detect the metal binding metallothionein-like protein in these extracts. The [³⁵S] cysteine labelling of large samples prior to extraction may allow more detailed analysis of extracts and allow the detection of cysteine rich peptides on subsequent purifications, for example via HPLC.

8.5 Evidence for the PsMT_A protein in crude root extracts

A band of apparent molecular weight 11 500 was detected in a crude extract of [³⁵S] cysteine labelled *P. sativum* roots (figure 7.11B). The band was much more intense following electrophoresis of an extract from seedlings grown in iron deficient conditions. Northern analysis confirmed that the *PsMT_A* gene was more strongly expressed in roots of these seedlings (figure 7.13). The band was not evident in the Coomassie blue stained gel (figure 7.11A) suggesting that it represented a particularly cysteine rich component. The migration of the band observed on this gel is consistent with that previously observed for recombinant PsMT_A (Kille *et al.* 1991). A doublet of cysteine rich spots was detected by two-dimensional electrophoresis of [³⁵S] cysteine labelled root extract (figure 7.15C). The bands were not apparent in the equivalent gel with an extract from iron supplemented seedlings. The migration on the isoelectric focusing phase of the gel (between pH 4 and 5) would be consistent with the predicted properties of PsMT_A. It is noted that the [³⁵S] peak attributed to PsMT_A following gel filtration chromatography of a root extract mixed with labelled recombinant PsMT_A appeared to be a doublet (figure 7.10).

The isoelectric point for the cadmium binding protein (phytochelatin) of *N. tabacum* was estimated to be 3.15 (Reese and Wagner 1987). It cannot be ruled out that a phytochelatin complex would migrate to a similar position on an isoelectric focusing gel as that observed for the spots in figure 7.15C. It is well known, that oxidized phenolics react with amine and sulphhydryl groups on proteins increasing their negative charge in elevated pH (cited in Bartolf *et al.* 1980). Phytochelatin has, proportionally, a much higher cysteine content than the putative metallothionein-like protein and it is possible that a similar effect in pea extracts might cause phytochelatin to have very high mobility during electrophoresis. The bands observed on polyacrylamide gels might have too high an apparent molecular weight for phytochelatin. In addition the extracts were from seedlings grown in media lacking copper and zinc. *De novo* synthesis of phytochelatin would not be elevated under these conditions and so phytochelatin may not be highly labelled with [³⁵S] cysteine.

8.6 Concluding remarks

It has been demonstrated that the products of the plant metallothionein-like genes are capable of binding metal both *in vitro* and *in vivo*. It was demonstrated that zinc was associated with recombinant PsMT_A and AtMT-t2 protein isolated from *E. coli* and that the AtMT-t2 protein

restored zinc tolerance to a metallothionein deficient strain of *Synechococcus*. Expression of the type-3 metallothionein-like gene and *AtMT-12* gene in copper metallothionein deficient yeast has been reported to restore a degree of copper tolerance (Zhou and Goldsbrough 1994). The northern analysis of *PsMT_A* expression presented in this thesis demonstrates that the gene does respond to variations in the exogenous concentrations of copper, iron and zinc. However, this response was more complex than has been observed for metallothionein in other organisms, for example *CUP1* in yeast (Thorvaldsen *et al.* 1993). Factors other than exogenous metal concentrations may be involved in the response. The observation that expression of *PsMT_A* could be induced by low copper concentrations and responded rapidly to changes in exogenous metal concentration may be particularly significant. It may indicate that the product of the gene is involved in a copper deficiency response, possibly involved in copper uptake or transport. Alternatively expression of the gene may be expressed as part of a stress response induced by the very low copper levels. The likelihood of this latter hypothesis has been increased by the identification of a putative ethylene responsive element within the *PsMT_A* promoter element. Ethylene has been implicated in other nutritive stresses in higher plants, for example phosphate and nitrogen starvation (He *et al.* 1992).

If *PsMT_A* expression is part of an ethylene mediated response it still raises the question as to what the function of the native protein might be. Expression of the *PsMT_A* gene in roots of seedlings grown in media not supplemented with copper, zinc or iron may indicate that *PsMT_A* could function as a holoprotein *in planta*. This seems unlikely due to the high cysteine content and metallothionein-like structure of the cysteine rich domains. In this case the metal binding capacity of the recombinant protein may have been impaired during the original purification procedure from *E. coli* or the subsequent ion exchange and gel filtration chromatography procedures. If the *PsMT_A* does function as a holoprotein during ethylene stress responses then potentially it could function as a general thiol reductant.

In addition to the stress response ethylene mediated gene regulation also occurs during different developmental stages of the plant, such as germination, fruit ripening, abscission of leaves, and senescence of flowers (Yang and Hoffman 1984). There are reports of expression of metallothionein-like genes in a number of plant species during many of these stages (references and summary in section 8.1). It is possible that the plant metallothionein-like gene products may be involved in the regulation of intercellular trace metals during cellular development. Preliminary data from reporter gene experiments with the *PsMT_A*

promoter in *A. thaliana* indicate that in addition to high expression in root tissue (Robinson and co-workers, unpublished), there is high expression from the *PsMT_A* promoter in leaf hydathodes, senescing cotyledons and in the anthers and stigma during different stages of flower development.

A key development in the research into the plant metallothionein-like genes and their products will be the isolation of the active proteins from plant tissue. In the present experiments the quantity of a low molecular weight zinc complex recovered by ion exchange chromatography decreased in response to an elevated concentration of exogenous iron. Expression of the *PsMT_A* gene is also reduced under such conditions. The response of a copper component identified in the same extracts was less consistent. It is quite possible that there was significant loss of metal from complexes due to oxidation during the isolation procedure. This could account for the variability in the quantity of copper complex recovered by ion exchange chromatography and also for the variability in the recovery of the components Cu-A and Cu-B by gel filtration chromatography. Extraction procedures using an inert gas atmosphere may be important in the isolation of a plant metallothionein-like gene product. The use of [³⁵S] cysteine *in planta* labelling techniques detected differentially expressed protein bands by polyacrylamide electrophoresis. This removes the problem of loss of metal from the protein during purification. The use of *in planta* labelling in combination with the chromatographic technique may be a more sensitive technique for the detection of cysteine rich peptides than the detection of bound metal.

8.7 Future work

8.7.1 Isolation of the translational products of plant metallothionein-like genes from plant tissue

As stated previously the isolation of plant metallothionein-like gene products will be a key area in the development of research in this field. Important information which needs to be determined includes; which, if any, metals are associated with the native protein, localisation of the native protein both at the tissue and cellular level, which, if any, cellular components the native protein may be associated with, what is the half life of the native protein and is it involved in transport. The production of a functional antibody to a metallothionein-like protein would be an important tool in determining many of these questions. Alternatively an

- Pearson, W.R. and Lipman, D.J. (1988) Improved tools for biological sequence analysis. *Proc. Natl. Acad. Sci. USA* **85** pp. 2444-2448.
- Phillips, D.C. and North, A.C.T. (1978) *Protein structure* (second edition). Ed. Head, J.J., Carolina Biological Supply Company, USA.
- Pickering, I.J., George, G.N., Dameron, C.T., Kurze, B., Winge, D.R. and Dance, I.G. (1993) X-ray absorption spectroscopy of cuprous thiolate clusters in proteins and model systems. *J. Am. Chem. Soc.* **115** pp. 9498-9505.
- Plocke, D.J. and Kägi, J.H.R. (1992) Spectral characteristics of cadmium-containing phytochelatin complexes isolated from *Schizosaccharomyces pombe*. *Eur. J. Biochem.* **207** pp. 201-205.
- Premakumar, R., Winge, D.R., Wiley, R.D. and Rajogpalan, K.V. (1975) Copper-chelatin; isolation from various eukaryotic sources. *Arch. Biochem. Biophys.* **170** pp. 278-288.
- Prinz, R. and Weser, U. (1975) Naturally occurring Cu-thionein in *Saccharomyces cerevisiae*. *J. Phys. Chem.* **356** pp. 767-776.
- Pountney, D.L. and Vašák, M. (1992) Spectroscopic studies on metal distribution in Co(II)/Zn(II) mixed-metal clusters in rabbit liver metallothionein 2. *Eur. J. Biochem.* **209** pp. 335-341.
- Pountney, D.L., Schauwecker, I., Zarn, J. and Vašák, M. (1994) Formation of mammalian Cu₈-metallothionein *in vitro*: Evidence for the existence of two Cu(I)₄-thiolate clusters. *Biochemistry* **33** pp. 9699-96705.
- Raguzzi, F., Lesuisse, E. and Crichton, R.R. (1988) Iron storage in *Saccharomyces cerevisiae*. *FEBS Letters* **231** No.1 pp. 253-258.
- Rauser, W.E. (1987) Changes in the glutathione content of maize seedlings exposed to cadmium. *Plant Sci.* **51** pp. 171-175.
- Rauser, W.E. (1990) Phytochelatins. *Annu. Rev. Biochem.* **59** pp. 61-86.
- Rauser, W.E. and Meuwly, P. (1993) Part of the cadmium is bound by certain thiolate isopeptides. *Plant Phys.* **102** p.163.
- Reese, R.N. and Wagner, G.J. (1987a) Properties of tobacco (*Nicotiana tabacum*) cadmium-binding peptide(s): unique non-metallothionein Cd ligands. *Biochem J.* **241** pp. 641-647.
- Reese, R.N. and Wagner, G.J. (1987b) Effects of buthionine sulphoxamine on Cd-binding peptide levels in suspension-cultured tobacco cells treated with Cd, Zn or Cu. *Plant Physiol.* **84** pp. 574-577.
- Reese, R.N. and Winge, D.R. (1988) Sulphide stabilization of the cadmium- γ -glutamyl peptide complex of *Schizosaccharomyces pombe*. *J. Biol. Chem.* **263** pp. 12832-12835.

- Reese, R.N., Mehra, R.K., Tarbet, E.B. and Winge, D.R. (1988) Studies on the gamma-glutamyl Cu-binding peptide from *Schizosaccharomyces pombe*. *J. Biol. Chem.* **263** pp. 4186-4192.
- Reese, R.N., White, C.A. and Winge, D.R. (1992) Cadmium -sulphide crystallites in Cd-(γ -EC)_nG peptide complexes from tomato. *Plant Physiol.* **98** pp. 225-229.
- Rennenberg, H. (1982) Glutathione metabolism and possible roles in higher plants. *Phytochemistry* **21** pp. 2771.
- Richards, M.P. (1989) Recent developments in trace element metabolism and function: Role of metallothionein in copper and zinc metabolism. *J.Nutr.* **119** pp. 1062-1070.
- Riordan, J.R. and Richards, V. (1980) Human fetal liver contains both zinc- and copper- rich forms of metallothionein. *J. Biol. Chem.* **255** pp. 5380-5383.
- Rhee, I.K., Lee, K.S. and Huang, P.C. (1990) Metallothioneins with interchain hinges expanded by insertion mutagenesis. *Protein Engineering* **3** pp. 205-213
- Robinson, N.J. and Thurman, D.A. (1986) Isolation of a copper complex and its rate of appearance in roots of *Mimulus guttatus*. *Planta* **169** pp. 92-97.
- Robinson, N.J. and Jackson, P.J. (1986) 'Metallothionein-like' metal complexes in angiosperms; their structure and function. *Physiol. Plant* **67** pp. 499-506.
- Robinson, N.J., Barton, K., Naranjo, C.M., Sillerud, L.O., Trehwella, J., Watt, K. and Jackson, P.J. (1987) Characterisation of metal peptides from cadmium resistant plant cells. In *Metallothionein II: Proceedings of the second international meeting on metallothionein and other low-molecular-weight, metal-binding proteins*. Kägi, J.H.R. and Kojima, Y. Eds., Birkhauser Verlag, Basel.
- Robinson, N.J., Ratliff, R.L., Anderson, P.J., Delhaize, E., Berger, J.M. and Jackson, P.J. (1988) Biosynthesis of poly(gamma-glutamylcysteinyl)glycines in cadmium-resistant *Datura innoxia* cells. *Plant Sci.* **56** pp. 197-204.
- Robinson, N.J. (1989) Algal metallothioneins: secondary metabolites and proteins. *J. Appl. Phyc.* **1** pp. 5-18.
- Robinson, N.J. (1990) Metal-binding polypeptides in plants. In *Heavy metal tolerance in plants: Evolutionary aspects.*; Shaw, A., Ed.; CRC Press, Inc.
- Robinson, N.J., Evans, I.M., Mulcrone, J., Bryden, J. and Tommey, A.M. (1992) Genes with similarity to metallothionein genes and copper, zinc ligands in *Pisum sativum* L. *Plant and Soil* **146** pp. 291-298.
- Robinson, N.J., Tommey, A.M., Kuske, C. and Jackson, P.J. (1993) Plant metallothioneins. *Biochem. J.* **295** pp. 1-10.

- Romera, F.J. and Alcántara, E. (1994) Iron-deficiency stress responses in cucumber (*Cucumis sativus* L.) roots. A possible role for ethylene. *Plant Physiol.* **105** pp. 1133-1138.
- Rost, B. and Sander, C. (1993) Prediction of protein structure at better than 70% accuracy. *J. Mol. Biol.* **232** pp. 584-599.
- Rost, B. and Sander, C. (1994) Combining evolutionary information and neural networks to predict protein secondary structure. *Proteins* **19** pp. 55-72.
- Sadler, I., Suda, K., Schatz, G., Kaudewitz, F. and Haid, A. (1984) Sequencing of the nuclear gene for the yeast cytochrome-C1 precursor reveals an unusually complex amino terminal presequence. *EMBO J.* **3** pp. 2137-2143.
- Salt, D.E., Thurman, D.A., Tomsett, A.B. and Sewell, A.K. (1989) Copper phytochelatin of *Mimulus guttatus*. *Proc. R. Soc. London.* **236** pp. 79-89.
- Sambrook, J., Fritsch, E.F. and Maniatis, T. (1989) *Molecular Cloning: A Laboratory Manual* (2nd Edition). Cold Spring Harbour Press, New York.
- Sanger, F., Nickel, S. and Coulson, A.R. (1977) DNA sequencing with chain-terminating inhibitors. *Proc. Natl. Acad. Sci. USA* **74** pp. 5463-5467.
- Schägger, H. and von Jagow, G. (1987) Tricine-sodium dodecyl sulphate-polyacrylamide gel electrophoresis for the separation of proteins in the range from 1 to 100 kDa. *Anal. Biochem.* **166** pp. 368-379.
- Schat, H. and Kalff, M.M.A. (1992) Are phytochelatin involved in differential metal tolerance or do they merely reflect metal-imposed strain. *Plant Physiol.* **99** pp. 1475-1480.
- Scheller, H.V., Huang, B., Hatch, E. and Goldsborough, P.B. (1987) Phytochelatin synthesis and glutathione levels in response to heavy metals in tomato cells. *Plant Physiol.* **85** pp. 1031-1035.
- Schultz, C.L. and Hutchinson, T.C. (1988) Evidence against a key role for metallothionein-like protein in the copper tolerance mechanism of *Deschampsia cespitosa* (L.) Beauv. *New Phytol.* **110** pp. 163-171.
- Shaw, F.C., Petering, D.H., Weber, D.N. and Gingrich, D.J. (1989) Inorganic studies of the cadmium binding peptides from *Euglena gracillus*. in *Metal Ion Homeostasis*, Hamer, D.H. and Winge, D.R. Eds. Liss Inc., New York.
- Shi, J., Lindsay, W.P., Huckle, J.W., Morby, A.P. and Robinson, N.J. (1992) Cyanobacterial metallothionein gene expressed in *Escherichia coli*. Metal binding properties of the expressed protein. *FEBS Letters* **303** pp. 159-163.
- Shojima, S., Nishizawa, N-K., Fushiya, S., Nozoe, S., Irifune, T. and Mori, S. (1990) Biosynthesis of phytosiderophores. *Plant Phys.* **93** pp. 1497-1503.

- Silar, P., Butler, G. and Thiele, D.J. (1991) Heat shock transcription of the yeast metallothionein gene. *Mol. Cell. Biol.* **11** No. 3 pp. 1232-1238.
- Sinclair, J. and Rickwood, D. (1981) Two-dimensional gel electrophoresis. *Gel electrophoresis of proteins: a practical approach*. Eds. Hames, B.D. and Rickwood, D. IRL Press Limited, England.
- Smith, D.B. and Johnson, K.S. (1988) Single-step purification of polypeptides expressed in *Escherichia coli* as fusions with glutathione-S-transferase. *Gene* **67** pp. 31-40.
- Smith, D.B. and Corcoran, L.M. (1990) Expression and purification of glutathione-S-transferase fusion proteins. In *Current protocols in molecular biology* **2** p. 16.7.1. Ausubel, F.M. *et al.* Eds. John Wiley and Sons, New York.
- Snowden, K.C. and Gardner, R.C. (1993) Five genes induced by aluminium in wheat (*Triticum aestivum* L.) roots. *Plant Phys.* **103** pp. 855-861.
- Southern, E. (1975) Detection of specific sequences among DNA fragments separated by gel electrophoresis. *J. Mol. Biol.* **98** 503-517.
- Speiser, D.M., Abrahamson, S.L., Banuelos, G. and Ow, D. (1992) *Brassica juncea* produces a phytochelatin-cadmium-sulphide complex. *Plant Physiol.* **99** pp. 817-821.
- Steffens, J.C., Hunt, D.F. and Williams, B.G. (1986) Accumulation of non-protein metal-binding polypeptides from (gamma-glutamyl-cysteinyl)_n-glycine in selected cadmium-resistant tomato cells. *J. Biol. Chem.* **261** pp. 13879-13882.
- Steffens, J.C. (1990) The heavy metal binding peptides of plants. *Annu. Rev. Plant Physiol. Plant Mol. Biol.* **41** pp. 553-575.
- Stillman, M.J. and Zelazowski, A.J. (1988) Domain specificity in metal binding to metallothionein. *J. Biol. Chem.* **263** pp. 6128-6133.
- Stillman, M.J. and Zelazowski, A.J. (1989) Domain specificity of Cd²⁺ and Zn²⁺ binding to rabbit liver metallothionein 2. *Biochem. J.* **262** pp. 181-188.
- Swofford and Olsen (1990) Phylogeny reconstruction. In *Molecular Systematics*. Eds. Hillis, D.M. and Moritz, C. Sinauer Associates Inc., USA.
- Tamai, K.T., Gralla, E.B., Ellerby, L.M., Valentine, J.S. and Thiele, D.J. (1993) Yeast and mammalian metallothioneins functionally substitute for yeast copper-zinc superoxide dismutase. *Proc. Natl. Acad. Sci. USA* **90** pp. 8013-8017.
- Tardat, B. and Touati, D. (1991) Two global regulators repress the anaerobic expression of MnSOD in *Escherichia coli*: Fur (ferric uptake regulation) and Arc (aerobic respiration control). *Mol. Micro.* **5** pp. 455-465.

- Taylor, G.J. (1987) Exclusion of metals from the symplasm: a possible mechanism of metal tolerance in higher plants. *J. Plant Nutr.* **10** pp. 1213-1222.
- Theil, E.C. (1987) Ferritin: structure, gene regulation, and cellular function in animals, plants and microorganisms. *Annu. Rev. Biochem.* **56** pp. 289-315.
- Thiele, D.J. and Hamer, D.H. (1986) Tandemly duplicated upstream control sequences mediate copper-induced transcription of the *Saccharomyces cerevisiae* copper-metallothionein gene. *Mol. Cell. Biol.* **6** pp. 1158-1163.
- Thiele, D.J. (1988) *ACE1* regulates expression of the *Saccharomyces cerevisiae* metallothionein gene. *Mol. Cell. Biol.* **8** pp. 2745-2752.
- Thiele, D.J. 1992. Metal-regulated transcription in eukaryotes. *Nucleic Acids Research* **20** pp. 1183-1191.
- Thoraldsen, J.L., Sewell, A.K., McCowen, C.L. and Winge, D.R. (1993) Regulation of metallothionein genes by the ACE1 and AMT1 transcription factors. *J. Biol. Chem.* **268** No. 17 pp. 12512-12518.
- Thumann, J., Grill, E., Winacker, E.-L. and Zenk, M.H. (1991) Reactivation of metal-requiring apoenzymes by phytochelatin-metal complexes. *FEBS Letters* **284** pp. 66-69.
- Thurman, D.A., Salt, D.E. and Tomsett, A.B. (1989) In *Metal Ion Homeostasis*. Hamer, D. and Winge, D. eds. Alan R. Liss, New York.
- Tohoyama, H., Inouhe, M., Joho, M. and Murayama, T. (1990) Resistance to cadmium is under the control of the *CAD2* gene in the yeast *Saccharomyces cerevisiae*. *Curr. Genet.* **18** pp. 181-185.
- Tommey, A.M., Shi, J., Lindsay, W.P., Urwin, P.E. and Robinson, N.J. (1991) Expression of the pea gene *PsMT_A* in *E. coli*. Metal binding properties of the expressed protein. *FEBS Letters* **292** pp. 48-52.
- Tomsett, A.B. and Thurman, D.A. (1988) Molecular biology of metal tolerance in plants. *Plant Cell Env.* **11** pp. 383-394.
- Toye, B. Immunological characterization of a cloned fragment containing the species specific epitope from the major outer membrane protein of *Chlamydia trachomatis*. *Infect Immun.* **58** pp. 3909-3913.
- Tukendorf, A. and Rauser, E.E. (1990) Changes in glutathione and phytochelatin in roots of maize seedlings exposed to cadmium. *Plant Sci.* **70** pp. 155-166.
- Turner, J.S., Morby, A.P., Whitton, B.A., Gupta, A. and Robinson, N.J. (1993) Construction of Zn²⁺/Cd²⁺ hypersensitive cyanobacterial mutants lacking a functional metallothionein locus. *J. Biol. Chem.* **268** No. 6, pp. 4494-4498.

- Vallee, B.L. and Ulmer, D. (1972) Biochemical effects of mercury, cadmium and lead. *Ann. Rev. Biochem.* **41** pp. 91-128.
- Vallee, B.L. and Auld, D.S. (1990) Zinc coordination, function, and structure of zinc enzymes and other proteins. *Biochemistry* **29**, No. 24, pp. 5647 - 5659.
- Vallee, B.L. and Auld, D.S. (1993) Zinc: Biological functions and coordination motifs. *Acc. Chem. Res.* **26**, pp. 543-551.
- Vašák, M., Galdes, A., Hill, A.O., Kägi, J.H.R., Bremner, I. And Young, B.W. (1980) Investigation of the structure of metallothioneins by proton nuclear magnetic resonance spectroscopy. *Biochemistry* **19** pp. 416-425.
- Vašák, M., Galdes, A.H., Hill, A.O., Kägi, J.H.R., Bremner, I. and Young, B.W. (1980) Investigation of the structure of metallothionein by proton nuclear magnetic resonance spectroscopy. *Biochemistry* **19** pp. 416-425.
- Vašák, M. and Kägi, J.H.R. (1981) Metal thiolate clusters in cobalt(II)-metallothionein. *Proc. Nat. Acad. Sci. USA* **78** p. 6709-6713.
- Vašák, M., Hawkes, G.E., Nicholson, J.K. and Sadler, P.J. (1985) ¹¹³Cd NMR studies of reconstituted seven-cadmium metallothionein; evidence for structural flexibility. *Biochemistry* **24** pp. 740-747.
- Vögeli-Lange, R. and wagner, G.J. (1990) Subcellular localization of cadmium and cadmium-binding peptides in tobacco leaves. *Plant Phys.* **92** pp. 1086-1093.
- von Heijne, G. (1983) Patterns of amino acids near signal sequence cleavage sites. *Eur. J. Biochem.* **133** pp 17-21.
- Wagner, G.J and Trotter, M.M. (1982) Inducible cadmium binding complexes of cabbage and tobacco. *Plant Phys.* **69** pp. 804-809.
- Wagner, G.J. (1984) Characterization of a cadmium-binding complex of cabbage leaves. *Plant Phys.* **76** pp. 797-805.
- Welch, J., Fogel, S., Buchmann, C. and Karin, M. (1989) The *CUP2* gene product regulates the expression of the *CUP1* gene, coding for yeast metallothionein. *EMBO J.* **8** pp. 255-260.
- Welch, R.M. and LaRue, T.A. (1990) Physiological characterisation of Fe accumulation in the 'bronze' mutant of *Pisum sativum* L., cv 'sparkle' E107 (*brz brz*). *Plant Physiol.* **93** pp. 723-729.
- Welch, R.M., Norvell, W.A., Schaefer, S.C., Shaff, J.E. and Kochian, L.V. (1993) Induction of iron(III) and copper (II) reduction in pea (*Pisum sativum* L.) roots by Fe and Cu status: Does the root-cell plasmalemma Fe(III)-chelate reductase perform a general role in regulating cation uptake. *Planta* **190** pp. 555-561.

- Weser, U., Mutter, W. and Hartmann, H.-J. (1986) The role of Cu(I)-thiolate clusters during the proteolysis of Cu-thionein. *FEBS Letters* **197** pp. 258-262.
- Willner, H., Vařák, M. and Kägi, J.H.R. (1987) Cadmium thiolate clusters in metallothionein - spectrophotometric and spectropolarimetric features. *Biochemistry* **26** pp. 6287-6292.
- Winge, D.R. and Miklossy, K.-A. (1982) Domain nature of metallothionein. *J. Biol. Chem.* **257** pp. 3471-3476.
- Winge, D.R., Nielson, K.B., Gray, W.R. and Hamer, D.H. (1985) Yeast metallothionein: sequence and metal binding properties. *J. Biol. Chem.* **260** pp. 14464-14470.
- Wright, C.F., McKenney, K., Hamer, D.H., Byrd, J. and Winge, D.R. (1987) Structural functional studies of the amino terminus of yeast metallothionein. *J. Biol. Chem.* **262** pp. No. 27 pp. 12912-12919.
- Wright, C.F., Hamer, D.H. and McKenney, K. (1988) Autoregulation of the yeast copper metallothionein gene depends on metal binding. *J. Biol. Chem.* **263** No. 3 pp. 1570-1574.
- Yamashoji, S. and Kajimoto, G. (1986) Decrease of NADH in yeast cells by external ferricyanide reduction. *Biochim. Biophys. Acta* **852** pp. 25-29.
- Yang, S.F. and Hoffman, N.E. (1984) Ethylene and biosynthesis in higher plants. *Ann. Rev. Plant Physiol.* **35** pp. 155-189.
- Zarembinski, T.I. and Theologis, A. (1994) Ethylene biosynthesis and action: a case of conservation. *Plant Mol. Biol.* **26** pp. 1579-1597.
- Zelazowski, A.J., Gasyna, Z. and Stillman, M.J. (1989) Silver binding to rabbit liver metallothionein - circular dichroism and emission study of silver-thiolate cluster formation with apometallothionein and the α -fragments and β -fragments. *J. Biol. Chem.* **264** pp. 17091-17099.
- Zeng, J., Vallee, B.L. and Kägi, J.H.R. (1991a) Zinc transfer from transcription factor IIA fingers to thionein clusters. *Proc. Natl. Acad. Sci. USA* **88** pp. 9984-9988.
- Zeng, J., Heuchel, R., Schaffner, W. and Kägi, J.H.R. (1991b) Thionein (apometallothionein) can modulate DNA binding and transcription activation by zinc finger containing factor SP1. *FEBS Letters* **279** No. 2 pp. 310-312.
- Zhang, F., Römheld, V. and Marschner, H. (1991) Role of the root apoplasm for iron accumulation by wheat plants. *Plant Physiol.* **97** pp. 1302-1305.
- Zhou, J. and Goldsbrough, P.B. (1994) Functional homologs of fungal metallothionein genes from *Arabidopsis*. *Plant Cell* **6** pp. 875-884.

- Zhou, P and Thiele, D.J. (1991) Isolation of a metal activated transcription factor from *Candida glabrata* by complementation in *Saccharomyces cerevisiae*. *Proc. Natl. Acad. Sci. USA* **88** pp. 6112-6116.
- Zhou, P., Szczyypka, M.S., Sosinowski, T. and Thiele, D.J. (1992) Expression of a yeast metallothionein gene family is activated by a single metalloregulatory transcription factor. *Mol. Cell. Biol.* **12** pp. 3766-3775.
- Zhou, P. and Thiele, D.J. (1993) Copper and gene regulation in yeast. *Biofactors* **4** pp. 105-115.

